DISSERTATION

submitted to the
Combined Faculties of the Natural Sciences and Mathematics
of the Ruperto Carola University of Heidelberg, Germany,
for the degree of
Doctor of Natural Sciences

Put forward by
SEBASTIAN OHMER

Born in Hanau, Germany

Oral examination: December 19th, 2017

New Symmetry Concepts for Spacetime and Unification

Referees:
Prof. Dr. Dr. h.c. Manfred Lindner
and
Prof. Dr. Tilman Plehn

Abstract:
In this dissertation, we present new concepts of spacetime and unification for physics beyond the Standard Model. Our ansatz is to decouple new physics from the electroweak scale but still provide a solution to the hierarchy problem and allow for a viable dark matter candidate. Nevertheless, we always emphasize the testability. We first motivate the decoupling of Standard Model extensions from the electroweak scale by discussing the left-right symmetric theory with the minimal number of propagating degrees of freedom to account for Majorana neutrinos. Furthermore, we motivate the decoupling by showing the viability of Majorana dark matter in the context of a minimal consistent theory of local baryon number. Combining these ideas, we then introduce the 433 theory which is based on the gauge group $SU(4)_C \otimes SU(3)_L \otimes SU(3)_R$. The 433 theory is an UV completion of the Standard Model in four dimensions which can be realized at low energy scales. As the 433 theory lacks an inherent dark matter candidate, we consider Bose-Einstein condensate dark matter as an alternative symmetry-motivated dark matter candidate. We put forward a new method to probe such superfluid dark matter with gravitational waves. After presenting a solution to the hierarchy problem and a testable dark matter candidate, we question the unique role of supersymmetry to mix global internal and external symmetries. Subsequently, we introduce a new spacetime concept and demonstrate how spacetime symmetries can father the three Standard Model generations.

Zusammenfassung:
In dieser Dissertation stellen wir neue Konzepte für die Raumzeit und die Vereinheitlichung der fundamentalen Kräfte vor. Wir präsentieren eine neue Lösung für das Hierarchieproblem und erörtern mögliche Dunkle Materie Kandidaten. Dabei vertreten wir den Standpunkt, dass die Physik jenseits des Standard Models von der elektroschwachen Skala entkoppelt ist. Die Überprüfbarkeit unserer Ideen steht dabei immer im Vordergrund. Zuerst motivieren wir das Entkoppeln von der elektroschwachen Skala mit der Diskussion der links-rechts symmetrischen Theorie mit der minimalen Anzahl propagierender Freiheitsgrade, welche Majorana Neutrinos realisieren können. Weiterhin motivieren wir das Entkoppeln durch eine Studie der Majorana Dunklen Materie in der minimalen konsistenten Theorie von lokaler Baryonenzahl. Anschließend verbinden wir diese Ideen in der 433 Theorie, einer Eichtheorie basierend auf der Eichsymmetrie $SU(4)_C \otimes SU(3)_L \otimes SU(3)_R$. Die 433 Theorie ist eine UV Vervollständigung des Standard Models in vier Dimensionen, welche bei niedrigen Energien realisiert werden kann. Weil die 433 Theorie keinen intrinsischen Dunkle Materie Kandidaten hat, behandeln wir den alternativen und durch Symmetrien motivierten Dunkle Materie Kandidaten eines Bose-Einstein Kondensates. Dabei stellen wir eine neue Methode zum Erforschen dieser Suprafllüssigkeit als Dunkle Materie mittels Gravitationswellen vor. Nachdem wir eine Lösung für das Hierarchieproblem und überprüfbare Dunkle Materie Kandidaten eingeführt haben, hinterfragen wir die Rolle von Supersymmetrie beim Vermischen von globalen internen und externen Symmetrien. Daraufhin stellen wir ein neues Raumzeitkonzept vor und demonstrieren, wie Raumzeitsymmetrien die Ursache für die drei Standard Model Generationen sein können.

Contents

CHAPTER 1

INTRODUCTION

PARTICLE PHYSICS is considered to be in a crisis. The beautiful and appealing theoretical ideas developed during the last forty years are currently being tested and seem to fail us. Pressure is building up and we are in the dark what the future will bring. In such turbulent times, it is up to us to seize the steering wheel, to put forward new ideas, and to guide the way.

We study physics because we have the deep unsettling desire to understand. There is no guarantee that the quest for knowledge is easy, there is not even a guarantee for success. We mostly improve by failure. Challenging the respected ideas of supersymmetry and unification, we try to advertise new concepts for physics beyond the Standard Model.

The approaches we take in this thesis are guided by symmetry and minimality. We interpret the current experimental evidence such that the physics beyond the Standard Model is decoupled from the electroweak scale. The goal of this thesis is to provide alternative ideas for the road ahead.

The starting point is the Standard Model, which is shortly recapitulated in section 1.1. The main motivation for physics beyond the Standard Model is then given in section 1.2, before we clarify the importance of symmetries as a guiding principle in section 1.3.

Chapter 2 then focuses on bottom-up extensions of the Standard Model. In section 2.1, we discuss left-right symmetric theories and introduce the left-right symmetric theory with the minimal number of propagating degrees of freedom which can account for Majorana neutrinos. A special emphasize is put on the testability of the theory at the LHC. Section 2.2 is dedicated to the Standard Model extension by local baryon number. We again shortly recap the extension with the minimal number of new particles before discussing the properties of the intrinsic dark matter candidate. Even though the dark matter candidate will generically be too heavy to be directly produced at the LHC, we also comment on possible signals of local baryon number at particle colliders.

In chapter 3, we argue in favor of a new approach towards the hierarchy problem. We construct the first UV completion of the Standard Model in four dimensions which can be realized at low energies. Such a theory enables us to lower the Planck scale significantly and to lessen the tension between the electroweak scale and the Planck scale. The theory we discuss is based on the gauge group $SU(4)_C \otimes SU(3)_L \otimes SU(3)_R$ and combines the ideas of left-right symmetric theories and extensions by local baryon number. Again, we also stress the predictability of the theory. We point out the possibility of falsification by determining the reheating temperature in the early Universe and possible probes at particle colliders. We comment on a possible extension with true gauge unification in section 3.2.

Unfortunately, the discussed UV completions of the Standard Model lack the intrinsic dark matter candidate of other Standard Model extensions by local baryon number. We therefore consider alternative dark matter candidates which are induced by anomalous global symmetries in chapter 4. Axion-like particles are often a generic feature of Standard Model extensions. They allow for the interesting possibility of forming Bose-Einstein condensates (BECs) of galactic size. Such a dark matter candidate has vastly different properties compared to the intrinsic dark matter candidate of local baryon number in section 2.2.1. Probing BEC dark matter is therefore difficult. We propose a new method relying on multi-messenger gravitational wave astronomy in section 4.3.

Before closing, we discuss alternatives to supersymmetry in chapter 5. Our focus is however not supersymmetry alternatives solving the hierarchy problem as we introduced low scale Standard Model UV completions in chapter 3, but on alternatives to mix global spacetime and particle symmetries. The Coleman-Mandula theorem constrains such a mixing severely and we review the no-go theorem in section 5.1. We then consider theoretical concepts which have the potential to circumvent the Coleman-Mandula theorem in section 5.2, before turning to spacetime modifications in section 5.3. The new spacetime structure we introduce will allow for a mixing of internal and external symmetries and can additionally explain the appearance of the Standard Model generations and their mass differences.

We conclude and give an outlook for future developments in chapter 6. For the sake of readability, some results were banished to the appendix, whereas, for other results, we have to refer the interested reader to the peer-reviewed articles.

Disclaimer

While writing this thesis, the presented results were already published in peer-reviewed journals.

- Section 2.1 is based on “Simple Left-Right Theory: Lepton Number Violation at the LHC” in collaboration with Pavel Fileviez Pérez and Clara Murgui [1].
- Section 2.2 mainly considers results presented in “Leptobaryons as Majorana Dark Matter” in collaboration with Hiren H. Patel [2]. However, the minimal theory of leptobaryons was first introduced in “Minimal Theory for Lepto-Baryons” together with Pavel Fileviez Pérez and Hiren H. Patel [3] and was an essential part of the author’s master thesis.
- The low scale UV completions of the Standard Model presented in chapter 3 were first published in “Unification and Local Baryon Number” in collaboration with Pavel Fileviez Pérez [4].
- Section 4.3 elaborates on the results of “Gravitational waves as a new probe of Bose–Einstein condensate Dark Matter” in collaboration with P. S. Bhupal Dev and Manfred Lindner [5].
- Chapter 5 is based on the ideas published in “Emerging Internal Symmetries from Effective Spacetimes” in collaboration with Manfred Lindner [6].

1.1 The Standard Model of Particle Physics

The Standard Model of particle physics is known as one of the most precise theories ever invented. Experiments with state-of-the-art Penning traps are able to measure the electron g factor to a precision of 0.28 parts in one trillion (10^{12}) [7]. However, only since 2012 has the Standard Model been complete. In the year 2012, the ATLAS and CMS [8, 9] detector at the Large Hadron Collider (LHC) in Switzerland announced the discovery of the Higgs boson. In this section, we shortly discuss the main features of the Standard Model.

The Standard Model is a gauge theory based on the gauge group

$$G_{\text{SM}} = SU(3)_C \otimes SU(2)_L \otimes U(1)_Y \,. \tag{1.1}$$

It was first introduced by Glashow, Weinberg and Salam in the 1960s [10, 11, 12]. In the following discussion of the Standard Model, we split the Standard Model Lagrangian as follows

$$\mathcal{L}^{\text{SM}} = \mathcal{L}^{\text{SM}}_{\text{gauge}} + \mathcal{L}^{\text{SM}}_{\text{scalar}} + \mathcal{L}^{\text{SM}}_{\text{fermion}} \,. \tag{1.2}$$

We will now discuss the individual contributions separately.

- $\mathcal{L}^{\text{SM}}_{\text{gauge}}$ contains the kinetic terms of the twelve Standard Model gauge fields

$$\mathcal{L}^{\text{SM}}_{\text{gauge}} = -\frac{1}{4}(F^{\mu\nu}_G)_a (F_{G\,\mu\nu})^a - \frac{1}{4}(F^{\mu\nu}_W)_b (F_{W\,\mu\nu})^b - \frac{1}{4}F^{\mu\nu}_B F_{B\,\mu\nu} \,, \tag{1.3}$$

  where $(F^{\mu\nu}_G)_a$, $(F^{\mu\nu}_W)_b$ and $F^{\mu\nu}_B$ are the respective field strength tensors of the gluon fields G^μ_a belonging to the $SU(3)_C$ symmetry, the weak fields W^μ_b corresponding to the $SU(2)_L$ symmetry, and the hypercharge field B^μ originating from the local abelian $U(1)_Y$ symmetry with $a \in \{1, \dots, 8\}$ and $b \in \{1, 2, 3\}$. The field strength tensor is thereby defined as $F^{\mu\nu} = \frac{i}{g}[D^\mu, D^\nu] = (F^{\mu\nu})_a T^a$ with covariant derivative $D^\mu = \partial^\mu + ig(A^\mu)_a T^a$ where $(A^\mu)_a$ and T^a are the respective gauge fields and gauge symmetry generators. The gauge coupling g characterizes the coupling strength of the associated gauge interactions [1].

- $\mathcal{L}^{\text{SM}}_{\text{scalar}}$ describes the Higgs doublet $H \sim (1, 2, 1/2)$ and the spontaneous symmetry breaking in the Standard Model

$$\mathcal{L}^{\text{SM}}_{\text{scalar}} = (D^\mu H)^\dagger (D_\mu H) - \frac{\lambda}{2}\left(H^\dagger H - \frac{1}{2}v^2\right)^2 \,. \tag{1.4}$$

  The scalar potential has the classical minimum

$$\langle H \rangle = \frac{1}{\sqrt{2}}\begin{pmatrix} 0 \\ v \end{pmatrix} \,, \tag{1.5}$$

[1] Through all of this thesis we use natural units with $c = \hbar = 1$.

Fermionic particle content of the Standard Model

particle	$SU(3)_C$	$SU(2)_L$	$U(1)_Y$
left-handed quarks $Q_L = \begin{pmatrix} u_L \\ d_L \end{pmatrix}$	3	2	1/6
right-handed up-type quarks u_R	3	1	2/3
right-handed down-type quarks d_R	3	1	-1/3
left-handed leptons $\ell_L = \begin{pmatrix} \nu_L \\ e_L \end{pmatrix}$	1	2	-1/2
right-handed charged leptons e_R	1	1	-1

Table 1.1: The Standard Model fermions and their quantum numbers.

and therefore the vacuum state is not invariant under the symmetry transformations of G_{SM}. This phenomenon is known as spontaneous symmetry breaking [13, 14, 15] and is responsible for the gauge boson and fermion masses in the Standard Model. Furthermore, the non-trivial vacuum expectation value of the Higgs breaks the electroweak symmetry of the Standard Model

$$SU(3)_C \otimes SU(2)_L \otimes U(1)_Y \xrightarrow{\langle H \rangle \neq 0} SU(3)_C \otimes U(1)_{\text{EM}} \,. \tag{1.6}$$

The spontaneous breaking of the gauge symmetry G_{SM} leads to a mass mixing of the neutral component of the weak gauge fields and the hypercharge gauge field. A linear combination of the weak and hypercharge gauge fields becomes massive and is known as the Z boson, whereas another linear combination stays massless and is known as the photon γ.

The Weinberg angle parametrizes the mixing of the neutral component of the weak gauge field and the hypercharge gauge field

$$\cos(\theta_W) = \frac{g_L}{g_Y^2 + g_L^2} \quad \text{and} \quad \sin(\theta_W) = \frac{g_Y}{\sqrt{g_Y^2 + g_L^2}} \,, \tag{1.7}$$

where g_Y and g_L are the hypercharge and weak gauge couplings, respectively. The Higgs and gauge boson masses are then given by

$$M_H = \sqrt{\lambda} v \,, \quad M_W = \frac{g_L v}{2} \,, \quad M_Z = \frac{g_L v}{2\cos(\theta_W)} \,. \tag{1.8}$$

- $\mathcal{L}^{\text{SM}}_{\text{fermion}}$ accounts for the kinetic terms and interactions of the Standard Model fermions. The fermionic particle content of the Standard Model is shown in Table 1.1.

The Lagrangian of the Standard Model fermions is given by

$$\begin{aligned}\mathcal{L}^{\text{SM}}_{\text{fermion}} =& \bar{Q}_{L\alpha}(i\not{D})Q_{L\alpha} + \bar{u}_{R\alpha}(i\not{D})u_{R\alpha} + \bar{d}_{R\alpha}(i\not{D})d_{R\alpha} \\ &+ \bar{\ell}_{L\alpha}(i\not{D})\ell_{L\alpha} + \bar{e}_{R\alpha}(i\not{D})e_{R\alpha} - y^{(l)}_{\alpha\beta}\,\bar{\ell}_{L\alpha}H\,e_{R\beta} \\ &- y^{(u)}_{\alpha\beta}\,\bar{Q}_{L\alpha}\,\tilde{H}u_{R\beta} - y^{(d)}_{\alpha\beta}\,\bar{Q}_{L\alpha}\,H\,d_{R\beta}\,,\end{aligned} \tag{1.9}$$

with $\not{D} = \gamma_\mu D^\mu$ and Dirac gamma matrices $\gamma_\mu = (\gamma_0, \gamma_1, \gamma_2, \gamma_3)$. We further defined $\tilde{H} = i\sigma_2 H^*$. The Yukawa couplings $y^{(l)}_{\alpha\beta}$, $y^{(u)}_{\alpha\beta}$, and $y^{(d)}_{\alpha\beta}$ are given by 3×3 matrices in flavor space.

The non-trivial vacuum expectation value of the Higgs field induces a mass for the Standard Model fermions via the Yukawa interactions after electroweak symmetry breaking. The fermion mass matrices are given by

$$(m_f)_{\alpha\beta} = y^{(f)}_{\alpha\beta}\frac{v}{\sqrt{2}} \quad \text{with} \quad f \in \{u, d, l\}\,. \tag{1.10}$$

Note that the mass matrices are not diagonal in general. However, we can further define a bi-unitary transformation of the left- and right-handed fermion fields which diagonalizes the mass matrices

$$(V^f_L)^\dagger y^{(f)} V^f_R = \text{diag}(m^f_1, m^f_2, m^f_3)\,,$$

where m^f_1, m^f_2, and m^f_3 are the first, second, and third generation mass eigenvalues of the associated Standard Model fermions $f \in \{u, d, l\}$. The bi-unitary transformation of the quark fields leads to a mixing of different quark flavors in weak charged current interactions. The mixing is described by the unitary Cabibbo-Kobayashi-Maskawa (CKM) matrix [16, 17] $V_{\text{CKM}} = (V^u_L)^\dagger V^d_L$. The CKM matrix has four free parameters which describe the quark mixing, three angles and one phase. Due to the phase of the CKM matrix, we find explicit CP violation in the Standard Model.

The bi-unitary transformation of the charged leptons does not lead to a mixing of the lepton flavors because neutrinos are massless in the Standard Model. Upon the introduction of neutrino masses, this picture changes. The Pontecorvo-Maki-Nakagawa-Sakata (PMNS) matrix [18, 19] was introduced to describe the neutrino mixing. The PMNS matrix has again at least four free parameters, three angles, and one phase. If neutrinos are Majorana particles, two additional phases enter the mixing matrix. The phases of the PMNS matrix are also a source of explicit CP violation.

After this short walk-through of the Standard Model of particle physics, we now turn towards physics beyond it. In chapter 2, we will construct explicit bottom-up extensions of the Standard Model. We will embed the Standard Model in a more complete theory in chapter 3 and modify the spacetime structure in chapter 5. The discussed extensions always tackle phenomena beyond the Standard Model by concepts of new symmetries.

1.2 Beyond the Standard Model

The Standard Model is a remarkable theory, but it is not flawless. In this section, we introduce two shortcomings of the Standard Model: dark matter and the hierarchy problem. It is widely believed that these two problems require new physics close to the electroweak scale and thus could be experimentally tested and solved in near future. Of course these are not the only challenges the Standard Model faces, but these are the two problems which drive the field of high energy physics at the moment.

In this thesis, we will put forward new solutions to these problems and also elaborate on new possibilities to probe existing solutions. Our main focus thereby will be to detach these problems from the electroweak scale and thus explain the null results at current experiments. While doing so, we will also encounter other deficits of the Standard Model which we introduce in the appropriate sections. These deficits range from neutrino masses, parity violation, proton stability, baryon asymmetry in the Universe, and origin of the Standard Model gauge structure to the strong CP problem, the appearance of three Standard Model fermion generations, and the fermion mass hierarchies. All these problems are important and we will present or comment on possible solutions. Nevertheless, none of them is conventionally as closely linked to the electroweak scale as dark matter and the hierarchy problem. Hence, none of them is under such experimental pressure as dark matter and the hierarchy problem.

Dark Matter

With all the praises for the Standard Model, we should not forget that only about 5% of the energy density of the Universe is described by the Standard Model. About 27% of the energy density of the Universe is contributed by dark matter and roughly 68% is in the form of dark energy [20]. In this thesis, we take the point of view that a cosmological constant is responsible for the accelerated expansion of the Universe and accounts for the dark energy. However, we expect that the physics explaining the smallness of the cosmological constant is unrelated to the ideas presented.

The most notable aspect of dark matter is the overwhelming experimental evidence. We have a variety of discrepancies between observational data and our theoretical predictions which are all hinting towards the concept of dark matter. Even more strikingly, the experimental evidence covers a wide range of distances. At galactic scales, we find modifications of galaxy rotation curves [21, 22]. At the scale of galaxy clusters, we find undeniable shifts of the center-of-mass in cluster collisions [23, 24]. At cosmological scales, we find enhancement and damping in the baryon acoustic spectrum [25, 20]. There are attempts to explain these observations by a modification of gravity [26, 27]. However, due to this wide spread in energy, we interpret these results as a strong hint towards a new stable electrically neutral particle species.

Dark matter is not a particularly new problem of cosmology. Zwicky already discovered in 1933 that the galaxies of the Coma-cluster move faster as their observed gravitational potential suggests [28]. Further experimental evidence for dark matter stems from the abundance of light elements at Big Bang nucleosynthesis (BBN) [29]. The observed abundance is too small to explain the observed large scale structure of the Universe. These observations are supported by N-body simulations which have to include a dark matter component to match the observed large scale structure [30]. Finally, a more recent indication for dark matter comes from studies of weak gravitational lensing [31].

Weakly interacting massive particles (WIMPs) have been the preferred dark matter candidate over the past decades. A stable particle with weak scale interactions and a mass in the multi-GeV range has just the right properties to account via the freeze-out mechanism for the observed dark matter relic abundance. This is known as the WIMP miracle. Moreover, WIMPs are extremely well motivated in the most respected Standard Model extensions. The lightest supersymmetric particle, for example, is an ideal dark matter candidate [32]. Furthermore, most gauge extensions of the Standard Model predict stable particles which are also exemplary dark matter candidates.

WIMPs are by far not the only dark matter candidates. Other proposed dark matter candidates are axion-like particles [33, 34], scalar extensions of the Standard Model [35, 36], keV sterile neutrinos [37] or primordial black holes [38, 39]. All of these dark matter candidates interact very weakly with Standard Model particles, can be produced in the early Universe, and are stable on cosmological time scales. However, they can differ in their velocity distributions. The observations suggest that the dominant dark matter contribution has to originate from a non-relativistic particle species. Such non-relativistic dark matter is referred to as cold dark matter. Sterile neutrino dark matter, in contrast, would only be partly non-relativistic if at all in thermal equilibrium. Partly non-relativistic and partly relativistic dark matter scenarios are generally referred to as warm dark matter. Recent results even imply that a dark matter mixture with non-relativistic and relativistic degrees of freedom may have a better agreement with the measured small scale structure of the Universe [40, 41].

As the search for dark matter is one of the most important quests of modern physics, and also due to the variety of possible dark matter candidates, a global experimental endeavor started. Direct detection experiments such as XENON1T try to measure the dark matter-nucleon scattering in large underground laboratories [42, 43]. Gamma ray observatories like H.E.S.S. search for dark matter annihilation products [44, 45, 46]. The ATLAS and CMS detectors at the LHC try to identify new stable particles [47]. More specialized experiments, for example ADMX, search specifically for axion-like particles as dark matter [48]. Gravitational wave detectors such as LIGO [49] can search for primordial black holes.

In this thesis, we will consider two very different dark matter candidates. In section 2.2, we enlarge the Standard Model gauge symmetry by local baryon number. As the Standard Model with gauged baryon number is not a consistent theory due to the non-vanishing anomalies, we have to predict new particles. Upon the spontaneous breaking of local baryon number, the lightest new particle is automatically stable and a dark matter candidate. In the extension presented in section 2.2, the dark matter candidate will be a Standard Model singlet Majorana fermion. We will see that, due to the Majorana nature, the proposed dark matter candidate behaves as heavy WIMP dark matter.

Our second dark matter candidates are axion-like particles which we discuss in chapter 4. We thereby focus on the interesting property that axion-like particles can form Bose-

Einstein condensates of galactic size. Such BEC dark matter is however difficult to distinguish from other dark matter candidates with large scale structure observations. We therefore propose a novel method to probe BEC dark matter with repulsive self-interactions via gravitational waves in section 4.3.

The Hierarchy Problem

With the discovery of the Higgs boson, we have confirmed the existence of fundamental scalar particles. The most peculiar aspect of fundamental scalars is the fact that they are highly sensitive to UV physics. The Higgs mass is the only dimensionful coupling of the Standard Model Lagrangian and thus the only relevant operator. Embedding the Standard Model in an UV complete theory, we find that the measured physical Higgs mass is given by

$$M_H^2 = (M_H^0)^2 + \delta M_H^2 \,, \tag{1.11}$$

where M_H^0 is the bare Higgs mass and δM_H represents the high energy corrections to the Higgs mass induced by the high energy theory.

If we assume that the Standard Model is valid up to the Planck scale and that a more fundamental theory emerges at this scale, the high energy corrections in equation (1.11) are given by

$$\delta M_H^2 = C_{\mathrm{Pl}} \frac{M_{\mathrm{Pl}}^2}{16\pi^2} \,, \tag{1.12}$$

with the coupling C_{Pl} depending on the gauge couplings, Yukawa couplings, and Higgs self-couplings of the theory. As the Planck scale is assumed to be of the order $M_{\mathrm{Pl}} \sim 10^{19}$ GeV, we find that the bare Higgs mass M_H^0 has to almost exactly cancel the high energy corrections to allow for an electroweak scale physical Higgs mass. Such a theory is considered to be fine-tuned. It is important to note that the hierarchy problem is not a flaw of the Standard Model per se. The problem arises as we are embedding the Standard Model into a more fundamental theory at scales far above the electroweak scale.

The Standard Model fermion masses are in contrast protected from UV corrections by the chiral symmetry of the Standard Model at high energies. There are only two known symmetries which could protect the Higgs mass from UV corrections. The first possibility is supersymmetry [50, 51] and the second is conformal symmetry [52, 53]. Supersymmetry is a modification of the spacetime structure which introduces a new particle with opposite statistics for every Standard Model particle. The new bosons and fermions only give rise to mass corrections of the Standard Model Higgs proportional to the supersymmetry breaking scale. Hence, if the supersymmetry breaking scale is close to the electroweak scale, the mass corrections are small and we would consider the theory natural. On the other hand, conformal symmetry forbids dimensionful couplings completely. The Higgs mass is established by an anomalous breaking of the conformal symmetry.

In this thesis, we take the approach that the Planck scale, the scale where gravity becomes strongly coupled, is not at 10^{19} GeV but significantly lower at 10^7 GeV. We would then still consider the physical Higgs mass to be fine-tuned. However, by lowering the Planck scale by twelve orders of magnitude, the tuning is significantly lessened. The Planck scale can be lowered for example with the introduction of large extra dimensions [54]. We are able to take this point of view as we construct the first UV completion of the Standard Model in four dimensions which can be realized at energy scales as low as 10^7 GeV without giving rise to proton decay in chapter 3.

The constructed UV completion of the Standard Model further introduces four additional scales between the electroweak scale and the lowered Planck scale. The high energy corrections of the Higgs mass then take the form

$$\delta M_H^2 = C_1 \frac{M_1^2}{16\pi^2} + C_2 \frac{M_2^2}{16\pi^2} + C_3 \frac{M_3^2}{16\pi^2} + C_4 \frac{M_4^2}{16\pi^2} + C_{\mathrm{Pl}} \frac{M_{\mathrm{Pl}}^2}{16\pi^2} \,. \tag{1.13}$$

Although the four scales in between the electroweak scale and the lowered Planck scale at 10^7 GeV do not resolve the fine-tuning of the theory, they do give rise to the possibility of a new mechanism such as the clockwork mechanism [55] which could lead to a cancellation of the contributions of the five scales to the Higgs mass.

1.3 Symmetries in Physics

To solve problems efficiently, we generally start to simplify and to abstract. Such an approach is especially sensible if the problem is too complex to grasp initially. As we are abstracting, we try to categorize and search for hidden relations. Symmetries are often our first choice. If considering the mechanics of billiard balls or the quantum theory of many-body systems, symmetries make nature accessible. It is unsurprising that symmetries are considered to be one of the most important fundamental principles of physics.

Symmetry is an abstract phrase. What does a physicist actually mean by a symmetry? A symmetry in fundamental physics is a special transformation property of the system which does not change the outcome of experiments. Assuming that the laws of physics are describable by the principle of least action, we define a symmetry by a transformation of the action which changes the action by, at most, a total derivative. A total derivative leads to surface terms which vanish for appropriate field configurations. The only exception are non-abelian gauge theories, as discussed in section 4.1. The action S is defined as

$$S = \int \mathrm{d}^4x \, \mathcal{L}(\Phi_i, \partial\Phi_i) \,, \tag{1.14}$$

where Φ_i are arbitrary scalar, spinor, vector, and metric tensor fields. Noether's theorem [56] then links symmetry transformations of the action S to conserved charges. Conserved charges allow us to label quantum states.

We distinguish two types of symmetry transformations: spacetime and internal symmetries. Spacetime transformations are symmetry transformations which act on the integral measure d^4x and on fields in non-trivial spacetime symmetry representations. Translations and rotations are, for instance, spacetime symmetries. Internal symmetry transformations on the other hand do not transform the integration measure d^4x, but only act on the fields in the Lagrangian. The Standard Model gauge symmetry is an example for an internal symmetry.

The special standing of symmetries in fundamental particle physics became evident with the development of quantum mechanics at the beginning of the 20th century. Eugene Wigner recognized that elementary particles have to be identified with the irreducible representations of the spacetime symmetry group [57].

However, it was not only the importance of spacetime symmetries which unmasked symmetries as a superb guiding principle. After the discovery of gauge theories and the success of describing quantum electrodynamics (QED) as an abelian $U(1)_{\mathrm{EM}}$ gauge theory and quantum chromodynamics (QCD) as a non-abelian $SU(3)_C$ gauge theory, the prominence of symmetries finally became undeniable. The Standard Model of particle physics, which is the most precise theory known [7], is based on a $SU(3)_C \otimes SU(2)_L \otimes U(1)_Y$ gauge theory which is spontaneously broken to $SU(3)_C \otimes U(1)_{\mathrm{EM}}$ via the Higgs-Englert mechanism, as discussed in section 1.1.

Of course, symmetries also serve as a guiding principle for physics beyond the Standard Model. The appearance of extremely small or extremely large numbers as fundamental quantities is always a striking and puzzling phenomenon. To relate such entities to natural order one quantities, symmetries are required. A prime example is the Peccei-Quinn symmetry which was invented to explain the smallness of the vacuum angle of QCD θ_{QCD}.

However, not only can the Peccei-Quinn symmetry explain the observed vacuum angle of QCD, it also leads to an interesting and testable phenomenology. The axion, the pseudo-Goldstone boson of the Peccei-Quinn symmetry, is a potential dark matter candidate. In general, axion-like particles have to be extremely light and weakly interacting. Fascinatingly, they could form macroscopic Bose-Einstein condensates of galactic size. We discuss axion-like particles and Bose-Einstein condensate dark matter in chapter 4. Thereby, special emphasize is given to a new method of probing Bose-Einstein condensate dark matter with gravitational waves [5].

On the other hand, an exemplary extremely large number which requires explanation is the proton lifetime. The lifetime of the proton exceeds the age of the Universe by at least three times. The proton carries baryon number which is an accidental global symmetry of the Standard Model. Intriguing results from quantum gravity suggest that global symmetries cannot exist in nature (see section 2.2). By promoting baryon number from a global symmetry to a local symmetry, we can evade such consistency conflicts. Additionally, we thereby also stabilize the proton and explain the long lifetime. The phenomenology of the minimal Standard Model extension with local baryon number [3, 2] is discussed in section 2.2. “Minimal” in this context refers to the minimal number of additional fermionic multiplets to have a consistent anomaly free quantum theory.

So far, we have only tried to enlarge the symmetry structure of the Standard Model. However, there are also symmetries which are explicitly broken and they unsettle us. The spacetime we observe suggests that there should exist three discrete spacetime symmetries: parity P, charge conjugation C, and time reversal T. The CPT theorem [58, 59, 60] even guarantees that a local, causal, and Lorentz invariant field theory with Poincaré invariant vacuum and bound Hamiltonian is invariant under CPT transformations. Nevertheless, the Wu experiment was the first experimental proof that the discrete parity symmetry P is broken in nature [61]. Today, we even know that all the individual discrete spacetime symmetries are broken. As a consequence, the CP symmetry is explicitly broken by the CKM matrix in the Standard Model (see section 1.1). A possible mechanism to explain why parity is violated in the Standard Model is the spontaneous symmetry breaking in left-right symmetric theories [62, 63, 64, 65]. In left-right symmetric theories, the discrete parity symmetry P can be restored at high energies. As the theory spontaneously breaks to the Standard Model, the parity symmetry P is broken as well. We discuss left-right symmetric theories in section 2.1. We thereby introduce the left-right symmetric theory with the minimal number of degrees of freedom which can account for Majorana neutrinos [1].

As symmetries should help us to understand the structure of nature, it is a valid question to ask: What is special about a gauge theory based on $SU(3)_C \otimes SU(2)_L \otimes U(1)_Y$? Group theoretical embeddings of the Standard Model try to address this question. We will construct a low scale UV completion of the Standard Model which is testable in chapter 3. Consequently, we will combine the ideas of local baryon number and left-right symmetry. The gauge theory we introduce is based on $SU(4)_C \otimes SU(3)_L \otimes SU(3)_R$ and is the minimal non-abelian gauge theory which can be broken to the Standard Model with local baryon number and is left-right symmetric [4]. “Minimal” in this context refers to the minimal rank of the gauge group. We will also touch on the more symmetric gauge theory based on $SU(4)_C \otimes SU(4)_L \otimes SU(4)_R$.

Until now, we distinguished between spacetime and internal symmetries. Such a distinction is supported by the Coleman-Mandula theorem [66]. The theorem demands that the symmetry describing a scattering process in a relativistic and interacting quantum field theory has to factor into spacetime and particle symmetries. This is a frustrating result as we expect that the most fundamental theory of everything should treat spacetime and particles on an equal footing. We discuss the Coleman-Mandula theorem and possibilities to nonetheless mix spacetime and particle symmetries without supersymmetry in chapter 5. Our focus thereby is on non-supersymmetric theories with a modified spacetime structure [6]. As we are introducing new concepts for spacetime, we also change Wigner’s notion of elementary particles.

This discussion shows that symmetries are a recurring theme in physics. Symmetries will also be the repeating and connecting topic of this thesis, which spans from gauge extensions of the Standard Model to new notions of spacetime.

Chapter 2

Minimal Extensions guided by Symmetries

In this chapter, we discuss two bottom-up extensions of the Standard Model. Our focus is thereby on theories which are decoupled from the electroweak scale, minimal, and testable with current and future experiments. We start with the discussion of the left-right symmetric theory with the minimal number of beyond the Standard Model particles which can account for Majorana neutrinos in the next section. The model was first introduced by us in [1]. The Majorana neutrino mass is generated at the one-loop level via a new singly charged scalar field. As a consequence, the theory predicts light right-handed Majorana neutrinos. The new singly charged scalar field and the light right-handed Majorana neutrinos will allow for the testability of the theory at the LHC.

We then turn from left-right symmetric theories to extensions of the Standard Model by local baryon number. The Standard Model extension by local baryon number with the least number of new fermionic multiplets was discovered in an earlier work [3] and the topic of the master thesis of the author. The new fermionic multiplets were named leptobaryons since they carry baryon and lepton number but are color singlets. In this thesis, we focus on the discussion of the phenomenology of the minimal theory of leptobaryons which is based on work published in [2]. Extending the Standard Model gauge group by gauged baryon number leads to a new stable particle. In the minimal theory of leptobaryons, we assume that the new stable particle is a neutral Majorana fermion and thus an ideal dark matter candidate. We will investigate the properties of such a dark matter candidate and make a connection to possible signals at a particle collider such as the LHC.

2.1 Minimal Left-Right Symmetric Theory

Left-right symmetric theories [62, 63, 64, 65] are based on the gauge group

$$G_{\text{LR}} = SU(3)_C \otimes SU(2)_L \otimes SU(2)_R \otimes U(1)_{B-L}. \tag{2.1}$$

We could further impose a discrete left-right parity which links $SU(2)_L$ and $SU(2)_R$ representations. Note that we could also choose charge conjugation as a discrete left-right symmetry [67]. However, to later have a viable left-right symmetric theory at low energies, we have to assume that the discrete left-right parity is explicitly broken (see section 2.1.1). The Standard Model fermions are embedded in the following representations

$$\begin{aligned} Q_L &= \begin{pmatrix} u_L \\ d_L \end{pmatrix} \sim (3,2,1,1/3)\,, \quad Q_R = \begin{pmatrix} u_R \\ d_R \end{pmatrix} \sim (3,1,2,1/3)\,, \\ \ell_L &= \begin{pmatrix} \nu_L \\ e_L \end{pmatrix} \sim (1,2,1,-1)\,, \quad \ell_R = \begin{pmatrix} \nu_R \\ e_R \end{pmatrix} \sim (1,1,2,-1)\,. \end{aligned}$$

For the electric charge, we use the convention

$$Q_{\text{EM}} = T_L^3 + T_R^3 + \frac{Y_{(B-L)}}{2}\,, \tag{2.2}$$

where $Y_{(B-L)}$ is the generator of $U(1)_{B-L}$ and T_L^3 and T_R^3 are the symmetry generators of $SU(2)_L$ and $SU(2)_R$, respectively [68].

In left-right symmetric theories, the Standard Model quarks and leptons become massive once a bi-doublet Higgs acquires a non-trivial vacuum expectation value. The bi-doublet Higgs is given in matrix notation by

$$\Phi = \begin{pmatrix} \phi_1^0 & \phi_2^+ \\ \phi_1^- & \phi_2^0 \end{pmatrix} \sim (1,2,2,0)\,.$$

If the Yukawa interactions of the bi-doublet Higgs with the Standard Model fermions are given by

$$\mathcal{L} \supset \bar{Q}_L \left(Y_1 \Phi + Y_2 \tilde{\Phi} \right) Q_R + \bar{\ell}_L \left(Y_3 \Phi + Y_4 \tilde{\Phi} \right) \ell_R + \text{h.c.}\,, \tag{2.3}$$

where $\tilde{\Phi} = \sigma_2 \Phi^* \sigma_2$, then the charged fermion masses read as

$$m_U = Y_1 v_1 + Y_2 v_2^*, \tag{2.4}$$
$$m_D = Y_1 v_2 + Y_2 v_1^*, \tag{2.5}$$
$$m_E = Y_3 v_2 + Y_4 v_1^*, \tag{2.6}$$

where v_1 and v_2 are the vacuum expectation values of the fields ϕ_1^0 and ϕ_2^0, respectively.

In this simplest scenario, neutrinos are Dirac particles with mass matrix given by

$$m_\nu^D = Y_3 v_1 + Y_4 v_2^*. \tag{2.7}$$

Nonetheless, in the region of parameter space where $v_2 \ll v_1$ and $Y_3 \ll Y_4$, we find small Dirac neutrino masses [69]. In this limit, the lepton masses approximately take the form

$$m_E \approx Y_4 v_1^*, \tag{2.8}$$

$$m_\nu^D \approx v_1 \left(Y_3 + m_E \frac{v_2^*}{|v_1|^2} \right). \tag{2.9}$$

To break the left-right symmetric theory to the Standard Model

$$SU(2)_R \otimes U(1)_{B-L} \to U(1)_Y \,,$$

additional Higgses have to be added. The left-right symmetric Higgs sector with the minimal number of additional propagating degrees of freedom which can accomplish the symmetry breaking is given by [65]

$$H_L = \begin{pmatrix} h_L^+ \\ h_L^0 \end{pmatrix} \sim (1,2,1,1) \quad \text{and} \quad H_R = \begin{pmatrix} h_R^+ \\ h_R^0 \end{pmatrix} \sim (1,1,2,1)\,.$$

The left-right symmetry is broken as H_R develops the vacuum expectation value

$$\langle H_R \rangle = \frac{1}{\sqrt{2}} \begin{pmatrix} 0 \\ v_R \end{pmatrix} \,. \tag{2.10}$$

It is thus important to acknowledge that the left-right symmetric theory with the minimal number of beyond the Standard Model particles predicts Dirac neutrinos.

However, since the neutrinos ν_R do not carry electric charge, there is the possibility that neutrinos are their own anti-particles and hence Majorana particles. This possibility is theoretically especially attractive because it is a necessary condition to have a seesaw mechanism [70, 71, 72, 73, 74]. The seesaw mechanism explains the smallness of the neutrino masses compared to the other Standard Model fermion masses. We will discuss Majorana neutrinos and different realizations of the seesaw mechanism in left-right symmetric theories in the next section.

2.1.1 Majorana Neutrinos in Left-Right Symmetric Theories

In left-right symmetric models, two tree-level realizations of Majorana neutrino masses are known. We will shortly introduce these possibilities before we propose a new radiative seesaw mechanism and show the advantages.

- **Type I and Type II seesaw mechanism:** The minimal number of left-right symmetric propagating scalar degrees of freedom which can break $SU(2)_R \otimes U(1)_{B-L}$ to $U(1)_Y$ are the previously introduced Higgs doublets H_L and H_R. However, we can also accomplish the symmetry breaking by introducing two Higgs triplets [74, 75, 76, 77, 78] instead

  $$\Delta_L \sim (1,3,1,2) \quad \text{and} \quad \Delta_R \sim (1,1,3,2)\,.$$

  We then find the following additional interactions of the Higgs triplets and Standard Model fermions

  $$\mathcal{L} \supset \lambda_\Delta \ell_L^T C i\sigma_2 \Delta_L \ell_L + \lambda_\Delta \ell_R^T C i\sigma_2 \Delta_R \ell_R + \text{h.c.}\,. \tag{2.11}$$

  Upon the general vacuum expectation value assignment

  $$\langle\Phi\rangle = \begin{pmatrix} v_1 & 0 \\ 0 & v_2 \end{pmatrix}, \quad \langle\Delta_L\rangle = \begin{pmatrix} 0 & 0 \\ v_L & 0 \end{pmatrix}, \quad \langle\Delta_R\rangle = \begin{pmatrix} 0 & 0 \\ v_R & 0 \end{pmatrix}, \tag{2.12}$$

  the neutrino mass matrix in the basis $(\nu\,\nu^c)_L$ takes the form

  $$m_\nu^{I+II} = \begin{pmatrix} 2\lambda_\Delta v_L & Y_3 v_1 + Y_4 v_2^* \\ Y_3 v_1 + Y_4 v_2^* & -2\lambda_\Delta^* v_R^* \end{pmatrix}. \tag{2.13}$$

  After diagonalizing the mass matrix m_ν^{I+II}, we find in the limit $v_R \gg v_1, v_2$ and for $v_L \to 0$ the approximate mass eigenvalues

  $$m_{\nu_L}^{I+II} \approx \lambda_\Delta \frac{f(v_1,v_2)}{v_R} + \frac{(Y_3 v_1 + Y_4 v_2^*)^2}{\lambda_\Delta v_R}\,, \tag{2.14}$$

  $$m_{\nu_R}^{I+II} \approx \lambda_\Delta v_R\,, \tag{2.15}$$

  where $f(v_1,v_2) = a(v_1^2+v_2^2) + b v_1 v_2$ with coefficients a and b functions of various scalar potential couplings. Hence, the smallness of the left-handed neutrino mass can be understood as a consequence of $v_R \gg v_1, v_2$. Heavy right-handed neutrinos are the reason for light left-handed neutrinos.

- **Type III seesaw mechanism:** In the context of the minimal consistent left-right symmetric Higgs sector with the Higgs doublets H_L and H_R, we can account for Majorana neutrinos at tree-level by introducing two fermionic triplets [79, 80]

  $$\rho_L \sim (1,3,1,0) \quad \text{and} \quad \rho_R \sim (1,1,3,0)\,.$$

The Majorana mass terms and additional Yukawa couplings are then given by

$$\begin{aligned}\mathcal{L} \supset\ & \lambda_\rho \ell_L^T C i\sigma_2 \rho_L H_L + \lambda_\rho \ell_R^T C i\sigma_2 \rho_R H_R \\ & + m_\rho \mathrm{Tr}\left(\rho_L^T C \rho_L\right) + m_\rho \mathrm{Tr}\left(\rho_R^T C \rho_R\right) + \text{h.c.}\,.\end{aligned} \tag{2.16}$$

In the basis $(\nu\, \nu^c\, \rho^c)_L$, we thus find the mass matrix

$$m_\nu^{III} = \begin{pmatrix} 0 & Y_3 v_1 + Y_4 v_2^* & 0 \\ Y_3 v_1 + Y_4 v_2^* & 0 & -\frac{1}{2\sqrt{2}}\lambda_\rho v_R \\ 0 & -\frac{1}{2\sqrt{2}}\lambda_\rho v_R & m_\rho \end{pmatrix}, \tag{2.17}$$

with the general vacuum expectation value assignment

$$\langle\Phi\rangle = \begin{pmatrix} v_1 & 0 \\ 0 & v_2 \end{pmatrix}, \quad \langle H_L\rangle = \frac{1}{\sqrt{2}}\begin{pmatrix} 0 \\ v_L \end{pmatrix}, \quad \langle H_R\rangle = \frac{1}{\sqrt{2}}\begin{pmatrix} 0 \\ v_R \end{pmatrix}, \tag{2.18}$$

where $v_R \neq v_L$ to spontaneously break the left-right symmetry. We further assume $v_L = 0$ for simplicity [64, 80]. After integrating out ρ and ρ^c, we approximately find

$$m_{\nu_L}^{III} \approx \frac{8 m_\rho (Y_3 v_1 + Y_4 v_2^*)^2}{\lambda_\rho^2 v_R^2}, \quad m_{\nu_R}^{III} \approx \frac{\lambda_\rho^2 v_R^2}{8 m_\rho}, \quad m_{\rho_R}^{III} \approx m_\rho\,. \tag{2.19}$$

To integrate out ρ and ρ^c, we assumed $m_\rho \gg v_R \gg v_1, v_2$. Again, the mass of the left-handed neutrinos is suppressed by the mass of the right-handed neutrinos. However, the right-handed neutrino mass is now also suppressed by the fermionic triplet mass.

Radiative Seesaw Mechanism

After reviewing the type I+II and III seesaw mechanism in left-right symmetric theories, we now turn to a radiative seesaw mechanism [81]. The motivation to turn from a tree-level process to a quantum loop process is Ockham's razor and the principle of minimality. Without experimental evidence, we should try to describe nature with the least number of degrees of freedom possible. By introducing an arbitrary number of specialized particles, any data can be fitted and any phenomena can be described. However, by doing so, a deeper connection between the observations is lost. As physicists it is our main objective to search for and understand these wondrous connections. We therefore rely on the minimal left-right symmetric Higgs sector which can give mass to the Standard Model fermions and further breaks the left-right symmetry

$$\Phi \sim (1,2,2,0)\,, \quad H_L \sim (1,2,1,1)\,, \quad H_R \sim (1,1,2,1)\,.$$

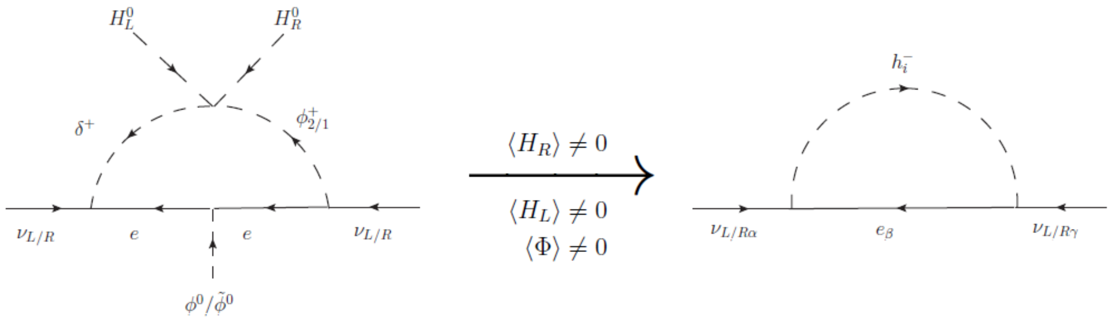

Figure 2.1: Neutrino mass generation at the quantum level.

To further generate Majorana masses for the neutrinos which allows for a seesaw mechanism, we add a singly charged scalar field [82, 1]

$$\delta^+ \sim (1, 1, 1, 2) \,.$$

Note that no new fermionic degrees of freedom are needed compared to the type III seesaw mechanism and that one scalar degree of freedom less is introduced compared to the type I+II seesaw mechanism. The relevant interactions to generate the Majorana neutrino masses are given by

$$\mathcal{L} \supset \lambda_L \ell_L \ell_L \delta^+ + \lambda_R \ell_R \ell_R \delta^+ + \lambda_1 H_L^T i\sigma_2 \Phi H_R \delta^- + \lambda_2 H_L^T i\sigma_2 \tilde{\Phi} H_R \delta^- + \text{h.c.}\,. \tag{2.20}$$

To calculate the neutrino masses at low energies, we have to transform into the broken symmetry phase. Before symmetry breaking, we find the five charged scalar fields, $\phi_1^\pm$, $\phi_2^\pm$, $h_R^\pm$, $h_L^\pm$, and $\delta^\pm$. We introduce the 5×5 rotation matrix V which diagonalizes the charged Higgs mass matrix and relates the scalar fields in the broken and unbroken symmetry phase

$$\left(\phi_1^+ \, \phi_2^+ \, h_L^+ \, h_R^+ \, \delta^+\right)^T = V \left(h_1^+ \, h_2^+ \, h_3^+ \, h_4^+ \, h_5^+\right)^T . \tag{2.21}$$

The rotation matrix V depends on the scalar couplings. The full scalar potential is given in the Appendix 7.2.

For illustration, we show the loop diagram in Figure 2.1 which generates the Majorana neutrino masses in the broken and unbroken symmetry phase. The diagram in the unbroken phase illustrates the dependence of the process on the couplings in the Lagrangian (2.20) which is hidden inside the rotation matrix V in the broken phase.

The neutrino mass matrix generated at one-loop level in the basis $(\nu\, \nu^c)_L$ then reads

$$m_\nu^{\text{1-loop}} = \begin{pmatrix} m_\nu^L & m_\nu^D \\ \left(m_\nu^D\right)^T & m_\nu^R \end{pmatrix} , \tag{2.22}$$

where

$$(m_\nu^L)^{\alpha\gamma} = \frac{1}{4\pi^2}\lambda_L^{\alpha\beta} m_{e_\beta} \sum_i \text{Log}\left(\frac{M_{h_i}^2}{m_{e_\beta}^2}\right) V_{5i}\left[(Y_3^\dagger)^{\beta\gamma}V_{2i}^* - (Y_4^\dagger)^{\beta\gamma}V_{1i}^*\right] + \alpha \leftrightarrow \gamma, \tag{2.23}$$

$$(m_\nu^R)^{\alpha\gamma} = \frac{1}{4\pi^2}\lambda_R^{\alpha\beta} m_{e_\beta} \sum_i \text{Log}\left(\frac{M_{h_i}^2}{m_{e_\beta}^2}\right) V_{5i}\left[(Y_3)^{\beta\gamma}V_{1i}^* - (Y_4)^{\beta\gamma}V_{2i}^*\right] + \alpha \leftrightarrow \gamma\,. \tag{2.24}$$

Studying the mass matrix (2.22), we learn that in the region of parameter space where $m_\nu^L, m_\nu^R \ll m_\nu^D$ we find quasi-Dirac neutrinos. This region of parameter space corresponds to small couplings λ_L and λ_R [83, 84]. Quasi-Dirac neutrinos have the unusual property of a large mixing of active and sterile neutrinos. However, in order to have a seesaw mechanism, we have to require $\lambda_L \ll \lambda_R$. We therefore assume that the discrete left-right parity is explicitly broken by the Yukawa and scalar interactions. The explicit breaking of the discrete left-right parity further avoids the domain wall problem when considering a low left-right symmetry scale [85]. If we then additionally assume that $m_\nu^D \ll m_\nu^R$, we find a low scale seesaw mechanism with masses approximately given by

$$m_{\nu_L} \approx -\left(m_\nu^D\right)^T \left(m_\nu^R\right)^{-1}\left(m_\nu^D\right) \quad \text{and} \quad m_{\nu_R} \approx m_\nu^R\,. \tag{2.25}$$

Hence, although the Majorana neutrino masses are generated at the one-loop level, we can still find a suppression of the active neutrino masses.

We can estimate the scale of the right-handed Majorana neutrino mass by noting that the sum over the charged Higgs masses weighted by the combination of mixing matrix entries and Yukawa couplings in equation (2.24) is strongly constraining the scale of the neutrino masses due to the unitarity of the mixing matrix V. There is no lower bound on the right-handed neutrino Majorana mass since the masses turn to zero when the charged Higgs masses are degenerated. However, we can infer an upper bound by assuming a conservative scenario where the couplings λ_R, Y_3, and Y_4 are of order one. We further assume a single generation for simplicity because the contribution of the tau mass dominates over the contribution of the muon and electron mass inside the loop of Figure 2.1 since $m_\tau \gg m_\mu, m_e$.

Due to the unitarity of the mixing matrix, the maximum value that the logarithms in equation (2.24) could acquire is roughly two times the largest difference between the order of magnitudes of the charged Higgs masses. We could assume the extreme case in which one charged Higgs has a mass of the order of the electroweak scale, $\mathcal{O}(10^2\text{GeV})$, and another charged Higgs has a mass of the order of the Plank scale, $\mathcal{O}(10^{19}\text{GeV})$. The upper theoretical bound for the right-handed Majorana neutrino mass would then be

$$M_\nu^R \lesssim 150\,\text{GeV}\,. \tag{2.26}$$

In a more plausible scenario, the mass scales of the charged Higgses in a low scale left-right symmetric theory are expected to be in the multi-TeV range, $\mathcal{O}(10^3 - 10^4\mathrm{GeV})$. Therefore, the estimation for a more realistic upper limit is

$$M_\nu^R \lesssim (0.4 - 0.8)\ \text{GeV}\,. \tag{2.27}$$

In summary, we find relatively light right-handed neutrinos. Hence, in order for the seesaw mechanism to still explain the smallness of the left-handed neutrino masses, we have to assume that $v_2 \ll v_1$ and $Y_3 \ll Y_4$. We therefore require already comparatively small Dirac neutrino masses m_ν^D as shown in equation (2.9). In the Appendix 7.3, we demonstrate that the separation of the vacuum expectation values, $v_2 \ll v_1$, of the bi-doublet Higgs is possible.

2.1.2 Gauge Bosons in the Minimal Left-Right Symmetric Theory

In this section, we start the discussion of the different possibilities to probe the minimal left-right symmetric theory with Majorana neutrinos. By enlarging the Standard Model gauge group G_{SM} to the left-right symmetric gauge group G_{LR}, we introduce additional gauge bosons. In order to understand the gauge symmetry structure of nature, we have to examine the gauge boson properties [64].

In left-right symmetric theories, we find the charged gauge bosons $W_R^\pm$ and a neutral gauge boson Z_{BL} in addition to the Standard Model gauge bosons. In the basis $(W_L^+ \, W_R^+)$ the charged gauge boson mass matrix reads as

$$\mathcal{M}_\pm^2 = \begin{pmatrix} \frac{g_L^2}{2}(\frac{1}{2}v_L^2 + v_1^2 + v_2^2) & -g_L g_R v_1 v_2 \\ -g_L g_R v_1 v_2 & \frac{g_R^2}{2}(\frac{1}{2}v_R^2 + v_1^2 + v_2^2) \end{pmatrix}, \tag{2.28}$$

where g_L and g_R are the gauge couplings of $SU(2)_L$ and $SU(2)_R$. We can diagonalize the mass matrix by a single rotation where the mixing angle is approximately

$$\tan(2\theta_{\text{LR}}) \approx 8\frac{g_L}{g_R}\frac{v_1 v_2}{v_R^2}. \tag{2.29}$$

In the limit $v_R \gg v_L, v_1, v_2$, we find $\theta_{\text{LR}} \to 0$ such that $W_L^\pm$ and $W_R^\pm$ do not mix and are effectively mass eigenstates. The mass of $W_R^\pm$ is then given by

$$M_{W_R} \approx \frac{g_R}{2} v_R . \tag{2.30}$$

Moreover, the mass matrix for the neutral gauge bosons in the basis $(W_L^3 \, W_R^3 \, Z_{BL})$ can be written as

$$M_0^2 = \frac{1}{4}\begin{pmatrix} 2g_L^2(\frac{1}{2}v_L^2 + v_1^2 + v_2^2) & -2g_L g_R(v_1^2 + v_2^2) & -g_L g_{BL} v_L^2 \\ -2g_L g_R(v_1^2 + v_2^2) & 2g_R^2(\frac{1}{2}v_R^2 + v_1^2 + v_2^2) & -g_R g_{BL} v_R^2 \\ -g_L g_{BL} v_L^2 & -g_R g_{BL} v_R^2 & g_{BL}^2(v_L^2 + v_R^2) \end{pmatrix}. \tag{2.31}$$

To diagonalize the 3×3 mass matrix of the neutral gauge bosons, three rotations are necessary. However, in the limit $v_L \to 0$, we can decompose these three rotations and first apply two rotations to decouple the photon. We find that the photon decouples once we apply the rotations

$$\begin{aligned} W_L^0 &= \cos(\theta_W)\, Z_L + \sin(\theta_W)\, A\,, \\ W_R^0 &= \cos(\theta_R)\, Z_R - \sin(\theta_W)\sin(\theta_R)\, Z_L + \cos(\theta_W)\sin(\theta_R)\, A\,, \\ Z_{BL}^0 &= -\sin(\theta_R)\, Z_R - \sin(\theta_W)\cos(\theta_R)\, Z_L + \cos(\theta_W)\cos(\theta_R)\, A\,, \end{aligned}$$

where we defined $\tan(\theta_R) = g_{BL}/g_R$ and the Weinberg angle is given by $\tan(\theta_W) = g_Y/g_L$. In this scenario, the gauge coupling of the Standard Model hypercharge is defined as

$$g_Y = \frac{g_{BL} g_R}{\sqrt{g_{BL}^2 + g_R^2}} \,. \tag{2.32}$$

In the $(Z_R \; Z_L \; A)$ basis the mass matrix is now given by

$$M_0^2 = \begin{pmatrix} M_{RR}^2 & M_{LR}^2 & 0 \\ M_{LR}^2 & M_{LL}^2 & 0 \\ 0 & 0 & 0 \end{pmatrix} , \tag{2.33}$$

with

$$M_{RR}^2 = \frac{v_R^2}{4}\left(g_{BL}^2 + g_R^2\right) + (v_1^2 + v_2^2)\,\frac{g_R^4}{2(g_{BL}^2 + g_R^2)} \,, \tag{2.34}$$

$$M_{LR}^2 = -(v_1^2 + v_2^2)\,\frac{g_R^2\sqrt{g_L^2 g_R^2 + g_{BL}^2(g_L^2 + g_R^2)}}{2(g_{BL}^2 + g_R^2)} \,, \tag{2.35}$$

$$M_{LL}^2 = (v_1^2 + v_2^2)\,\frac{g_L^2 g_R^2 + g_{BL}^2(g_L^2 + g_R^2)}{2(g_{BL}^2 + g_R^2)} \,. \tag{2.36}$$

We can further diagonalize the 2×2 submatrix by a single rotation. We define the mixing angle by

$$\tan(2\theta_{BL}) \approx -\frac{4 g_R^2 \sqrt{g_L^2 g_R^2 + g_{BL}^2(g_L^2 + g_R^2)}}{(g_{BL}^2 + g_R^2)^2}\,\frac{v_1^2 + v_2^2}{v_R^2} \,. \tag{2.37}$$

In the limit $v_R^2 \gg v_1^2 + v_2^2$, the mixing angle θ_{BL} vanishes and thus Z_L and Z_R do not mix. Electroweak precision tests constrain the mixing angle θ_{BL} to be smaller than 10^{-3} and thus the limit $v_R^2 \gg v_1^2 + v_2^2$ seems to be realized in nature [86]. The Z' mass in this limit is then given by

$$M_{Z'} \simeq \frac{\sqrt{g_{BL}^2 + g_R^2}}{g_R} M_{W_R} \overset{g_L = g_R}{\simeq} 1.2\, M_{W_R} \,, \tag{2.38}$$

where $g_L = g_R$ is a reasonable assumption because we expect the gauge couplings to be identical at the left-right symmetry scale. Only for $g_L = g_R$ are the left- and right-handed interactions identical at the left-right symmetry scale. The current limit on the new charged gauge boson mass $M_{W_R} \gtrsim 3$ TeV [67, 87, 88, 89] therefore translates into a limit on the new neutral gauge boson mass $M_{Z'} \gtrsim 3.6$ TeV.

The new heavy gauge bosons can decay to all Standard Model fermions. Additionally, they can also decay to the right-handed neutrinos in the minimal left-right symmetric theory with Majorana neutrinos because the right-handed neutrino mass is of order $\mathcal{O}(1\,\text{GeV})$ as was derived in the previous section. The new charged gauge boson W_R^+ decays as

$$W_R^+ \to \overline{q_d} q_u ,\; \bar{e}\nu_L ,\; \bar{e}\nu_R \,, \tag{2.39}$$

where generation and flavor indices are implicit and $q_d \in \{d, s, b\}$ and $q_u \in \{u, c, t\}$. The decays of the new neutral gauge boson $Z^{'}$ are

$$Z^{'} \to \bar{q}q, \bar{e}e, \overline{\nu_L}\nu_L, \overline{\nu_R}\nu_R, \delta^+\delta^- \,, \tag{2.40}$$

where again the generation and flavor indices are implicit. Note that in left-right symmetric theories with Higgs triplets the right-handed neutrinos ν_R are mostly considered to be heavy to realize the type I+II seesaw mechanism [74, 78]. As a consequence, the gauge bosons cannot decay to right-handed neutrinos ν_R. The minimal left-right symmetric theory with Majorana neutrinos therefore predicts a larger leptonic branching ratio compared to such a scenario.

The partial decay widths of W_R^+ are given in the Appendix 7.1.1. We find

$$\text{BR}(W_R^+ \to \overline{q_d}q_u) \simeq 60\% \,, \quad \text{BR}(W_R^+ \to \bar{e}\nu_L) \simeq 20\% \,, \quad \text{BR}(W_R^+ \to \bar{e}\nu_R) \simeq 20\% \,,$$

for the branching ratios. Comparing these results to the standard left-right symmetric theory with Higgs triplets and heavy Majorana neutrino masses

$$\text{BR}(W_R^+ \to \overline{q_d}q_u) \simeq 75\% \,, \quad \text{BR}(W_R^+ \to \bar{e}\nu_L) \simeq 25\% \,,$$

we can distinguish the two theories by measuring the baryonic branching of the new right-handed charged current.

In Figure 2.2, we show the total width and the leptonic width of the charged gauge boson W_R^+ as a function of M_{W_R}. The solid lines allow for the decay $W_R^+ \to \bar{e}\nu_R$, whereas the dashed lines do not. By measuring $\Gamma_{W_R}^{\text{tot}}$ to more than 25% accuracy, we can experimentally verify if the decay $W_R^+ \to \bar{e}\nu_R$ is kinematically allowed. To clarify, if the decay $W_R^+ \to \bar{e}\nu_R$ was discovered, we could not conclude that the minimal left-right symmetric theory with Majorana neutrinos was realized in nature. However, the minimal left-right symmetric theory with Majorana neutrinos predicts light right-handed neutrinos and thus $W_R^+ \to \bar{e}\nu_R$ is a necessary condition for the theory to be realized in nature.

The partial decay widths of $Z^{'}$ are again given in the Appendix 7.1.2. We find for the branching

$$\begin{aligned}&\text{BR}(Z^{'} \to \bar{q}q) \simeq 90.5\% \,, \quad \text{BR}(Z^{'} \to \bar{e}e) \simeq 7.4\% \,, \quad \text{BR}(Z^{'} \to \overline{\nu_L}\nu_L) \simeq 0.1\% \,, \\ &\text{BR}(Z^{'} \to \overline{\nu_R}\nu_R) \simeq 0.1\% \,, \quad \text{BR}(Z^{'} \to \delta^+\delta^-) \simeq 1.8\% \,.\end{aligned}$$

The baryonic decays dominate the width of the $Z^{'}$. Changes in the leptonic branching will change the total width negligibly such that it is difficult to distinguish experimentally if the decays $Z^{'} \to \overline{\nu_R}\nu_R$ are kinematically allowed or forbidden.

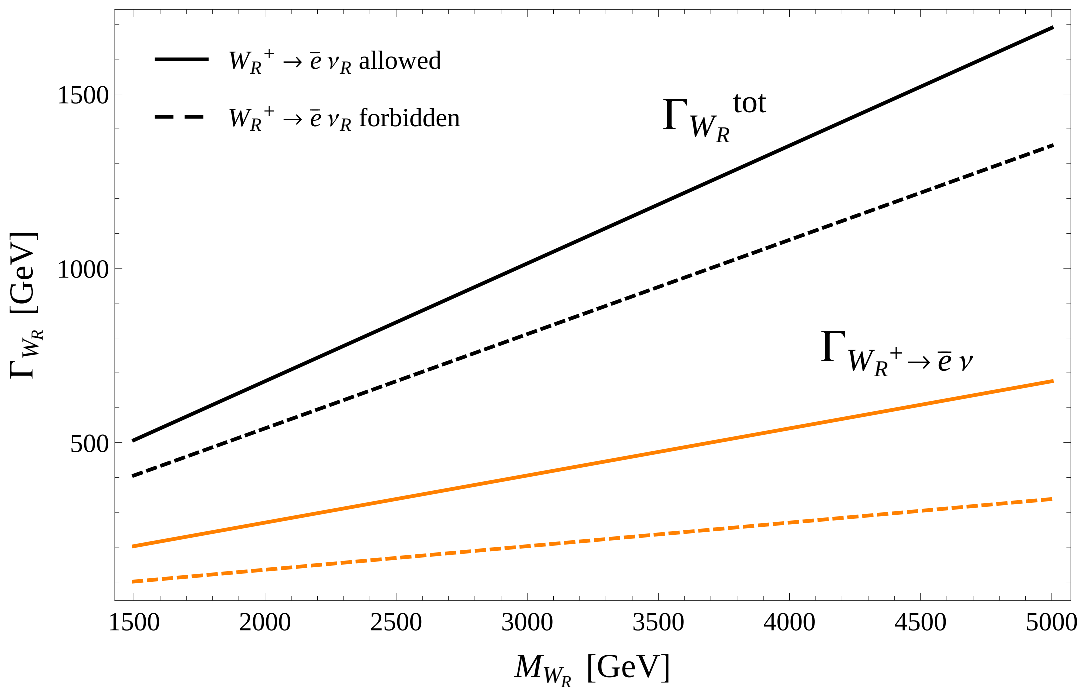

Figure 2.2: Total and leptonic width of W_R^+ as a function of M_{W_R}. The solid lines correspond to the discussed minimal left-right symmetric model with Majorana neutrinos where $W_R^+ \to \bar{e}\nu_R$ is allowed and the dashed lines to the standard left-right symmetric theories where $W_R^+ \to \bar{e}\nu_R$ is forbidden.

2.1.3 Minimal Left-Right Symmetric Theory at the LHC

We have introduced the minimal left-right symmetric theory with Majorana neutrinos and have studied the theoretical properties. Now, we have to ask: How can we test this theory?

In the last section, we already compared the branching ratios of the new heavy gauge bosons $W_R^\pm$ and $Z^{'}$ in the minimal left-right symmetric theory with Majorana neutrinos to the standard left-right symmetric theory with Higgs triplets and heavy right-handed neutrinos. However, since the leptonic decays are subdominant, the partial widths of the new heavy gauge bosons $W_R^\pm$ and $Z^{'}$ would have to be measured very precisely to discriminate the models.

As the theory predicts Majorana neutrinos, it breaks lepton number by two units. The standard LHC signature of lepton number violation by two units in left-right symmetric theories is same-sign dileptons with two accompanying jets [90]. However, since the minimal left-right symmetric theory with Majorana fermions predicts light right-handed Majorana neutrinos the decay length of ν_R is too large to observe such total lepton number violation at the LHC [67, 91]. These long decay lengths are however an opportunity for the future SHiP experiment at CERN [92]. SHiP will be able to test the interesting region of GeV right-handed neutrinos ν_R and TeV right-handed currents W_R. Neutrinoless double beta decay which is an experimental test of lepton number violation by two units is unfortunately also suppressed for light right-handed Majorana neutrinos [93].

Nevertheless, we can search for the family lepton number violation of δ^+ at the LHC. The charged scalar singlet δ^+ which generates the Majorana neutrino mass at the quantum level violates family lepton number via the couplings $\lambda_L \ell_L \ell_L \delta^+$ and $\lambda_R \ell_R \ell_R \delta^+$ in the Lagrangian (2.20). We can produce the charged scalar singlet δ^+ at the LHC via the Drell-Yan process

$$pp \to \gamma, Z, Z^{'} \to \delta^+ \delta^- \,.$$

The charged scalar singlet δ^+ mixes with the other singly charged scalars Φ_1^+, Φ_2^+, h_L^+ and h_R^+ of the theory. Due to this mixing the charged scalar singlet δ^+ could not only decay to leptons, but also to quarks. However, since the couplings $\lambda_1 H_L^T i\sigma_2 \Phi H_R \delta^-$ and $\lambda_2 H_L^T i\sigma_2 \tilde{\Phi} H_R \delta^-$ which are responsible for the mixing of the charged scalar degrees of freedom also enter the generation of the Majorana neutrino mass, we expect the couplings λ_1 and λ_2 to be small and thus the mixing to be small. As a consequence, the charged scalar singlet δ^+ will dominantly decay leptonically. At the LHC, we can then search for the process

$$pp \to \gamma, Z, Z^{'} \to \delta^+ \delta^- \to e_i^+ e_j^- E_T^{\text{miss}} \,.$$

The only Standard Model background which can mimic two leptons of different flavor and missing transverse energy in the final state is WW production where subsequently the Standard Model W decays leptonically. However, we can evade this background by applying a cut on the charged leptons transverse momentum p_T^e where we require $p_T^e > M_W$ [94].

The partonic production cross section of the charged scalar singlet is given by

$$\sigma(\bar{q}q \to \delta^+\delta^-)(\hat{s}) = \frac{N_C(\hat{s} - 4M_\delta^2)^{\frac{3}{2}}}{12\pi\sqrt{\hat{s}}} \left(|V^q|^2 + |A^q|^2\right) , \tag{2.41}$$

with

$$V^q = \frac{e^2 Q^q}{\hat{s}} + \frac{V_Z^q a_Z}{\hat{s} - M_Z^2 + i\Gamma_Z M_Z} + \frac{V_{Z'}^q a_{Z'}}{\hat{s} - M_{Z'}^2 + i\Gamma_{Z'} M_{Z'}} , \tag{2.42}$$

$$A^q = \frac{A_Z^q a_Z}{\hat{s} - M_Z^2 + i\Gamma_Z M_Z} + \frac{A_{Z'}^q a_{Z'}}{\hat{s} - M_{Z'}^2 + i\Gamma_{Z'} M_{Z'}} . \tag{2.43}$$

We defined $\hat{s} = s\tau$ as the partonic center-of-mass energy and N_C as the number of colors in the Standard Model. Furthermore, Γ_Z is the total decay width of the Z boson and $\Gamma_{Z'}$ the total decay width of $Z^{'}$. The Feynman rules which define the couplings in equation (2.42) and (2.43) are given in the Appendix 7.4. The hadronic cross section at a proton-proton collider with center-of-mass energy s can then be computed by evaluating

$$\sigma(pp \to \delta^+\delta^-)(s) = \int_{\tau_0}^{1} \mathrm{d}\tau \frac{\mathrm{d}\mathcal{L}_{\bar{q}q}^{pp}}{\mathrm{d}\tau} \sigma(\bar{q}q \to \delta^+\delta^-)(\hat{s}) , \tag{2.44}$$

with the parton luminosity defined as

$$\frac{\mathrm{d}\mathcal{L}_{\bar{q}q}^{pp}}{\mathrm{d}\tau} = \int_{\tau_0}^{1} \frac{\mathrm{d}x}{x} \left[f_{\bar{q}/p}(x,\mu)\, f_{q/p}\left(\frac{\tau}{x},\mu\right) + f_{\bar{q}/p}\left(\frac{\tau}{x},\mu\right) f_{q/p}(x,\mu) \right] , \tag{2.45}$$

and threshold $\tau_0 = 4M_\delta^2/s$.

In Figure 2.3, we show the $\delta^+\delta^-$ production cross section at the LHC with center-of-mass energy $\sqrt{s} = 13$ TeV as a function of the charged scalar singlet mass M_δ. We used the MSTW 2008 proton distribution functions [95] to calculate the hadronic cross section. As the theory approaches the resonant regime $M_{Z'} \sim 2M_\delta$, the $\delta^+\delta^-$ production cross section increases significantly and makes the theory testable at the LHC.

We can further calculate the number of events expected for the final state $e_i^+ e_j^- E_T^{\text{miss}}$

$$N(pp \to e_i^+ e_j^- E_T^{\text{miss}}) = \sigma(pp \to \delta^+\delta^-)\, \text{BR}(\delta^+ \to \overline{e_i}\nu)\, \text{BR}(\delta^- \to \bar{\nu} e_j)\, \mathcal{L} , \tag{2.46}$$

where $\mathcal{L}$ is the measured luminosity. Figure 2.4 shows isocurves of number of events $N(pp \to e_i^+ e_j^- E_T^{\text{miss}})$ at a proton-proton collider with $\sqrt{s} = 13$ TeV and $\mathcal{L} = 50$ fb^{-1}. We observe that for $M_\delta < 800$ GeV and a leptonic branching BR$(\delta^+ \to \bar{e}\nu) > 0.6$, we would be able to detect more than 100 events.

We also show contours of constant expected number of events of $pp \to e_i^+ e_j^- E_T^{\text{miss}}$ in the $M_\delta - M_{Z'}$ mass plane in Figure 2.5. As the mass of the charged scalar singlet M_δ decreases, the number of observed events becomes more and more independent of the neutral gauge boson mass $M_{Z'}$. This is due to the fact that the $\delta^+\delta^-$ production is now dominantly mediated by the Standard Model gauge bosons Z and γ. If the charged scalar

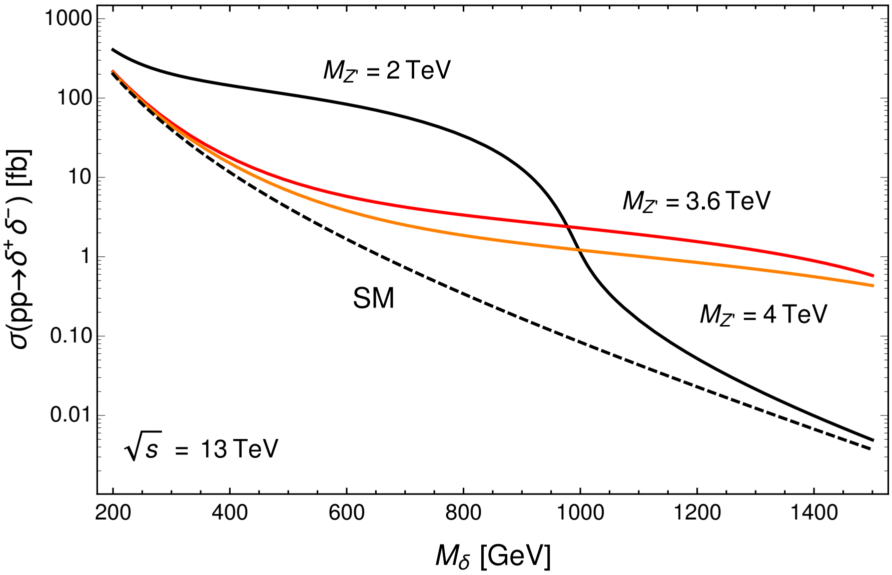

Figure 2.3: The $\delta^+\delta^-$ production cross section at a proton-proton collider with center-of-mass energy $\sqrt{s} = 13$ TeV as a function of M_δ.

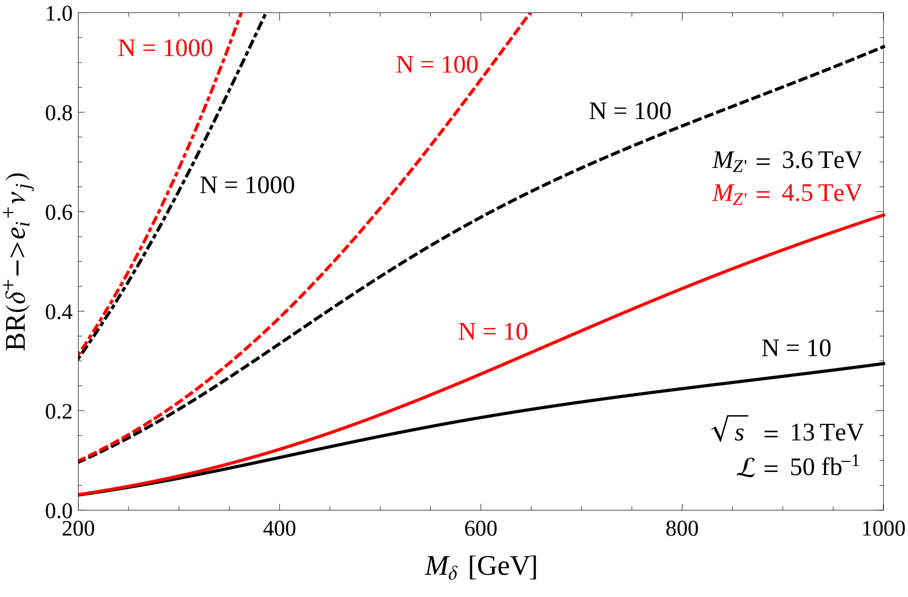

Figure 2.4: Contours of the expected number of events of the process $pp \to e_i^+ e_j^- E_T^{\text{miss}}$ at a proton-proton collider with $\sqrt{s} = 13$ TeV and collected luminosity $\mathcal{L} = 50$ fb^{-1}. Black lines correspond to $M_{Z'} = 4.5$ TeV and red lines represent $M_{Z'} = 3.6$ TeV.

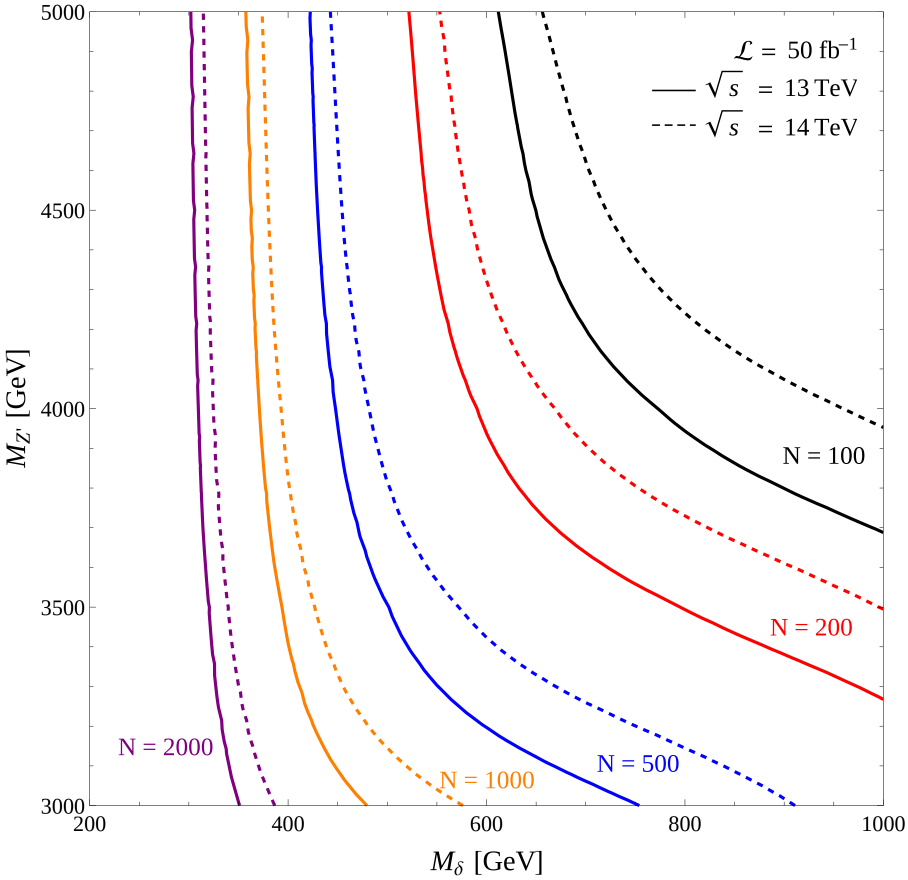

Figure 2.5: Contours of expected number of events of $pp \to e_i^+ e_j^- E_T^{\text{miss}}$ at a proton-proton collider in the $M_\delta - M_{Z'}$ mass plane.

singlet is heavy, $M_\delta > 800$ GeV, the neutral gauge boson mass has to be below 4 TeV to have a sizable number of events at the LHC with a collected luminosity of $\mathcal{L} = 50$ fb^{-1}. The rise in the number of events for $M_{Z'} < 4$ TeV is due to the Z' resonance in the production cross section $\sigma(pp \to \delta^+\delta^-)$ (see Figure 2.3).

2.1.4 Summary

In this section, we discussed left-right symmetric theories. We first stressed the fact that the left-right symmetric theory with the minimal number of propagating degrees of freedom predicts Dirac neutrinos. However, to realize the appealing idea of Majorana fermions, we introduced the minimal left-right symmetric theory with Majorana neutrinos. The left-right symmetry G_{LR} is broken to the Standard Model gauge symmetry G_{SM} by the Higgs doublet H_R. Furthermore, the Majorana neutrino masses are generated at the one-loop level via a new singly charged scalar field $\delta^{\pm}$. Strikingly, the theory predicts light right-handed Majorana neutrinos.

As a consequence, the decay channel $W_R^+ \to \bar{e}\nu_R$ is open and the leptonic branching ratio of W_R is larger as compared to the standard left-right symmetric theory with Higgs triplets and heavy right-handed neutrinos. Due to the light right-handed Majorana neutrinos, the usual searches for lepton number violation by two units at the LHC are inapplicable as the decay length of ν_R is too long. The charged scalar singlet $\delta^{\pm}$ however also induces family lepton number violation. We can probe the family lepton number violation at the LHC by searching for the process $pp \to \delta^+\delta^- \to e_i^+ e_j^- E_T^{\text{miss}}$. The lepton flavor violation can also be tested in rare processes such as $\mu \to e\gamma$ and $\mu \to e$ conversion, as discussed in [96]. For more details on the minimal left-right symmetric theory with Majorana neutrinos the interested reader is directed to the master thesis of Clara Murgui [97].

2.2 Minimal Theory of Leptobaryons

Baryon and lepton number are accidental global symmetries of the Standard Model of particle physics. However, when considering a theory which combines the three fundamental forces of the Standard Model with gravity, it is assumed that these global symmetries are broken [98, 99]. If a black hole carries the global baryon charge Q_{B}, it will still carry the global baryon charge Q_{B} after Hawking radiation [100, 101] shrank the black hole to a quantum black hole of Planck scale size. However, the upper bound of the Bekenstein entropy limits the amount of information a black hole of a given size can carry [102, 103]. If Q_{B} is therefore a large quantity, which we would assume since a collapsing star consists dominantly of baryonic matter, the information provided by Q_{B} violates the Bekenstein entropy bound [104]. We would therefore conclude that there are no global symmetries in a theory of quantum gravity.

We further observe experimentally that the proton is an extremely stable particle where the current lower bounds on the proton lifetime are of the order $\tau_p \gtrsim \mathcal{O}(10^{34}\text{ yrs.})$ [105]. Conventional Grand Unified Theories (GUTs) such as $SU(5)$ and $SO(10)$ generically predict proton decay [106, 107, 108, 109] by combining baryons and leptons in the same multiplets. As a consequence, these theories can only be realized at extremely high scales. The energy scale of GUTs is considered to be $M_{\mathrm{GUT}} \sim 10^{14-16}$ GeV. As a result, no new physics is expected between the electroweak scale ($\sim 10^2$ GeV) and the GUT scale ($\sim 10^{14-16}$ GeV). This paradigm is known as the great desert [110].

We intent to change this frustrating picture by stabilizing the proton similarly to how the electron is stabilized by electrodynamics. Consequently, we introduce two new fundamental interactions. We promote the global baryonic and leptonic symmetries to local symmetries [111, 112, 113, 114, 3]

$$G_{BL} = SU(3)_C \otimes SU(2)_L \otimes U(1)_Y \otimes U(1)_B \otimes U(1)_\ell \,. \tag{2.47}$$

Ad hoc, this theory is not anomaly free. In the Standard Model with three right-handed neutrinos ν_R, we still find the non-vanishing anomalies [111]

$$\begin{aligned} \mathcal{A}(SU(2)_L^2 \otimes U(1)_B) = \frac{3}{2}\,, \quad \mathcal{A}(U(1)_Y^2 \otimes U(1)_B) = -\frac{3}{2}\,, \\ \mathcal{A}(SU(2)_L^2 \otimes U(1)_\ell) = \frac{3}{2}\,, \quad \mathcal{A}(U(1)_Y^2 \otimes U(1)_\ell) = -\frac{3}{2}\,. \end{aligned} \tag{2.48}$$

New fermionic degrees of freedom in addition to the three right-handed neutrinos ν_R have to be introduced to the Standard Model to cancel these anomalies. The minimal number of new multiplets required to have a consistent gauge theory is four. These new fields are called "leptobaryons" [3] since they carry baryon and lepton number but no color and are given by

$$\begin{aligned} \Psi_L \sim (1, 2, 1/2, 3/2, 3/2)\,, \quad \Psi_R \sim (1, 2, 1/2, -3/2, -3/2)\,, \\ \Sigma_L \sim (1, 3, 0, -3/2, -3/2)\,, \quad \chi_L \sim (1, 1, 0, -3/2, -3/2)\,. \end{aligned} \tag{2.49}$$

Apart from the photon and the gluon we do not observe any other massless gauge boson. The gauge groups $U(1)_B$ and $U(1)_\ell$ are therefore broken by the Higgs-Englert mechanism [13, 14, 15]. The two additional scalar fields are denoted by

$$H_{\text{B}} \sim (1,1,0,3,3) \quad \text{and} \quad H_{\text{L}} \sim (1,1,0,0,2)\,, \tag{2.50}$$

with the vacuum expectation values defined as

$$\langle H_{\text{B}} \rangle = \frac{v_{\text{B}}}{\sqrt{2}} \quad \text{and} \quad \langle H_{\text{L}} \rangle = \frac{v_{\text{L}}}{\sqrt{2}}\,. \tag{2.51}$$

It is important to note that in this minimal model, the baryon numbers of the leptobaryons and H_{B} are completely determined and there is no freedom in choosing the baryonic charge as in contrast to the model proposed in [114].

The most general interactions of the leptobaryons are

$$\begin{aligned} -\mathcal{L} \;\supset\; & h_1 \bar{\Psi}_R H \chi_L + h_2 H^\dagger \Psi_L \chi_L + h_3 H^\dagger \Sigma_L \Psi_L + h_4 \bar{\Psi}_R \Sigma_L H \\ & + y_\Psi\, \bar{\Psi}_R \Psi_L H_{\text{B}}^* + y_\chi\, \chi_L \chi_L H_{\text{B}} + y_\Sigma \,\text{Tr}\, \Sigma_L^2 H_{\text{B}} \\ & + Y_\nu\, \ell_L H \nu^c + \lambda_R\, \nu^c \nu^c H_{\text{L}} \;+\; \text{h.c.}, \end{aligned} \tag{2.52}$$

where the right-handed neutrinos are denoted by $\nu^c = (\nu_R)^c$ and the Standard Model Higgs is given by $H \sim (1,2,1/2,0,0)$. The baryonic gauge boson Z_{B} acquires the mass

$$M_{Z_{\text{B}}} = 3 g_{\text{B}} v_{\text{B}}\,, \tag{2.53}$$

upon the spontaneous breaking of $U(1)_{\text{B}}$. The mass of the leptobaryons is given by

$$m_{\Psi,\Sigma,\chi} = \frac{y_{\Psi,\Sigma,\chi}}{\sqrt{2}} v_{\text{B}}\,, \tag{2.54}$$

for negligible couplings $h_1, h_2, h_3, h_4 \to 0$. We will comment on the naturalness of this limit in section 2.2.1.

We have motivated gauging baryon number by stabilizing the proton and thus explaining the huge lower bound on the proton lifetime. However, since no long-range baryonic interactions are observed, the gauge symmetry has to be broken. Thus, we have to make sure that we do not reintroduce proton decay. The baryonic scalar field H_{B} which breaks local baryon number spontaneously carries baryon charge $B_{H_{\text{B}}} = 3$ and therefore only introduces $\Delta B = \pm 3$ interactions. The first higher order operator which mediates proton decay is hence given by

$$\mathcal{O}_{\text{proton}} = \frac{c_{\text{B}}}{\Lambda_{\text{B}}^{15}} (Q_L Q_L Q_L \ell_L)^3 H_{\text{B}}^*\,. \tag{2.55}$$

Due to the enormous suppression of Λ_{B}^{-15}, we can break local baryon number at the electroweak scale and still be in agreement with the measured bounds on the proton lifetime.

Note that we gauged baryon and lepton number. By adding three right-handed neutrinos ν_R to the Standard Model, we symmetrized the anomalies in equation (2.48). Thus, by constructing a consistent anomaly free theory for baryon number, we automatically construct a consistent anomaly free theory for lepton number by assigning the same lepton number as baryon number to the new fermions. In the following, we will assume that $U(1)_\ell$ is broken at a higher scale than $U(1)_\mathrm{B}$ hence that $v_\mathrm{L} \gg v_\mathrm{B}$. As a consequence, we neglect the new heavy gauge boson Z_L associated with the broken $U(1)_\ell$ gauge symmetry and the leptonic scalar H_L. Gauged lepton number was studied in [115, 116].

Baryon Asymmetry with Gauged Baryon Number

It is puzzling that there is more matter than anti-matter in the Universe. During the Big Bang and inflation matter and anti-matter should have been created in the same amounts and all dependence on the initial conditions washed out. Sakharov discovered very early three necessary conditions [117] to create the observed matter anti-matter asymmetry in the Universe:

1. Departure from thermal equilibrium,
2. C and CP violation,
3. Baryon number violation.

How can we satisfy the third condition when promoting baryon number to a local symmetry?

By assuming that $U(1)_\ell$ is broken at a higher scale than $U(1)_\mathrm{B}$, we can create an initial $(B-L)$ asymmetry in the early Universe via the decays of the heavy right-handed neutrinos ν_R. This mechanism is also known in leptogenesis [118, 119]. The non-perturbative Standard Model sphaleron process is modified due to the new gauge symmetry and the presence of additional fermions with non-trivial $SU(2)_L$ charge. The 't Hooft vertex takes the form

$$\mathcal{O}_{\text{'t Hooft}} = (Q_L Q_L Q_L \ell_L)^3 \bar{\Psi}_R \Psi_L \Sigma_L^4 \,. \tag{2.56}$$

The modified sphalerons which conserve baryon number transfer the initial $(B-L)$ asymmetry to a final baryon asymmetry in the early Universe. The transfer coefficient was calculated in [3] which was part of the author's master thesis

$$\Delta B_f^{\mathrm{SM}} = \frac{32}{99} \Delta(B-L)_{\mathrm{SM}} \approx 0.32\, \Delta(B-L)_{\mathrm{SM}} \,, \tag{2.57}$$

where $\Delta(B-L)_{\mathrm{SM}}$ is the initial $(B-L)$ asymmetry and ΔB_f^{SM} is the final baryon number asymmetry. To compare, the known Standard Model transfer coefficient which is given by [120]

$$\Delta B_f^{\mathrm{SM}} = \frac{28}{79} \Delta(B-L)_{\mathrm{SM}} \approx 0.35\, \Delta(B-L)_{\mathrm{SM}} \,, \tag{2.58}$$

differs only slightly.

Electroweak Observables of Gauged Baryon Number

As in any new theory, we have to make sure that the proposed new particles are not in conflict with the existing precision measurements of the Standard Model. The electroweak oblique parameters [121, 122] for example quantify corrections to the electroweak gauge boson propagators due to new physics. The decoupling theorem however states [123] that new vector-like fermions contribute to the oblique parameters as $1/\Lambda_{\text{BSM}}^2$, where Λ_{BSM} is the mass scale of the new vector-like fermions. For vanishing Yukawa couplings to the Standard Model Higgs ($h_1, h_2, h_3, h_4 \to 0$) the leptobaryons become vector-like such that contributions to the electroweak oblique parameters are negligible [124]. See section 2.2.1 for a comment on the naturalness of this limit.

We further assume that there is no kinetic mixing of Z_{B}^μ and B^μ. Hence, there are no corrections to the electroweak ρ-parameter which measures the relative strength of charged and neutral currents in the Standard Model [125].

The scalar potential for H and H_{B} is given by

$$\begin{aligned} V(H, H_{\text{B}}) = &- \mu^2 H^\dagger H + \lambda (H^\dagger H)^2 - \mu_B^2 H_{\text{B}}^* H_{\text{B}} \\ &+ b(H_{\text{B}}^* H_{\text{B}})^2 + a H^\dagger H H_{\text{B}}^* H_{\text{B}} \,. \end{aligned} \tag{2.59}$$

The portal term $aH^\dagger H H_{\text{B}}^* H_{\text{B}}$ introduces a mixing of the Standard Model Higgs H and the baryonic Higgs H_{B}. Constraints on the signal strength measurements of the Standard Model Higgs at the LHC [126] give

$$|\theta| \lesssim 0.35 \,, \tag{2.60}$$

where θ is the mixing angle of H and H_{B}. The mixing angle θ is defined as

$$\begin{pmatrix} h' \\ h'_{\text{B}} \end{pmatrix} = \begin{pmatrix} \cos\theta & \sin\theta \\ -\sin\theta & \cos\theta \end{pmatrix} \begin{pmatrix} h \\ h_{\text{B}} \end{pmatrix}, \quad \text{where} \quad -\tfrac{\pi}{4} < \theta < \tfrac{\pi}{4} \,, \tag{2.61}$$

with

$$\begin{aligned} H^T &= \left(h^\pm,\, \tfrac{1}{\sqrt{2}}(v + h' + i\phi^0)\right), \\ H_{\text{B}} &= \tfrac{1}{\sqrt{2}}(v_{\text{B}} + h'_{\text{B}} + i\phi_{\text{B}}) \,, \end{aligned} \tag{2.62}$$

and $v = 246$ GeV [127].

We will assume a small mixing angle for our phenomenological study to be consistent with the LHC constraint (2.60). Because the mixing angle is derived from the marginal operator $H^\dagger H H_{\text{B}}^* H_{\text{B}}$ it is only logarithmically sensitive to UV physics. In the low energy leptobaryon theory considered here, radiative corrections at the one-loop level are proportional to itself. The independent renormalization begins at the two-loop level with the process shown in Figure 2.6. We conclude that it is reasonable to consider small mixing of H and H_{B} and that it is further stable against quantum corrections.

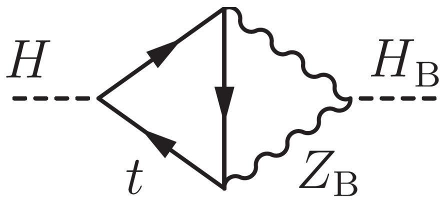

Figure 2.6: Quantum loop contributing to the Higgs mixing angle θ.

Leptobaryon Mass Bound

As is well known in the literature, the top quark potentially destabilizes the vacuum of the Standard Model Higgs because the top quark is heavier than the Standard Model Higgs [128]. Similarly, the leptobaryons will destabilize the scalar potential in the direction of H_B if the mass scale of the leptobaryons is much larger than the mass of H_B.

We approximate this effect by solving the one-loop $\overline{\mathrm{MS}}$ renormalization group equation for the quartic baryonic Higgs self-coupling

$$\mu\frac{\mathrm{d}b}{\mathrm{d}\mu} = \frac{1}{16\pi^2}\big[-4y_\psi^4 - 3y_\Sigma^4 - y_\chi^4 + 2a^2 + 486g_\mathrm{B}^4 \\ + 2b(-54g_\mathrm{B}^2 + 4y_\psi^2 + 3y_\Sigma^2 + y_\chi^2) + 20b^2\big]\,, \quad (2.63)$$

with the initial conditions at the scale $\mu_0 = (M_{H_\mathrm{B}} + M_{Z_\mathrm{B}})/2$ taking the form

$$y_{\Psi,\Sigma,\chi} = 3\sqrt{2}g_\mathrm{B}\frac{m_{\Psi,\Sigma,\chi}}{M_{Z_\mathrm{B}}} \quad \text{and} \quad b_0 = \frac{9g_\mathrm{B}^2}{2}\frac{M_{H_\mathrm{B}}^2}{M_{Z_\mathrm{B}}^2}\,. \quad (2.64)$$

We now demand self-consistency on the theory by requiring that the quartic self-coupling b does not become negative at mass scales below the leptobaryon masses $m_{\Psi,\Sigma,\chi}$ [2].

To derive an upper bound on the leptobaryon masses $m_{\Psi,\Sigma,\chi}$, we simplify the differential equation (2.63) by assuming that the leptobaryon masses are degenerate, $y_\Psi = y_\Sigma = y_\chi$, and by neglecting the running of all other couplings in equation (2.63). This is justified by the low scale at which the quartic self-coupling b becomes negative. We then find

$$\mu\frac{\mathrm{d}b}{\mathrm{d}\mu} \simeq -\frac{1}{2\pi^2}y_\Psi^4\,, \quad (2.65)$$

which we can solve for the condition $b(\mu = m_{\Psi,\Sigma,\chi}) = 0$. The quartic self-coupling of the baryonic Higgs b thus vanishes at the mass scale of the leptobaryons for

$$m_{\Psi,\Sigma,\chi} = \sqrt{\frac{\pi M_{Z_\mathrm{B}} M_{H_\mathrm{B}}}{3g_\mathrm{B}}\frac{1}{W(x)^{\frac{1}{4}}}} \quad \text{with} \quad x = \frac{16\pi^2 M_{Z_\mathrm{B}}^2 M_{H_\mathrm{B}}^2}{9g_\mathrm{B}^2(M_{H_\mathrm{B}} + M_{Z_\mathrm{B}})^4}\,, \quad (2.66)$$

where $W(x)$ is the Lambert W function. The Lambert W function is bounded from above,

$W(x) \lesssim 2$ for $x \lesssim 20$, such that we find the theoretical upper bound

$$m_{\Psi,\Sigma,\chi} \lesssim 0.86\sqrt{\frac{M_{Z_\mathrm{B}} M_{H_\mathrm{B}}}{g_\mathrm{B}}}\,, \tag{2.67}$$

on the leptobaryon masses to have a stable vacuum. We can infer from equation (2.67) that the leptobaryon masses should be of the same order of magnitude as the baryonic gauge boson mass M_{Z_B} and the baryonic Higgs mass M_{H_B} unless the gauge coupling g_B is extremely small.

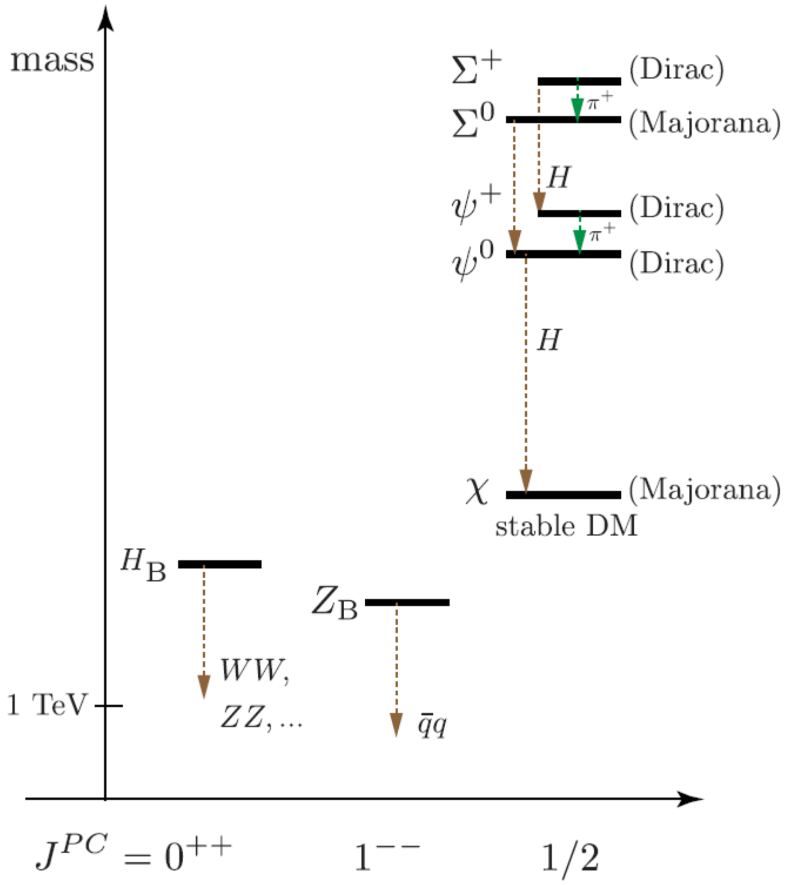

Figure 2.7: Mass spectrum of the minimal theory of leptobaryons considered in this study.

2.2.1 Leptobaryons as Dark Matter

Apart from solving the consistency problems of global baryon number and theories of quantum gravity, the minimal theory of leptobaryons has the advantage of introducing a dark matter candidate in addition to stabilizing the proton. Analyzing the Lagrangian in equation (2.52), we observe that after breaking $U(1)_\mathrm{B}$ spontaneously there still remains a remnant Z_2 symmetry in the leptobaryon sector

$$(Z_2)_\mathrm{DM} : \Psi \to -\Psi \,, \quad \overline{\Psi} \to -\overline{\Psi} \,, \quad \vec{\Sigma} \to -\vec{\Sigma} \,, \quad \chi \to -\chi \,. \tag{2.68}$$

Note that this symmetry is not forced on the theory artificially but emerges automatically from the gauge symmetry structure. The accidental Z_2 symmetry secures that the lightest leptobaryon is a stable particle. Here, we assume that the lightest leptobaryon is the Standard Model singlet Majorana fermion χ. Thus, χ is a potential dark matter candidate.

In the following, we assume a mass spectrum of the theory as shown in Figure 2.7. The leptobaryons Σ and Ψ can decay to χ via the emission of Higgs quanta. Note that we assumed the couplings h_1, h_2, h_3, and h_4 to be negligibly small to avoid constraints from the electroweak oblique parameters as discussed in the previous section. This is technically natural because in the limit $h_1, h_2, h_3, h_4 \to 0$ the Lagrangian (2.52) gains the discrete symmetry

$$\begin{aligned}
(Z_2)_\Psi :& \quad \Psi \to -\Psi \text{ and } \overline{\Psi} \to -\overline{\Psi}\,, \\
(Z_2)_\Sigma :& \quad \vec{\Sigma} \to -\vec{\Sigma}\,, \\
(Z_2)_\chi :& \quad \chi \to -\chi\,.
\end{aligned} \tag{2.69}$$

Nevertheless, we require the couplings to be non-vanishing such that Σ and Ψ can decay to χ in the early Universe. The electroweak self-energies induce a mass splitting in the leptobaryon multiplets such that the charged components can decay to the neutral components of the multiplets via pion emission [129].

As a side remark, we would like to mention that in principle Σ_0 and Ψ_0 could also contribute to the dark matter relic density such that we would find multicomponent dark matter. For multicomponent dark matter to be feasible, the leptobaryons would either have to be mass degenerate or the Yukawa couplings h_1, h_2, h_3, and h_4 would have to vanish. However, in the next section we will focus on the phenomenology of the sole Majorana dark matter candidate χ.

Dark Matter Relic Density

We assume that in the early hot and dense Universe, all particles were in thermal equilibrium. As the Universe expands and cools down, the heavier particles start to freeze-out as the temperature drops below their mass. The heavier leptobaryons will decay to the lightest leptobaryon χ. However, as the temperature drops below the mass of χ the remnant Z_2 symmetry in the leptobaryon sector forbids any further decays. The relic abundance of χ today is therefore fixed by its freeze-out temperature T_f.

To calculate today's dark matter relic abundance of χ, we have to solve the Lee-Weinberg equation [130]

$$\frac{\mathrm{d}Y}{\mathrm{d}x} = Z(x)\Big(Y_{\text{eq}}^2(x) - Y^2(x)\Big)\,, \tag{2.70}$$

with $Y(x) = n(s)/s(x)$ where $n(x)$ is the dark matter number density and $s(x)$ is the entropy density. Furthermore, we defined $x = m_\chi/T$ and

$$Z(x) = \sqrt{\frac{\pi}{45}}\frac{m_\chi M_{\text{Pl}}}{x^2}\Big(\sqrt{g_*}\langle v_{\text{Mol}}\sigma\rangle(x)\Big)\,. \tag{2.71}$$

The thermally averaged cross section is given by [131]

$$\langle v_{\text{Mol}}\sigma\rangle(x) = \int_{4m_\chi}^{\infty} \mathrm{d}s\,\sigma(s)\left(\frac{\sqrt{s}(s-4m_\chi^2)K_1(\frac{x\sqrt{s}}{m_\chi})}{8m_\chi^5 K_2^2(x)}\right)x\,, \tag{2.72}$$

with K_1 and K_2 being the modified Bessel functions of the second kind. We use the full thermally averaged cross section because the phenomenologically interesting region of parameter space will depend on the threshold and resonance behavior of the dark matter annihilation cross section. The equilibrium distribution of the number density is

$$Y_{\text{eq}}(x) = \frac{45}{4\pi^4}\frac{g_\chi}{g_*}x^2 K_2(x)\,, \tag{2.73}$$

with $g_\chi = 2$ the internal degrees of freedom of the Majorana fermion χ and g_* the relativistic degrees of freedom where the temperature dependence of g_* is neglected.

To solve the Lee-Weinberg equation, we rewrite the differential equation (2.70) in terms of the difference of the true number density and the equilibrium number density, $\Delta(x) = Y(x) - Y_{\text{eq}}(x)$, and find

$$\frac{\mathrm{d}\Delta(x)}{\mathrm{d}x} + \frac{\mathrm{d}Y_{\text{eq}}(x)}{\mathrm{d}x} = -Z(x)\Big(\Delta^2(x) + 2\Delta(x)Y_{\text{eq}}(x)\Big)\,. \tag{2.74}$$

We define the freeze-out temperature T_f as the temperature where $\Delta(x) = \delta \cdot Y_{\text{eq}}(x)$ with δ a fixed order one number and thus are left with

$$\frac{1}{Y_{\text{eq}}^2(x)}\frac{\mathrm{d}Y_{\text{eq}}(x)}{\mathrm{d}x} = -Z(x)\frac{\delta(\delta+2)}{\delta+1}\bigg|_{x=x_f}\,. \tag{2.75}$$

For large x, the modified Bessel functions with $|\arg(x)| < 3\pi/2$ can be approximated by

$$K_{1,2}(x) \simeq \sqrt{\frac{\pi}{2x}}e^{-x}\,, \tag{2.76}$$

and hence we get

$$Y_{\text{eq}}(x) = \frac{45}{4\sqrt{2}\pi^{\frac{7}{2}}}\frac{g_\chi}{g_*}x^{\frac{3}{2}}e^{-x}\,. \tag{2.77}$$

Using the large x expansion and plugging this result into the above equation gives

$$x_f \simeq \log\left(\frac{\delta(\delta+2)}{\delta+1}\sqrt{\frac{45}{32}}\frac{g_\chi m_\chi M_{\text{Pl}}\langle v_{\text{Mol}}\sigma\rangle(x_f)}{\pi^3\sqrt{g_* x_f}}\right)\,, \tag{2.78}$$

which can be solved numerically.

After the dark matter decouples, we can neglect $Y_{\text{eq}}(x)$ in the Lee-Weinberg equation and are left with

$$\frac{\mathrm{d}Y(x)}{\mathrm{d}x} = -Z(x)Y^2(x)\,. \tag{2.79}$$

This differential equation can be solved analytically and has the solution [132]

$$Y(x_0) = \frac{Y(x_f)}{1 + Y(x_f)\int_{x_f}^{x_0} Z(x)\mathrm{d}x} \,. \tag{2.80}$$

We further numerically approximate the solution to

$$Y(x_0) \simeq \frac{1}{\int_{x_f}^{x_0} Z(x)\mathrm{d}x} \,, \tag{2.81}$$

and then find today's dark matter relic density to be given by

$$\Omega_{\mathrm{DM}} = \frac{m_\chi s_0}{\rho_c} Y(x_0) \,, \tag{2.82}$$

with $s_0 = 2970\,\mathrm{cm}^{-3}$ and $\rho_c = 1.05394 \cdot 10^{-5} h^2 \mathrm{GeV}/\mathrm{cm}^3$.

Hence, the freeze-out temperature which determines today's dark matter relic density crucially depends on the dark matter annihilation cross section. If the dark matter annihilates too violently, no dark matter can survive until today. However, if the dark matter annihilates too slow, too much dark matter would populate the Universe. We therefore have to analyze the annihilation properties of χ carefully to see if it truly is a proper dark matter candidate.

The possible annihilation channels in the limit of no scalar mixing, $\theta \to 0$, are

$$\chi\chi \to \bar{q}q,\ Z_{\mathrm{B}}H_{\mathrm{B}},\ Z_{\mathrm{B}}Z_{\mathrm{B}},\ H_{\mathrm{B}}H_{\mathrm{B}} \,.$$

The corresponding Feynman diagrams with the leading partial wave contributions are shown in Figure 2.8. Note that because χ is a Majorana fermion it only couples via an axial coupling to the baryonic gauge boson Z_{B}. As a consequence, the s-channel annihilation $\chi\chi \to Z_{\mathrm{B}} \to \bar{q}q$ is velocity suppressed. Only the annihilation channels $\chi\chi \to Z_{\mathrm{B}}Z_{\mathrm{B}},\ Z_{\mathrm{B}}H_{\mathrm{B}}$ with an incoming S-wave in Figure 2.8 are not velocity suppressed.

In Figure 2.9, we show the dark matter relic abundance today as a function of the dark matter mass m_χ for fixed $M_{Z_{\mathrm{B}}}$, $M_{H_{\mathrm{B}}}$, α_{B}, and θ to demonstrate the general behavior. Thereby, we defined the baryonic coupling strength as

$$\alpha_{\mathrm{B}} = \frac{g_{\mathrm{B}}^2}{4\pi} \,. \tag{2.83}$$

The horizontal red line corresponds to the observed dark matter relic abundance by Planck, $\Omega_{\mathrm{DM}}h^2 \simeq 0.12$ [20]. We see that there are basically two regions which can satisfy the observed relic abundance. In the following, we will divide the dark matter discussion of χ in a resonant and non-resonant annihilation regime. In the resonant regime, the velocity suppressed s-channel annihilation $\chi\chi \to Z_{\mathrm{B}} \to \bar{q}q$ is the dominant annihilation channel. For this annihilation channel to be effective, the mass of the dark matter candidate χ has to be close to half the mass of the baryonic gauge boson Z_{B}, $m_\chi \simeq M_{Z_{\mathrm{B}}}/2$. Hence, the dark matter in the resonant regime will be relatively light. In the non-resonant regime the dom-

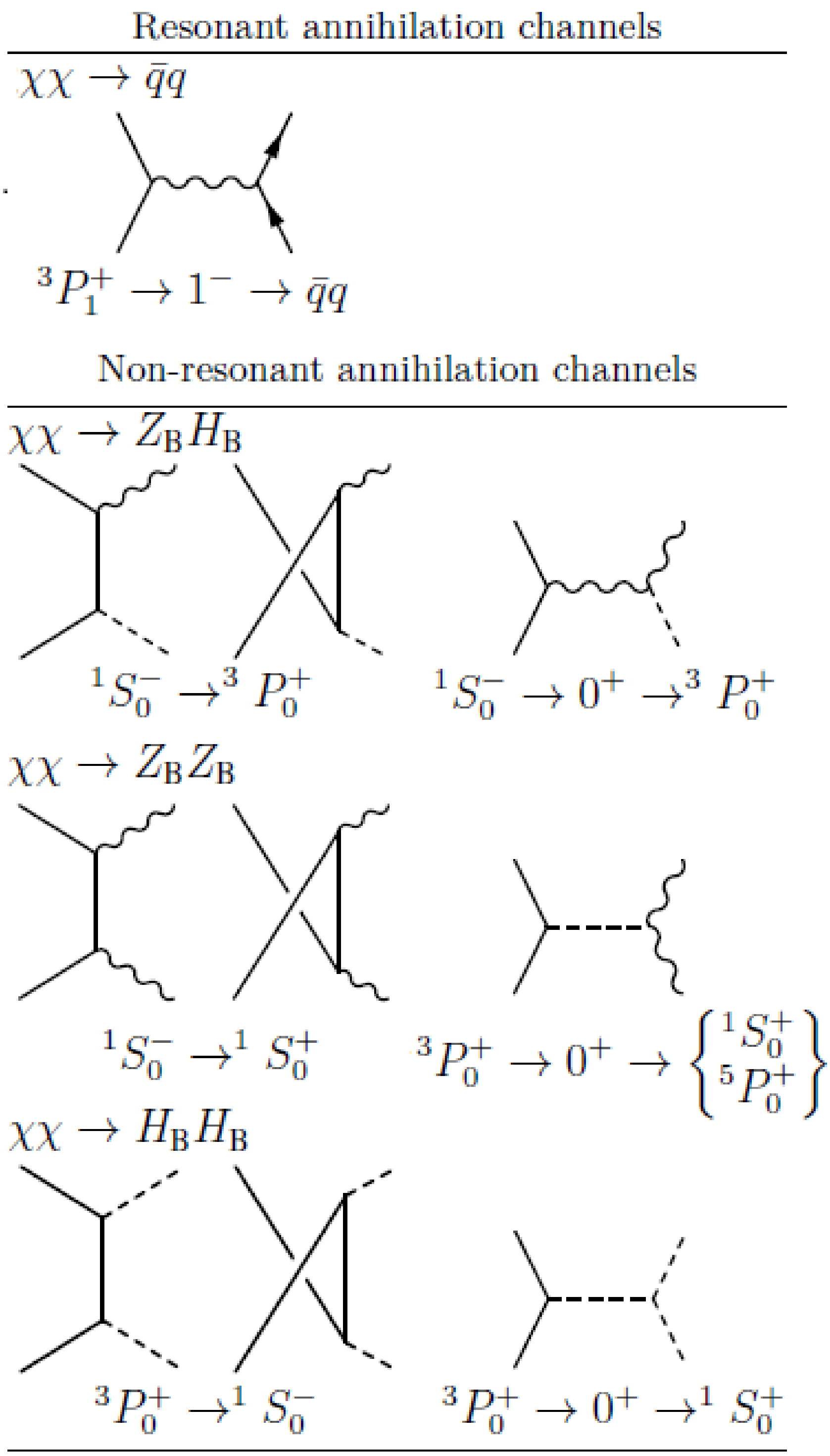

Figure 2.8: Dark matter annihilation channels in the limit of vanishing scalar mixing, $\theta \to 0$, with lowest non-vanishing partial waves.

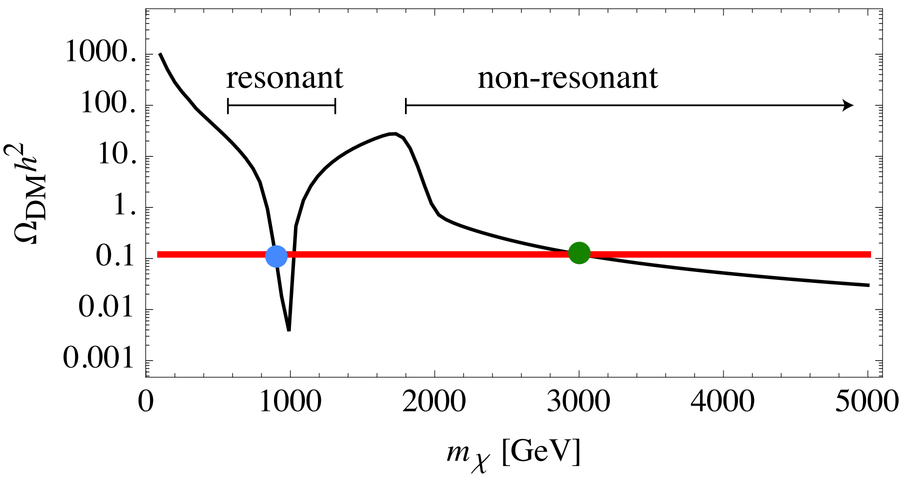

Figure 2.9: Today's dark matter relic abundance as a function of the dark matter mass for fixed M_{Z_B}, M_{H_B}, α_B, and θ. The horizontal red line corresponds to the measured abundance by Planck [20]. The blue and green dot indicate the dark matter masses which correspond to our observed Universe. We will separate our dark matter analysis in a resonant (blue dot) and non-resonant (green dot) annihilation regime.

inant annihilation channels are the velocity unsuppressed channels $\chi\chi \to Z_\mathrm{B} Z_\mathrm{B},\, Z_\mathrm{B} H_\mathrm{B}$. Note that we will find fairly heavy dark matter in this regime since we have to require $m_\chi \gtrsim M_{H_\mathrm{B}} \simeq M_{Z_\mathrm{B}}$ for the annihilation channels to be kinematically allowed.

Dark Matter Direct Detection

In principle, the dark matter phenomenology of the minimal theory of leptobaryons depends on five free parameters

$$M_{Z_\mathrm{B}},\, M_{H_\mathrm{B}},\, m_\chi,\, \alpha_\mathrm{B},\, \theta\,. \tag{2.84}$$

Apart from the constraint on the dark matter abundance, we can also apply the constraints from direct detection experiments such as XENON1T [42] to further confine the allowed parameter space. The processes contributing to the spin-independent dark matter-nucleon scattering are shown in Figure 2.10. We again include the leading partial wave contribution to show that the gauge boson mediated scattering is velocity suppressed due to the Majorana nature of χ. The cross section for the gauge boson mediated scattering is given by

$$\sigma_\mathrm{SI}(Z_\mathrm{B}) = 18\pi\alpha_\mathrm{B}^2 \frac{3m_N^2}{M_{Z_\mathrm{B}}^4} v_\mathrm{DM}^2\,, \tag{2.85}$$

where m_N is the nucleon mass, v_DM is the effective dark matter velocity given by $v_\mathrm{DM} = 0.0093c$ [2] and we are considering the regime $m_\chi \gg m_N$.

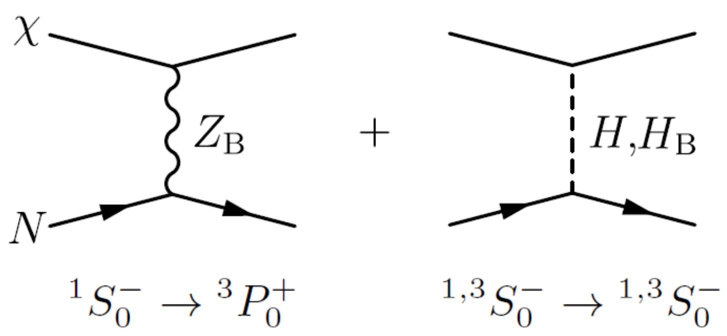

Figure 2.10: The processes contributing to the spin-independent dark matter-nucleon scattering with lowest non-vanishing partial waves. The gauge boson exchange is velocity suppressed. Whereas, the Higgs exchange is mixing angle suppressed.

The Higgs mediated scattering is mixing angle suppressed. To calculate the scattering of χ with a nucleon N via the exchange of the baryonic Higgs $H_{\rm B}$, we use the effective Lagrangian

$$\mathcal{L}_{\rm eff}^{DD} = f_q m_q \chi\chi\bar{q}q + f_G \chi\chi G^a_{\mu\nu} G^{a\,\mu\nu} \,, \tag{2.86}$$

where

$$f_q = \frac{g_{\rm B} B_{H_{\rm B}} \sin(\theta)\cos(\theta) m_\chi}{2 M_{Z_{\rm B}} v_H} \frac{M_{H_{\rm B}}^2 - M_H^2}{M_{H_{\rm B}}^2 M_H^2} \,, \tag{2.87}$$

and

$$f_G = -\frac{\alpha_s g_{\rm B} B_{H_{\rm B}} \sin(\theta)\cos(\theta) m_\chi}{24\pi M_{Z_{\rm B}} v_H} \frac{M_{H_{\rm B}}^2 - M_H^2}{M_{H_{\rm B}}^2 M_H^2} \sum_{a=c,b,t} c_a \,, \tag{2.88}$$

with $c_a = 1 + \frac{11}{4\pi}\alpha_s(m_a)$ and $B_{H_{\rm B}}$ the baryon number of $H_{\rm B}$. In the low energy limit where the initial velocity vanishes, $|\vec{p_i}| = 0$, and thus also the transferred momentum vanishes, the scattering amplitude is given by

$$\begin{aligned} i\mathcal{M} &= 2if_q \bar{u}(p_\chi)u(p_\chi) \sum_q m_q \langle N|\bar{q}q|N\rangle + 2if_G \bar{u}(p_\chi)u(p_\chi)\langle N|G^a_{\mu\nu}G^{a\,\mu\nu}|N\rangle \\ &= 4if_q m_N^2 \bar{u}(p_\chi)u(p_\chi) \Bigg[\sum_q \frac{m_q}{m_N} \langle\tilde{N}|\bar{q}q|\tilde{N}\rangle \\ &\qquad\qquad + \frac{2}{27}\left(1 - \sum_q \frac{m_q}{m_N}\langle\tilde{N}|\bar{q}q|\tilde{N}\rangle\right) \sum_{a=c,b,t} c_a \Bigg] \,, \end{aligned} \tag{2.89}$$

where we used lattice conventions $|N\rangle = \sqrt{2m_N}|\tilde{N}\rangle$ [133] and

$$\frac{1}{m_N}\langle\tilde{N}|G^a_{\mu\nu}G^{a\,\mu\nu}|\tilde{N}\rangle = -\frac{8\pi}{9\alpha_s}\left(1 - \sum_q \frac{m_q}{m_N}\langle\tilde{N}|\bar{q}q|\tilde{N}\rangle\right). \tag{2.90}$$

For the spin-independent direct detection cross section we therefore find

$$\begin{aligned}\sigma_{\text{SI}}(H,\, H_{\text{B}}) =& \frac{8}{\sqrt{2}}\frac{G_F\alpha_{\text{B}}B_{H_{\text{B}}}^2\sin^2(\theta)\cos^2(\theta)m_\chi^4 m_N^4}{(m_\chi + m_N)^2 M_{Z_{\text{B}}}^2}\frac{(M_{H_{\text{B}}}^2 - M_H^2)^2}{M_{H_{\text{B}}}^4 M_H^4} \\ &\times\left|\sum_q \frac{m_q}{m_N}\langle\tilde{N}|\bar{q}q|\tilde{N}\rangle + \frac{2}{27}\left(1 - \sum_q \frac{m_q}{m_N}\langle\tilde{N}|\bar{q}q|\tilde{N}\rangle\right)\sum_{a=c,b,t} c_a\right|^2,\end{aligned} \tag{2.91}$$

where $1/v^2 = 4G_F/\sqrt{2}$ was used. From lattice calculations we take as input [133] $c_c = 1.32$, $c_b = 1.19$, $c_t = 1$, and

$$\left|\sum_q \frac{m_q}{m_p}\langle\tilde{N}|\bar{q}q|\tilde{N}\rangle + \frac{2}{27}\left(1 - \sum_q \frac{m_q}{m_p}\langle\tilde{N}|\bar{q}q|\tilde{N}\rangle\right)\sum_{a=c,b,t} c_a\right| = 0.3155\,, \tag{2.92}$$

$$\left|\sum_q \frac{m_q}{m_n}\langle\tilde{N}|\bar{q}q|\tilde{N}\rangle + \frac{2}{27}\left(1 - \sum_q \frac{m_q}{m_n}\langle\tilde{N}|\bar{q}q|\tilde{N}\rangle\right)\sum_{a=c,b,t} c_a\right| = 0.31772\,. \tag{2.93}$$

The total spin-independent direct detection cross section is then given by

$$\sigma_{\text{SI}} = \sigma_{\text{SI}}(Z_{\text{B}}) + \sigma_{\text{SI}}(H,\, H_{\text{B}})\,. \tag{2.94}$$

Note that there is no interference term due to the different contributing partial waves.

Resonant Dark Matter

We will first discuss the resonant dark matter regime. The dark matter annihilation is governed by the process $\chi\chi \to Z_{\text{B}} \to \bar{q}q$ with the annihilation cross section given by

$$\sigma_{\text{res}} = 9\pi\alpha_{\text{B}}\sqrt{1 - \frac{4m_\chi^2}{s}}\,\frac{M_{Z_{\text{B}}}\Gamma_{Z_{\text{B}}}\text{Br}(Z_{\text{B}} \to \sum\bar{q}q)}{(s - M_{Z_{\text{B}}}^2)^2 + M_{Z_{\text{B}}}^2\Gamma_{Z_{\text{B}}}^2}\,. \tag{2.95}$$

The partial decay widths of the leptophobic gauge boson Z_{B} are given in the Appendix 7.5. Note that we neglect the process $\chi\chi \to H,\, H_{\text{B}} \to \bar{q}q$ since it is mixing angle and velocity suppressed. This further has the advantage that the annihilation cross section is then independent of the baryonic Higgs mass $M_{H_{\text{B}}}$ and the scalar mixing angle θ as can be inferred from equation (2.95). We will therefore restrict ourselves to the regime of zero scalar mixing ($\theta \to 0$). Moreover, the spin-independent dark matter-nucleon scattering is now mediated by the gauge boson exchange which is given by equation (2.85). We are

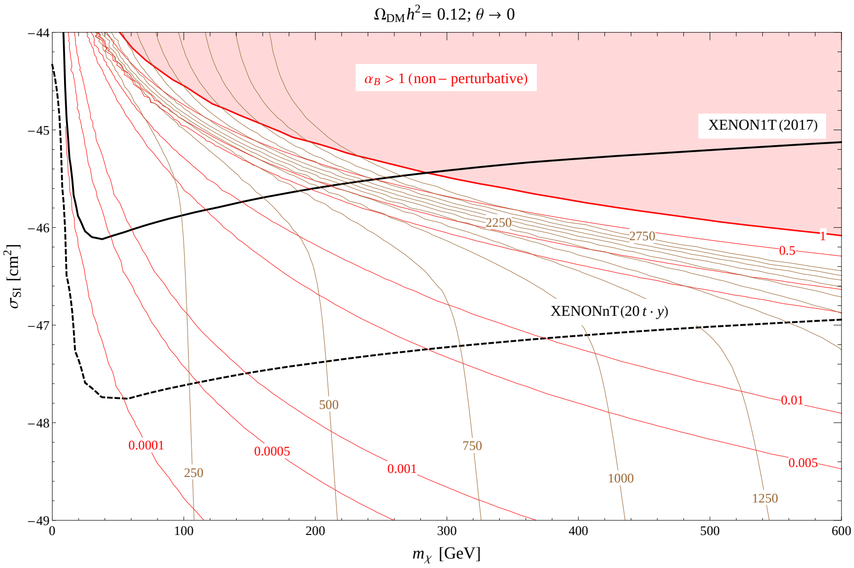

Figure 2.11: Contours of constant M_{Z_B} (brown, in GeV) and α_B (red) in the m_χ-σ_SI plane in agreement with the measured dark matter abundance ($\Omega_\mathrm{DM}h^2 = 0.12$) and in the limit $\theta \to 0$. The upper right region is excluded because large non-perturbative coupling constants are required to satisfy the dark matter density constraints. We show the current limit on direct detection by XENON1T [134] (black, solid) and the projected limit by XENONnT [43] (black, dashed).

thus left with only three independent parameters $(M_{Z_\mathrm{B}},\, m_\chi,\, \alpha_\mathrm{B})$ for the discussion of the resonant dark matter scenario.

To constrain the allowed parameter space, we can invert the direct detection cross section to find the baryonic coupling strength α_B as a function of the baryonic gauge boson mass M_{Z_B} and spin-independent dark matter-nucleon scattering cross section σ_SI

$$\alpha_\mathrm{B}(M_{Z_\mathrm{B}},\, \sigma_\mathrm{SI}) = \frac{M_{Z_\mathrm{B}}^2}{\alpha_\mathrm{B} m_N v_\mathrm{DM}} \sqrt{\frac{\sigma_\mathrm{SI}}{54\pi}}\,. \tag{2.96}$$

Inserting equation (2.96) into equation (2.95), we can then numerically determine M_{Z_B} for a fixed dark matter mass m_χ such that the Majorana fermion χ saturates the observed dark matter relic density. In Figure 2.11, we show the contours of constant M_{Z_B} in brown in GeV and contours of constant α_B in red consistent with the observed dark matter relic abundance in the m_χ-σ_SI plane.

For light baryonic gauge bosons, $M_{Z_\mathrm{B}} \lesssim 1250$ GeV, the dark matter relic abundance fixes the dark matter mass m_χ. Thus, the brown contours show the narrow resonance behavior already observed in Figure 2.9. We always find $m_\chi < M_{Z_\mathrm{B}}/2$ because we chose the lower dark matter mass of the resonance peak (blue dot in Figure 2.9) for our analysis. We can exclude the shaded region in the upper right corner of Figure 2.11 because large non-perturbative coupling constants are needed to satisfy the dark matter relic abundance constraints. The current limit from XENON1T [134] and the projected limit for the XENONnT experiment [43] are shown in black in Figure 2.11. The current direct detection limit from XENON1T probes dark matter with $m_\chi \lesssim 300$ GeV. The XENONnT experiment can then rule out dark matter with $m_\chi \lesssim 600$ GeV and coupling constants $\alpha_\mathrm{B} \gtrsim 0.05$.

Non-Resonant Dark Matter

We now turn to the non-resonant dark matter scenario. The dominant velocity unsuppressed annihilation channels are $\chi\chi \to Z_\mathrm{B} H_\mathrm{B},\ Z_\mathrm{B} Z_\mathrm{B}$. The thermally averaged annihilation cross sections of these two channels are given by

$$\langle v\sigma(\chi\chi \to Z_\mathrm{B} S_\mathrm{B})\rangle = \frac{81\alpha_\mathrm{B}^2 \pi \cos^2\theta}{64\, m_\chi^4 M_{Z_\mathrm{B}}^4} \lambda(4m_\chi^2, M_{Z_\mathrm{B}}^2, M_{H_\mathrm{B}}^2)^{3/2}\,, \tag{2.97}$$

$$\langle v\sigma(\chi\chi \to Z_\mathrm{B} Z_\mathrm{B})\rangle = \frac{81\pi\alpha_\mathrm{B}^2}{4m_\chi} \frac{(m_\chi^2 - M_{Z_\mathrm{B}}^2)^{3/2}}{(M_{Z_\mathrm{B}}^2 - 2m_\chi^2)^2}\,, \tag{2.98}$$

with $\lambda(a,b,c) = a^2 + b^2 + c^2 - 2ab - 2ac - 2bc$. In contrast to the resonant dark matter scenario, the annihilation cross sections depend on all five free parameters given in (2.84).

The upper limit on the scalar mixing angle from the Higgs signal strength measurements at the LHC suggests a small mixing angle (see equation (2.60)). We will therefore start with an analysis in the limit $\theta \to 0$. Later, we will see that this is a reasonable initial starting point.

In the limit $\theta \to 0$, we can fix the parameters M_{Z_B}, M_{H_B}, and α_B and determine m_χ such that it saturates the observed dark matter relic abundance. Contours of constant dark matter mass in GeV (black) for fixed $M_{H_\mathrm{B}} = 1000$ GeV (upper panel) and fixed $\alpha_\mathrm{B} = 0.001$ (lower panel) are shown in Figure 2.12. The bounds from direct detection are now used to derive an upper bound on the scalar mixing angle θ.

The dominant contribution to the dark matter-nucleon scattering in this scenario is the velocity unsuppressed Higgs exchange. The direct detection cross section is therefore mixing angle suppressed. For a fixed dark matter mass m_χ, we can hence derive the maximal mixing angle which is in agreement with the experimental constraints from XENON1T [134]. Our approach is illustrated in Figure 2.13.

The upper bound on the scalar mixing angle is included in dashed blue contours in Figure 2.12. We see that the derived limits on the mixing angle, $|\theta| \lesssim 0.05$, are much stronger than the constraints from the Higgs signal strength measurement at the LHC [126]. The small mixing angles also justify our initial assumption of $\theta \to 0$ for the annihilation processes.

In the upper panel, we observe that the dark matter mass m_χ required to saturate the observed dark matter relic abundance increases as the coupling constant α_B decreases. This can be understood by consulting Figure 2.9 where the dark matter relic abundance increases as the coupling constant α_B is lowered because the dark matter annihilates slower. The intersection point of the dark matter relic abundance and the observed abundance (green dot in Figure 2.9) is shifted to heavier dark matter masses.

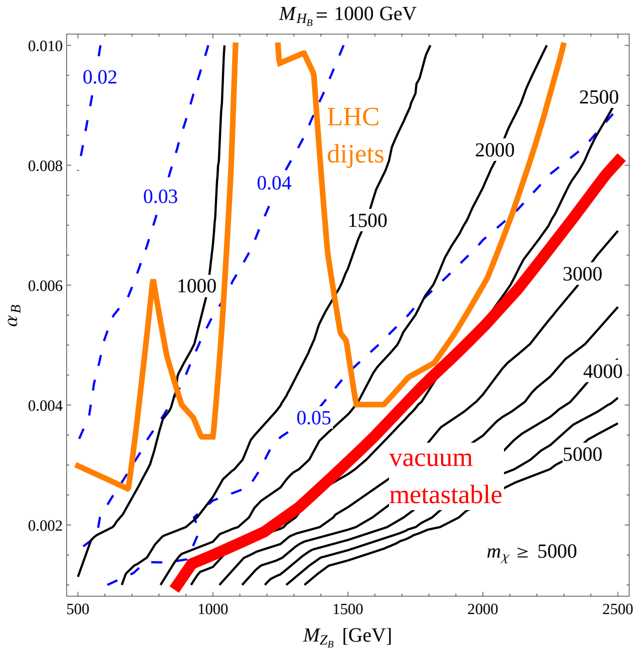

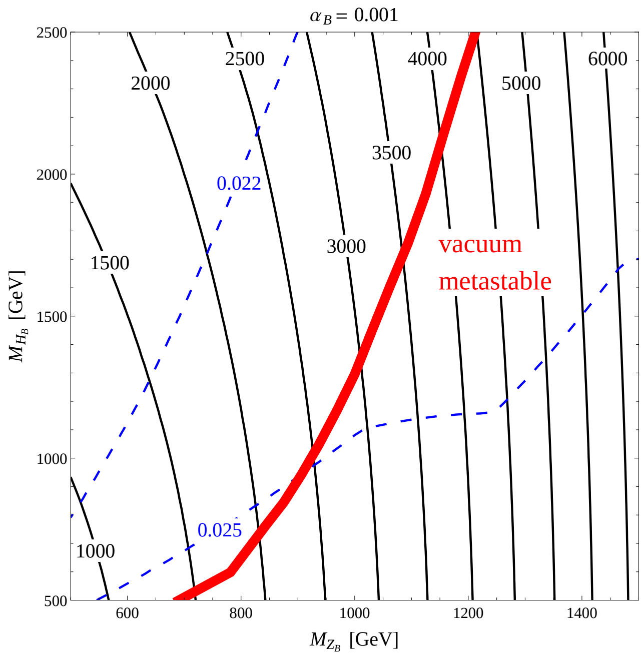

Figure 2.12: Contours of constant dark matter mass m_χ (black, in GeV) saturating the observed dark matter relic abundance for fixed $M_{H_B} = 1000$ GeV (upper panel) and fixed $\alpha_B = 0.001$ (lower panel) in the limit $\theta \to 0$. Upper bounds on the scalar mixing angle θ are derived from the direct detection limit of the XENON1T experiment [134] (blue, dashed). The upper bound on the dark matter mass from requiring the vacuum in the direction of the baryonic Higgs H_B to be stable at energies below the dark matter mass (see equation (2.67)) is shown in red. For fixed $M_{H_B} = 1000$ GeV (upper panel) the constraints from dijet searches at the LHC (discussed in section 2.2.2) are given in orange.

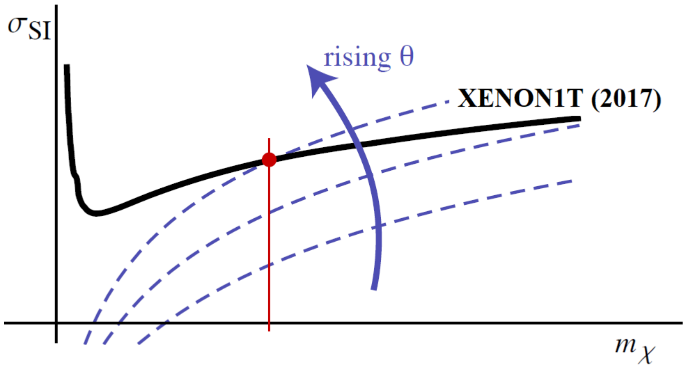

Figure 2.13: The spin-independent direct detection cross section as a function of the dark matter mass m_χ for different scalar mixing angles θ and fixed $M_{Z_{\mathrm{B}}}$, $H_{H_{\mathrm{B}}}$, and α_{B}. For a given dark matter mass determined by requiring relic density saturation (red line), we derive an upper bound on the scalar mixing angle by considering the intersection of σ_{SI} with the XENON1T bound (black) [134].

Furthermore, in the lower panel, we see that the dark matter mass m_χ increases as the baryonic gauge boson mass $M_{Z_{\mathrm{B}}}$ and baryonic Higgs mass $M_{H_{\mathrm{B}}}$ increase. This behavior is expected as at least one of the annihilation channels $\chi\chi \to Z_{\mathrm{B}}Z_{\mathrm{B}}$, $Z_{\mathrm{B}}H_{\mathrm{B}}$, $H_{\mathrm{B}}H_{\mathrm{B}}$ has to remain open.

As the dark matter mass increases to satisfy the constraint on the observed dark matter relic density, the upper limit on the dark matter mass from requiring the vacuum to be stable in the direction of the baryonic Higgs H_{B} at energies below the dark matter mass becomes important. This consistency limit of the theory was discussed in section 2.2 and is shown in Figure 2.12 as red line. In the region to the right of the red contour, the vacuum becomes metastable at energies below the dark matter mass and new physics is required to stabilize the theory.

Moreover, in the upper panel, we show the constraints from dijet searches at the LHC which are discussed in the next section as orange line. The absence of dijet resonances at the LHC generically forces the theory to smaller couplings to suppress the dijet production. However, as the coupling constant α_{B} decreases, the consistency condition of no new physics below the dark matter mass to stabilize the scalar potential becomes important (see equation (2.67)) and requires $M_{Z_{\mathrm{B}}} \lesssim 800$ GeV. For baryonic gauge boson masses $M_{Z_{\mathrm{B}}} \gtrsim 2000$ GeV the LHC constraints weaken because of the limited center-of-mass energy of $\sqrt{s} = 13$ TeV. Larger coupling constants $\alpha_{\mathrm{B}} \gtrsim 0.005$ are then still allowed.

2.2.2 Leptobaryons at the LHC

In this section, we discuss the discovery potential of the minimal theory of leptobaryons at the LHC. As we learned in the last section, there are in principle two different regimes which allow for the Majorana fermion χ to be a valid dark matter candidate. For our LHC study of the minimal theory of leptobaryons, we will focus on the non-resonant dark matter scenario because the masses of m_χ and M_{Z_B} are not as closely tuned as in the resonant dark matter scenario. The allowed parameter space therefore suggests $m_\chi \gtrsim M_{Z_\mathrm{B}}, M_{H_\mathrm{B}}$. Because the Z_2 symmetry (2.68) which stabilizes the lightest leptobaryon requires that the leptobaryons have to be produced at least pairwise at the LHC, searching for the dark matter candidate χ is challenging. It thus seems to be much more promising to investigate the properties of the new gauge symmetry $U(1)_B$ and the symmetry breaking mechanism at the LHC. As we will see, we can then still indirectly probe the quantum numbers of the leptobaryons.

Baryonic Gauge Boson Z_B at the LHC

The leptophobic gauge boson Z_B can be produced at the LHC via the processes

$$pp \to Z_\mathrm{B} \to jj,\; Z_\mathrm{B} H_\mathrm{B}\,.$$

We will first consider the dijet resonances and touch on the associated production in the next section. In the mass range $m_\chi \gtrsim M_{Z_\mathrm{B}}$, the baryonic gauge boson Z_B will only decay to quarks. Because the Z_B only couples to baryon number it branches uniformly to all quark flavors in the limit of negligible phase space factors. In order to confirm the leptophobic nature of Z_B, we thus have to search for resonances in the dijet channel with the corresponding absence of dilepton resonances. For a given flavor of initial and final state quarks the partonic cross section of the dijet production is given by

$$\hat{\sigma}(\bar{q}_i q_i \to Z_\mathrm{B} \to \bar{q}_f q_f) = \frac{1}{972\pi} \frac{g_\mathrm{B}^4 \hat{s}}{(\hat{s} - M_{Z_\mathrm{B}}^2)^2 + M_{Z_\mathrm{B}}^2 \Gamma_{Z_\mathrm{B}}}\,, \tag{2.99}$$

where we assumed massless quarks and $\sqrt{\hat{s}}$ is the partonic center-of-mass energy. The total decay width of Z_B in this scenario is given by $\Gamma_{Z_\mathrm{B}} = g_\mathrm{B}^2 M_{Z_\mathrm{B}}/(6\pi)$. The production cross section of dijet resonances (2.99) only depends on the gauge coupling g_B and the baryonic gauge boson mass M_{Z_B}. We can therefore derive an upper bound on the coupling g_B as a function of M_{Z_B} from the absence of dijet resonances at ATLAS [135, 136] and CMS [137, 138, 139, 140]. The upper bound on g_B as a function of M_{Z_B} for different experimental studies at the LHC is shown in Figure 2.14 where we used the MSTW 2008 parton distribution functions to calculate the hadronic cross section [95].

Apart from a small open window at $M_{Z_\mathrm{B}} \sim 1200$ GeV, the LHC rules out leptophobic gauge bosons with $M_{Z_\mathrm{B}} \lesssim 2000$ GeV for $g_\mathrm{B} \gtrsim 0.2$. The upper bound on g_B weakens for larger baryonic gauge boson masses ($M_{Z_\mathrm{B}} \gtrsim 2500$ GeV) because the center-of-mass energy of the LHC is too small to probe this region effectively. We indicated with a dotted box the non-resonant dark matter study of the upper panel of Figure 2.12. Additionally,

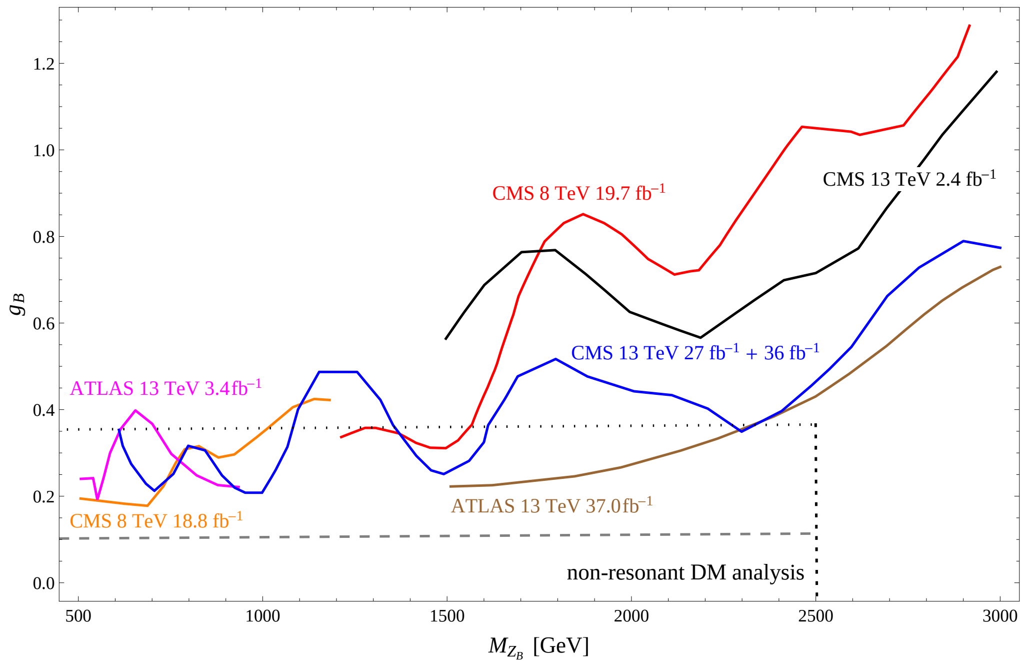

Figure 2.14: Upper limit of $g_{\rm B}$ as a function of the leptophobic gauge boson mass $M_{Z_{\rm B}}$ from the absence of dijet resonances at ATLAS [135, 136] and CMS [137, 138, 139, 140].

we also indicated with a gray dashed line $\alpha_{\rm B} = 0.001$ which was fixed in the non-resonant dark matter study in the lower panel of Figure 2.12. Note that the combination of the derived upper limit of $g_{\rm B}$ was used in the upper panel of Figure 2.12 to constrain the non-resonant dark matter scenario.

As a side remark, if the decays $Z_{\rm B} \to \chi\chi,\ \bar{\Psi}\Psi,\ \Sigma\Sigma$ are allowed, they will dominate the decay width of $Z_{\rm B}$ since the leptobaryons have a larger baryon charge than the Standard Model quarks. The different partial decay widths of $Z_{\rm B}$ are given in the Appendix 7.5.

Baryonic Higgs $H_{\rm B}$ at the LHC

The baryonic Higgs $H_{\rm B}$ inherits the Standard Model Higgs production channels at the LHC [141]. The relevant production channels are shown in Figure 2.15. The only additional production channels compared to the Standard Model Higgs are the associated production with a baryonic gauge boson and the new contribution to vector boson fusion from the baryonic gauge boson $Z_{\rm B}$.

In the upper panel of Figure 2.16, we show the production cross section of the baryonic Higgs $H_{\rm B}$ at a proton-proton collider with center-of-mass energy $\sqrt{s} = 14$ TeV for fixed $\alpha_{\rm B}$, $|\theta|$, and $M_{Z_{\rm B}}$ as a function of the baryonic Higgs mass $M_{H_{\rm B}}$. As for the Standard Model Higgs, gluon fusion dominates the production at the LHC. However, vector boson fusion becomes the dominant production process for $M_{H_{\rm B}} \gtrsim 1150$ GeV.

Moreover, in the lower panel of Figure 2.16, we display the $H_{\rm B}$ production cross sec-

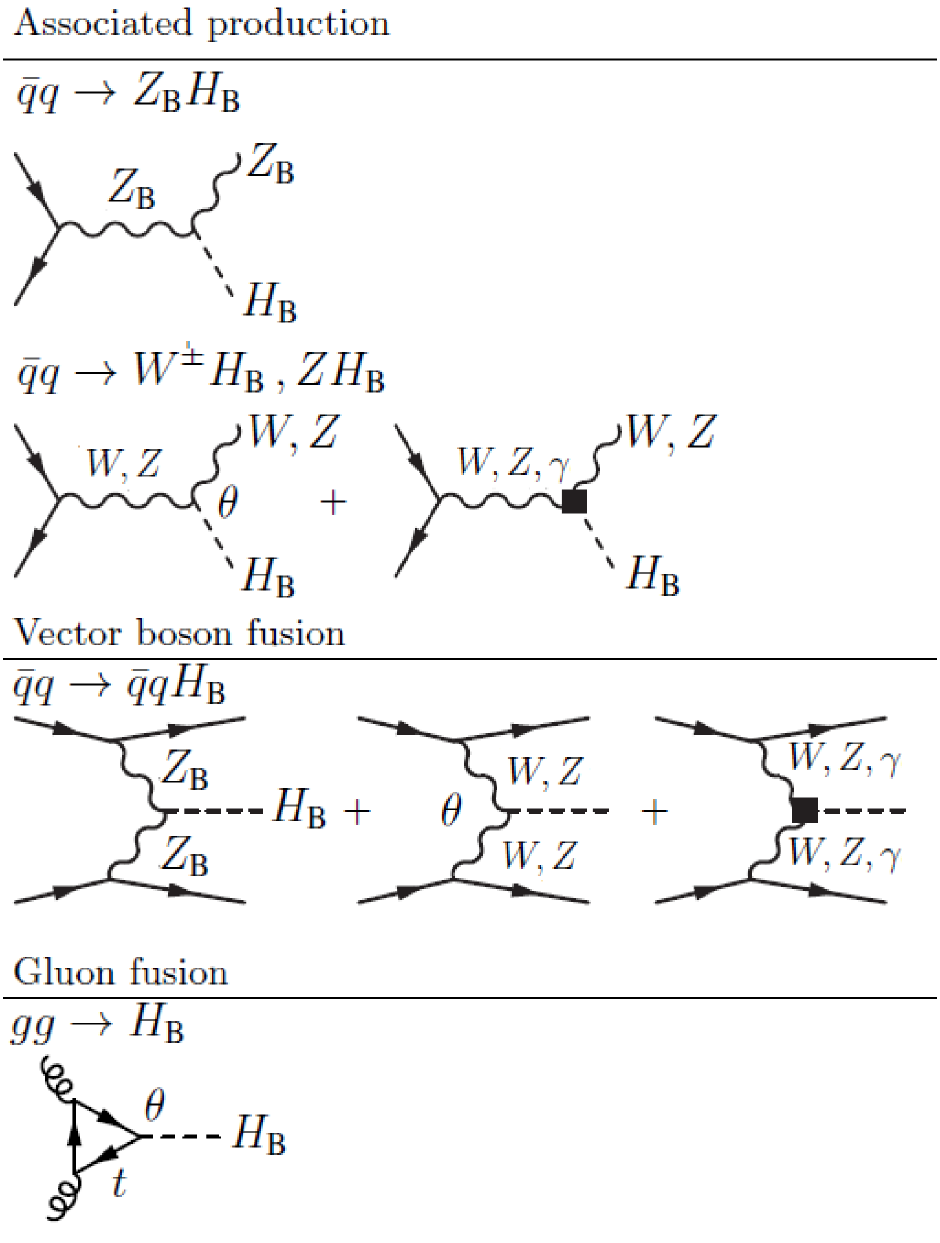

Figure 2.15: The production channels of the baryonic Higgs H_B at a proton-proton collider. Vertices marked with θ are mixing angle suppressed. For vertices marked with a square, one-loop contributions of the leptobaryons are taken into account.

tion at the LHC with $\sqrt{s} = 14$ TeV for fixed $\alpha_{\rm B}$, $M_{H_{\rm B}}$, and $M_{Z_{\rm B}}$ as a function of the mixing angle $|\theta|$. Note that for small mixing angles ($|\theta| \lesssim 0.02$) the associated production with a baryonic gauge boson $Z_{\rm B}$ is the leading contribution. In this limit, the associated production can also become relevant for the dijet searches discussed in section 2.2.2. Furthermore, the current upper bound from direct detection experiments on the scalar mixing angle (see section 2.2.1, $|\theta| \lesssim 0.05$) suggests that we will be in the regime of tiny mixing angles in the near future.

After producing the baryonic Higgs $H_{\rm B}$ at the LHC, we have to study the decay profile in order to identify it correctly. The tree-level partial decay widths of $H_{\rm B}$ are given in the Appendix 7.6. If kinematically allowed, the baryonic Higgs decays to pairs of leptobaryons and leptophobic gauge bosons dominate

$$H_{\rm B} \to \chi\chi, \bar{\Psi}\Psi, \Sigma\Sigma, Z_{\rm B} Z_{\rm B} \,. \tag{2.100}$$

Our dark matter analysis however suggests $m_\chi \gtrsim M_{H_{\rm B}}$ such that the decay to leptobaryons is kinematically forbidden if we require the lightest leptobaryon χ to saturate the observed dark matter relic abundance. If also the decay to baryonic gauge bosons $Z_{\rm B}$ is kinematically forbidden, we have to take one-loop processes into account to capture the decay properties of $H_{\rm B}$ into Standard Model electroweak gauge bosons correctly for small scalar mixing angles θ. The Feynman diagrams representing the mixing angle and loop suppressed decays of the baryonic Higgs $H_{\rm B}$ into electroweak gauge bosons $W^\pm$, Z, and γ are shown in Figure 2.17.

The leading contributions at the one-loop level come from the heavy leptobaryons Ψ and Σ running inside the loop in Figure 2.17. In the following, we take the limit $m_\Psi, m_\Sigma \to \infty$ and calculate the effective couplings of the physical baryonic Higgs $h_{\rm B}$ to the electroweak gauge bosons $W^\pm$, Z, and γ. We find the effective Lagrangian

$$\begin{aligned}
\mathcal{L}_{\rm eff}^{H_{\rm B}} = &\frac{g_{\rm B}}{8\pi^2 M_{Z_{\rm B}}} \sum_f \Big[e^2 Q_f^2 \, h_{\rm B} F_{\mu\nu} F^{\mu\nu} + \frac{g_L^2}{\cos^2(\theta_{\rm w})} \left(T_f^3 - Q_f \sin^2(\theta_{\rm w}) \right)^2 \, h_{\rm B} Z_{\mu\nu} Z^{\mu\nu} \\
&+ \frac{2 e g_L}{\cos(\theta_{\rm w})} Q_f \left(T_f^3 - Q_f \sin^2(\theta_{\rm w}) \right) \, h_{\rm B} F_{\mu\nu} Z^{\mu\nu} \Big] \\
&+ \frac{g_{\rm B}}{8\pi^2 M_{Z_{\rm B}}} \sum_F \left[g_L^2 c_F^{(W)} \, h_{\rm B} W^+_{\mu\nu} W^{-\mu\nu} \right] ,
\end{aligned} \tag{2.101}$$

with the first sum over the isospin components $f = \{\psi^+, \psi^0, \Sigma^+, \Sigma^0\}$ and the second sum over the entire multiplets $F = \{\Psi, \Sigma\}$ where $c_\Psi^{(W)} = 1$ and $c_\Sigma^{(W)} = 2$. Here, $\theta_{\rm w}$ is the electroweak Weinberg angle, Q_f is the electric charge and T_f^3 is the $SU(2)_L$ isospin of the components ψ^+, ψ^0, Σ^+, and Σ^0. The branching of the baryonic Higgs $H_{\rm B}$ as a function of the scalar mixing angle $|\theta|$ for fixed $\alpha_{\rm B}$, $M_{H_{\rm B}}$, $M_{Z_{\rm B}}$, and m_χ including the one-loop contributions from the leptobaryons Ψ and Σ is then shown in Figure 2.18.

For large mixing angles, $|\theta| > 10^{-3}$, the mixing angle suppressed decays dominate and the baryonic Higgs $H_{\rm B}$ inherits the Standard Model Higgs decay modes apart from the additional decay mode $H_{\rm B} \to HH$. However, for smaller mixing angles, $|\theta| < 10^{-3}$,

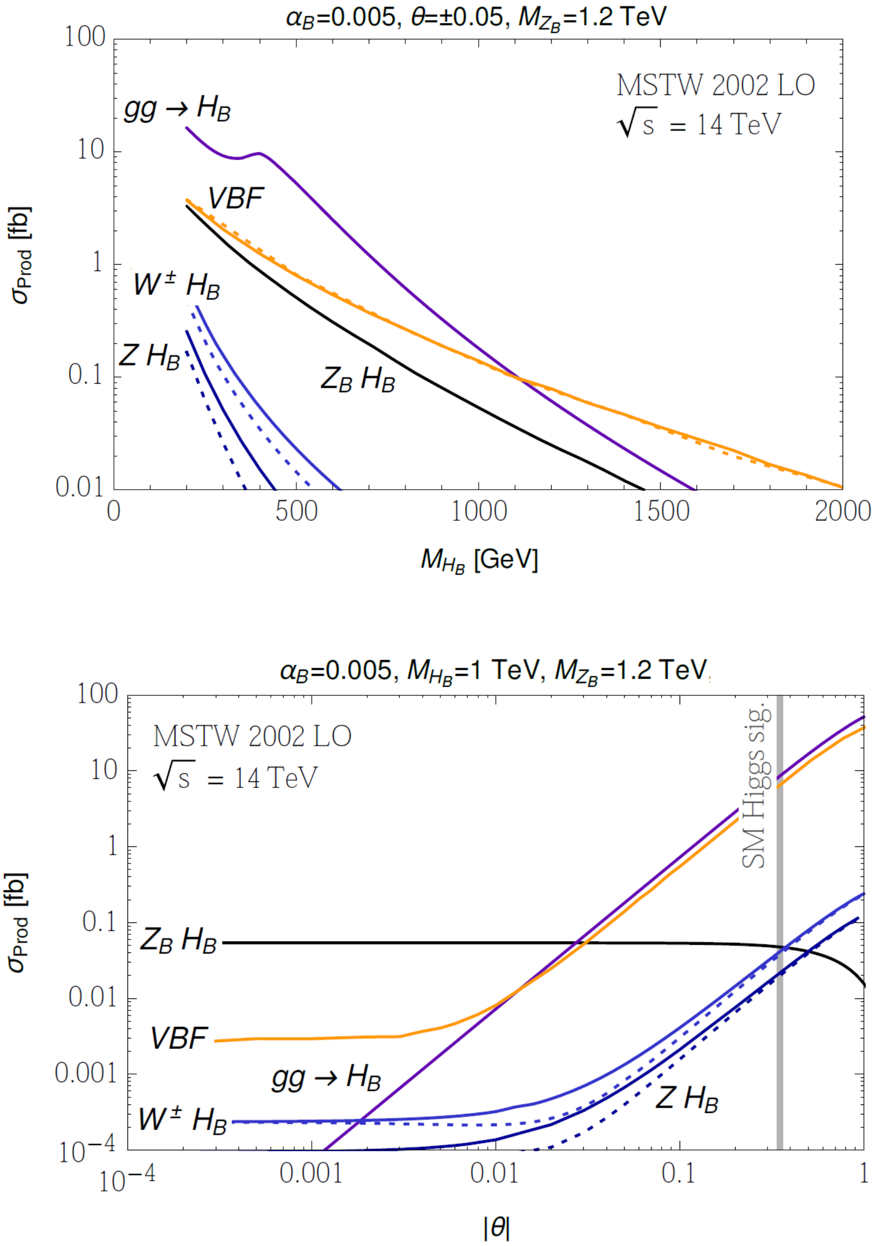

Figure 2.16: The production cross section of the baryonic Higgs H_{B} at the LHC with a center-of-mass energy $\sqrt{s} = 14$ TeV as a function of the baryonic Higgs mass $M_{H_{\mathrm{B}}}$ (upper panel) and the scalar mixing angle $|\theta|$ (lower panel). The hadronic production cross sections were computed with CalcHEP 3.4 using the MSTW 2002 parton distribution functions [142]. Solid lines correspond to $\theta > 0$ whereas dashed lines are given by $\theta < 0$. The processes contributing to vector boson fusion (VBF) and associated production are given in Figure 2.15. The upper limit on the scalar mixing angle $|\theta| \leq 0.35$ from Higgs signal strength measurements [126] is given by the vertical gray line in the lower panel.

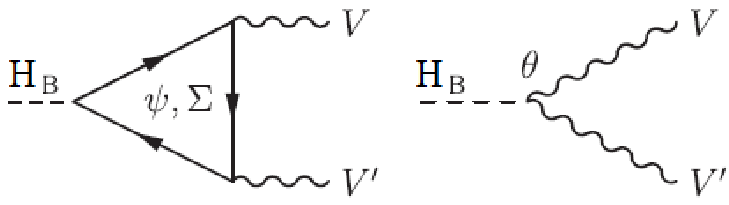

Figure 2.17: Feynman graphs illustrating the loop suppressed (left) and mixing angle suppressed (right) decays of the baryonic Higgs H_{B} to electroweak gauge bosons $V, V' \in \{W^{\pm}, Z, \gamma\}$.

the loop suppressed decay channels start to become dominant and the H_{B} decay profile is significantly different compared to the Standard Model Higgs decay profile. The decay channels $H_{\mathrm{B}} \to Z\gamma, \gamma\gamma$ increase drastically for small mixing angles, whereas the decay modes $H_{\mathrm{B}} \to HH, \bar{t}t$ become irrelevant.

We can estimate the relative partial widths of H_{B} in the limit $\theta \to 0$ by squaring the effective couplings in equation (2.101) and taking into account a factor $1/2$ for the ZZ and $\gamma\gamma$ decay mode to respect the indistinguishability of the final state particles. The relative branching ratios of the baryonic Higgs H_{B} are then given by

$$\Gamma_{WW} : \Gamma_{ZZ} : \Gamma_{Z\gamma} : \Gamma_{\gamma\gamma} = 20 : 7 : 3 : 1\,. \tag{2.102}$$

We can compare the relative branching (2.102) to the relative branching of the leptobaryon model discussed in [114]

$$\Gamma_{WW} : \Gamma_{ZZ} : \Gamma_{Z\gamma} : \Gamma_{\gamma\gamma} = 2 : 1 : 10^{-3} : 1\,. \qquad \text{(model in [114])} \tag{2.103}$$

Especially, the branching to $Z\gamma$ is significantly increased in the minimal leptobaryon model because of the presence of the $SU(2)_L$ triplet Σ. Therefore, even if the leptobaryons are too heavy to be directly produced at the LHC, we can still draw conclusions about the quantum numbers of the leptobaryons from the loop mediated decays of the baryonic Higgs H_{B} for small mixing angles $|\theta|$ at the LHC. Furthermore, due to the different decay profiles of different leptobaryon models, we can even distinguish between sets of anomaly canceling fermions. Note however that the relative branching in equation (2.102) is subject to finite mass correction. Nevertheless, we expect that the relative decay strengths do not change significantly.

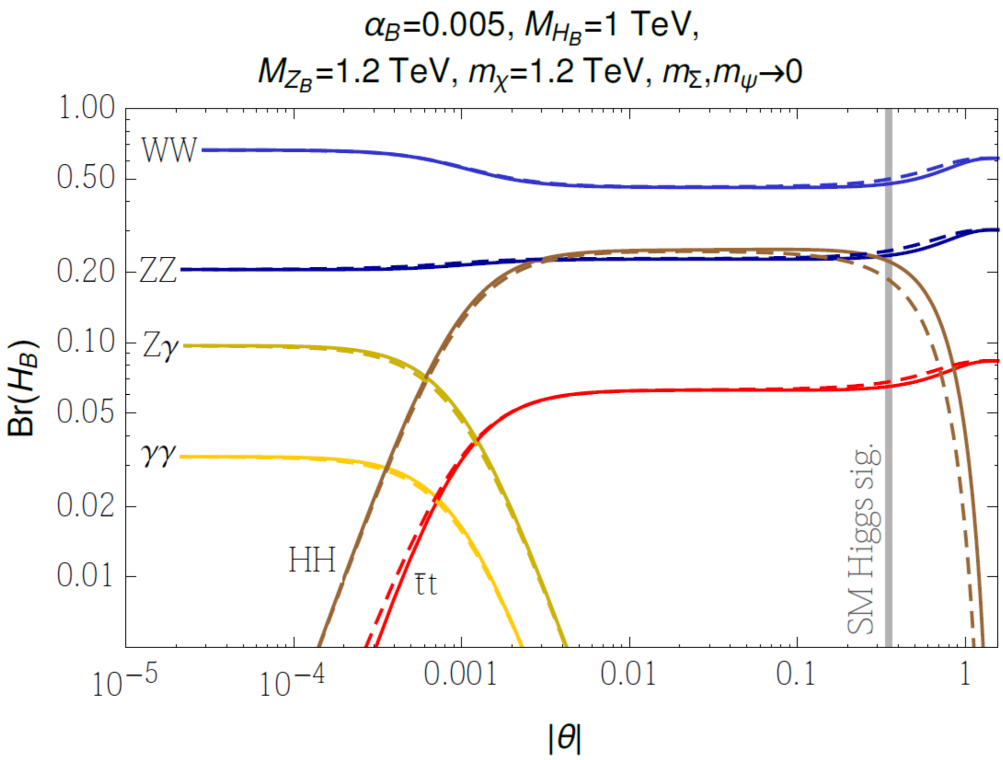

Figure 2.18: The branching ratio of the baryonic Higgs H_B as a function of the scalar mixing angle $|\theta|$ below the $H_\mathrm{B} \to Z_\mathrm{B} Z_\mathrm{B}$ threshold. The one-loop contributions to the branching ratios were computed with Package-X [143]. The solid lines correspond to $\theta > 0$ whereas dashed lines show the results for $\theta < 0$. The upper bound on the scalar mixing angle from Higgs signal strength measurements [126], $|\theta| \leq 0.35$, is represented by the vertical gray line.

2.2.3 Summary

In this section, we studied the minimal theory of leptobaryons. We argued that the scale of baryon number violation can be as low as the electroweak scale without being in conflict with current bounds from proton decay. However, the scale of baryon number violation is not restricted to be at the electroweak scale and can be interpreted as a free parameter. After a short introduction to the model, we focused on the dark matter phenomenology of the leptobaryons. The lightest leptobaryon is automatically stabilized by a remnant Z_2 symmetry. We assumed that the lightest leptobaryon is the Standard Model singlet Majorana fermion χ. Investigating the dark matter relic density, we found two viable dark matter regimes. In the resonant dark matter regime, the dark matter annihilation is dominated by $\chi\chi \to Z_\text{B} \to \bar{q}q$ such that we find relatively light dark matter, $m_\chi \simeq M_{Z_\text{B}}/2$. However, current dark matter direct detection experiments push the resonant dark matter scenario to more tuned regimes.

The non-resonant dark matter scenario leads to interesting phenomenology as it can constrain the scalar mixing angle θ stronger than Higgs studies at the LHC. Moreover, the dark matter in the non-resonant regime is fairly heavy, $m_\chi \gtrsim M_{Z_\text{B}}, M_{H_\text{B}}$, such that we can apply the internal consistency condition that the heavy leptobaryons should not destabilize the scalar potential in the direction of H_B at mass scales below their mass.

Finally, we turned to the discovery potential of the leptophobic gauge boson Z_B and baryonic Higgs H_B at the LHC. The absence of dijet resonances pushes the leptophobic gauge boson Z_B to larger masses and smaller couplings g_B. The baryonic Higgs H_B displays an interesting decay profile where for small scalar mixing angles the loop mediated decays to $Z\gamma$ and $\gamma\gamma$ become sizable.

CHAPTER 3

LOW SCALE UNIFICATION - TESTING THE ORIGIN OF SYMMETRIES

IN THIS CHAPTER, we extend and combine the ideas of the previous section. We construct an UV complete non-abelian left-right symmetric gauge theory which can be broken to the Standard Model with gauged baryon number at low energy scales. Grand Unified Theories (GUTs) explain the particle content and structure of the Standard Model by embedding the Standard Model into a more fundamental theory with enhanced symmetries. The Standard Model of particle physics is then a low energy realization of a theoretically more appealing theory. However, conventional Grand Unified Theories have to be implemented at the GUT scale, $M_{\text{GUT}} \sim 10^{14-16}$ GeV, to be consistent with the lower limits on the proton lifetime [109]. Therefore, the theoretically beautiful idea of unification is nearly untestable.

In this work, we attempt to lower the UV completion scale of the Standard Model by constructing an UV complete theory which can be broken to the Standard Model with local baryon number. As we already saw in section 2.2, we can stabilize the proton by promoting baryon number to a gauge symmetry. Thus, we can evade the limits on the proton lifetime and realize the UV complete theory at low scales.

Why is the stabilization of the proton not only of phenomenological importance, but also the key to soften the hierarchy problem?
Interpreting the Standard model as a low energy effective field theory, we find at leading order the dimension six proton mediating operator [144, 145]

$$\mathcal{L} \supset \frac{c_p}{\Lambda_p^2} Q_L Q_L Q_L \ell_L \,. \tag{3.1}$$

If an UV completion of the Standard Model does not forbid or suppress this higher-dimensional operator, then current experimental bounds require

$$\Lambda_p \gtrsim 10^{14-16} \text{ GeV}, \tag{3.2}$$

for order one couplings ($c_P \simeq \mathcal{O}(1)$). Not only is a huge separation of scales imposed by the theoretical considerations on the Planck scale, but a huge separation of scales is also enforced by our experimental observations. To evade these experimental constraints, to lower the UV completion scale of the Standard Model, and to alleviate the hierarchy problem, a stabilization of the proton is crucial. Now, the next question we have to answer is: What is the structure of the gauge theory which can be broken to $G_{\text{SM}} \otimes U(1)_B$ at low energies?

In order to have a well defined baryon number, quarks and leptons cannot be in the same multiplet. An example of such a theory is the minimal left-right symmetric theory discussed in section 2.1. Moreover, see [146] for a discussion of gauged baryon number in the context of left-right symmetric theories. However, left-right symmetric theories are not an UV complete theory because the abelian $U(1)_{B-L}$ gauge symmetry leads to a Landau pole at high energies. At energies above the Landau pole, the theory is invalid.

We can embed the left-right symmetric gauge theory into the non-abelian gauge theory $SU(3)_C \otimes SU(3)_L \otimes SU(3)_R$ known as trinification [147, 148, 149, 150, 151, 152]. Trinification has a well defined baryon number. As in the Standard Model, baryon number is a global symmetry of the theory. The theory which we construct is based on the non-abelian gauge group $SU(4)_C \otimes SU(3)_L \otimes SU(3)_R$ [4]. Baryon number is thus the fourth color of $SU(4)_C$. This gauge group is also the symmetry group with the minimal rank to embed trinification with local baryon number. We will also extend these ideas and discuss a gauge theory based on the even more symmetric symmetry group $SU(4)_C \otimes SU(4)_L \otimes SU(4)_R$. Note that, in contrast to the last section, we discuss a top-down extension of the Standard Model in this sector.

An UV completion of the Standard Model at low scales is not only testable, but by lowering the UV completion scale of the Standard Model, we also allow for a new approach towards the hierarchy problem. We do not know the scale of quantum gravity and large extra dimensions could lower the Planck scale significantly [54]. Moreover, by putting forward a low scale UV completion which incorporates the ideas of left-right symmetric theories and local baryon number, we predict a variety of new scales. These new scales can attenuate the hierarchy problem further.

3.1 The 433 Theory

The theory presented in this section is the first experimentally valid UV completion of the Standard Model extension of local baryon number. It is further an UV complete theory which can be realized at low energy scales such that in contrast to conventional Grand Unified Theories it can be tested at the LHC and future colliders. The theory is minimal in the sense that the gauge group has the lowest possible rank to embed trinification and gauged baryon number.

We consider the gauge group

$$G_{433} = SU(4)_C \otimes SU(3)_L \otimes SU(3)_R \,, \tag{3.3}$$

with the Standard Model fermions embedded in

$$Q \sim (4, \bar{3}, 1) \,, \quad Q^c \sim (\bar{4}, 1, 3) \,, \quad L \sim (1, 3, \bar{3}) \,.$$

Note that as G_{433} is a non-abelian gauge group, it illustrates the charge quantization in the Standard Model. However, this theory is again not anomaly free with non-vanishing anomalies

$$\begin{aligned} &\mathcal{A}(SU(3)_L^3) = -\frac{1}{8} \,, \quad \mathcal{A}(SU(3)_R^3) = \frac{1}{8} \,, \\ &\mathcal{A}(SU(4)_C \otimes SU(3)_L^2) = -\frac{3}{2} \,, \quad \mathcal{A}(SU(4)_C \otimes SU(3)_R^2) = \frac{3}{2} \,. \end{aligned} \tag{3.4}$$

To cancel the anomalies familywise and have a consistent theory, we have to introduce three copies of the additional fermions

$$\Psi^c \sim (1, 3, 1) \quad \text{and} \quad \eta \sim (1, 1, \bar{3}) \,.$$

In matrix notation, we see how the Standard Model fermions and new fermions are aligned in the multiplets. The colored multiplets are given by

$$Q = \begin{array}{c} \xrightarrow{\qquad SU(3)_L \qquad} \\ \begin{pmatrix} d_r & u_r & D_r \\ d_b & u_b & D_b \\ d_g & u_g & D_g \\ \Psi_d & \Psi_u & \Psi_D \end{pmatrix} \end{array} \Bigg\downarrow {\scriptstyle SU(4)_C} = \begin{pmatrix} \mathfrak{q} \\ \Psi \end{pmatrix} \,,$$

$$Q^c = \begin{array}{c} \xrightarrow{\qquad SU(4)_C \qquad} \\ \begin{pmatrix} d^c_{\bar{r}} & d^c_{\bar{b}} & d^c_{\bar{g}} & \eta^c_d \\ u^c_{\bar{r}} & u^c_{\bar{b}} & u^c_{\bar{g}} & \eta^c_u \\ D^c_{\bar{r}} & D^c_{\bar{b}} & D^c_{\bar{g}} & \eta^c_D \end{pmatrix} \end{array} \Bigg\downarrow {\scriptstyle SU(3)_R} = \begin{pmatrix} \mathfrak{q}^c & \eta^c \end{pmatrix} \,.$$

The quark multiplets Q and Q^c contain, apart from the Standard Model quarks $q = (d\, u)$ and anti-quarks $q^c = (d^c\, u^c)^T$, an additional heavy down-type quark D and anti-quark

D^c. We further find the colorless fractional charged fields Ψ and η^c inside the quark multiplets. These new exotic particles form Dirac fermions with the additional fermions Ψ^c and η which were required by anomaly cancellation. The additional fermions are given by

$$\Psi^c = \overset{\xrightarrow{\hspace{6em}SU(3)_L\hspace{6em}}}{\begin{pmatrix}\Psi^c_d & \Psi^c_u & \Psi^c_D\end{pmatrix}} \quad \text{and} \quad \eta = \begin{pmatrix}\eta_d \\ \eta_u \\ \eta_D\end{pmatrix} \Big\downarrow {\scriptstyle SU(3)_R}\,.$$

Note that the new colorless fermions carry the same fractional electric charge as the Standard Model quarks

$$\begin{aligned}
Q_{\text{EM}}(\Psi_u) &= +2/3\,, \quad Q_{\text{EM}}(\Psi_d) = Q_{\text{EM}}(\Psi_D) = -1/3, \\
Q_{\text{EM}}(\Psi^c_u) &= -2/3\,, \quad Q_{\text{EM}}(\Psi^c_d) = Q_{\text{EM}}(\Psi^c_D) = +1/3, \\
Q_{\text{EM}}(\eta_u) &= +2/3\,, \quad Q_{\text{EM}}(\eta_d) = Q_{\text{EM}}(\eta_D) = -1/3, \\
Q_{\text{EM}}(\eta^c_u) &= -2/3\,, \quad Q_{\text{EM}}(\eta^c_d) = Q_{\text{EM}}(\eta^c_D) = +1/3\,.
\end{aligned} \tag{3.5}$$

Moreover, in matrix notation the lepton multiplet is given by

$$L = \overset{\xrightarrow{\hspace{6em}SU(3)_R\hspace{6em}}}{\begin{pmatrix} N_1 & E^+ & \nu \\ E^- & N_2 & e^- \\ \nu^c & e^+ & N_3 \end{pmatrix}} \Big\downarrow {\scriptstyle SU(3)_L}\,.$$

The lepton multiplet L contains the Standard Model leptons $e^\pm$ and ν. Lepton number is therefore explicitly broken. In contrast to the last section, we thus cannot automatically also construct a theory of local lepton number. We further find the right-handed neutrino ν^c in L. Additionally, new heavy singly charged leptons $E^\pm$ and three new neutral leptons N_1, N_2, and N_3 are included in L.

Normalizing the Gell-Mann matrices such that $\lambda^8 = 1/\sqrt{3}\,\text{diag}(1,1,-2)$ and defining the generators of $SU(3)_{L,R}$ such that $\text{Tr}(T^a_{L,R}T^b_{L,R}) = \delta^{ab}_{L,R}/2$, we can identify $T^a_{L,R} = \lambda^a_{L,R}/2$. We then find for the known conserved electroweak charges

$$Q_{\text{EM}} = T^3_L + Y \quad \text{with} \quad Y = T^3_R + \frac{1}{2}Y_{(B-L)}\,, \tag{3.6}$$

and with

$$Y_{(B-L)} = -\frac{2}{\sqrt{3}}T^8_L - \frac{2}{\sqrt{3}}T^8_R\,. \tag{3.7}$$

The generators of $SU(4)_C$ are normalized such that $\lambda^{15}_C = 1/\sqrt{6}\,\text{diag}(1,1,1,-3)$ and $\text{Tr}(T^a_C T^b_C) = \delta^{ab}_C/2$ where $T^a_C = \lambda^a_C/2$. The conserved charge corresponding to local baryon number is then given by

$$Y_B = 2\sqrt{\frac{2}{3}}T_C^{15}\,. \tag{3.8}$$

The Higgs sector of the theory is composed of

$$\xi \sim (15,1,1)\,,\quad S \sim (4,1,1)\,,\quad \Phi_1 \sim (1,3,\bar{3})\,,\quad \Phi_2 \sim (1,3,\bar{3})\,,\quad \Phi_3 \sim (1,3,\bar{3})\,.$$

Note that ξ has no tree-level interactions with the fermions in the theory. Yet, ξ will develop the vacuum expectation value

$$\langle \xi \rangle = v_C\, T_C^{15}\,, \tag{3.9}$$

which breaks $SU(4)_C$ such that

$$SU(4)_C \to SU(3)_C \otimes U(1)_B\,.$$

Baryon number as the fourth color was first discussed in [153, 154]. These theories are however by comparison not UV complete and cannot embed the Standard Model with gauged baryon number. In matrix notation, the scalar degrees of freedom S and Φ_i with $i \in \{1,2,3\}$ are given by

$$S = \begin{pmatrix} S_r \\ S_b \\ S_g \\ S_B \end{pmatrix} \Bigg\downarrow_{SU(4)_C} = \begin{pmatrix} S_C \\ S_B \end{pmatrix}\,,$$

$$\xrightarrow{\quad SU(3)_R \quad}$$

$$\Phi = \begin{pmatrix} \varphi_1^0 & \varphi^+ & H_L^0 \\ \varphi^- & \varphi_2^0 & H^- \\ H_R^0 & H^+ & \phi^0 \end{pmatrix} \Bigg\downarrow_{SU(3)_L} = \begin{pmatrix} \phi & H_L \\ H_R & \phi^0 \end{pmatrix}\,.$$

The scalar field S consists of three colored degrees of freedom $S_C = (S_r, S_b, S_g)^T$ and a complete Standard Model singlet S_B. The scalar fields S_C and S_B carry baryon number. Therefore, as S_B develops a non-trivial vacuum expectation value, it breaks $U(1)_B$. The scalar bi-triplets Φ_i consist of a $SU(2)_L \otimes SU(2)_R$ bi-doublet ϕ_i, a left-handed Higgs doublet $(H_L)_i$, a right-handed Higgs doublet $(H_R)_i$, and a new Standard Model singlet $(\phi^0)_i$.

The interactions of the quark fields and the scalar sector are described by

$$\begin{aligned} -\mathcal{L}_Q = & QQ^c(y_1\Phi_1 + y_2\Phi_2 + y_3\Phi_3) + \eta\Psi^c(k_1\Phi_1^\dagger + k_2\Phi_2^\dagger + k_3\Phi_3^\dagger) \\ & + y_\Psi Q\Psi^c S^\dagger + y_\eta \eta Q^c S + \text{h.c.}\,. \end{aligned} \tag{3.10}$$

Expanding the quark interactions, we find for the individual components

$$
\begin{aligned}
QQ^c\Phi = \; Q^iQ^c_a\Phi^i_a = & \, dd^c\varphi^0_1 + uu^c\varphi^0_2 + du^c\varphi^+ + ud^c\varphi^- \\
& + dD^cH^0_L + Dd^cH^0_R + Du^cH^+ + uD^cH^- + DD^c\phi^0 \, .
\end{aligned}
\tag{3.11}
$$

Now and below, we use the convention that $SU(3)_L$ indices will be written in upper case with $\{i,j,k\}$ and $SU(3)_R$ indices in lower case with $\{a,b,c\}$. Note that the summation over the $SU(4)_C$ indices is implicit. The terms $dD^cH^0_L$ and $Dd^cH^0_R$ will lead to mass mixing of the Standard Model down-type quarks and the new heavy quarks. See the Appendix 7.7 for a discussion of the fermion mixing. Furthermore, we can also expand the new exotic quark interactions

$$
\begin{aligned}
Q\Psi^cS^\dagger = & \, u_r\Psi^c_uS^*_{\bar{r}} + u_b\Psi^c_uS^*_{\bar{b}} + u_g\Psi^c_uS^*_{\bar{g}} + d_r\Psi^c_dS^*_{\bar{r}} + d_b\Psi^c_dS^*_{\bar{b}} + d_g\Psi^c_dS^*_{\bar{g}} \\
& + D_r\Psi^c_DS^*_{\bar{r}} + D_b\Psi^c_DS^*_{\bar{b}} + D_g\Psi^c_DS^*_{\bar{g}} + \Psi_u\Psi^c_uS^*_B + \Psi_d\Psi^c_dS^*_B + \Psi_D\Psi^c_DS^*_B \, , \\
\eta Q^cS = & \, \eta_uu^c_{\bar{r}}S_r + \eta_uu^c_{\bar{b}}S_b + \eta_uu^c_{\bar{g}}S_g + \eta_dd^c_{\bar{r}}S_r + \eta_dd^c_{\bar{b}}S_b + \eta_dd^c_{\bar{g}}S_g \\
& + \eta_DD^c_{\bar{r}}S_r + \eta_DD^c_{\bar{b}}S_b + \eta_DD^c_{\bar{g}}S_g + \eta_u\eta^c_uS_B + \eta_d\eta^c_dS_B + \eta_D\eta^c_DS_B \, ,
\end{aligned}
\tag{3.12}
$$

where the color indices are shown explicitly for clarity. The gauge invariance forces the colored scalars S_C to always interact with a colored quark and a colorless fractional charged fermion. The fractional charged fermions receive a mass contribution from S_B as S_B develops a vacuum expectation value (see section 3.1.1).

The interactions of the leptonic fields with the scalar degrees of freedom are described by

$$
-\mathcal{L}_L = \frac{1}{2}LL(h_1\Phi_1 + h_2\Phi_2 + h_3\Phi_3) + \text{h.c.} \, . \tag{3.13}
$$

Expanding the totally asymmetric interactions of the leptonic fields, we find for the individual components

$$
\begin{aligned}
\frac{1}{2}LL\Phi = & \, \frac{1}{2}\epsilon^{ijk}\epsilon_{abc}L^i_aL^j_b\Phi^k_c \\
= & \, (N_2N_3 - e^-e^+)\varphi^0_1 + (e^+\nu - E^+N_3)\varphi^- + (e^-\nu^c - E^-N_3)\varphi^+ \\
& + (N_1N_3 - \nu\nu^c)\varphi^0_2 + (E^+e^- - \nu N_2)H^0_R + (E^-e^+ - \nu^cN_2)H^0_L \\
& + (\nu E^- - N_1e^-)H^+ + (\nu^cE^+ - N_1e^+)H^- + (N_1N_2 - E^-E^+)\phi^0 \, .
\end{aligned}
\tag{3.14}
$$

The totally asymmetric interaction forbids tree-level Majorana mass terms for the leptons. Yet, the theory generates Majorana masses at loop level (see section 3.1.2). In addition, the interaction terms $(E^+e^- - \nu N_2)H^0_R$ and $(E^-e^+ - \nu^cN_2)H^0_L$ will lead to a mass mixing of the singly charged fermions $E^\pm$ and $e^\pm$, and the neutral fermions ν and N_1. Again, see the Appendix 7.7 for the complete tree-level fermion mass matrices. As ϕ^0 acquires a vacuum expectation value the beyond the Standard Model fermions $E^\pm$, N_1, and N_2

obtain a mass (see section 3.1.2).

As the scalar field ξ acquires the vacuum expectation value (3.9), it breaks $SU(4)_C$

$$SU(4)_C \otimes SU(3)_L \otimes SU(3)_R \to SU(3)_C \otimes SU(3)_L \otimes SU(3)_R \otimes U(1)_B \,.$$

We thus found a model of trinification where the former global symmetry of baryon number was promoted to a $U(1)$ gauge symmetry and embedded in a non-abelian gauge theory. Upon symmetry breaking, the colored fields decompose as

$$\begin{aligned}
Q &\to \underset{\sim(3,\bar{3},1,1/3)}{\mathfrak{q}} + \underset{\sim(1,\bar{3},1,-1)}{\Psi}\,, \\
Q^c &\to \underset{\sim(\bar{3},1,3,-1/3)}{\mathfrak{q}^c} + \underset{\sim(1,1,3,1)}{\eta^c}\,, \\
S &\to \underset{\sim(3,1,1,-1/3)}{S_C} + \underset{\sim(1,1,1,1)}{S_B}\,.
\end{aligned}$$

The interactions in the quark sector then take the form

$$\begin{aligned}
-\mathcal{L}_Q = {} & y_i \left(\mathfrak{q}\mathfrak{q}^c + \Psi\eta^c\right)\Phi_i + k_i \eta\Psi^c\Phi_i^\dagger \\
& + y_\Psi \left(\mathfrak{q}\Psi^c S_C^\dagger + \Psi\Psi^c S_B^*\right) + y_\eta \left(\eta\mathfrak{q}^c S_C + \eta\eta^c S_B\right) + \text{h.c.}\,,
\end{aligned} \tag{3.15}$$

with $i \in \{1, 2, 3\}$.

So far, we have mainly presented how the Standard Model fermions are embedded and interact in the 433 theory. As we are breaking G_{433} to trinification with gauged baryon number, the question arises: What are the bounds on the symmetry breaking scales? We will give an overview of the symmetry breaking pattern and the scales involved in the next section. Moreover, we have to explicitly show the stability of the proton to ensure the possibility of a low scale UV completion.

3.1.1 Symmetry Breaking and Scales

We now first discuss the overall symmetry breaking structure before we turn to the individual steps of the symmetry breaking in the next section. The general symmetry breaking pattern we follow is displayed below.

$$\boxed{SU(4)_C \otimes SU(3)_L \otimes SU(3)_R}$$

$$\langle \xi \rangle \neq 0$$

$$\boxed{SU(3)_C \otimes SU(3)_L \otimes SU(3)_R \otimes U(1)_B}$$

$$\langle \phi^0 \rangle \neq 0$$

$$\boxed{SU(3)_C \otimes SU(2)_L \otimes SU(2)_R \otimes U(1)_{B-L} \otimes U(1)_B}$$

$$\langle H_R^0 \rangle \neq 0$$

$$\boxed{SU(3)_C \otimes SU(2)_L \otimes U(1)_Y \otimes U(1)_B}$$

As the color adjoint field ξ breaks $SU(4)_C$ to $SU(3)_C \otimes U(1)_B$, the symmetry group reduces to trinification with local baryon number. Trinification is discussed in the literature as independent UV completion of the Standard Model [147, 148, 149, 150, 151, 152]. The scalar bi-triplets Φ_i break the trinification gauge group via a left-right symmetric theory to the Standard Model gauge symmetry

$$3_C 3_L 3_R \xrightarrow{\Lambda_{33}} 3_C 2_L 2_R 1_{B-L} \xrightarrow{\Lambda_R} 3_C 2_L 1_Y \,,$$

with Λ_{33} the scale of trinification breaking and Λ_R the scale of left-right symmetry breaking.

The intermediate left-right symmetric theory is constrained by LHC studies for new charged currents (see section 2.1.2). The most optimistic lower limit on the scale of left-right symmetry breaking is obtained by considering the perturbative upper limit of the $SU(2)_R$ gauge coupling ($g_R \to 4\pi$). We can then derive from equation (2.30) the lower bound

$$\Lambda_R \gtrsim 500\,\text{GeV}. \tag{3.16}$$

We will see in the next section that the new down-type quarks D and anti-quarks D^c as well as the new charged leptons $E^\pm$ acquire a mass proportional to the trinification breaking scale Λ_{33}. The absence of these new particles at the LHC leads to lower mass bounds in the TeV range for these new particles [155]. Therefore, if we assume order one couplings, the trinification breaking scale Λ_{33} is also experimentally bounded from below with

$$\Lambda_{33} \gtrsim 10^3 \text{ GeV}. \tag{3.17}$$

The breaking of baryon number is orthogonal to the symmetry breaking of trinification. Baryon number can therefore be broken before, after, or even in between the breaking of trinification.

Upon the breaking of $U(1)_B$, the new fermions Ψ, Ψ^c, η, and η^c acquire a mass. Baryon number is broken once the baryonic scalar S_{B} develops a vacuum expectation value

$$\langle S_B \rangle = \frac{v_B}{\sqrt{2}}\,. \tag{3.18}$$

We then find the following mass terms in the Lagrangian

$$-\mathcal{L}_Q \supset m_\Psi \left(\Psi_u \Psi_u^c + \Psi_d \Psi_d^c + \Psi_D \Psi_D^c\right) + m_\eta \left(\eta_u \eta_u^c + \eta_d \eta_d^c + \eta_D \eta_D^c\right)\,, \tag{3.19}$$

where

$$m_\Psi = y_\Psi \frac{v_B^*}{\sqrt{2}} \quad \text{and} \quad m_\eta = y_\eta \frac{v_B}{\sqrt{2}}\,. \tag{3.20}$$

In the limit $v_B \to \infty$ the new fermions decouple from the theory and the theory reduces to the known theory of trinification. Again, the non-observation of new fractional charged fermions at the LHC [156] leads to an experimental lower bound on the scale of baryon number violation in the TeV range

$$v_B \gtrsim 10^3 \,\text{GeV}\,. \tag{3.21}$$

As the color adjoint field ξ does not have tree-level interactions with the fermions of the theory, the bounds on the scale of $SU(4)_C$ breaking stem from LHC constraints on new colored gauge bosons [156]. In section 3.1.3, we will show that upon the $SU(4)_C$ breaking by $\langle\xi\rangle$, we find three complex massive gauge bosons with mass proportional to v_C. The lower bound on the vacuum expectation value v_C is therefore also in the TeV range

$$v_C \gtrsim 10^3 \,\text{GeV}\,. \tag{3.22}$$

In summary, we just argued that the full symmetry breaking of the 433 theory can be realized in the multi-TeV range. Thereby, none of the scales is related to the electroweak scale, but all of them are testable at the LHC and future colliders.

However, in order to be able to break the theory at such low energy scales, the proton has to be stable. Analyzing the theory, we find that proton decay is mediated by the dimension nine operator

$$\mathcal{O}_{\text{proton}} = c_p \frac{QQQL\Phi\Phi S^\dagger}{(\Lambda_{433})^5} \,. \tag{3.23}$$

Hence, the decay of the proton is suppressed by the 433 scale Λ_{433} to the fifth power. The proton decay rate thus scales as

$$\Gamma_p \sim \frac{m_p^5 \langle\Phi\rangle^4 \langle S\rangle^2}{(\Lambda_{433})^{10}} \,, \tag{3.24}$$

with m_p the mass of the proton. Following our previous discussion, we assume $\langle S\rangle \sim 10^3$ GeV and also $\langle\Phi\rangle \sim 10^3$ GeV. Thus, for the theory to be in agreement with the lower limit on the proton lifetime $\tau(p \to e^+\pi^0) \gtrsim 10^{34}$ yrs. [105], the lower bound for physics beyond the 433 theory is given by

$$\Lambda_{433} \gtrsim 10^7 \text{ GeV}. \tag{3.25}$$

Note that the scale of minimum validity of the 433 theory is thus seven to nine orders of magnitude smaller than the GUT scale. However, proton decay is not as suppressed as in the bottom-up approach to gauged baryon number discussed in section 2.2.

The 433 theory is at least valid until $\Lambda_{433} \sim 10^7$ GeV. Any new kind of physics beyond the 433 theory can be realized at scales above Λ_{433} without being in conflict with the current proton lifetime bounds. Nevertheless, the remarkable feature of the 433 theory is that we are not in need of new physics beyond. The 433 theory is based on a non-abelian gauge symmetry and is thus valid for arbitrary high energy scales. Moreover, as large extra dimensions can lower the Planck scale, we could even expect a theory of quantum gravity to be realized at $\Lambda_{433} \sim 10^7$ GeV. By proposing the 433 theory and demonstrating the possibility of a consistent UV completion in four dimensions at energy scales as low as 10^{3-4} GeV, we have significantly diminished the amount of fine-tuning required by a low Higgs mass. Without argument, the proton decay scale Λ_{433} is still well separated from the electroweak scale. Yet, the tuning involved looks less intimidating:

$$\frac{M_H^2}{\Lambda_{433}^2} \simeq 10^{-10} \quad \text{compared to} \quad \frac{M_H^2}{M_{\text{Pl}}^2} \simeq 10^{-26} \,. \tag{3.26}$$

A possible solution to the now arising little hierarchy could originate in the four additional scales of the 433 theory (Λ_R, Λ_{33}, Λ_B, and Λ_C). For example, a symmetry relating the Higgs mass contributions such that they cancel could be at work. Also, the newly proposed clockwork mechanism could be responsible for a small electroweak Higgs mass [55]. However, further investigations are necessary to address the little hierarchy problem in the 433 theory.

Note that, in pure trinification, proton decay is mediated via a dimension eight operator. Thus, the proton decay scale of pure trinification can be as low as 10^8 GeV. By gauging baryon number, we could hence lower the potential scale of quantum gravity further by one order of magnitude. In the next section, we discuss the theory of trinification with gauged baryon number and investigate the individual symmetry breaking steps to the Standard Model with local baryon number.

3.1.2 Trinification and Effective Left-Right Symmetric Theory

In this section, we discuss the individual symmetry breaking steps of the 433 theory in more detail. The theory known as trinification is a gauge theory based on the symmetry group

$$G_{333} = SU(3)_C \otimes SU(3)_L \otimes SU(3)_R \,, \tag{3.27}$$

with the Standard Model fermions in the representations

$$\mathfrak{q} \sim (3, \bar{3}, 1) \,, \quad \mathfrak{q}^c \sim (\bar{3}, 1, 3) \,, \quad L \sim (1, 3, \bar{3}) \,.$$

However, due to the breaking of $SU(4)_C$ with the color adjoint Higgs field ξ, we find a gauge theory based on

$$G_{333\mathrm{B}} = SU(3)_C \otimes SU(3)_L \otimes SU(3)_R \otimes U(1)_B \,,$$

with three generations of additional fermions

$$\Psi \sim (1, \bar{3}, 1) \,, \quad \Psi^c \sim (1, 3, 1) \,, \quad \eta \sim (1, 1, \bar{3}) \,, \quad \eta^c \sim (1, 1, 3) \,.$$

Moreover, these fermions are the minimal number of additional fermionic degrees of freedom to have a consistent theory which promotes the global baryon number symmetry of trinification to a local symmetry. The anomalies are canceled familywise.

As the neutral components of the bi-triplet scalar fields Φ_i acquire a vacuum expectation value, trinification is broken to a left-right symmetric theory and finally to the Standard Model. Symmetry breaking would only require the presence of one scalar bi-triplet. However, as the scalar fields develop a vacuum expectation value, they induce a mass for the fermions. In order to reproduce the measured Standard Model fermion masses, at least two scalar bi-triplets are needed. Nonetheless, with only two scalar bi-triplets, a fine-tuning of the Yukawa couplings of the order of 10^8 is necessary to satisfy current constraints on the neutrino masses and at the same time satisfy the constraints on the masses of new heavy down-type quarks D and charged fermions $E^{\pm}$ [147]. To avoid any fine-tuning concerning the Standard Model fermion masses, we therefore require three scalar bi-triplets Φ_i.

For simplicity, we will consider the following vacuum expectation value assignment for the three scalar bi-triplets

$$\langle \Phi_1 \rangle = \begin{pmatrix} v_1 & 0 & \hat{0} \\ 0 & \hat{0} & 0 \\ \hat{0} & 0 & \hat{0} \end{pmatrix} , \langle \Phi_2 \rangle = \begin{pmatrix} \hat{0} & 0 & \hat{0} \\ 0 & v_2 & 0 \\ \hat{0} & 0 & \hat{0} \end{pmatrix} , \langle \Phi_3 \rangle = \begin{pmatrix} \hat{0} & 0 & \hat{0} \\ 0 & \hat{0} & 0 \\ v_R & 0 & v_{33} \end{pmatrix} , \tag{3.28}$$

with the hierarchy of scales $v_{33} \gg v_R \gg v_1, v_2$ (see symmetry breaking pattern in section 3.1.1). Note that in principle, further neutral components of the scalar fields which are denoted by $\hat{0}$ in equation (3.28) could develop a vacuum expectation value and contribute to the symmetry breaking. However, to reproduce the observed Standard Model, the above vacuum expectation value assignment is sufficient. Our discussion can be viewed as the limit $v_{33}, v_R, v_1, v_2 \gg \hat{0}$.

The vacuum expectation value $\langle(\phi^0)_3\rangle = v_{33}$ breaks trinification to a left-right symmetric theory

$$SU(3)_L \otimes SU(3)_R \xrightarrow{\langle(\phi^0)_3\rangle = v_{33}} SU(2)_L \otimes SU(2)_R \otimes U(1)_{B-L} \,.$$

Upon symmetry breaking, the colored and fractional charged fermionic fields decompose as

$$\begin{aligned}
\mathfrak{q} &\to \underset{\sim(3,\bar{2},1,1/3,1/3)}{q} + \underset{\sim(3,1,1,-2/3,1/3)}{D}\,, \\
\mathfrak{q}^c &\to \underset{\sim(\bar{3},1,2,-1/3,-1/3)}{q^c} + \underset{\sim(\bar{3},1,1,2/3,-1/3)}{D^c}\,, \\
\Psi &\to \underset{\sim(1,\bar{2},1,1/3,-1)}{\Psi_q} + \underset{\sim(1,1,1,-2/3,-1)}{\Psi_D}\,, \\
\Psi^c &\to \underset{\sim(1,2,1,-1/3,0)}{\Psi^c_q} + \underset{\sim(1,1,1,2/3,0)}{\Psi^c_D}\,, \\
\eta &\to \underset{\sim(1,1,\bar{2},1/3,0)}{\eta_q} + \underset{\sim(1,1,1,-2/3,0)}{\eta_D}\,, \\
\eta^c &\to \underset{\sim(1,1,2,-1/3,1)}{\eta^c_q} + \underset{\sim(1,1,1,2/3,1)}{\eta^c_D}\,.
\end{aligned}$$

The symmetry breaking separates the Standard Model quarks q and anti-quarks q^c from the heavy down-type quarks D and anti-quarks D^c. The fundamental and anti-fundamental representations of $SU(3)_L$ and $SU(3)_R$ are broken to $SU(2)_L$ and $SU(2)_R$ doublets and singlets, respectively, whereas the bi-triplet lepton field decomposes as

$$L \to \underset{\sim(1,2,\bar{2},0,0)}{\mathfrak{L}} + \underset{\sim(1,2,1,-1,0)}{\ell} + \underset{\sim(1,1,\bar{2},1,0)}{\ell^c} + \underset{\sim(1,1,1,0,0)}{N_3}\,.$$

The Standard Model leptons are detached from the fermionic bi-doublet $\mathfrak{L}$ and the Standard Model singlet N_3. The scalar bi-triplets decompose similarly

$$\Phi \to \underset{\sim(1,2,\bar{2},0,0)}{\phi} + \underset{\sim(1,2,1,-1,0)}{H_L} + \underset{\sim(1,1,\bar{2},1,0)}{H_R} + \underset{\sim(1,1,1,0,0)}{\phi^0}\,.$$

Like the leptons, the left-handed and right-handed Higgs doublets are decoupled from the scalar bi-doublet ϕ and the scalar field responsible for the breaking of trinification ϕ^0.

The lepton interactions in the effective left-right symmetric theory are then given by

$$\begin{aligned}
-\mathcal{L}_L \supset \epsilon_{ab}\epsilon^{nm}\, h_i \Big(&\frac{1}{2}\mathfrak{L}^n_a \mathfrak{L}^m_b \phi^0_i + \mathfrak{L}^n_a N_3 (\phi_i)^m_b - \ell^n \ell^c_a (\phi_i)^m_b \\
&+ \ell^n \mathfrak{L}^m_a (H_{R\,i})_b - \mathfrak{L}^n_a \ell^c_b (H_{L\,i})^m\Big)\,,
\end{aligned} \tag{3.29}$$

with the convention that $\{n, m\}$ stand for $SU(2)_L$ indices and $\{a, b\}$ are $SU(2)_R$ indices. We defined $\epsilon^{12} = \epsilon_{12} = -\epsilon^{21} = -\epsilon_{21} = 1$ and $\epsilon^{nn} = \epsilon_{aa} = 0$. The asymmetric nature of the leptonic interaction in trinification is still present. The quark interactions now take the form

$$\begin{aligned}
-\mathcal{L}_Q \supset y_i \Big(& qq^c\phi_i + qD^c(H_L)_i + Dq^c(H_R)_i + DD^c(\phi^0)_i \\
& + \Psi_q\eta_q^c\phi_i + \Psi_q\eta_D^c(H_L)_i + \Psi_D\eta_q^c(H_R)_i + \Psi_D\eta_D^c(\phi^0)_i \Big) \\
& + k_i \left(\eta_q\Psi_q^c\phi_i^\dagger + \eta_q\Psi_D^c(H_L)_i^\dagger + \eta_D\Psi_q^c(H_R)_i^\dagger + \eta_D\Psi_D^c(\phi^0)_i^* \right) \\
& + y_\Psi \left(q\Psi_q^c S_C^* + D\Psi_D^c S_C^* + \Psi_q\Psi_q^c S_B^* + \Psi_D\Psi_D^c S_B^* \right) \\
& + y_\eta \left(\eta_q q^c S_C + \eta_D D^c S_C + \eta_q\eta_q^c S_B + \eta_D\eta_D^c S_B \right) \,.
\end{aligned} \tag{3.30}$$

Breaking trinification creates the mass terms

$$-L \supset m_L(N_1N_2 - E^+E^-) + m_D(DD^c + \Psi_D\eta_D^c) + m_{\eta\Psi}\eta_D\Psi_D^c \,, \tag{3.31}$$

with

$$m_L = h_3 v_{33} \,, \quad m_D = y_3 v_{33} \,, \quad m_{\eta\Psi} = k_3 v_{33} \,. \tag{3.32}$$

The new leptons $\mathfrak{L}$, additional down-type quarks D, and anti-quarks D^c and new fractional charged fermions Ψ, Ψ^c, η, and η^c decouple from the theory as $v_{33} \to \infty$. It is important to note that the new fermions needed for the anomaly cancellations upon promoting baryon number to a gauge symmetry (Ψ, Ψ^c, η, and η^c) can acquire heavy vector-like masses even if baryon number is broken at a lower scale then trinification. The only beyond the Standard Model fermion apart from the right-handed neutrino ν^c which does not have a tree-level mass contribution proportional to the breaking scale of trinification is the neutral lepton N_3. However, one-loop mass corrections give

$$m_{N_3} \sim \frac{h_3 v_{33}}{16\pi^2} \,, \tag{3.33}$$

such that also N_3 decouples from the theory as $v_{33} \to \infty$ [147, 151]. We will discuss the one-loop mass contributions to N_3 in more detail below.

In the limit where we integrate out the new heavy fermions with mass terms proportional to v_{33}, we find the simple left-right symmetric theory

$$\begin{aligned}
-L \supset & \; qq^c \left(y_1\phi_1 + y_2\phi_2 + y_3\phi_3 \right) \\
& - \epsilon_{ab}\epsilon^{nm} \left(h_1\ell^n\ell_a^c(\phi_1)_b^m + h_2\ell^n\ell_a^c(\phi_2)_b^m + h_3\ell^n\ell_a^c(\phi_3)_b^m \right) \,.
\end{aligned} \tag{3.34}$$

Note that this left-right symmetric theory differs significantly from the left-right symmetric theory presented in section 2.1 because the theory inherits the $SU(3)_L \otimes SU(3)_R$ invariant interactions. We thus also see from the Lagrangian in equation (3.34) that a single bi-doublet ϕ could not reproduce the Standard Model fermion masses in contrast to the left-right symmetric theory presented in section 2.1.

As the left-right symmetry is broken to the Standard Model gauge symmetry by the vacuum expectation value $\langle (H_R^0)_3 \rangle = v_R$,

$$SU(2)_R \otimes U(1)_{B-L} \xrightarrow{\langle (H_R^0)_3 \rangle = v_R} U(1)_Y \,, \tag{3.35}$$

the Standard Model down-type anti-quarks d^c, negative charged leptons e^-, and left-handed neutrinos ν become mixed mass eigenstates with the heavy down-type anti-quarks D^c, heavy negative charged leptons E^-, and heavy neutral leptons N_1, respectively. We will take the limit $v_R \ll v_{33}$ for clarity in the following discussion such that the mixing of these fermionic degrees of freedom can be neglected. The details of the fermion mixing and the full tree-level mass terms can be found in the Appendix 7.7.

The Standard Model fermions acquire their mass once the vacuum expectation values $\langle (\varphi_1^0)_1 \rangle = v_1$ and $\langle (\varphi_2^0)_2 \rangle = v_2$ develop and break the Standard Model gauge symmetry

$$SU(2)_L \otimes U(1)_Y \xrightarrow{\langle (\varphi_1^0)_1 \rangle = v_1,\, \langle (\varphi_2^0)_2 \rangle = v_2} U(1)_{EM} \,.$$

We then find the following Standard Model fermion masses

$$m_d = y_1 v_1 \,, \quad m_u = y_2 v_2 \,, \quad m_e = h_1 v_1 \,, \quad m_\nu = h_2 v_2 \,. \tag{3.36}$$

Note that the neutrinos only have a Dirac mass at tree-level. However, one-loop corrections will again induce Majorana mass terms for the neutrinos. This is expected since lepton number is explicitly broken by the lepton multiplet L.

Radiative Neutrino Masses

To show the one-loop contributions to the neutrino masses qualitatively, we work in a simplified model with only one scalar bi-triplet Φ [151]. The relevant interactions are given by

$$\mathcal{L} \supset -M_\Phi^2 \Phi \Phi^* - \lambda \Phi\Phi\Phi - \frac{h}{2} L L \Phi + \text{h.c.} \,. \tag{3.37}$$

The cubic scalar interaction $\lambda\Phi\Phi\Phi$ is crucial for the Majorana mass generation at one-loop order. Due to the asymmetric nature of this scalar interaction, Majorana masses for N_3 and ν^c are generated at the one-loop level. However, no Majorana mass term is generated for ν. Hence, in contrast to the radiative neutrino masses in section 2.1.1, we do not have to assume left-right parity violation by the Yukawa couplings.

Until now, we have been working in the limit $v_{33} \gg v_R$ to avoid fermion mass mixing and simplify the fermion mass discussion. However, to not only generate a Majorana mass term for N_3, we have to relax this assumption to also generate an one-loop Majorana mass for ν^c. For the full fermion masses and the relevant interactions including mixing, we again refer to the Appendix 7.7. The one-loop diagrams responsible for the Majorana masses of N_3 and ν^c are given in the unbroken symmetry phase in Figure 3.1.

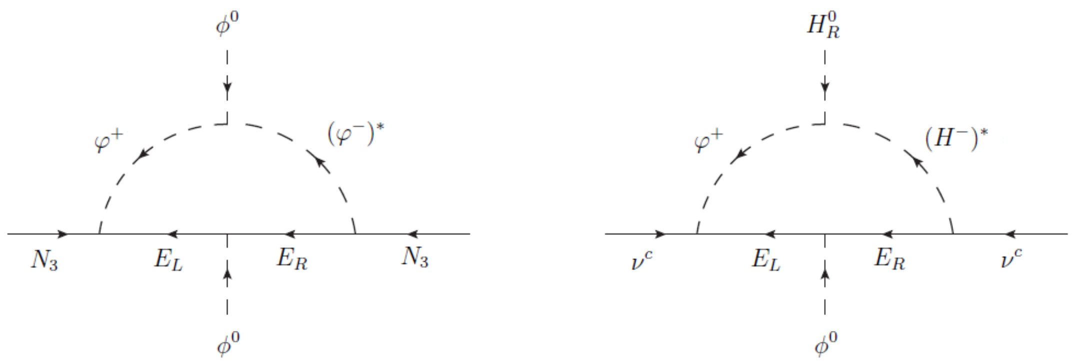

Figure 3.1: One-loop Majorana masses in the unbroken symmetry phase for N_3 and ν^c.

In contrast to section 2.1.1, only four charged scalars contribute to the one-loop neutrino masses in our simplified model. When taking all three scalar bi-triplets into account, twelve scalars contribute. We define the charged scalar mixing by

$$\left((\varphi^-)^* \;\varphi^+ \;(H^-)^* \;H^+\right)^T = U \left(h_1^+ \;h_2^+ \;h_3^+ \;h_4^+\right)^T , \tag{3.38}$$

and then find the one-loop Majorana mass contributions

$$\begin{aligned}
(m_{N_3}^{\text{1-loop}})^{\alpha\gamma} &= \frac{\cos(\alpha)}{16\pi^2} m_L h^{\alpha\beta} \sum_i \text{Log}\left(\frac{M_{h_i}^2}{m_{L_\beta}^2}\right) U_{2i} h^{\beta\gamma} U_{1i}^* + \alpha \leftrightarrow \gamma \\
&= \frac{\cos(\alpha)}{16\pi^2} m_L F_{N_3}^{\alpha\gamma} , \\
(m_{\nu^c}^{\text{1-loop}})^{\alpha\gamma} &= \frac{\sin(\alpha)}{16\pi^2} m_L h^{\alpha\beta} \sum_i \text{Log}\left(\frac{M_{h_i}^2}{m_{L_\beta}^2}\right) U_{2i} h^{\beta\gamma} U_{3i}^* + \alpha \leftrightarrow \gamma \\
&= \frac{\sin(\alpha)}{16\pi^2} m_L F_{\nu^c}^{\alpha\gamma} , \\
(m_{\nu^c N_3}^{\text{1-loop}})^{\alpha\gamma} &= \frac{m_L}{16\pi^2} \left(\sin(\alpha) F_{N_3}^{\alpha\gamma} - \cos(\alpha) F_{\nu^c}^{\alpha\gamma}\right) ,
\end{aligned} \tag{3.39}$$

with charged scalar masses M_{h_i} and mixing angle $\tan(\alpha) = v_R/v_{33}$. Note that we neglected one-loop contributions from fermions with masses at the electroweak scale. The neutral fermion mass matrix in the basis $(\nu\, \nu^c\, N_3)$ is then given by

$$m_{\nu\,\nu^c N_3}^{\text{1-loop}} = \begin{pmatrix} 0 & -m_\nu & 0 \\ -m_\nu & m_{\nu^c}^{\text{1-loop}} & m_{\nu^c N_3}^{\text{1-loop}} \\ 0 & m_{\nu^c N_3}^{\text{1-loop}} & m_{N_3}^{\text{1-loop}} \end{pmatrix} \simeq m_L \begin{pmatrix} 0 & \mathcal{O}(\epsilon) & 0 \\ \mathcal{O}(\epsilon) & \mathcal{O}(1) & \mathcal{O}(1) \\ 0 & \mathcal{O}(1) & \mathcal{O}(1) \end{pmatrix} , \tag{3.40}$$

where in the second step we defined m_ν/m_L as $\mathcal{O}(\epsilon)$. The neutrino mass matrix (3.40) has two eigenvalues of order $\mathcal{O}(1)$ and one eigenvalue of order $\mathcal{O}(\epsilon^2)$ [151]. We therefore approximately find in our simplified model at the one-loop level

$$m_{N_3} \sim m_L \,, \quad m_{\nu^c} \sim m_L \,, \quad m_\nu^{\text{1-loop}} \sim \frac{m_\nu^2}{m_L} \,. \tag{3.41}$$

The neutrino mass is therefore suppressed by the mass of the heavy new charged fermions $E^\pm$. Even if the above calculation is only a rough estimation of the Majorana neutrino masses for N_3 and ν^c in the 433 theory, we expect that the full calculation with all three scalar bi-triplets yields a similar result. After discussing the symmetry breaking pattern and the induced fermion masses in detail, we will turn to the new additional gauge bosons in the next section.

3.1.3 Leptophobic and Trinification Gauge Bosons

In this section, we shift our focus from the fermions of the theory to the gauge bosons. The $SU(4)_C$ gauge bosons can be decomposed in matrix form as

$$A_C^\mu = \begin{pmatrix} G^\mu & X^\mu/\sqrt{2} \\ (X^\mu)^*/\sqrt{2} & 0 \end{pmatrix} + Z_B^\mu T_C^{15}. \tag{3.42}$$

As the scalar field ξ breaks $SU(4)_C$ to $SU(3)_C \otimes U(1)_B$, we find:

- Three complex massive leptophobic gauge bosons $X^\mu \sim (3,1,1,4/3)$ with mass given by $M_X = \sqrt{2/3} g_C v_C$.

- One massless leptophobic gauge boson $Z_\mathrm{B}^\mu \sim (1,1,1,0)$ which mediates the conserved $U(1)_B$ symmetry.

- Eight massless Standard Model gluons $G^\mu \sim (8,1,1,0)$ corresponding to the color $SU(3)_C$ gauge symmetry.

At the scale of baryon number violation, the massive gauge bosons X^μ receive an additional mass contribution

$$M_X^2 = \frac{2}{3} g_C^2 v_C^2 + \frac{1}{4} g_C^2 v_B^2 \,, \tag{3.43}$$

with $g_B = \sqrt{3/8}\, g_C$ at the symmetry breaking scale v_B. In addition, once local baryon number is broken the leptophobic gauge boson Z_B^μ acquires the mass

$$M_{Z_\mathrm{B}} = g_B v_B \,. \tag{3.44}$$

Note the difference in the leptophobic gauge boson mass M_{Z_B} compared to the minimal theory of leptobaryons in section 2.2. The different coefficient is due to the different baryon numbers of S_B ($B_{S_\mathrm{B}} = 1$) and H_B ($B_{H_\mathrm{B}} = 3$).

The leptophobic nature of the gauge bosons manifests in the decays. The complex colored gauge boson X^μ decays to quarks and new fractional charged fermions if kinematically allowed

$$X^\mu \to \bar{\Psi}\mathsf{q}, \overline{\mathsf{q}^c}\eta^c \,. \tag{3.45}$$

The gauge boson Z_B couples to baryon number and decays to pairs of quarks and, if kinematically allowed, to pairs of new fractional charged fermions

$$Z_B \to \bar{\mathsf{q}}\mathsf{q}, \bar{\Psi}\Psi, \overline{\mathsf{q}^c}\mathsf{q}^c, \overline{\eta^c}\eta^c \,. \tag{3.46}$$

Turning to the trinification sector, we write the trinification gauge bosons in matrix form as

$$A^{\mu}_{L,R} = \begin{pmatrix} \frac{1}{2}\left(W^3_{L,R} + \frac{1}{\sqrt{3}}C_{L,R}\right) & \frac{1}{\sqrt{2}}W^+_{L,R} & \frac{1}{\sqrt{2}}B^0_{L,R} \\ \frac{1}{\sqrt{2}}W^-_{L,R} & \frac{1}{2}\left(-W^3_{L,R} + \frac{1}{\sqrt{3}}C_{L,R}\right) & \frac{1}{\sqrt{2}}B^-_{L,R} \\ \frac{1}{\sqrt{2}}B^0_{L,R} & \frac{1}{\sqrt{2}}\tilde{B}^+_{L,R} & -\frac{2}{\sqrt{3}}C_{L,R} \end{pmatrix}, \tag{3.47}$$

with the subscripts L and R labeling the $SU(3)_L$ and $SU(3)_R$ gauge bosons, respectively. Upon breaking trinification to an effective left-right symmetric theory via the vacuum expectation value v_{33}, we find:

- Four left-handed massive gauge bosons

$$\begin{aligned} B_L &= \begin{pmatrix} B^0_L \\ B^-_L \end{pmatrix} \sim (1,2,1,-1,0)\,, \\ \tilde{B}_L &= \begin{pmatrix} \tilde{B}^0_L & \tilde{B}^+_L \end{pmatrix} \sim (1,\bar{2},1,1,0)\,, \end{aligned} \tag{3.48}$$

  with the fermionic decay channels

$$B_L \to \bar{q}D, \overline{\Psi_q}\Psi_D, \overline{\Psi^c_D}\Psi^c_q, \overline{\ell^c}\mathfrak{L}, \overline{N_3}\ell\,. \tag{3.49}$$

- Four right-handed massive gauge bosons

$$\begin{aligned} B_R &= \begin{pmatrix} B^0_R \\ B^-_R \end{pmatrix} \sim (1,1,2,-1,0)\,, \\ \tilde{B}_R &= \begin{pmatrix} \tilde{B}^0_R & \tilde{B}^+_R \end{pmatrix} \sim (1,1,\bar{2},1,0)\,, \end{aligned} \tag{3.50}$$

  where the possible fermionic decay channels are given by

$$B_R \to \overline{D^c}q^c, \overline{\eta^c_D}\eta^c_q, \overline{\eta_q}\eta_D, \overline{\mathfrak{L}}\ell, \overline{\ell^c}N_3\,. \tag{3.51}$$

- One mixed massive gauge boson

$$C = \cos(\theta_{33})C_R - \sin(\theta_{33})C_L \sim (1,1,1,0,0)\,, \tag{3.52}$$

  with $\tan(\theta_{33}) = g_L^2/g_R^2$. The possible fermionic decays are

$$\begin{aligned} C \to\ & \bar{q}q, \bar{D}D, \overline{q^c}q^c, \overline{D^c}D^c, \overline{\Psi_q}\Psi_q, \overline{\Psi_D}\Psi_D, \overline{\Psi^c_q}\Psi^c_q, \overline{\Psi^c_D}\Psi^c_D, \\ & \overline{\eta_q}\eta_q, \overline{\eta_D}\eta_D, \overline{\eta^c_q}\eta^c_q, \overline{\eta^c_D}\eta^c_D, \bar{\ell}\ell, \overline{\ell^c}\ell^c, \overline{\mathfrak{L}}\mathfrak{L}, \overline{N_3}N_3\,. \end{aligned} \tag{3.53}$$

- One mixed massless gauge boson coupling to $B-L$

$$Z_{BL} = \cos(\theta_{33})C_L + \sin(\theta_{33})C_R \sim (1,1,1,0,0)\,. \tag{3.54}$$

The $B-L$ gauge coupling is thereby defined as

$$g_{BL} = \frac{\sqrt{3}}{2} \frac{g_L g_R}{\sqrt{g_L^2 + g_R^2}} \,. \tag{3.55}$$

As the $U(1)_{B-L}$ gauge symmetry is broken, Z_{BL} acquires a mass. The possible fermionic decay channels then are

$$\begin{aligned} Z_{BL} \to\ & \bar{q}q, \bar{D}D, \overline{q^c}q^c, \overline{D^c}D^c, \overline{\Psi_q}\Psi_q, \overline{\Psi_D}\Psi_D, \overline{\Psi_q^c}\Psi_q^c, \overline{\Psi_D^c}\Psi_D^c, \\ & \overline{\eta_q}\eta_q, \overline{\eta_D}\eta_D, \overline{\eta_q^c}\eta_q^c, \overline{\eta_D^c}\eta_D^c, \bar{\ell}\ell, \overline{\ell^c}\ell^c, \bar{\mathfrak{L}}\mathfrak{L}, \overline{N_3}N_3 \,. \end{aligned} \tag{3.56}$$

Note that we suppressed spacetime indices for clarity. The mass terms of the gauge bosons in the Lagrangian can be written as

$$-\mathcal{L} \supset \frac{M_{B_L}^2}{2} \tilde{B}_L B_L + \frac{M_{B_R}^2}{2} \tilde{B}_R B_R + \frac{M_C^2}{2} \tilde{C} C \,, \tag{3.57}$$

with masses

$$M_{B_L} = 2 g_L v_{33} \,, \quad M_{B_R} = 2 g_R v_{33} \,, \quad M_C = \sqrt{2(g_L^2 + g_R^2)} v_{33} \,. \tag{3.58}$$

The resulting left-right symmetric theory breaks to the Standard Model once the right-handed Higgs doublet $(H_R)_3$ acquires the vacuum expectation value v_R. The gauge bosons of a left-right symmetric theory broken by a right-handed Higgs doublet are discussed in detail in section 2.1.2.

3.1.4 Cosmology of the 433 Theory

In section 2.2.1, we learned that upon the breaking of local baryon number the lightest leptobaryon is stabilized by a remnant Z_2 symmetry. We further required that the lightest leptobaryon was an electrically neutral particle and hence a potential dark matter candidate. The situation now in the context of the 433 theory is very similar. Upon the breaking of local baryon number, an inherited Z_2 symmetry stabilizes the lightest particle in the new sector

$$\begin{aligned}(Z_2)_{\rm C}: \quad & \Psi \to -\Psi\,, \quad \Psi^c \to -\Psi^c\,, \quad \eta \to -\eta\,, \quad \eta^c \to -\eta^c\,, \\ & S_C \to -S_C\,, \quad X^\mu \to -X^\mu\,. \end{aligned} \tag{3.59}$$

However, the new sector consists of fractional charged fermions Ψ, Ψ^c, η, and η^c, colored scalar bosons S_C, and colored gauge bosons X^μ. The 433 theory therefore predicts stable fractional charged fermions and/or stable colored bosons. In cosmology, neither stable fractional charged particles nor a stable colored boson which due to confinement would form exotic bound states were observed. To avoid conflicts with cosmology, we therefore have to require that the reheating temperature in the early Universe was below the mass scale of the lightest new exotic particle. We can then avoid the production of these fields after inflation. In principle, we find three different kinematic regimes:

- **Scenario A:** The fractional charged fermions are the lightest new particles. We then have to allow for the following decay channels to be open such that the heavier new fields can decay to the fractional charged particles

$$\begin{aligned} S_C &\to \Psi + \Psi^c + X^\mu, \\ S_C &\to \eta + \eta^c + X^\mu, \\ X^\mu &\to \overline{\Psi} + q,\, \overline{q^c} + \eta^c\,. \end{aligned}$$

  The upper bound on the reheating temperature is hence given by

$$T^A_{RH} \ll \frac{1}{\sqrt{2}} y_{\Psi,\eta} v_B\,. \tag{3.60}$$

- **Scenario B:** The colored gauge boson X^μ is the lightest stable particle. We therefore require the following decay channels to be open

$$\begin{aligned} S_C &\to \Psi + \Psi^c + X^\mu, \\ S_C &\to \eta + \eta^c + X^\mu, \\ \Psi &\to (X^\mu)^* + \bar{q}, \\ \eta^c &\to X^\mu + \overline{q^c}. \end{aligned}$$

Now, the upper bound on the reheating temperature is given by

$$T_{RH}^{B} \ll g_C \sqrt{\frac{2}{3} v_C^2 + \frac{1}{4} v_B^2}\,. \tag{3.61}$$

- **Scenario C:** The colored scalar boson S_C is the lightest exotic field. For the new particles to be able to decay to S_C, the following decay channels have to be open

$$\begin{aligned} X^\mu &\rightarrow S_C + S_B, \\ \Psi &\rightarrow \bar{q} + S_C, \\ \eta &\rightarrow q^c + S_C\,. \end{aligned}$$

  We then require for the reheating temperature in the early Universe

$$T_{RH}^{C} \ll M_{S_C}. \tag{3.62}$$

The strongest current constraint on the reheating temperature in the early Universe comes from a combination of BBN, cosmic microwave background (CMB) and large scale structure bounds, $T_{RH} \gtrsim 4.7$ MeV [157]. As motivated in section 3.1.1, we want to break $SU(4)_C$ and local baryon number in the multi-TeV regime. On these grounds, we also expect the new particles to have masses in the TeV regime such that we can search for them at particle colliders. The 433 theory is therefore in full agreement with cosmology for a reheating temperature below the TeV scales.

It is important to note that the prediction of a low reheating temperature allows for the falsifiability of the 433 theory. If we discover the new exotic particles in the multi-TeV range, but at the same time have hints towards a high scale reheating temperature, then the 433 theory is in conflict with cosmology and has to be ruled out.

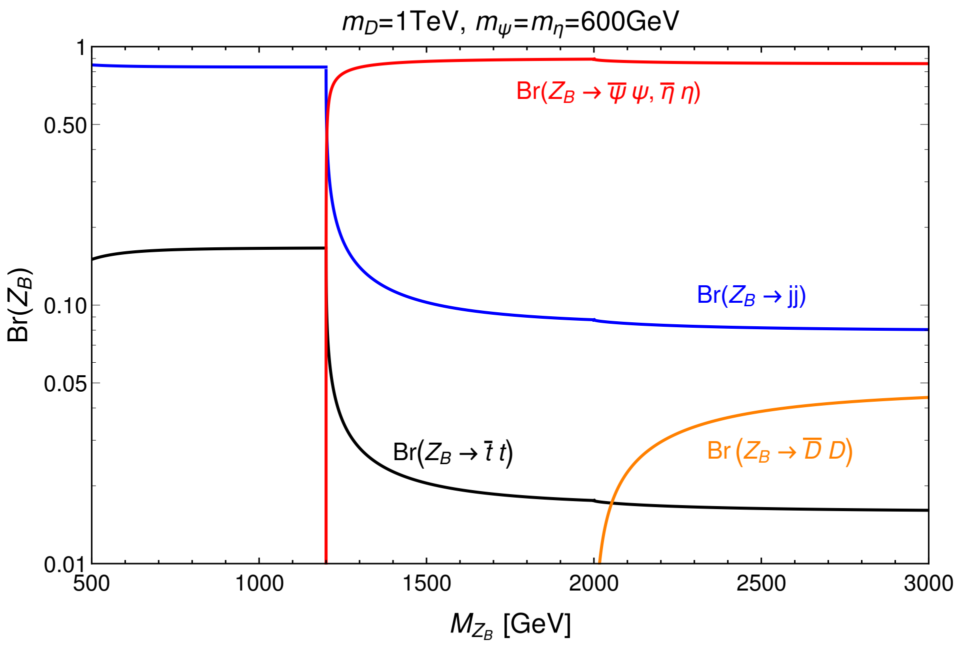

Figure 3.2: The branching ratios of the leptophobic gauge boson $Z_{\rm B}$ as a function of $M_{Z_{\rm B}}$.

3.1.5 433 Theory at Particle Colliders

Our main motivation to discuss the 433 theory was the search for an UV completion of the Standard Model of particle physics which can be realized at low energy scales and thus is also testable at current and future particle colliders. The testability of the 433 theory at particle colliders is the topic of this section.

The theory again predicts a leptophobic gauge boson $Z_{\rm B}$ which was already discussed in section 2.2.2. If we assume that the decays of $Z_{\rm B}$ to the new fractional charged particles Ψ, Ψ^c, η, and η^c, and to the new heavy down-type quarks D and anti-quarks D^c are kinematically forbidden, we can apply the LHC constraints from dijet searches displayed in Figure 2.14. The presence of the heavy D quarks and D^c anti-quarks would reduce the branching to Standard Model quarks by approximately 33%. This is expected as the three new D quarks and D^c anti-quarks carry the same baryon number as the Standard Model quarks and anti-quarks.

As $Z_{\rm B}$ couples to baryon number, the partial decay width to a pair of fermions $\bar{f}f$ is given by

$$\Gamma(Z_{\rm B} \to \bar{f}f) = N_C \frac{g_{\rm B}^2 B_f^2}{12\pi} M_{Z_{\rm B}} \left(1 + 2\frac{m_f^2}{M_{Z_{\rm B}}^2}\right) \sqrt{1 - 4\frac{m_f^2}{M_{Z_{\rm B}}^2}}\,, \tag{3.63}$$

with baryon number B_f and mass m_f. The branching ratio of $Z_{\rm B}$ as a function of $M_{Z_{\rm B}}$ for $m_D = 1$ TeV and $m_\Psi = m_\eta = 600$ GeV is shown in Figure 3.2. We see that for $M_{Z_{\rm B}} \leq 1.2$ TeV, the decay to two jets dominates over the $t\bar{t}$ channel. However, as soon as the decays to the new fermions $\bar{\Psi}\Psi$ and $\overline{\eta^c}\eta^c$ are kinematically allowed, they dominate

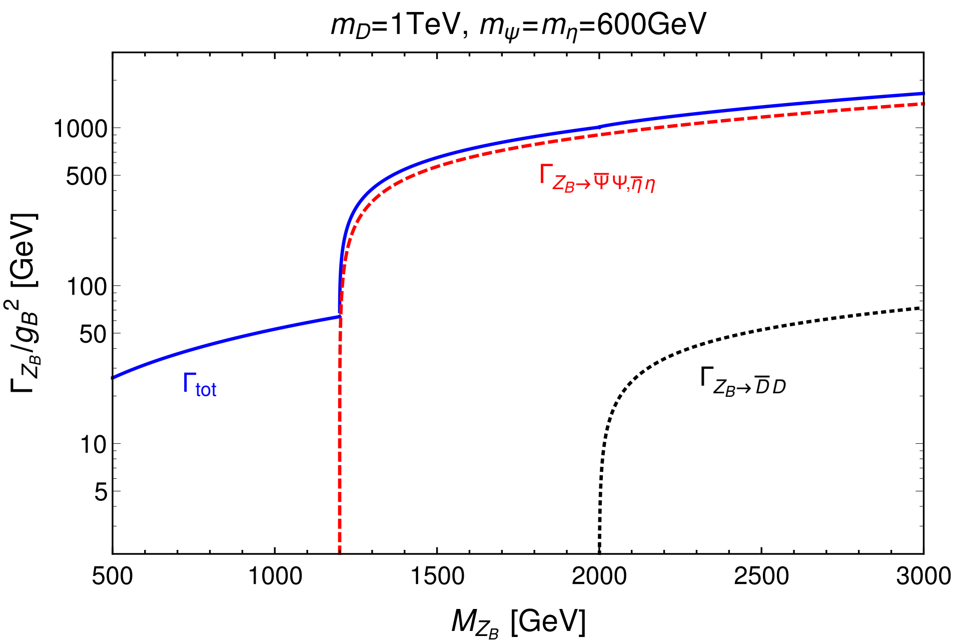

Figure 3.3: The decay width of the leptophobic gauge boson $Z_{\rm B}$ as function of $M_{Z_{\rm B}}$.

because of the three times larger baryon charge of Ψ and η^c. The decay to $\bar{D}D$ is then only of minor importance. The total decay width of $Z_{\rm B}$ as a function of $M_{Z_{\rm B}}$ is given in Figure 3.3. The leptophobic gauge boson $Z_{\rm B}$ has a large width if the decays to fractional charged particles are allowed.

However, the theory also predicts new colored and fractional charged fields. If the colored fields X^μ and S_C are stable, they can be produced pairwise via QCD interactions and we can expect exotic signatures such as the formation of R-hadrons at the LHC [156]. Otherwise, if the fractional charged particles Ψ, Ψ^c, η, and η^c are stable, we can search for charged tracks at the ATLAS and CMS detector. Moreover, since there is an additional gauge boson $Z_{\rm B}$ in the theory compared to the Standard Model, the production process

$$p\,p \to \gamma^*,\, Z^*,\, Z_{\rm B}^* \to \bar{\Psi}\Psi,\, \bar{\eta}\eta\,, \tag{3.64}$$

is enhanced and the experimental bounds on long lived charged particles are stronger [156]. This, however, also opens up the possibility of resonant production of the fractional charged fermions which can increase the production cross section significantly (compare discussion in section 2.1.3).

3.2 444 Unification

The last section was focused on the 433 theory. The 433 theory is the first UV completion of the Standard Model in four dimensions which can be realized at energy scales as low as 10^{3-4} GeV. On the other hand, the 433 theory is only an UV completion of the Standard Model. The theory lacks a common origin of the gauge interactions. It therefore still remains a mystery why nature chose the gauge group G_{433}. What singles out this UV complete theory?

In this section, we therefore turn to the gauge group

$$G_{444} = SU(4)_C \otimes SU(4)_L \otimes SU(4)_R \,. \tag{3.65}$$

This theory has the advantage that by enforcing a discrete Z_3 symmetry, all gauge interactions are identical. We can hence achieve the unification of the gauge interactions in contrast to the 433 theory. Note that the bottom-up unification of the Standard Model gauge interactions in a theory of local baryon number at low energies was discussed in an earlier work [158] as part of the author's master thesis.

In the context of the 444 theory, the Standard Model fermions are embedded in

$$Q \sim (4, \bar{4}, 1)\,, \quad Q^c \sim (\bar{4}, 1, 4)\,, \quad L \sim (1, 4, \bar{4})\,.$$

It is important to appreciate that we do not have to add additional fermions to the theory for consistency, since it is already anomaly free. In matrix notation the fermionic fields are given by

$$Q = \begin{array}{c} \xrightarrow{\qquad\qquad SU(4)_L \qquad\qquad} \\ \begin{pmatrix} d_r & u_r & D_r & \chi_r \\ d_b & u_b & D_b & \chi_b \\ d_g & u_g & D_g & \chi_g \\ \Psi_d & \Psi_u & \Psi_D & \chi_\Psi \end{pmatrix} \end{array} \Bigg\downarrow {\scriptstyle SU(4)_C} = \begin{pmatrix} \mathfrak{q} & \chi \\ \Psi & \chi_\Psi \end{pmatrix} ,$$

$$Q^c = \begin{array}{c} \xrightarrow{\qquad\qquad SU(4)_C \qquad\qquad} \\ \begin{pmatrix} d^c_{\bar{r}} & d^c_{\bar{b}} & d^c_{\bar{g}} & \Psi^c_d \\ u^c_{\bar{r}} & u^c_{\bar{b}} & u^c_{\bar{g}} & \Psi^c_u \\ D^c_{\bar{r}} & D^c_{\bar{b}} & D^c_{\bar{g}} & \Psi^c_D \\ \chi^c_{\bar{r}} & \chi^c_{\bar{b}} & \chi^c_{\bar{g}} & \chi^c_\Psi \end{pmatrix} \end{array} \Bigg\downarrow {\scriptstyle SU(4)_R} = \begin{pmatrix} \mathfrak{q}^c & \Psi^c \\ \chi^c & \chi^c_\Psi \end{pmatrix} ,$$

$$L = \begin{array}{c} \xrightarrow{\qquad\qquad SU(4)_R \qquad\qquad} \\ \begin{pmatrix} N_1 & E^+ & \nu & l_{d^c} \\ E^- & N_2 & e^- & l_{u^c} \\ \nu^c & e^+ & N_3 & l_{D^c} \\ l_d & l_u & l_D & N_4 \end{pmatrix} \end{array} \Bigg\downarrow {\scriptstyle SU(4)_L} = \begin{pmatrix} \mathfrak{L} & \ell & l_{q^c} \\ \ell^c & N_3 & l_{D^c} \\ l_q & l_D & N_4 \end{pmatrix} .$$

Compared to the 433 theory, the colored multiplets Q and Q^c are complemented by the electrically neutral quarks χ and anti-quarks χ^c. Moreover, the leptonic bi-triplet has evolved to a leptonic bi-quad. The leptonic bi-quad now also incorporates fractional charged leptons where the electric charge is given by

$$
\begin{aligned}
Q_{\text{EM}}(l_u) &= +\frac{2}{3} = -Q_{\text{EM}}(l_{u^c}), \\
Q_{\text{EM}}(l_d) &= -\frac{1}{3} = -Q_{\text{EM}}(l_{d^c}), \\
Q_{\text{EM}}(l_D) &= -\frac{1}{3} = -Q_{\text{EM}}(l_{D^c}) \,.
\end{aligned}
\tag{3.66}
$$

In addition, the leptonic bi-quad now contains four additional neutral leptons N_1, N_2, N_3, and N_4 per generation compared to left-right symmetric theories with the Standard Model neutrinos ν and right-handed neutrinos ν^c. The conserved electroweak charges are still given by (3.6) and (3.7).

The minimal left-right symmetric Higgs sector which can break G_{444} to the Standard Model is given by

$$
\begin{aligned}
&\Sigma \sim (15, 4, \bar{4})\,, \quad S \sim (4, 1, 1)\,, \quad S_L \sim (1, 4, 1)\,, \quad S_R \sim (1, 1, 4)\,, \\
&\Phi_1 \sim (1, 4, \bar{4})\,, \quad \Phi_2 \sim (1, 4, \bar{4})\,.
\end{aligned}
$$

We had to introduce S_L and S_R to break the remnant diagonal abelian symmetry which remains after Σ breaks G_{444}. Actually, to break the abelian symmetry, only one scalar field would be needed. However, to conserve the discrete Z_3 symmetry necessary for true gauge unification, we include S_L and S_R. In the 433 theory, we had to introduce three scalar bi-triplets to have realistic Standard Model fermion masses without fine-tuning. By giving Σ non-trivial $SU(4)_L \otimes SU(4)_R$ charges, we only have to add two bi-quad scalar fields.

We can write the fundamental scalars S, S_L, and S_R in matrix notation as

$$
S = \begin{pmatrix} S_C^r \\ S_C^b \\ S_C^g \\ S_B \end{pmatrix} \Bigg\downarrow_{SU(4)_C} , \quad
S_L = \begin{pmatrix} S_L^{d^c} \\ S_L^{u^c} \\ S_L^{D^c} \\ S_L^{\chi^c} \end{pmatrix} \Bigg\downarrow_{SU(4)_L} , \quad
S_R = \begin{pmatrix} S_R^{d^c} \\ S_R^{u^c} \\ S_R^{D^c} \\ S_R^{\chi^c} \end{pmatrix} \Bigg\downarrow_{SU(4)_R} .
$$

The scalar fields $S_L^{q^c}$ and $S_R^{q^c}$ carry fractional electric charge, whereas $S_L^{\chi^c}$ and $S_R^{\chi^c}$ are electrically neutral and can acquire vacuum expectation values. The scalar bi-quad can be written in matrix notation as

$$
\Phi = \begin{array}{c} \xrightarrow{\hspace{6em} SU(4)_R \hspace{6em}} \\ \begin{pmatrix} \varphi_1^0 & \varphi^+ & H_L^0 & \varphi_{d^c} \\ \varphi^- & \varphi_2^0 & H^- & \varphi_{u^c} \\ H_R^0 & H^+ & \phi_1^0 & \varphi_{D^c} \\ \varphi_d & \varphi_u & \varphi_D & \phi_2^0 \end{pmatrix} \end{array} \Bigg\downarrow_{SU(4)_L} = \begin{pmatrix} \varphi & H_L & \varphi_{q^c} \\ H_R & \phi_1^0 & \varphi_{D^c} \\ \varphi_q & \varphi_D & \phi_2^0 \end{pmatrix} .
$$

Compared to the bi-triplet scalar fields in trinification, the bi-quad scalars Φ_1 and Φ_2 contain the fractional charged components φ_q and φ_{q^c}, and an additional neutral scalar ϕ_2^0. The scalar ϕ_2^0 contributes to the breaking of $SU(4)_L \otimes SU(4)_R$ as it develops a vacuum expectation value. The electric charges of the fractional charged scalars are given by

$$\begin{aligned} Q_{\mathrm{EM}}(\varphi_u) &= +\frac{2}{3} = -Q_{\mathrm{EM}}(\varphi_{u^c}) = -Q_{\mathrm{EM}}(S_R^{u^c}) = -Q_{\mathrm{EM}}(S_L^{u^c})\,, \\ Q_{\mathrm{EM}}(\varphi_d) &= -\frac{1}{3} = -Q_{\mathrm{EM}}(\varphi_{d^c}) = -Q_{\mathrm{EM}}(S_R^{d^c}) = -Q_{\mathrm{EM}}(S_L^{d^c})\,, \\ Q_{\mathrm{EM}}(\varphi_D) &= -\frac{1}{3} = -Q_{\mathrm{EM}}(\varphi_{D^c}) = -Q_{\mathrm{EM}}(S_R^{D^c}) = -Q_{\mathrm{EM}}(S_L^{D^c})\,. \end{aligned} \tag{3.67}$$

The scalar Σ can be decomposed in color space as

$$\Sigma = \begin{pmatrix} \Sigma_8 & \Sigma_3 \\ \Sigma_{\bar{3}} & 0 \end{pmatrix}_C + \Sigma_\Phi T_C^{15}\,.$$

The theory hence predicts a color adjoint scalar Σ_8, a color fundamental scalar Σ_3, and a color anti-fundamental field $\Sigma_{\bar{3}}$. Moreover, the scalar field Σ_Φ behaves as the bi-quad scalars Φ_1 and Φ_2 and will be responsible for the symmetry breaking.

The symmetry breaking pattern we are considering is given below.

$$\boxed{SU(4)_C \otimes SU(4)_L \otimes SU(4)_R}$$

$$\langle S_L \rangle \neq 0,\ \langle S_R \rangle \neq 0 \ \Big|\ \langle \Sigma_\Phi \rangle \neq 0$$

$$\boxed{SU(3)_C \otimes SU(3)_L \otimes SU(3)_R \otimes U(1)_B}$$

$$\langle \Sigma_\Phi \rangle \neq 0 \ \Big|\ \langle \Phi \rangle \neq 0$$

$$\boxed{SU(3)_C \otimes SU(2)_L \otimes U(1)_Y \otimes U(1)_B}$$

The quark interactions in the 444 theory take the simple form

$$-\mathcal{L}_Q = Q Q^c (y_1 \Phi_1 + y_2 \Phi_2 + y_\Sigma \Sigma) + \text{h.c.}\,. \tag{3.68}$$

In contrast, the leptonic field does not interact with the scalar sector at the renormalizable-level. Nonetheless, lepton masses can be generated by the dimension five Weinberg operator

$$-\mathcal{L}_L = \frac{h_{nm}}{\Lambda} L L \Phi_n \Phi_m + \frac{\lambda_{nm}}{\Lambda} L \Phi_n^\dagger L \Phi_m^\dagger + \text{h.c.}\,, \tag{3.69}$$

with

$$LL\Phi\Phi = \frac{1}{4}\epsilon^{ijkl}\epsilon_{abcd}L^i_a L^j_b \Phi^k_c \Phi^l_d \quad \text{and} \quad L\Phi^\dagger L\Phi^\dagger = L^i_a(\Phi^\dagger)^i_a L^j_b(\Phi^\dagger)^j_b\,, \tag{3.70}$$

where we use the convention that $SU(4)_L$ indices are written in upper case with $\{i, j, k, l\}$ and $SU(4)_R$ indices in lower case with $\{a, b, c, d\}$. Both couplings h_{nm} and λ_{nm} are symmetric in lepton flavor and in scalar flavor space

$$h_{nm} = h_{mn} \quad \text{and} \quad \lambda_{nm} = \lambda_{mn}\,. \tag{3.71}$$

Actually, the charged lepton masses are only generated by the totally asymmetric dimension five operator. However, there are also two possibilities to generate renormalizable lepton masses:

- **Scenario A:** We can add a scalar bi-sextet ϱ

  $$\varrho \sim (1, 6, 6)\,,$$

  which gives rise to the interaction

  $$-\mathcal{L}_L \supset h^\varrho_{nm} L_n L_m \varrho = \frac{h^\varrho}{4} L^i_a L^j_b \varrho^{ij}_{ab}\,. \tag{3.72}$$

  Note that ϱ is completely asymmetric

  $$\varrho^{ij}_{ab} = -\varrho^{ji}_{ab} = \varrho^{ij}_{ba} = \varrho^{ji}_{ba}\,, \tag{3.73}$$

  and hence the Yukawa coupling h^ϱ_{nm} has to be asymmetric in lepton flavor space, $h^\varrho_{nm} = -h^\varrho_{mn}$.

- **Scenario B:** Adding a scalar bi-tenplet ς

  $$\varsigma \sim (1, \overline{10}, 10)\,,$$

  we find that the following gauge invariant interaction can be included in the Lagrangian of the theory

  $$-\mathcal{L}_L \supset h^\varsigma L\varsigma L = \frac{h^\varsigma}{2} L^i_a \varsigma^{ij}_{ab} L^j_b\,. \tag{3.74}$$

  The bi-tenplet ς is in contrast to the bi-sextet ϱ completely symmetric.

Upon the following generic vacuum expectation value assignment which is inspired by our previous discussion in the 433 theory

$$\langle\Phi_1\rangle = \begin{pmatrix} v_1 & 0 & \hat{0} & 0 \\ 0 & \hat{0} & 0 & 0 \\ \hat{0} & 0 & \hat{0} & 0 \\ 0 & 0 & 0 & \hat{0} \end{pmatrix}, \qquad \langle\Phi_2\rangle = \begin{pmatrix} \hat{0} & 0 & \hat{0} & 0 \\ 0 & v_2 & 0 & 0 \\ v_R & 0 & v_{33} & 0 \\ 0 & 0 & 0 & \hat{0} \end{pmatrix},$$

$$\langle\Sigma_\Phi\rangle = \begin{pmatrix} v_1^C & 0 & \hat{0} & 0 \\ 0 & v_2^C & 0 & 0 \\ v_R^C & 0 & v_{33}^C & 0 \\ 0 & 0 & 0 & v_{44} \end{pmatrix},$$

the mass terms of the quarks take the form

$$\begin{aligned} -\mathcal{L}_Q \supset & \left(y_2 v_2 + \frac{y_\Sigma}{2\sqrt{6}} v_2^C\right) u^c u + \left(y_2 v_2 - \frac{3y_\Sigma}{2\sqrt{6}} v_2^C\right) \Psi_u^c \Psi_u \\ & + \begin{pmatrix} d^c & D^c \end{pmatrix} \begin{pmatrix} y_1 v_1 + \frac{y_\Sigma}{2\sqrt{6}} v_1^C & y_2 v_R + \frac{y_\Sigma}{2\sqrt{6}} v_R^C \\ 0 & y_2 v_{33} + \frac{y_\Sigma}{2\sqrt{6}} v_{33}^C \end{pmatrix} \begin{pmatrix} d \\ D \end{pmatrix} \\ & + \begin{pmatrix} \Psi_d^c & \Psi_D^c \end{pmatrix} \begin{pmatrix} y_1 v_1 - \frac{3y_\Sigma}{2\sqrt{6}} v_1^C & y_2 v_R - \frac{3y_\Sigma}{2\sqrt{6}} v_R^C \\ 0 & y_2 v_{33} - \frac{3y_\Sigma}{2\sqrt{6}} v_{33}^C \end{pmatrix} \begin{pmatrix} \Psi_d \\ \Psi_D \end{pmatrix} \\ & + m_\chi \chi \chi^c - 3 m_\chi \chi_\Psi \chi_\Psi^c \,, \end{aligned} \tag{3.75}$$

with neutral fermion mass

$$m_\chi = \frac{y_\Sigma}{2\sqrt{6}} v_{44} \,. \tag{3.76}$$

Note that $\hat{0}$ again denotes additional neutral scalar degrees of freedom which could develop a vacuum expectation value.

In order to have a mass separation of the light Standard Model quarks and the new heavy quarks, large Yukawa couplings are needed. This is due to the fact that the same couplings in equation (3.75) give mass to the down-type quarks and the exotic fermions Ψ. If we take the limit of massless down-type quarks, we find the relation

$$y_1 v_1 = -\frac{y_\Sigma}{2\sqrt{6}} v_1^C \,. \tag{3.77}$$

The mass of the exotic fermion Ψ_d is then given by

$$m_{\Psi_d} = -2\frac{y_\Sigma}{\sqrt{6}} v_1^C \,, \tag{3.78}$$

where v_1^C contributes to the electroweak symmetry breaking and is therefore bounded by $v_1^C \leq 174$ GeV. With the latest LHC bounds [156], we have to require $m_{\Psi_d} \geq 600$ GeV and thus $y_\Sigma \geq 4.2$. Similarly, large Yukawa couplings are needed for the different leptonic interactions to establish a mass separation of the Standard Model leptons and the new heavy leptons. Unfortunately, large Yukawa couplings can lead to Landau poles which signal the breakdown of the theory.

From a theoretical perspective the 444 theory appears to be more appealing at first glance because of the gauge unification. However, the absence of new heavy quarks and leptons at the LHC has led to severe constraints on the masses of such new particles [155, 156]. The large Yukawa couplings required in the 444 theory to accommodate for such heavy new particles makes the theory unattractive.

3.3 Summary

In this section, we developed the first experimentally valid UV completion of the Standard Model in four dimensions which can be realized at scales as low as 10^{3-4} GeV. Note that such a theory radically changes the discouraging picture of conventional Grand Unified Theories which are untestable at current and future particle colliders.

The first theory we presented was based on the gauge group $SU(4)_C \otimes SU(3)_L \otimes SU(3)_R$ and realizes the idea of local baryon number as fourth color. This is also the only known experimentally valid theory where the Standard Model extension of local baryon number can be embedded. The 433 theory predicts stable fractional charged and/or colored fields. As a consequence, the reheating temperature in the early Universe has to be below the mass scale of these new stable exotic fields. Moreover, the stable exotic fields lead to striking signals at the LHC such as charged tracks and/or the formation of R-hadrons.

To close, we discussed a gauge symmetry based on the symmetry group $SU(4)_C \otimes SU(4)_L \otimes SU(4)_R$. This theory is not only an UV completion of the Standard Model, but also gives rise to gauge unification as the interactions are indistinguishable upon imposing a discrete Z_3 symmetry. However, this theory requires large Yukawa couplings in order to be in agreement with experimental bounds from the LHC. Further investigations are needed to decide if such a theory could be realized in our Universe.

The results of this section allow for a radically different solution to the hierarchy problem. The enhanced symmetry structure of the 433 theory suppresses proton decay such that the scale of quantum gravity can be as low as 10^7 GeV. No further embedding apart for aesthetic reasons is needed. The 433 theory is valid for arbitrary high energy scales. We would like to emphasize that the non-abelian nature of the 433 theory also clarifies the charge quantization of the Standard Model and of the minimal extensions in chapter 2. Furthermore, by introducing a multitude of symmetry breaking scales above the electroweak scale, we find different additional contributions to the Higgs mass. Follow-up studies are necessary to conclude if a mechanism can relate the different additional Higgs mass contributions to ensure a natural electroweak scale Higgs mass.

CHAPTER 4

GLOBAL SYMMETRIES LEADING TO DARK MATTER - NEW PROBES

WE SAW in section 2.2.1 how an extension of the Standard Model gauge symmetry by local baryon number can lead to an explanation of the dark matter in the Universe. However, in section 3.1.4, we also pointed out that an UV completion of the Standard Model with gauged baryon number does not have to have a potential dark matter candidate. In this section, we will therefore focus on a different type of dark matter candidate which is however also motivated by new symmetries: axion-like particles.

Axion-like particles are inspired by the QCD axion which was introduced to solve the strong CP problem. However, we will be especially interested in the distinct feature that axion-like dark matter can form galactic Bose-Einstein condensates. We will introduce a new method to test axion-like dark matter with gravitational waves which was first developed in [5].

4.1 Axion-like Particles

Gerard 't Hooft noted in 1976 that non-abelian gauge theories have a non-trivial vacuum structure [159, 160]. The physical vacuum of a non-abelian gauge theory is the superposition of infinite degenerate vacuum states. We parametrize the physical vacuum by the vacuum angle θ which describes the alignment of the degenerate vacuum states. To account for the non-trivial vacuum structure, we also have to include the following term to our Lagrangian

$$\mathcal{L} \supset -\frac{c_\theta g^2 \theta}{32\pi^2} \mathrm{Tr}\left(G^{\mu\nu} \tilde{G}_{\mu\nu} \right) , \tag{4.1}$$

with the dual field strength tensor $\tilde{G}_{\mu\nu} = (1/2)\epsilon_{\mu\nu\alpha\beta} G^{\alpha\beta}$ and a model dependent dimensionless coupling constant c_θ. The term $\mathrm{Tr}(G^{\mu\nu}\tilde{G}_{\mu\nu})$ violates the discrete spacetime symmetries P and T but conserves C. Hence, the term also violates the CP symmetry. We already encountered CP violation in the Standard Model. By diagonalizing the quark mass matrix, we introduced the CKM matrix in section 1.1. The CKM phase is the source of explicit CP violation in the electroweak sector of the Standard Model.

Naively considering the Standard Model gauge group G_{SM}, we would expect two physical vacuum angles, an electroweak angle θ_{EW}, and a QCD vacuum angle θ_{QCD},

$$\mathcal{L}_{\text{SM}} \supset -\frac{g_L^2 \theta_{\text{EW}}}{32\pi^2} \text{Tr}\left(W^{\mu\nu}\tilde{W}_{\mu\nu}\right) - \frac{g_s^2 \theta_{\text{QCD}}}{32\pi^2} \text{Tr}\left(G^{\mu\nu}\tilde{G}_{\mu\nu}\right) . \tag{4.2}$$

However, only θ_{QCD} is physical in the Standard Model.

As was already mentioned in section 2.2, the Standard Model has the accidental global symmetries of baryon and lepton number. These global symmetries are anomalous at the quantum level. Introducing the baryonic and leptonic currents

$$J^\mu_{\text{B}} = \sum_q \tfrac{1}{3}\bar{q}\gamma^\mu q \quad \text{and} \quad J^\mu_{\text{L}} = \sum_{i=e,\mu,\tau} (\bar{\ell}_i \gamma^\mu \ell_i + \bar{\nu}_i \gamma^\mu \nu_i) , \tag{4.3}$$

we find

$$\partial_\mu J^\mu_{\text{B}} = \partial_\mu J^\mu_{\text{L}} = -\frac{3 g_L^2}{32\pi^2} \text{Tr}\left(W^{\mu\nu}\tilde{W}_{\mu\nu}\right) - \frac{3 g_Y^2}{32\pi^2} \text{Tr}\left(B^{\mu\nu}\tilde{B}_{\mu\nu}\right) . \tag{4.4}$$

Upon the symmetry transformation

$$Q_L \to e^{-i\frac{\alpha_B}{3}} Q_L , \qquad \ell_L \to e^{-i\alpha_L} \ell_L , \tag{4.5}$$

we thus find that the Lagrangian changes by

$$\delta\mathcal{L}_{\text{SM}} = \alpha_B \partial_\mu J^\mu_{\text{B}} + \alpha_L \partial_\mu J^\mu_{\text{L}} = -\frac{3 g_L^2 (\alpha_B + \alpha_L)}{32\pi^2} \text{Tr}\left(W^{\mu\nu}\tilde{W}_{\mu\nu}\right) . \tag{4.6}$$

Note that the terms proportional to $\text{Tr}(B^{\mu\nu}\tilde{B}_{\mu\nu})$ dropped out because $\text{Tr}(B^{\mu\nu}\tilde{B}_{\mu\nu})$ is a total derivative. Changing the Lagrangian by a total derivative leads to a surface term of the action. By choosing appropriate boundary conditions, $B^{\mu\nu} \to 0$ for $x^\mu \to \pm\infty$, the surface term vanishes. This statement is only valid because $B^{\mu\nu}$ is the field strength tensor of an abelian gauge symmetry. The expression $\text{Tr}(W^{\mu\nu}\tilde{W}_{\mu\nu})$ is also a total derivative. However, we cannot choose boundary conditions such that the surface term vanishes due to the non-trivial vacuum structure of non-abelian gauge theories [161, 162, 163]. By adjusting the global symmetry transformations to account for

$$\alpha_B + \alpha_L = -\frac{\theta_{\text{EW}}}{3} , \tag{4.7}$$

we can remove θ_{EW} from the Lagrangian. It was noted lately in [164] that in a theory with explicit baryon and lepton number violation θ_{EW} is physical and a new source of CP violation.

In QCD, the picture is different. There is no global symmetry of QCD which can be evoked to rotate θ_{QCD} away. QCD has the softly broken axial $U(1)$ symmetry

$$q_i \to e^{-i\alpha\gamma_5} q_i \quad \text{for} \quad i \in \{u, d, s, c, b, t\} , \tag{4.8}$$

with $\gamma_5 = i\gamma_0\gamma_1\gamma_2\gamma_3$. The Lagrangian however changes by

$$\delta\mathcal{L}_{\text{SM}} = -\frac{3g_s^2\alpha}{16\pi^2}\text{Tr}\left(G^{\mu\nu}\tilde{G}_{\mu\nu}\right) + 2i\alpha\bar{q}m_q\gamma_5 q\,. \tag{4.9}$$

Hence, a rotation given by $\alpha = -\theta_{\text{QCD}}/6$ would only shift θ_{QCD} from the topological term proportional to $\text{Tr}(G^{\mu\nu}\tilde{G}_{\mu\nu})$ to the quark mass matrix.

Attempts to measure the neutron electric dipole moment have set an upper bound on θ_{QCD} [165] given by

$$\theta_{\text{QCD}} \lesssim 10^{-10}\,. \tag{4.10}$$

Even though it is technically natural to expect θ_{QCD} to be small because for $\theta_{\text{QCD}} \to 0$ the QCD Lagrangian conserves CP, it is puzzling that nature chose such a small quantity. The question of the origin of such a small value for θ_{QCD} was dubbed the strong CP problem. In principle, there are three known possible solutions.

The first possibility is that the up-quark mass is zero at tree-level and only generated via non-perturbative processes [166, 167]. The axial symmetry of the up-quark would no longer be softly broken and thus would then allow us to rotate θ_{QCD} away. However, lattice computations show that the up-quark mass is non-zero and thus this is not considered a viable solution anymore [168].

The second possible solution is to assume that CP is an exact symmetry of QCD which is spontaneously broken. To spontaneously break the CP symmetry, a complex scalar field has to acquire a complex vacuum expectation value. In order to avoid constraints from electroweak precision measurements and account for a small vacuum angle, the available models have to be tuned. This makes this possibility less attractive [169, 170, 171, 172].

The preferred solution is to introduce a new anomalous global $U(1)_{PQ}$ symmetry which dynamically forces θ_{QCD} to be close to zero. The anomalous global $U(1)_{PQ}$ symmetry is referred to as Peccei-Quinn symmetry [173, 174]. For $U(1)_{PQ}$ to solve the strong CP problem, we have to introduce at least one scalar field ϕ which has a non-trivial $U(1)_{PQ}$ charge and spontaneously breaks $U(1)_{PQ}$. As an example, we define

$$\phi(x) = \varphi(x)e^{ia(x)} \quad \text{with} \quad \langle\varphi\rangle = \frac{f_a}{\sqrt{2}}\,. \tag{4.11}$$

We further have to request that at least one colored field has a non-trivial $U(1)_{PQ}$ charge. The literature mostly considers the two invisible axion benchmark models KSVZ [175, 176] and DFSZ [177, 178]. By spontaneously breaking the global $U(1)_{PQ}$ symmetry, the pseudoscalar field $a(x)$ becomes a pseudo Nambu-Goldstone boson. The field $a(x)$ is referred to as axion field [179, 180]. The axion is only a pseudo Nambu-Goldstone boson because the colored fields which are charged under the anomalous $U(1)_{PQ}$ symmetry introduce a topological term into the Lagrangian

$$\mathfrak{L} \supset -\xi \frac{a(x)}{f_a} \frac{g_s^2}{32\pi^2} \mathrm{Tr}\left(G^{\mu\nu}\tilde{G}_{\mu\nu}\right) , \tag{4.12}$$

due to the vacuum structure of QCD. This topological term breaks the classical shift symmetry of the axion field to a discrete shift symmetry

$$a(x) \to a(x) + 2\pi N \frac{f_a}{\xi} \quad \text{with} \quad N \in \mathbb{N}_+ . \tag{4.13}$$

Hence, the relevant Lagrangian for the axion dynamics takes the form

$$\begin{aligned} \mathcal{L} \supset & -\frac{\theta_{\text{QCD}} g_s^2}{32\pi^2} \mathrm{Tr}\left(G^{\mu\nu}\tilde{G}_{\mu\nu}\right) + \frac{1}{2}\partial_\mu a(x)\partial^\mu a(x) - \xi \frac{a(x)}{f_a}\frac{g_s^2}{32\pi^2} \mathrm{Tr}\left(G^{\mu\nu}\tilde{G}_{\mu\nu}\right) \\ & + \mathcal{L}_{\text{int}}\left(\partial a(x)/f_a\right) , \end{aligned} \tag{4.14}$$

where $\mathcal{L}_{\text{int}}$ describes the model dependent axion interactions with the fields of the theory [181]. The non-perturbative QCD instantons represented by the topological term (4.12) generate the effective axion potential

$$V(a) = \Lambda_{\text{QCD}}^4 \left(1 - \cos\left(\theta_{\text{QCD}} + \frac{\xi a(x)}{f_a}\right)\right) , \tag{4.15}$$

where $\Lambda_{\text{QCD}} \sim 220$ MeV is the scale of QCD [182, 183]. The minimum of the axion potential is then given by

$$\langle a \rangle = -\frac{f_a}{\xi}\theta_{\text{QCD}} . \tag{4.16}$$

Thus, by reinserting $a = \langle a \rangle + a_{\text{phys.}}$ into the Lagrangian (4.14), we remove the CP violating vacuum angle from the theory [184]. Here, $a_{\text{phys.}}$ is the physical axion field. Note that the QCD instantons generate the topological term and thus also the effective potential for the axion. This effective potential then forces the axion to remove the QCD vacuum angle by minimizing the action. The anomalous $U(1)_{PQ}$ symmetry cures the strong CP problem by exploiting the non-trivial vacuum structure of QCD.

The QCD axion is a valid dark matter candidate. It has no electric charge and the decay $a \to \gamma\gamma$ is suppressed such that the lifetime of the axion is much larger than the age of the Universe [183]. The only free parameter of the QCD axion is its mass m_a. Experimental limits from star evolution [185], SN1987a [186] and the cosmological energy density [183] require

$$10^{-5}\,\text{eV} \lesssim m_a \lesssim 1\,\text{eV} . \tag{4.17}$$

The QCD axion cannot be produced thermally in the early Universe. A thermal QCD axion would contribute to the effective number of relativistic degrees of freedom at BBN which is already tightly constrained [183]. However, the QCD axion can be produced non-thermally via the vacuum misalignment mechanism [187, 34, 188]. Expanding the axion potential (4.15) to first order, we find

$$V(a) \simeq m_a^2 \frac{a^2(x)}{2}, \tag{4.18}$$

with

$$m_a^2 = \xi^2 \frac{\Lambda_{\mathrm{QCD}}^4}{f_a^2}. \tag{4.19}$$

The equation of motion of the axion field in the early Universe is then given by

$$\ddot{a} + 3H\dot{a} + m_a^2 a = 0. \tag{4.20}$$

At early times, $H > m_a$, such that the Hubble friction dominates and the axion field is frozen at its initial value. At late times, $m_a > H$, the axion field starts to oscillate and we can interpret the energy density of the oscillations as dark matter [189]. Dedicated experiments such as ADMX [48] actively search for axion dark matter.

Inspired by the QCD axion, we can also construct extensions of the Standard Model with more general axion-like particles. Any non-abelian gauge extension of the Standard Model with an anomalous global symmetry potentially introduces an axion-like particle. Moreover, it was later recognized that theories with compactified extra dimensions such as Kaluza-Klein theories and string theories [190, 191] also contain axion-like particles. As the QCD axion, these new axion-like particles can be interesting dark matter candidates.

Axion-like particles are bosons. In order for these ultralight bosons to account for the energy density of dark matter, they have to be highly condensed in phase space. Besides, if the axion-like particles are dark matter, their total number has to be approximately conserved since dark matter decays have to be suppressed. If the axion-like particles further thermalize, they can form a Bose-Einstein condensate (BEC). In this context, a BEC is a single coherent macroscopic wave function with long range correlation [192]. The idea that dark matter halos could be composed of BECs was first developed in [193].

4.2 Bose-Einstein Condensate Dark Matter

In the last section, we introduced axion-like particles with the example of the QCD axion. Note that the QCD axion is motivated by an anomalous global symmetry and not an ad hoc dark matter candidate. Even if there is no remnant symmetry which stabilizes axion dark matter, the fact that the axion couplings are suppressed by the axion decay constant oppresses any possible decays.

The possibility that axion-like particles can form BECs opens new doors in dark matter phenomenology. Ordinary cold dark matter, such as the Majorana leptobaryon χ discussed in section 2.2.1, is confronted with a number of experimental problems at the galactic and sub-galactic scale, known as small scale crisis:

- **Core vs. Cusp problem:** N-body simulations of cold dark matter predict a cusp in the dark matter density profile of galaxies. However, the measured galactic density profiles show no cusp but a flat central core [194, 195, 196, 197].

- **Missing Satellite problem:** Every dark matter halo is accompanied by smaller halos, the satellite halos. Observations from the Virgo cluster show that much less accompanying satellite halos are observed than N-body simulations predict on the scale of galaxy clusters [198, 199, 200, 201].

- **Too-big-to-fail problem:** The N-body simulations do not only fail to give the correct number of galaxy cluster satellites, but also the satellites we observe are not as massive as predicted. Simulations predict such massive satellite halos that we could not have missed them while already observing smaller halos [202, 203, 204].

BEC dark matter is especially interesting because it has been claimed that BEC dark matter evades the small scale crisis of cold dark matter. Studies of BEC dark matter showed that the structure formation on galactic scales is suppressed which is in good agreement with the dark matter density profiles and satellites we observe [205]. In principle, there are two distinct classes of BEC dark matter:

- **BEC dark matter without self-interactions:** The quantum pressure of the localized particles stabilizes the dark matter halo against gravitational collapse. The de Broglie wavelength of the axion-like particles thus has to be of galactic size. The axion-like particles forming a BEC dark matter halo without self-interactions hence have to be very light

  $$m_a \sim 10^{-22}\text{eV}\,. \tag{4.21}$$

  This scenario is known as fuzzy dark matter in the literature [206, 207, 208, 209, 210, 211]. For a recent review see [212].

- **BEC dark matter with self-interactions:** A repulsive self-interaction of the axion-like particles can stabilize the dark matter halo and thus can allow for particles with smaller de Broglie wavelength [213, 214, 215, 216, 217]. Note that in general also an attractive self-interaction is possible. However, such systems tend to be unstable against gravitational perturbations and are more likely to form smaller density clumps such as Bose stars [218, 219, 220, 221, 222, 223]. Moreover, it was argued in [224] that only repulsive self-interactions lead to long-range correlations. We can estimate the mass range of the axion-like particles by demanding that the wavelengths of the particles have to be large enough to overlap in order to form a BEC. We then find

$$10^{-22}\,\mathrm{eV} \lesssim m_a \lesssim 1\,\mathrm{eV}\,. \tag{4.22}$$

Axion-like particles with repulsive self-interactions which form a BEC are therefore a particularly interesting dark matter candidate. The repulsive self-interaction allows for a broader mass range and much heavier particles compared to fuzzy dark matter. We will therefore focus on axion-like particles with a repulsive self-interaction in the following section. Note that due to the axion potential (4.15), the QCD axion always has an attractive self-interaction and thus does not form BEC dark matter halos. For a study of axion-like particles with a repulsive self-interaction see [217].

So far we have presented an alternative dark matter candidate, axion-like particles with repulsive self-interaction which form a BEC. However, the question arises: How can we distinguish this type of dark matter from ordinary cold dark matter?

Proposed methods range from an enhanced integrated Sachs-Wolfe effect [225], tidal torquing of galactic halos [226, 227, 228], and new effects on the cosmic microwave background matter power spectrum [229, 230]. However, neither of the considered methods has yet been successful. In February 2016, the LIGO collaboration announced the first detection of gravitational waves from a black hole-black hole merger [231]. This exceptional discovery has paved the way to new experimental methods to explore our Universe [232, 233]. In the next section, we propose a new method to probe BEC dark matter composed of bosons with repulsive self-interactions using multi-messenger gravitational wave astronomy.

4.3 Probing BEC Dark Matter with Gravitational Waves

We now propose a new method to test for BEC dark matter which consists of bosons with a repulsive self-interaction utilizing gravitational wave detectors [5]. Note that we focused our discussion on axion-like particles so far because they are well motivated particle candidates in a variety of beyond the Standard Model scenarios with anomalous global symmetries or compactified extra dimensions. However, our discussion on BEC dark matter is actually more general and in principle addresses all weakly interacting slim particles (WISPs) [234]. Our discussion thus also applies to light hidden-sector gauge bosons [235, 236, 237].

We first outline the general idea before turning to the quantitative analysis. We consider a gravitational wave which, for example, was emitted by a black hole-neutron star merger and passes through a BEC dark matter halo while traveling towards a gravitational wave detector on or around the Earth. A schematic outline of the general idea and the experimental set-up is shown in Figure 4.1.

While passing through the BEC halo, the gravitational wave scatters coherently in forward direction off the BEC phonons. The scattering induces a refractive index for the gravitational wave in the BEC medium. Thus, the gravitational wave is slowed down and does not propagate with the speed of light through the BEC dark matter halo. If the emitted gravitational wave has an electromagnetic or neutrino counterpart which we can measure on Earth, we can infer from the measured effective propagation speeds the microscopic properties of the BEC halo. The non-observation of a difference in the effective velocities constrains BEC dark matter severely.

To describe general BEC dark matter, we use a classical real scalar field $a(x)$ with the effective Lagrangian [238]

$$\mathcal{L}_{\text{BEC}} = \frac{1}{2}\partial_\mu a \partial^\mu a - \frac{1}{2} m_a^2 a^2 - \lambda_a a^4 \,, \tag{4.23}$$

where $\lambda_a > 0$ to account for a repulsive self-interaction. As the gravitational wave travels through the BEC dark matter halo, it excites phonon modes [239]. Thus, the gravitational wave interacts with the BEC medium. Note that such an interaction is unique for BEC dark matter and does not occur for ordinary cold dark matter. However, gravitational waves are also slowed down inside ordinary cold dark matter halos or any other energy density distribution in space. Due to the weakness of the gravitational interaction this effect is negligible [240, 241]. The phonon modes are excited as the gravitational wave undergoes coherent forward scattering in the BEC medium.

The optical theorem [242] links the forward scattering amplitude $f(0)$ to the refractive index

$$\eta_g = 1 + \frac{2\pi n f(0)}{k^2} \,, \tag{4.24}$$

with k being the wave number of the incident wave and n being the number density of

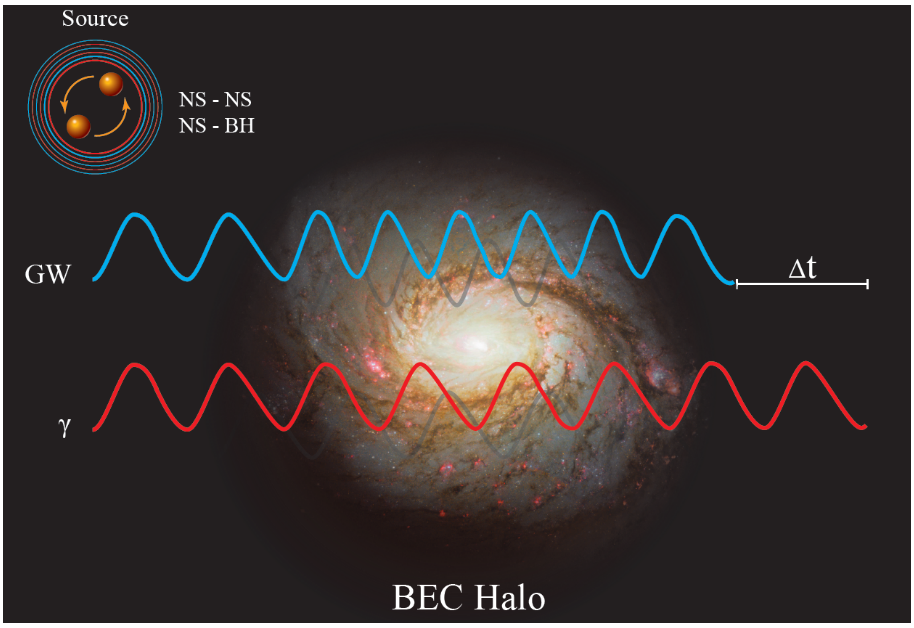

Figure 4.1: Schematic outline of the general idea how to probe BEC dark matter with gravitational waves.

scatterers. In general, the refractive index is a complex quantity

$$\eta_g = n_g - i\kappa_g \,. \tag{4.25}$$

By entering a medium, the wavelength of the incoming wave changes, $\lambda \to \eta_g/\lambda$, and as a result, so does the wave number, $k \to \eta_g k$. For a spherical wave $\Psi = \Psi_0 e^{-ikr}/r$, we thus find

$$\frac{\Psi_0}{r} e^{-ikr} \to \frac{\Psi_0}{r} e^{-i\eta_g kr} = \frac{\Psi_0}{r} e^{-\kappa_g kr} e^{-in_g kr} \,. \tag{4.26}$$

The complex refractive index η_g leads to two observable effects: The propagation speed of the wave changes $c_g = c/n_g$ and the amplitude of the wave is damped by $e^{-\kappa_g kr}$. We expect the wave absorption to be negligible because the energy of the gravitational wave does not suffice to excite the massive phonon modes in the BEC medium [239].

The optical theorem does not only link the refractive index η_g to the forward scattering amplitude $f(0)$, but also the imaginary part of the forward scattering amplitude to the total scattering cross section

$$\sigma_{\mathrm{BEC}}^{\mathrm{GW}} = \frac{4\pi}{k} \mathrm{Im}\left(f(0)\right) \,. \tag{4.27}$$

Hence, to calculate the refractive index for a gravitational wave in a BEC dark matter halo from first principles, we would have to calculate the cross section of the gravitational wave-phonon scattering. Since such a calculation is beyond this work, we estimate the refractive index of the gravitational wave in the BEC dark matter halo by relating the energy density of the incoming gravitational wave to the energy density of the massless phonon excitations.

From the Lagrangian given in equation (4.14), we can calculate the stress-energy tensor

$$T^{\mu\nu}_{\rm BEC} \;=\; \frac{\partial \mathcal{L}_{\rm BEC}}{\partial(\partial_\mu a)}\partial^\nu a - \eta^{\mu\nu}\mathcal{L}_{\rm BEC}\,, \tag{4.28}$$

with $\eta = \mathrm{diag}(1,-1,-1,-1)$. The background energy density $\rho_0 \equiv T^{00}_{\rm BEC}$ and pressure $p_0 \equiv T^{ii}_{\rm BEC}$ are then related by the equation of state [213]

$$p_0 \;=\; \frac{3}{2}\frac{\lambda_a}{m_a^4}\rho_0^2\,. \tag{4.29}$$

The speed of sound of the phonon modes can be derived from the equation of state by

$$c_s \;\equiv\; \left(\frac{\partial p_0}{\partial \rho_0}\right)^{1/2} \;=\; \left(\frac{3\lambda_a\rho_0}{m_a^4}\right)^{1/2}\,. \tag{4.30}$$

To estimate the energy density of the massless phonon modes, we assume that the dark matter halo is spherically symmetric. The phonons can therefore be described by an one-dimensional wave function with hard-wall boundary conditions. The average distance the gravitational wave propagates through a spherically symmetric halo with radius R is given by $\langle D_{\rm halo}\rangle = 4R/\pi$. Therefore, the energy spectrum of the massless phonon modes is [239]

$$\omega_l \;=\; \frac{l\pi c_s}{\langle D_{\rm halo}\rangle} \quad \text{with} \quad l \in \mathbb{N}_+\,. \tag{4.31}$$

As the gravitational wave travels through the BEC dark matter halo, it excites phonon modes. The minimum energy density required to excite massless phonon modes is determined by

$$\Delta\rho \;\equiv\; n_a\Delta\omega \;=\; \frac{n_a\pi^2 c_s}{4R}\,, \tag{4.32}$$

where n_a is the number density of phonons in the BEC medium and $\Delta\omega \equiv \omega_{l+1} - \omega_l$.

The energy density of the incoming gravitational wave is given by [243]

$$\rho_{\rm GW} \;=\; \frac{1}{4}M_{\rm Pl}^2\omega_{\rm GW}^2 h^2\,, \tag{4.33}$$

where h is the gravitational wave amplitude and $\omega_{\rm GW}$ is the gravitational wave frequency. Exploiting the linear dispersion relation of gravitational waves, we can relate the change of the wave number of the gravitational wave in the BEC medium to the minimum excitation energy density of the massless phonon modes by

$$\frac{\Delta\rho}{\rho_{\rm GW}} = 2\frac{\Delta k}{\omega_{\rm GW}}\,. \tag{4.34}$$

The refractive index of the gravitational wave in the BEC medium is then given by

$$n_g = 1 + \frac{\Delta k^2}{2\omega_{\rm GW}^2}\,, \tag{4.35}$$

where Δk can be thought of as an induced graviton mass if the gravitational wave were quantized.

A striking feature of BEC dark matter is its predictability. The radius of the dark matter halo is completely determined by the microscopic properties of the real scalar field [244, 245, 246]

$$R = 2\pi\sqrt{3\lambda_a}\,\frac{M_{\rm Pl}}{m_a^2}\,. \tag{4.36}$$

The phonon number density in the BEC medium is also determined by the mass of the axion-like particle m_a and the quartic coupling λ_a [5]

$$n_a = \left(\frac{6m_a^4}{\pi^2\lambda_a}\right)^{\frac{3}{4}}\zeta(3/2)\,. \tag{4.37}$$

The energy density distribution of a spherically symmetric BEC dark matter halo is given by [244]

$$\rho(r) = \rho_{\rm cr}\frac{\sin(\pi r/R)}{\pi r/R}\,. \tag{4.38}$$

We hence find $\rho(r\to 0) = \rho_{\rm cr}$. Thus, BEC dark matter predicts flat central core densities and solves the core vs. cusp problem. The average density is completely fixed by the central density

$$\rho_0 \equiv \langle\rho\rangle = \frac{3\rho_{\rm cr}}{\pi^2}\,. \tag{4.39}$$

We can therefore define the change in the refractive index as the gravitational wave travels through the BEC dark matter halo as

$$\delta n_g \equiv n_g - 1 = \sqrt{\frac{3}{2}}\frac{9m_a^6\rho_{\rm cr}\zeta^2(3/2)}{8\pi^3\lambda_a^{3/2}h^4\omega_{\rm GW}^4M_{\rm Pl}^6}\,, \tag{4.40}$$

which only depends on the gravitational wave amplitude h and frequency $\omega_{\rm GW}$, central density of the dark matter halo $\rho_{\rm cr}$, and the microscopic parameters m_a and λ_a. Since we can measure the central density of dark matter halos with sky surveys and the gravitational wave detectors determine the amplitude h and frequency ω_{GW} of a measured gravitational wave, we can constrain the $(m_a,\,\lambda_a)$-parameter space for fixed ρ_{cr}, h, and ω_{GW} by constraining the propagation speed of the gravitational wave.

To relate the change of the refractive index to the deviation of the gravitational wave velocity from the speed of light, we require that the gravitational wave is produced at a distance D from Earth and encounters a BEC dark matter halo with radius R while traveling to Earth. The fraction of distance which the gravitational wave propagates through the dark matter halo is then given by

$$x \;\equiv\; \frac{\langle D_{\mathrm{halo}}\rangle}{D} \;=\; \frac{4R}{\pi D}\,. \tag{4.41}$$

The time necessary for the gravitational wave to arrive on Earth while encountering the BEC halo is

$$\Delta\tau = x\frac{D}{c_g} + (1-x)\frac{D}{c}\,, \tag{4.42}$$

with c_g the propagation speed of the gravitational wave in the BEC medium and the speed of light $c = 1$ displayed explicitly. The effective speed with which the gravitational wave travels the distance D from its source to Earth is

$$c_{\mathrm{eff}} \;\equiv\; \frac{D}{\Delta\tau} \;=\; \frac{c_g}{x + (1-x)c_g}\,. \tag{4.43}$$

The deviation of the effective gravitational wave velocity with respect to the speed of light is then given by

$$\delta c_g \;\equiv\; 1 - c_{\mathrm{eff}} \;=\; \frac{x\delta n_g}{1 + x\delta n_g}\,. \tag{4.44}$$

Hence, we succeeded in relating the measurable change in the gravitational wave velocity δc_g to the microscopic properties m_a and λ_a of the BEC dark matter for fixed macroscopic quantities ρ_{cr}, D, h, and ω_{GW}.

The best current constraint on the gravitational wave velocity arises from the non-observation of gravitational Cherenkov radiation [247] and is given by

$$\delta c_g = 1 - c_g \lesssim 10^{-15}\,. \tag{4.45}$$

However, future multi-messenger experiments have the potential to tighten the bounds rapidly.

For example, the gamma-ray burst measured by Fermi-GBM [248] 0.4 seconds after LIGO detected GW150914 [231] gives with a typical time-of-flight analysis [249] $\delta c_g \lesssim 10^{-17}$ assuming that the gamma-ray burst and the gravitational wave have the same origin [250, 251, 252]. However, using modified dispersion relations typical for theories of quantum gravity, much stronger bounds can be deduced, $\delta c_g \lesssim 10^{-40}$ [253]. Even if the gamma-ray burst measured by Fermi-GBM is probably not correlated to the gravitational wave GW150914 as suggested by recent analysis [254, 255, 256, 257, 258, 259, 260] and the non-observation of a gamma-ray burst at AGILE [261], INTEGRAL [262], and SWIFT [263], this example demonstrates what can be expected from future multi-messenger searches.

During the preparation of this thesis, the LIGO and VIRGO collaborations announced the detection of a fourth gravitational wave. For the first time, a gravitational wave was detected by a three-detector network. The improved angular sky resolution is crucial for successful multi-messenger astronomy in the future [264].

In Figure 4.2, we numerically evaluate the relation (4.44) and constrain the $(m_a,\, \lambda_a)$-parameter plane for fixed $\rho_{\rm cr}$, D, h, and $\omega_{\rm GW}$. The central halo density was thereby fixed to $\rho_{\rm cr} = 0.04 M_\odot/{\rm pc}^3$ with solar mass $M_\odot$ [265]. In the upper panel, we further fixed $D = 400$ Mpc, $f = 35$ Hz and $h = 10^{-21}$ to illustrate the experimental reach of LIGO. The measured frequency f is related to the angular frequency of the gravitational wave via $w_{\rm GW} = 2\pi f$. The experimental limits eLISA can enforce on BEC dark matter with a repulsive self-interaction are displayed in the lower panel of Figure 4.2 for $D = 3$ Gpc, $f = 1$ mHz and $h = 10^{-20}$.

Studies of galaxy cluster collisions [266, 267, 268, 269, 270] and dark matter halo shapes [265, 271, 272, 273, 274] have severely constrained the dark matter self-interaction cross section per mass, $\sigma/m \sim (0.01 - 1){\rm cm}^2/{\rm g}$. The allowed region is given by the blue band in Figure 4.2.

Furthermore, the rotation curves of dark matter dominated low surface brightness galaxies and dwarf spheroidal galaxies have narrowed the allowed range of BEC dark matter halo radii, $R \sim (0.5 - 10)$ kpc [215, 244, 275, 276, 277]. Via equation (4.36), we can translate this bound to a constraint in the (m_a, λ_a)-parameter space. The allowed range of dark matter halo radii is given by the green band in Figure 4.2. The physically preferred point which is in agreement with the constraints on the dark matter self-interaction per mass and on the dark matter halo radii is indicated by a yellow square. Moreover, we regard any dark matter halo radii larger than one Mpc as nonphysical [244, 272]. Hence, the upper left region of the (m_a, λ_a)-parameter space is ruled out as indicated by the light purple shaded region in Figure 4.2.

A particular strong constraint can be derived from the effective number of relativistic degrees of freedom in the early Universe. Latest Planck results have put an upper limit on the additional relativistic degrees of freedom compared to the Standard Model, $\Delta N_{\rm eff} \lesssim 0.39$ [20]. The bound on $\Delta N_{\rm eff}$ is highly relevant for our discussion because $a(x)$ is an extremely light bosonic particle and hence will potentially alter $\Delta N_{\rm eff}$. The scalar field $a(x)$ behaves as radiation and contributes to $\Delta N_{\rm eff}$ if the scalar potential is dominated by the quartic interaction, $V(a) \sim \lambda_a a^4$. We therefore have to make sure that the transition from the radiation-like epoch of $a(x)$ to the matter-like epoch where the quadratic mass term dominates the scalar potential, $V(a) \sim (m_a^2/2)a^2$, has terminated before BBN [215, 277, 278]. We can derive a lower limit $m/\lambda^{1/4} \gtrsim 8.5$ eV from the considerations in [215]. In Figure 4.2, we translated the limit from $\Delta N_{\rm eff}$ to an upper bound on $\lambda_a(m_a)$ as indicated by the dashed black line. Note that the current Planck limit for $\Delta N_{\rm eff}$ is already in conflict with the physical preferred point. To rule out the suggested region by observed dark matter halo radii, we would have to measure $\Delta N_{\rm eff}$ to the precision of $\Delta N_{\rm eff} \lesssim 0.12$.

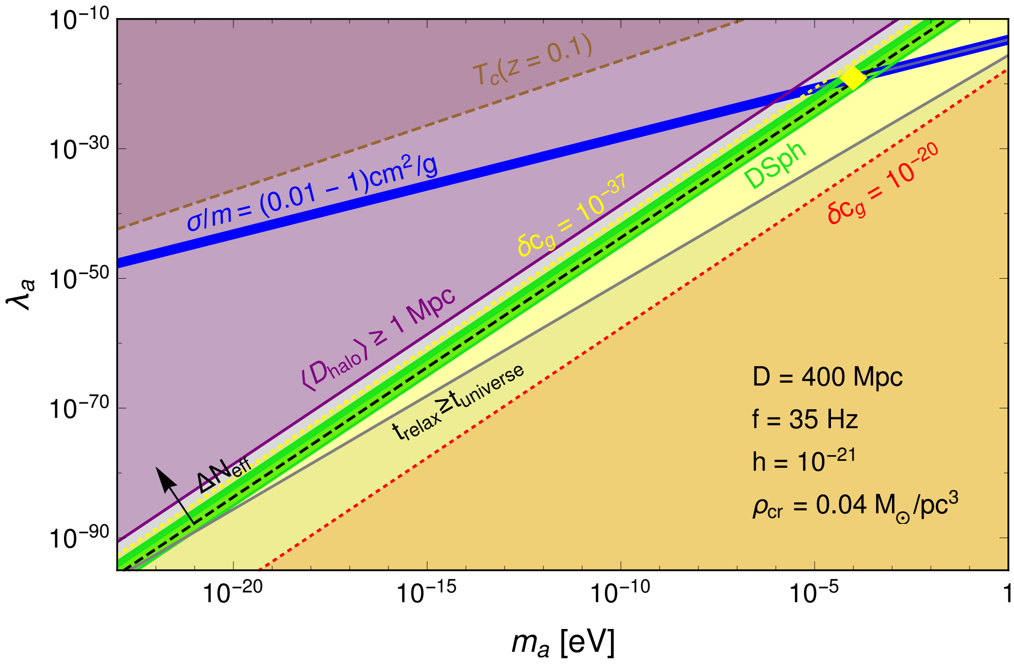

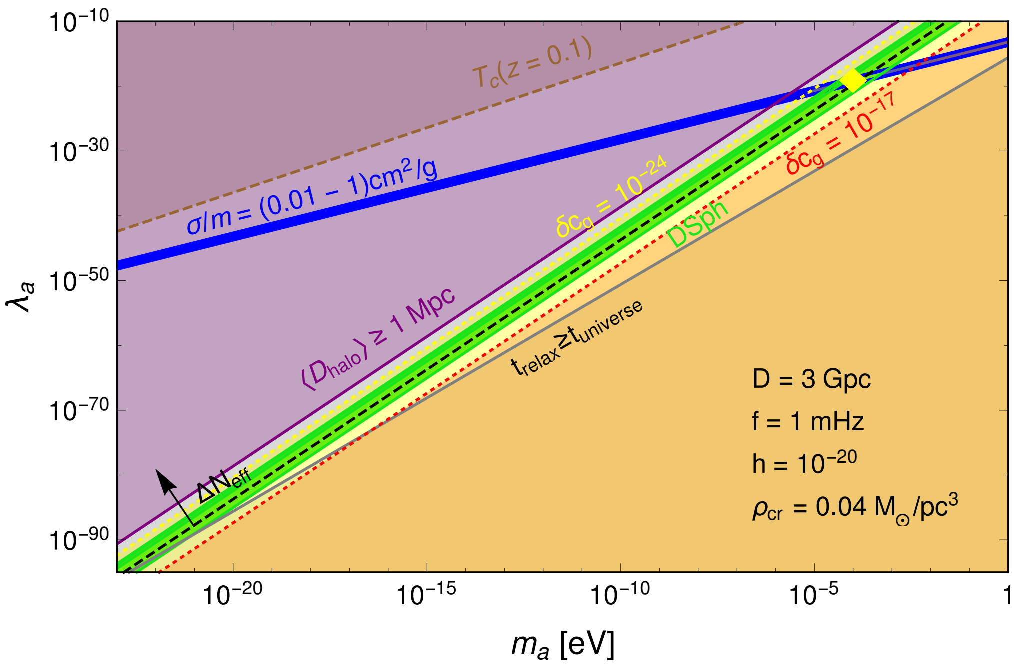

Figure 4.2: Constraints on $\lambda_a(m_a)$ for BEC dark matter with a repulsive self-interaction. The upper panel shows the constraints LIGO can enforce on the quartic self-interaction λ_a as a function of m_a for an upper bound of $\delta c_g \lesssim 10^{-20}$ (red shaded region) and $\delta c_g \lesssim 10^{-37}$ (yellow shaded region). The lower panel considers the future gravitational wave experiment eLISA. For future upper bounds of $\delta c_g \lesssim 10^{-17}$ (red shaded region) we can exclude yet unconstrained parameter space and for $\delta c_g \lesssim 10^{-24}$ (yellow shaded region) we are able to exclude BEC dark matter with repulsive self-interactions at eLISA. See the text below for a discussion of the different constraints shown.

In addition, a theoretical lower bound on $\lambda_a(m_a)$ can be derived from the relaxation time of the BEC halo. If the relaxation time of the BEC halo is larger than the age of the Universe, then the observed dark matter halos could not have formed [221, 279, 280]. Thus, the lower sand colored region in Figure 4.2 is excluded.

Furthermore, a relative weak constraint can be derived from the binary black hole merger event GW150914 detected by LIGO [231]. Assuming that the temperature of the BEC is comparable to the temperature of the visible Universe, we can require that the critical temperature below which a BEC forms, $T_c = (24m_a^2/\lambda_a)^{1/2}$ [281, 282, 283], is above the temperature of the Universe at redshift $z = 0.1$ when the gravitational wave GW150914 was emitted. The upper bound on $\lambda_a(m_a)$ from the critical temperature is given by the dark purple region in Figure 4.2.

We can infer from the upper panel in Figure 4.2 that if future multi-messenger networks such as AMON [284] are able to constrain the velocity of gravitational waves with a precision of $\delta c_g \lesssim 10^{-37}$, we can rule out BEC dark matter with a repulsive self-interaction with LIGO. The lower panel shows that in order for eLISA [285] to probe BEC dark matter with a repulsive self-interaction thoroughly, the multi-messenger searches have to constrain the propagation speed of gravitational waves at the level of $\delta c_g \lesssim 10^{-24}$.

In our discussion, we always assumed that the gravitational wave passes through a dark matter halo on its way to Earth. However, we can make sure that the gravitational wave encountered a dark matter halo by considering the deflection angle of a photon in a multi-messenger signal due to gravitational lensing [243]. The physical preferred point in Figure 4.2 corresponds to a dark matter halo with $R \sim 1$ kpc. Such a dark matter halo leads to a measurable deflection angle of $\delta\theta_{\text{def}} \simeq 10^{-7}$.

Moreover, equation (4.40) shows that the refractive index of a gravitational wave in a BEC is larger for lower frequency waves. This has the slight disadvantage that the Shapiro time delay is also larger for low frequency gravitational waves [286, 287, 288, 289, 290]. Therefore, the measured time delays in multi-messenger searches in the physically interesting region have to be handled with extra care for eLISA [285] and IPTA [291] which are in the low frequency regime.

4.4 Summary

In this section, we introduced axion-like particles as potential dark matter candidates. Axion-like particles are a well motivated extension of the Standard Model and can originate from anomalous global symmetries or compactified extra dimensions. Furthermore, axion-like particles have the striking feature to potentially form BECs of galactic size. These BEC dark matter halos are a possible solution to the cold dark matter small scale crisis. Due to the similarities in large scale structure formation, it is difficult to distinguish BEC dark matter from ordinary cold dark matter.

We therefore propose a new method to probe BEC dark matter with repulsive self-interactions using gravitational waves. A gravitational wave traveling through a BEC dark matter halo is slowed due to the interactions of the gravitational wave with the phonon modes. The interactions induce a refractive index. By measuring the time delay between a gravitational wave signal and an electromagnetic or neutrino counterpart in a multi-messenger search, we can constrain the deviation of the gravitational wave velocity from the speed of light. As BEC dark matter is extremely predictable, we can test the BEC dark matter paradigm for fixed macroscopic quantities: central dark matter halo core density ρ_{cr}, gravitational wave amplitude h and frequency f, and the distance D of the source of the multi-messenger signal from Earth. Constraining the gravitational wave propagation to the order of $\delta c_g \lesssim 10^{-37}$ would potentially rule out BEC dark matter at LIGO. However, eLISA has the potential to probe the interesting region of parameter space already for $\delta c_g \lesssim 10^{-24}$.

CHAPTER 5

INTERWEAVING GLOBAL SPACETIME AND PARTICLE SYMMETRIES

WHERE do we stand in theoretical particle physics? We have lots of prominent problems which should require a beyond the Standard Model solution. Some of the problems addressed in the previous chapters were the hierarchy problem, dark matter, neutrino masses, and proton stability. There are also problems such as the smallness of the cosmological constant which we neglected. However, the truth is that our favorite solutions to the hierarchy problem and dark matter which we thought are linked to the electroweak scale, supersymmetry and WIMPs, have yet not been found. Furthermore, their theoretical charm starts to crumble as we are forced to reduce couplings and increase masses to reconcile these theories with our experimental observations.

How should we go on with theoretical particle physics? We do not know. The breakdown of unitarity of the WW scattering amplitude was a guarantee that we could expect new physics at the electroweak scale and we found new physics: the Higgs boson. However, we do not have such a guarantee for future experiments. As our current ideas are tested and start to fail us, it seems mandatory that we open-mindedly also pursuit new ideas.

In this chapter, we want to introduce such a new idea. In contrast to low scale supersymmetry or WIMPs, this beyond the Standard Model approach is not directly linked to the electroweak scale. However, in this thesis, we advertised the ideas of low scale unification and axion-like dark matter such that we already decoupled the hierarchy problem and dark matter from the electroweak scale. We propose to move away from 4-dimensional Minkowski spacetime and investigate new possibilities. As a guiding principle, we require that the new spacetime structure should allow for the mixing of global internal and external symmetries. Internal symmetries are the conventional particle symmetries which we focused on in the previous sections such as global baryon number or the Peccei-Quinn symmetry, whereas external symmetries are the global spacetime symmetries. The global spacetime symmetry group associated with the conventional 4-dimensional Minkowski spacetime $\mathcal{M}_4$ is the Poincaré group $\mathcal{P}(1,3)$. We expect that in a truly fundamental theory the same analytic equations should describe spacetime and particles. Thus, the truly fundamental theory should also not distinguish between internal and external symmetries.

The famous Coleman-Mandula "no-go" theorem [66] shows under general assumptions that the full global symmetry group of a relativistic interacting theory has to factor into internal and external symmetries. The conventional way to circumvent the Coleman-

Mandula theorem is to move from ordinary symmetry algebras to graded symmetry algebras and thus introduce supersymmetry [292]. We will review the Coleman-Mandula theorem in the next section and point out different theoretical concepts which also allow us to mix global spacetime and particle symmetries without supersymmetry. Finally, we will discuss a new approach to spacetime and explicitly demonstrate the mixing of global internal and external symmetries in a toy model. We thereby focus on theories where spacetime is the direct product of 4-dimensional Minkowski spacetime and d orthogonal space-like dimensions. The toy model we construct shows how the three Standard Model generations and the fermion masses could be related to hidden spacetime symmetries. The ideas of this chapter are based on [6].

5.1 Coleman-Mandula Theorem

The Coleman-Mandula theorem is a general theorem of scattering theory [66]. We assume that the space of physical states is a Hilbert space which can be written as the direct sum of n-particle Hilbert spaces

$$\mathcal{H} = \mathcal{H}^{(1)} \oplus \mathcal{H}^{(2)} \oplus \ldots \,, \tag{5.1}$$

with $\mathcal{H}^{(n)}$ being the symmetrised Hilbert space from n one-particle Hilbert spaces

$$\mathcal{H}^{(n)} = \underbrace{\mathcal{H}^{(1)} \oplus \cdots \oplus \mathcal{H}^{(1)}}_{n\text{-times}} \,. \tag{5.2}$$

We then define the S-matrix as unitary operator on the Hilbert space $\mathcal{H}$ which describes scattering

$$S = 1 - i(2\pi)^D \delta^{(D)}(p - p')\, T \,, \tag{5.3}$$

where D is the number of spacetime dimensions and T the transition matrix.

For an unitary operator U on $\mathcal{H}$ to be a symmetry transformation of the S-matrix the following requirements have to be fulfilled:

(i) U maps one-particle states into one-particle states.
(ii) U acts on many particle states through the tensor product representation of one-particle states.
(iii) U commutes with S, $[U, S] = 0$.

The Coleman-Mandula theorem then states if G is a connected symmetry group of the S-matrix and

(I) G has a subgroup which is locally isomorphic to the Poincaré group,
(II) all physical particles have positive definite mass and there exists only a finite number of particles below an energy threshold E_{max},
(III) the S-matrix is an analytic function of the Mandelstam variables s and t,
(IV) the S-matrix is non-trivial at almost all energies,
(V) generators of G are representable as integrals in momentum space,

then G is locally isomorphic to the Poincaré group times an internal symmetry group.

The Coleman-Mandula theorem is a technical theorem. We will first try to convey the physical intuition [293, 294] of the theorem before turning to a more detailed sketch of the proof. Nevertheless, the interested reader is directed to [66, 295, 296] where the proper mathematical proof can be found.

To develop a physical intuition, we consider a $2 \to 2$ scattering process. The scattering process depends on the initial and final momenta. Thus, we would expect that the $2 \to 2$ scattering is described by 16 independent parameters in four dimensions. However, the scattering amplitude describing the scattering process has to respect the global spacetime symmetries which reduces the 16 independent parameters of the initial and final momenta to two independent parameters in 4-dimensional Minkowski spacetime.

The first condition we have to impose onto the scattering amplitude is Lorentz invariance and hence the amplitude has to be a Lorentz scalar. Secondly, we want to consider the scattering of physical particles and therefore the initial and final momenta have to be on the mass-shell. Finally, the $2 \to 2$ scattering process has to respect energy-momentum conservation. Counting the degrees of freedom and the imposed restrictions from Minkowski spacetime, we arrive at the known result that a $2 \to 2$ scattering process in $d+1$ dimensions with $d > 1$ only depends on the Mandelstam variables s and t.

If we would further demand that the scattering amplitude has to respect additional momentum dependent symmetries, only discrete values of s and t would be allowed. However, this is in conflict with our experimental observations where we find a continuous dependence of scattering on s and t. We therefore have to conclude that any further restrictions on the scattering amplitude have to be momentum independent. The generators of such a momentum independent symmetry transformation would commute with the momentum generators and would thus be named internal symmetries. We therefore arrive at the conclusion that the general symmetry structure of the S-matrix is given by

$$G \to \mathcal{P}(1,3) \otimes \text{“internal symmetries”}\,, \tag{5.4}$$

where $\mathcal{P}(1,3)$ is the Poincaré group in $3+1$ dimensions.

The proof of the no-go theorem as carried out by Coleman, Mandula [66], and later Weinberg [296] is tedious. Here, we will only go through the general structure and present the most important steps. We assume that A is a symmetry generator of the S-matrix and thus

$$\langle p'|\,[S,A]\,|p\rangle = 0\,. \tag{5.5}$$

The symmetry generator A should be a Lorentz invariant quantity and hence the operator $U^\dagger(\Lambda,a)A\,U(\Lambda,a)$ should also be an element of the algebra spanned by the symmetry generators of S where $U(\Lambda,a)$ is the unitary operator that implements Poincaré transformations on the physical Hilbert space $\mathcal{H}^{(1)}$ of one-particle states. We can then define the operator

$$f\cdot A = \int \mathrm{d}^4 a\, U^\dagger(1,a)A\,U(1,a)\tilde{f}(a)\,, \tag{5.6}$$

to explore how internal symmetries can modify the translational invariance of the symmetry generator A where $\tilde{f}$ is the Fourier transformed of a test function f. After a short calculation we find

$$f\cdot A\,|p\rangle = \int \mathrm{d}^4\,k\,|k\rangle\,\langle k|\,f\cdot A\,|p\rangle = \int \mathrm{d}^4\,k\,|k\rangle\,f(k-p)A(k,p)\,, \tag{5.7}$$

where we defined $A(k,p) = \langle k|\,A\,|p\rangle$. Translational invariance of the symmetry generator A restricts the general test function f only to depend on the difference of the initial and final 4-momenta.

The matrix element $A(k,p)$ is only non-vanishing if both 4-momenta p and k are on the mass-shell. We can now choose a region Δ in momentum space such that both p and

$p + \Delta$ are on the mass-shell and $\Delta \neq 0$. Furthermore, we choose the test function f such that $f \neq 0$ only for a sufficient small region around Δ. We would therefore find

$$f \cdot A \, |p\rangle = f(\Delta) A(p + \Delta, p) \, |p + \Delta\rangle \; , \tag{5.8}$$

where the modified symmetry generator $f \cdot A$ now connects the two states $|p\rangle$ and $|p + \Delta\rangle$. In general, if we choose Δ to be small, we will find for a 2→2 scattering process which obeys energy momentum conservation, $p+q = p'+q'$, that the momenta $q+\Delta$, $q'+\Delta$ and $p' + \Delta$ are not on the mass-shell. Hence, the matrix elements $A(q + \Delta, q)$, $A(q' + \Delta, q')$ and $A(p' + \Delta, p')$ have to vanish. If we demand that the modified symmetry generator $f \cdot A$ should also be an element of the algebra spanned by the symmetry generators of the S-matrix, then $f \cdot A$ has to commute with S which leads for a 2→2 scattering process to the relation

$$\begin{aligned} &\langle p' \, q' | \, S \Big(f \cdot A \, |p\rangle \otimes |q\rangle + |p\rangle \otimes f \cdot A \, |q\rangle \Big) \\ &\qquad\qquad\qquad = \Big(\langle p' | \, f \cdot A \otimes \langle q' | + \langle p' | \otimes \langle q' | \, f \cdot A \Big) S \, |p \, q\rangle \; , \end{aligned} \tag{5.9}$$

which simplifies to

$$\langle p' \, q' | \, S \, f \cdot A \, |p\rangle \otimes |q\rangle = f(\Delta) A(p + \Delta, p) \, \langle p' \, q' | \, S \, |p + \Delta \, q\rangle = 0 \, . \tag{5.10}$$

If the S-matrix would vanish for this scattering process, it would vanish for all scattering processes since we assumed that the S-matrix is an analytic function of the Mandelstam variables s and t. We can therefore always vary q, q' and p' to continuously describe all possible values of s and t. This is in contradiction with the assumption of non-trivial scattering for almost all energies. We thus have to conclude that $A(p+\Delta, p)$ has to vanish. There are two loopholes to prevent $A(p + \Delta, p)$ from being trivial.

- **A commutes with P^μ:** The matrix elements of the modified symmetry operator now take the form

  $$\langle p' | \, f \cdot A \, |p\rangle = \left(\int \mathrm{d}^4 a \tilde{f}(a) \right) \langle p' | \, A \, |p\rangle \; . \tag{5.11}$$

  The matrix elements of the symmetry generator A are now modified by a momentum independent constant. This momentum independent constant would correspond to an internal symmetry.

- **Equal initial and final momentum:** We neglected the possibility of $\Delta = 0$. The matrix element $A(p', p)$ is then only allowed to be non-vanishing for $p = p'$ and thus could be parametrized by

  $$A(p', p) = \delta^{(4)}(p' - p) \, a(p', p) \, . \tag{5.12}$$

The matrix elements of the modified symmetry generator $f \cdot A$ would then take the form

$$\langle p'|\, f \cdot A \,|p\rangle = f(0)\, a(p,p)\,, \tag{5.13}$$

and the modified symmetry generator $f \cdot A$ is hence given by

$$f \cdot A \,|p\rangle = f(0)\, a(p,p)\,|p\rangle\ . \tag{5.14}$$

We have just proven a powerful theorem already discovered by O'Raifeartaigh [297]: symmetry transformations cannot connect particles on different mass-shells. More general, a matrix element of a generator of the symmetry group of the S-matrix is only non-vanishing for equal initial and final 4-momenta. The matrix elements of the symmetry generators therefore have to be proportional to the delta distribution or derivatives of the delta distribution

$$\langle p'|\, A^{(N)}\,|p\rangle = \sum_{n=0}^{N} A^{(n)}(p)_{\mu_1\ldots\mu_n} \frac{\partial}{\partial p_{\mu_1}} \cdots \frac{\partial}{\partial p_{\mu_n}} \delta^{(4)}(p'-p)\,, \tag{5.15}$$

with

$$A^{(n)}(p)_{\mu_1\ldots\mu_n} \delta^{(4)}(p'-p) = \frac{1}{n!}\,\langle p'|\,[P_{\mu_1},[P_{\mu_2},\ldots[P_{\mu_n},A^{(n)}]]]\,|p\rangle\ . \tag{5.16}$$

The proof of the Coleman-Mandula theorem now reduces to the discussion of the different cases $N=0$, $N=1$, and $N>1$.

- $N=0$**:** The generators of the symmetry group are linear in the momentum

  $$A^{(0)} = a_\mu P^\mu + b\,\mathbb{I} + B\,, \tag{5.17}$$

  where B are generators of an internal symmetry group of the S-matrix which commute with the generators of the Poincaré group. The generators B have to transform trivially with respect to the Poincaré group due to the fact that the Poincaré group is non-compact and hence has no non-trivial finite-dimensional unitary representation. Non-relativistic theories which are only restricted by the Galilei group which is compact evade this constraint. This is precisely the loophole in the Coleman-Mandula theorem which we will later exploit with d orthogonal "non-relativistic" space-like dimensions.

- $N=1$**:** The generators of the symmetry group generate the Poincaré algebra

  $$A^{(1)}(p,p) = a_{\mu\nu} J^{\mu\nu} + A'^{(0)} \delta^{(4)}(p'-p)\,, \tag{5.18}$$

  where $J^{\mu\nu}$ are the generators of the homogeneous Lorentz group.

- $N>1$**:** The symmetry generators with more than one derivative acting on the delta distribution vanish.

This completes the proof of the Coleman-Mandula theorem and can be extended from the 4-dimensional Poincaré group to the $(d+1)$-dimensional Poincaré group [295].

5.2 Living without Supersymmetry

In the last section, we studied the Coleman-Mandula theorem. Now, we want to point out possibilities to circumvent the Coleman-Mandula theorem and allow for a mixing of internal and external symmetries. The preferred way around the no-go theorem is to introduce Grassmann coordinates and promote spacetime to a superspace [292]. However, since the concept of supersymmetry could not yet be experimentally verified, we want to explicitly focus on loopholes of the theorem which do not require supersymmetry.

- **Non-local interactions:** An underlying assumption of the Coleman-Mandula theorem is the existence of point-like fundamental particles and local interactions. We can therefore not apply the theorem to theories with extended fundamental objects. String theory is such an example. The Coleman-Mandula theorem does not hold for p-brane scattering [294]. Moreover, there are also attempts to construct string theories without supersymmetry [298].

  Non-local interactions also arise in theories with a fundamental length scale. Such a minimal length scale as the quanta of spacetime [299] seems to be very plausible when combining general relativity and quantum theory. A naive quantum mechanical treatment of a fundamental length scale reveals that the Hilbert space representations are no longer orthogonal due to the "fuzziness" of spacetime [300]. An example for theories with a fundamental length scale are κ-Poincaré algebras which are also linked to non-commutative spacetimes and exhibit non-linear commutation relations [301, 302]. However, a fully consistent quantum field theory with a fundamental length scale has not yet been found.

- **Local Spacetime Symmetries:** When considering particle symmetries, quantum gravity suggest that we should move from global symmetries to local symmetries (see the discussion in section 2.2). Inspired by this approach, we could also promote the global spacetime symmetries to local symmetries as is done in theories of loop quantum gravity for example. The Coleman-Mandula theorem is only applicable for global symmetries. Thus, non-trivial vacuum expectation values of the metric and Yang-Mills gauge fields can spontaneously break the local spacetime symmetries and evade the no-go theorem [303]. The unification of local particle and spacetime symmetries was studied in [304].

- **Modified Dispersion Relations:** The constant improvement of technology may make the experimental testing of theories of quantum gravity achievable in the future. A large class of quantum gravity models predict the modification of the relativistic dispersion relation at high energies [305, 306]. Such modified dispersion relations could be the first experimental hints for a theory of quantum gravity. Moreover, modified dispersion relations can indicate the breakdown of the Lorentz invariance of the theory. As relativistic Minkowski spacetime with global Poincaré symmetry is one of the fundamental concepts entering the Coleman-Mandula theorem, a deviation of this spacetime structure has the potential to evade the theorem.

However, whether mixing of global internal and external symmetries is feasible or not depends on the explicit structure of spacetime at high energies.

- **Effective Spacetime:** The spacetime we observe around us could only be a low energy realization of a more fundamental spacetime concept. Intrinsically non-relativistic Lifshitz theories received a lot of attention in recent years. This interest was triggered by Hořava in 2009 who showed that quantum gravity becomes power-counting renormalizable in $(3+1)$-dimensional Lifshitz spacetime for a dynamical critical exponent of $z = 3$ at high energies [307]. A general discussion of deviating from Lorentz symmetry in the UV to regulate quantum field theories can be found in [308]. Lifshitz spacetime is not invariant under Lorentz boosts and thus breaks Lorentz invariance explicitly. Therefore, Lifshitz theories are a good framework to study the possibility of mixing internal and external symmetries. However, Lifshitz theories also face problems reproducing the measured approximate Lorentz invariance at low energies [309].

  Moreover, theories which introduce d additional space-like dimensions can induce new effective spacetime structures as well. As an example, we will discuss theories which rely on a direct product structure of spacetime such that orthogonal non-relativistic extra dimensions can have global external symmetries which mix with global internal symmetries.

To summarize, we see that a variety of different ideas are available to enable a mixing of global internal and external symmetries without supersymmetry. All discussed concepts change the underlying assumptions of the Coleman-Mandula theorem about spacetime or fundamental particles. In the next section, we will modify the spacetime structure and demonstrate how spacetime symmetries can induce particle symmetries. Finally, we show how internal and external symmetries can mix to explain the three Standard Model generations.

5.3 Emerging Symmetries from Hidden Spaces

In 1937, Eugene P. Wigner developed a theory to describe the interactions of protons and neutrons [310]. Wigner introduced a $SU(4)$ invariant Hamiltonian where the $SU(4)$ symmetry mixes flavor and spin degrees of freedom. The eigenspace of the Hamiltonian was therefore spanned by the set $\{|p \uparrow\rangle, |p \downarrow\rangle, |n \uparrow\rangle, |n \downarrow\rangle\}$. Note that since Wigner was focusing on interactions of nuclei, he was using a non-relativistic Hamiltonian.

Later, in the early 1960s, the $SU(3)$ flavor symmetry of Gell-Mann and Ne'eman successfully described the interactions of various strongly interacting particles [311, 312]. This $SU(3)$ flavor symmetry for fixed spin could then be extended to a non-relativistic $SU(6)$ model where flavor and spin degrees of freedom are again mixed [313, 314, 315, 316, 317]. This development then led to attempts to construct a fully relativistic $SU(6)$ theory [318, 319, 320]. Promptly, several authors however pointed out various theoretical difficulties of such a relativistic $SU(6)$ theory [321, 322, 323]. A number of no-go theorems were the consequence with the Coleman-Mandula theorem being the strongest [324, 325, 326, 327, 297, 66].

The shortage of the relativistic theories to incorporate spin dependent symmetries roots in the fact that the semi-simple part of the Lorentz group is non-compact, $SO(1,3)$. Lorentz boosts are unbounded and thus there exist no non-trivial unitary finite-dimensional representations of the Lorentz group. Wigner's $SU(4)$ theory does not lead to inconsistencies because it is a non-relativistic theory where spacetime is described by the Galilean symmetry group. The semi-simple part of the Galilean group is given by $SO(3)$ and hence is compact, allowing for non-trivial unitary finite-dimensional representations.

In this section, we first introduce the concept of hidden spacetime symmetries by considering additional conserved momenta in the direction of extra dimensions. In the discussion of the Coleman-Mandula theorem in section 5.1, we argued that any further momentum dependent restrictions on the scattering amplitude on top of Lorentz invariance would only allow for discrete Mandelstam variables s and t in four dimensions. However, by introducing d space-like extra dimensions such that the global spacetime symmetry group factors into a direct product of the 4-dimensional Poincaré group and the symmetry group of the extra dimensions, we can demand that the scattering amplitude conserves charges which depend on the momentum in the extra dimensions without discretizing the scattering process.

Our discussion of the Coleman-Mandula theorem focused on the scattering of scalar degrees of freedom. However, we know from our experimental observations that not all particle wave functions transform trivially with respect to Lorentz transformations. There exist particles with spin in nature and these transform non-trivially with respect to spacetime rotations. Could therefore the symmetries of the S-matrix depend on the spin of the incoming and outgoing particles?

Inspired by Wigner's $SU(4)$ theory, we will introduce space-like extra dimensions which transform under rotations with respect to a compact symmetry group. Particles which transform non-trivially with regard to spacetime rotations in the extra dimensions will therefore have a hidden spin. As we demand that the rotations are described by a compact symmetry group, we will be allowed to combine particles with different hidden spin in the the same multiplet and thus finally mix spacetime and particle symmetries.

Translational Symmetries

To circumvent the Coleman-Mandula theorem, we are considering a D-dimensional spacetime with $D = 4 + d$. Furthermore, we require the d extra dimensions to be space-like to evade consistency issues related to causality [328, 329]. Finally, we assume that spacetime factors into the direct product of 4-dimensional Minkowski spacetime $\mathcal{M}_4$ and a d-dimensional hidden space Σ_d

$$\mathcal{M}_4 \times \Sigma_d \,. \tag{5.19}$$

As a consequence the global spacetime symmetry group also factors

$$\mathcal{P}(1,3) \otimes G_d \,, \tag{5.20}$$

where $\mathcal{P}(1,3)$ is the 4-dimensional Poincaré group and G_d is the symmetry group of Σ_d.

We first start by discussing translational invariant extra dimensions. Then, Noether's theorem [56] guarantees that the $(4+d)$-dimensional momentum defined as

$$P^A = \int \mathrm{d}^3x \, \mathrm{d}^d y \, T^{0A} \,, \tag{5.21}$$

with $A = (0, 1, \ldots, D-1)$, energy-momentum tensor T^{AB}, and spacetime coordinates $z^A = (x^\mu, y^a)$ with $\mu = (0, 1, 2, 3)$ and $a = (4, \ldots, D-1)$ is conserved

$$\partial_0 P^A = 0 \,. \tag{5.22}$$

Moreover, we assume that the particle mass

$$m^2 = P_A^\dagger P^A \quad \text{with} \quad A = (0, 1, \ldots, D-1) \,, \tag{5.23}$$

commutes with all symmetry group generators and is therefore a well-defined constant for all irreducible representations. The energy-momentum relation in D-dimensional spacetime is then given by

$$E^2 = m^2 + |\vec{p}|^2 + \left(p_4^2 + \cdots + p_{D-1}^2\right) \,. \tag{5.24}$$

This simple example already shows that the notion of internal and external symmetries changes as we move from four dimensions to D dimensions. Due to the required translational invariance of Σ_d, scattering processes have to respect the additional momentum conservation and thus scattering processes such as

$$(\vec{p}_A, p_D) + (\vec{p}_B, 0) \to (\vec{p}_A, 0) + (\vec{p}_B, 0) \,, \tag{5.25}$$

would be forbidden. From a 4-dimensional perspective the momentum generators P^a with

$a \in (4, \ldots, D-1)$ commute with the generators of the 4-dimensional Poincaré group. Therefore, the 4-dimensional Mandelstam variables s and t are not discretized by this additional conserved charge and nothing indicates a momentum dependence. Naively, we would therefore categorize the conserved charge as momentum independent in four dimensions and thus related to a new internal symmetry. Hence, the scattering process alone cannot reveal the true nature of the new conserved charge.

Note that this is not a contradiction to the Coleman-Mandula theorem. The Coleman-Mandula theorem is a theorem considering 4-dimensional Minkowski spacetime and not product spacetimes. The above example illustrates that the general symmetry group of the S-matrix can also factor as

$$G \to \mathcal{P}(1,3) \otimes G_d \otimes \text{“internal symmetries”}\,. \tag{5.26}$$

Thus, the factorization of the total global symmetry group of the theory can also include additional spacetime symmetries.

Kaluza-Klein number in theories with universal extra dimensions [330, 331] is an example of such additional spacetime symmetries. We only observe four large dimensions. Therefore, the extra dimensions have to be compactified to be phenomenologically viable. Hence, the translational invariance of the extra dimensions is explicitly broken and Kaluza-Klein number is therefore only a discrete quantum number. Moreover, theories with fermions require orbifolding which further breaks Kaluza-Klein number to Kaluza-Klein parity [331]. Such discrete symmetries arising from momentum conservation in extra dimensions could also explain the stability of dark matter [332, 333].

Rotational Symmetries

After starting the discussion with translational invariant spacetimes, we now move to rotational invariant additional spacetimes. Our observed 4-dimensional world is translational and rotational invariant. Therefore, it seems plausible that a hidden space could also have these properties. To define a rotation in the hidden space, we need at least two extra dimensions. For simplicity, we will thus assume that the product spacetime is given by

$$\mathcal{M}_4 \times \mathbb{R}^2\,. \tag{5.27}$$

The spacetime symmetry group is then

$$\mathcal{P}(1,3) \otimes \left(\mathbb{R}^2 \rtimes SO(2)\right)\,, \tag{5.28}$$

where $G_2 = \mathbb{R}^2 \rtimes SO(2)$.

Because of the two extra dimensions, we now find two conserved momenta

$$\partial_0 P^4 = 0 \quad \text{and} \quad \partial_0 P^5 = 0\,, \tag{5.29}$$

and one conserved angular momentum

$$\partial_0 L^{45} = 0\,, \tag{5.30}$$

where $L^{45} = y^4 p^5 - y^5 p^4$. When considering particle scattering, we can always define a reference frame where the initial angular momentum vanishes. Therefore, we neglect the angular momentum conservation in the following. However, an additional conserved angular momentum could lead to observable effects in the thermal plasma in the early Universe.

We can define a rotation matrix $R^{45}(\theta)$ in $\Sigma_2 = \mathbb{R}^2$ as

$$\begin{pmatrix} y'^4 \\ y'^5 \end{pmatrix} = \begin{pmatrix} \cos(\theta) & -\sin(\theta) \\ \sin(\theta) & \cos(\theta) \end{pmatrix} \begin{pmatrix} y^4 \\ y^5 \end{pmatrix}, \tag{5.31}$$

with rotation angle θ. A general particle wave function which transforms according to a non-trivial representation of $SO(2)$ will then transform as

$$\Psi(x^\mu, y^4, y^5) \to e^{-i\theta s_h}\, \Psi(x^\mu, y^4, y^5)\,, \tag{5.32}$$

with $s_h \in \mathbb{R}$ the "hidden" particle spin. Thus, the particles in the two extra dimensions behave as anyons. From a 4-dimensional point of view, the wave function transforms according to an internal $U(1)$ symmetry as the rotation generator of $R^{45}(\theta)$ commutes with all generators of $\mathcal{P}(1,3)$. The 4-dimensional $U(1)$ charge is then just given by the hidden spin of the particle. In contrast to the previous section, the hidden spin does not enter the energy-momentum relation and it is therefore even more difficult to distinguish global internal $U(1)$ symmetries from simple rotational symmetries in the hidden space.

Rotational symmetries in extra dimensions which induce symmetries in the 4-dimensional theory were considered in studies of the compactified chiral square [334, 335]. However, due to orbifold boundary conditions, the global $U(1)$ symmetry is broken to a discrete Z_8 symmetry. Such hidden rotational symmetries could also be an explanation for the stability of the proton [335].

Mixed Symmetries

In the last section, we saw how external symmetries in a higher dimensional spacetime can induce global seemingly internal symmetries in the 4-dimensional theory. The induced $U(1)$ symmetry in the last section was a byproduct of the fact that the particle wave function is in a representation of the spacetime symmetry group which transforms non-trivial with respect to rotations in the hidden space. However, we are not only searching for induced internal symmetries, but also for new spacetime concepts which allow a mixing of internal and external symmetries without supersymmetry. Therefore, we propose to interpret particles as irreducible representations of the product spacetime $\mathcal{M}_4 \times \Sigma_d$. Hence, we have to assume that spacetime is not an ordinary manifold, but arises effectively from a more fundamental theory. Furthermore, we have to be able to locally distinguish $\mathcal{M}_4$ and Σ_d. The more fundamental theory thus must have provided additional structure such as a condensate. Note especially that such a theory cannot be realized by compactifying a D-dimensional Minkowski spacetime since the Coleman-Mandula theorem is valid for spacetime symmetry groups $\mathcal{P}(1, D-1)$ with $D \geq 4$ [295].

Studying the Coleman-Mandula theorem, we learned that the non-compact semi-simple part of the Lorentz group is the reason why global spacetime and particle symmetries cannot mix. We will therefore choose the spacetime symmetry such that the semi-simple part of G_d is compact. As a concrete example, we construct a toy model where particles with different hidden spin are combined inside the same multiplet. Moreover, in the toy model, we can also understand the appearance of the three Standard Model generations due to the transformation properties of the Standard Model fermions in the hidden space.

We assume that spacetime is given by

$$\mathcal{M}_4 \times \mathbb{R}^3 \,. \tag{5.33}$$

In order to have a mixed global symmetry, we have to enlarge the spacetime symmetry. Normally, we would expect that the symmetry describing $\Sigma_3 = \mathbb{R}^3$ is given by $\mathbb{R}^3 \rtimes SU(2)$. However, we will assume that the spacetime symmetry is given by

$$\mathcal{P}(1,3) \otimes \left(\mathbb{R}^3 \rtimes SU(3)\right) \,. \tag{5.34}$$

We now consider a fermionic field Ψ which transforms as a spin $\frac{1}{2}$-representation of $\mathcal{P}(1,3)$ and as a fundamental representation of $SU(3)$. Note that in such a spacetime construction, all possible combinations of irreducible representations of $\mathcal{P}(1,3)$ and G_d are allowed in principle.

The fermionic field can then be expanded as

$$\Psi^{F\,f}(x^\mu, y^i) = \psi^F(x^\mu)\psi^f(y^i) \quad \text{with} \quad i \in (1,2,3) \,, \tag{5.35}$$

with the 4-dimensional spinor index $F \in (0,1,2,3)$ and the new additional index $f \in (1,2,3)$. Because $\Psi^{F\,f}$ is in the fundamental representation **3** of the global "non-relativistic" spacetime symmetry $SU(3)$, it transforms under spacetime rotations as

$$\Psi^{F\,f}(x^\mu, y^i) \to (e^{-i\alpha_N \lambda^N})^f_g \Psi^{F\,g}(x^\mu, y^i) \,, \tag{5.36}$$

with $N \in (1, \ldots, 8)$, α_N eight finite group parameters and λ^N the Gell-Mann matrices. The action of Ψ then is

$$\begin{aligned} S &= \int \mathrm{d}^4x \, \mathrm{d}^3y \left(\bar{\Psi}_{F\,f} \left(i\,(\gamma^\mu)^F_G \, \partial_\mu - \frac{\delta^F_G}{2M} \partial_i \partial^i \right) \Psi^{G\,f} - m \, \bar{\Psi}_{F\,f} \Psi^{F\,f} \right) \\ &= N \int \mathrm{d}^4x \Big(\bar{\psi}_F(x^\mu) \left(i\,(\gamma^\mu)^F_G \, \partial_\mu - m\,\delta^F_G \right) \psi^G(x^\mu) \Big) \\ &\quad + \int \mathrm{d}^4x \, \bar{\psi}_F(x^\mu) \psi^F(x^\mu) \int \mathrm{d}^3y \, \psi^\dagger_f(y^i) \left(-\frac{1}{2M} \partial_i \partial^i \right) \psi^f(y^i) \,, \,, \end{aligned} \tag{5.37}$$

where $\bar{\Psi}_{F\,f}(x^\mu, y^i) = \bar{\psi}_F(x^\mu)\psi^\dagger_f(y^i)$ and the normalization constant N was defined as

$$N = \left(\int \mathrm{d}^3y\, \psi^\dagger_f(y^i)\psi^f(y^i)\right) . \tag{5.38}$$

Note that the non-relativistic spacetime symmetry $SU(3)$ is responsible for the "non-relativistic kinetic term" $(1/2M)\partial_i\partial^i$ for the "static" fields $\psi^f(y^i)$. We refer to $\psi^f(y^i)$ as static fields because no time coordinate was introduced in the hidden space to avoid causality conflicts. The different static field configurations in the hidden space will be responsible for the varying Standard Model fermion masses.

As one dimension of the spacetime $\Sigma_3 = \mathbb{R}^3$ is compactified to a circle

$$\mathcal{M}_4 \times \mathbb{R}^3 \to \mathcal{M}_4 \times \mathbb{R}^2 \times S^1 \,, \tag{5.39}$$

the mixing of internal and external symmetries inside the global $SU(3)$ symmetry will become evident. The spacetime symmetry is explicitly broken by compactification to

$$\mathcal{P}(1,3) \otimes \left(\mathbb{R}^2 \rtimes U(1)_S \otimes U(1)_I\right) \,, \tag{5.40}$$

with an additional remnant discrete shift symmetry on S^1 induced from the former translational invariance. Upon the spacetime symmetry breaking, the former global $SU(3)$ symmetry decomposed into a global spacetime rotation $U(1)_S$ in the remaining two dimensional hidden plane and an internal $U(1)_I$ symmetry

$$SU(3) \to U(1)_S \otimes U(1)_I \,. \tag{5.41}$$

Thus, the fundamental representation of the global $SU(3)$ symmetry breaks down according to

$$\mathbf{3} \to ((s_h = 1/2), 1) + ((s_h = -1/2), 1) + ((s_h = 0), -2) \,.$$

The explicit spacetime symmetry breaking shows that states with different hidden spins were mixed in the fundamental $SU(3)$ multiplet and we hence demonstrated how internal and external symmetries mix in a non-relativistic hidden spacetime.

Due to the compactification of one extra dimension onto a circle, the static field $\psi^f(y^i)$ can now be expanded as

$$\psi^f(y^j, y^3) = \frac{1}{\sqrt{2\pi R}} \sum_l {\psi^{(l)}}^f(y^j)\, e^{i\frac{l}{R}y^3} \,, \tag{5.42}$$

with $j \in (1,2)$ where we fixed the coordinates such that the direction y^3 was compactified and R the compactification radius of S^1. After the compactification $\mathbb{R}^3 \to \mathbb{R}^2 \times S^1$, the individual components of the static field ${\psi^{(l)}}^f(y^j)$ no longer transform according to (5.36).

Now, the transformation properties with respect to $U(1)_S$ are given by

$$\begin{aligned}
&\psi^{(l)^1}(y^j) \to e^{-i\frac{\alpha_3}{2}}\psi^{(l)^1}(y^j)\,,\\
&\psi^{(l)^2}(y^j) \to e^{i\frac{\alpha_3}{2}}\psi^{(l)^2}(y^j)\,,\\
&\psi^{(l)^3}(y^j) \to \psi^{(l)^3}(y^j)\,,
\end{aligned}\tag{5.43}$$

and with respect to $U(1)_I$ by

$$\begin{aligned}
&\psi^{(l)^1}(y^j) \to e^{-i\frac{\alpha_8}{2\sqrt{3}}}\psi^{(l)^1}(y^j)\,,\\
&\psi^{(l)^2}(y^j) \to e^{-i\frac{\alpha_8}{2\sqrt{3}}}\psi^{(l)^2}(y^j)\,,\\
&\psi^{(l)^3}(y^j) \to e^{i\frac{\alpha_8}{\sqrt{3}}}\psi^{(l)^3}(y^j)\,.
\end{aligned}\tag{5.44}$$

The transformation properties also reflect the mixing of internal and external symmetries. The fields $\psi^{(l)^1}(y^j)$ and $\psi^{(l)^2}(y^j)$ have hidden spin $s_h = \pm 1/2$, whereas for $\psi^{(l)^3}(y^j)$ we find $s_h = 0$. The global abelian $U(1)_I$ symmetry is purely internal and shifts the fields $\psi^{(l)^f}(y^j)$ by a phase.

With the static field expansion given in equation (5.42), we can simplify the second term of the action (5.37) to

$$S \supset \int \mathrm{d}^4x\, \bar{\psi}_F(x^\mu)\psi^F(x^\mu) \int \mathrm{d}^2y\, \sum_l \psi_f^{(l)^\dagger}(y^j)\left(-\frac{1}{2M}\partial_j\partial^j - \frac{l^2}{2MR^2}\right)\psi^{(l)^f}(y^j)\,.\tag{5.45}$$

By then defining the mass contribution of the static field $\psi^f(y^j)$ in the hidden space as

$$\begin{aligned}
M_1 &= \int \mathrm{d}^2y\, \sum_l \psi_1^{(l)^\dagger}(y^j)\left(-\frac{1}{2M}\partial_j\partial^j - \frac{l^2}{2MR^2}\right)\psi^{(l)^1}(y^j)\,,\\
M_2 &= \int \mathrm{d}^2y\, \sum_l \psi_2^{(l)^\dagger}(y^j)\left(-\frac{1}{2M}\partial_j\partial^j - \frac{l^2}{2MR^2}\right)\psi^{(l)^2}(y^j)\,,\\
M_3 &= \int \mathrm{d}^2y\, \sum_l \psi_3^{(l)^\dagger}(y^j)\left(-\frac{1}{2M}\partial_j\partial^j - \frac{l^2}{2MR^2}\right)\psi^{(l)^3}(y^j)\,,
\end{aligned}\tag{5.46}$$

we can express the three generation Standard Model fermion masses m_1, m_2, and m_3 as

$$\begin{aligned}
m_1 &= m - M_1\,,\\
m_2 &= m - M_2\,,\\
m_3 &= m - M_3\,.
\end{aligned}\tag{5.47}$$

The three different mass contributions of the static field $M_{1,2,3}$ thus shift the bare fermion mass m to the measured Standard Model fermion masses.

The appearance of three Standard Model fermion generations is therefore linked to the transformation property of the fermionic field $\Psi^{F\,f}$ as fundamental representation of $SU(3)$ in the hidden space. The new additional index f is thus the Standard Model generation index. Moreover, the difference in the Standard Model fermion masses is due to the different static field configurations of ${\psi^{(l)}}^1(y^j)$, ${\psi^{(l)}}^2(y^j)$, and ${\psi^{(l)}}^3(y^j)$ in the hidden space.

This example is not in conflict with the Coleman-Mandula theorem. Instead, it shows that the Coleman-Mandula theorem is not applicable to all spacetime configurations. The outcome can differ significantly if we do not consider flat Minkowski spacetime. In our toy model, we are exploiting a direct product structure of spacetime to evade the Coleman-Mandula theorem. The additional spacetime symmetries G_d of the S-matrix can mix with global internal symmetries, if G_d contains a compact subgroup. The total symmetry group of the S-matrix then factors as

$$G \to \mathcal{P}(1,3) \otimes \text{“mixed } G_d \text{ and internal symmetries”}\,. \tag{5.48}$$

We therefore succeeded in mixing internal and external symmetries in a new class of spacetime models. It is important to stress again that an additional structure is necessary to locally distinguish $\mathcal{M}_4$ and Σ_d. Only with such additional structure can fundamental fields transform differently with respect to $\mathcal{M}_4$ and Σ_d. Furthermore, phenomenologically viable models are more complex as the presented toy model because interactions have to be included.

5.4 Summary

To summarize, we started by studying the assumptions entering the Coleman-Mandula theorem. After developing a physical intuition for the theorem, we outlined the important steps of the mathematical proof of the Coleman-Mandula theorem. Taking the non-observation of new physics at the electroweak scale apart from the Higgs boson as a motivation, we explored new possibilities to circumvent the no-go theorem and mix global particle and spacetime symmetries.

Finally, we turned to effective spacetime structures. We first examined how in a product spacetime external symmetries induce internal symmetries in the effective 4-dimensional theory. However, the key result of this chapter is the mixing of particle and spacetime symmetries in a novel class of spacetime models. Thereby, flat 4-dimensional Minkowski spacetime $\mathcal{M}_4$ is extended by a hidden d-dimensional space Σ_d which is described by a symmetry group with a compact subgroup. A local structure such as a condensate allows fundamental particles to distinguish $\mathcal{M}_4$ and Σ_d such that they can be in different representations regarding the spacetime symmetry groups of $\mathcal{M}_4$ and Σ_d. The different transformation properties then allow a mixing of the spacetime symmetry of Σ_d and global particle symmetries. As a theory of everything should not differentiate between internal and external degrees of freedom, such spacetime models could be an alternative to supersymmetric theories.

To demonstrate the application of such a mixing of internal and external symmetries, we constructed a toy model which can relate the appearance of three Standard Model generations to the transformation properties of the Standard Model fermions in two additional space-like dimensions. The mass hierarchies of the Standard Model generations are then due to different field configurations in the non-relativistic extra dimensions.

CHAPTER 6

CONCLUSIONS AND OUTLOOK

IN THIS THESIS, we introduced new avenues of theoretical particle physics beyond the established Standard Model. The lack of new physics at the LHC and other experiments stimulated us to turn our attention towards new physics which is decoupled from the electroweak scale. However, even if we were not arguing in favor of the standard lore of low scale supersymmetry and WIMPs, we did not lose track of the current experimental boundaries and constructed valid realistic symmetry-motivated models which are testable at current and future experiments.

In chapter 2, we pursued two bottom-up extensions of the Standard Model. As we are decoupling the new physics from the electroweak scale, we are in need of a new guiding principle. We therefore choose minimality as our guide. At first, we discussed left-right symmetric theories. The scale of left-right symmetry breaking is neither predicted nor bounded from above. We emphasized the fact that left-right symmetric theories with the minimal Higgs sector predict Dirac neutrinos. However, right-handed neutrinos allow for the theoretically attractive possibility of being Majorana fermions. The fermion mass hierarchy is still one of the open puzzles of the Standard Model. Nonetheless, the smallness of the neutrino masses is especially enigmatic. Majorana neutrinos enable the feasibility of a seesaw mechanism which has the potential to explain the smallness of the neutrino masses. We therefore developed the left-right symmetric theory with Majorana neutrinos and the minimal number of propagating degrees of freedom. The Majorana masses are generated at the one-loop level by a new singly charged scalar field $\delta^{\pm}$. The theory predicts light right-handed neutrinos ($M_{\nu}^{R} \sim 0.4 - 0.8$ GeV). This makes the theory testable, as the decay $W_R^+ \to \bar{e}\nu_R$ is generically allowed. In addition, lepton flavor violation becomes accessible at the LHC where we can search for the process $pp \to \delta^+\delta^- \to e_i^+ e_j^- E_T^{\text{miss}}$.

We then turned form left-right symmetric theories to $U(1)$ gauge extensions of the Standard Model. Thereby, we considered not just an arbitrary extension, but the well motivated Standard Model extension of local baryon number. Baryon number is an accidental global symmetry of the Standard Model. All tree-level processes respect baryon number. However, general considerations on quantum gravity suggest that nature should not allow for unbroken continuous global symmetries. Additionally, theories of gauged baryon number suppress proton decay and thus stabilize the proton. We discussed the Standard Model extension of gauged baryon number with the minimal number of new multiplets to have a consistent quantum theory. The theory automatically predicts a stable dark matter candidate: a Standard Model gauge singlet Majorana fermion. Due to the Majorana nature, the dark matter candidate has to be relatively heavy ($m_\chi \gtrsim 500$

GeV) in general to saturate the observed relic abundance. Nevertheless, the theory allows for a rich phenomenology and interesting complementarity of different experimental approaches. For example, direct detection experiments constrain the scalar mixing angle an order of magnitude stronger than current LHC measurements ($|\theta| \leq 0.05$). As for left-right symmetric theories, the scale of baryon number violation is not related to the electroweak scale. Nonetheless, the theory predicts a leptophobic gauge boson $Z_{\rm B}$ which we can discover at the LHC in dijet searches. Even if the inherent dark matter candidate is in general too heavy to be directly produced at the LHC, we can still reveal the quantum numbers of the leptobaryons by studying the loop-mediated baryonic Higgs decays to electroweak gauge bosons.

Switching gears, we moved from minimal bottom-up extensions of the Standard Model to top-down approaches. We discussed a consistent UV complete theory where the ideas of left-right symmetry and local baryon number could be embedded in chapter 3. The unification of the fundamental forces of nature into the simplest possible gauge structure is an appealing idea, as it paves the road towards a theory of everything. However, unified theories generically predict proton decay and therefore have to be exiled to high energy scales. These ideas are thus nearly untestable with earthbound experiments. By promoting baryon number to a gauge symmetry, we were able to stabilize the proton in section 2.2. We hence faced the question: Can we embed gauged baryon number in a non-abelian gauge theory and keep the proton stable? The answer was yes. We thereby discovered the first consistent UV completion of the Standard Model in four dimensions which can be realized at low energy scales (10^{3-4} GeV). The non-abelian gauge theory we proposed is based on the local symmetry group $SU(4)_C \otimes SU(3)_L \otimes SU(3)_R$. By suggesting such an UV completion of the Standard Model, we also took an unconventional point of view regarding the hierarchy problem. Due to the stability of the proton, the scale of quantum gravity can now be as low as 10^7 GeV. Furthermore, the theory introduces four additional scales between the electroweak scale and the scale of quantum gravity. This does not only lead to a rich phenomenology but could also allow for a mechanism to resolve the reduced hierarchy problem. Future studies are needed here. The 433 theory does not only account for local baryon number as fourth color, but it is also an UV completion of left-right symmetric theories with radiative Majorana neutrino masses. Although the theory is again not bound to the electroweak scale, it makes testable predictions. As argued in section 3.1.4, the 433 theory predicts a low reheating temperature to avoid the production of stable fractional charged fermions and/or stable colored bosons in the early Universe. The prediction of a low reheating temperature also allows falsifiability of the theory. Moreover, the predicted stable exotic particles make striking signals at particle colliders which we can search for.

A slight drawback of the 433 theory is the fact that it is an UV completion of the Standard Model but it does still distinguish the different gauge interactions. We therefore introduced an even more appealing gauge theory based on the symmetry group $SU(4)_C \otimes SU(4)_L \otimes SU(4)_R$. However, realistic experimentally valid fermion masses are problematic in this theory as they require large Yukawa couplings. Future investigations are necessary to decide if a different mass mechanism allows for a consistent theory.

A shortcoming of our proceeding from the bottom-up approaches in chapter 2 to a more restrictive top-down model in chapter 3 is the loss of the inherent stable dark matter candidate of the minimal Standard Model extension with gauged baryon number. We therefore shifted our focus towards a different dark matter candidate in chapter 4: axion-like particles. Axion-like particles are pseudo Nambu-Goldstone bosons of anomalous global symmetries and are also not linked to the electroweak scale. As the global symmetries responsible for the axion-like particles are anomalous, they are explicitly broken. Thus, in contrast to our discussion on baryon number, they do not have to be gauged to be consistent with the folk theorems of quantum gravity. Axion-like particles exhibit an especially interesting dark matter phenomenology. They can form BECs of galactic size which is a possible solution to the dark matter small scale crisis. Note that BEC dark matter is not restricted to axion-like particles, but is a possibility for stable weakly interacting light bosonic particles in general. Although, BEC dark matter is a promising dark matter scenario, it is difficult to distinguish from ordinary cold dark matter. We therefore proposed a new method to probe BEC dark matter with repulsive self-interactions via gravitational waves. Our method exploits the refractive index of the gravitational wave in the BEC dark matter halo. A sizable refractive index is unique to BEC dark matter. The gravitational wave is slowed down inside the dark matter halo such that we can measure a time delay of the gravitational wave with respect to a photon or neutrino in a multi-messenger signal. Because of the predictability of BEC dark matter, we can then relate the measured differences in propagation speed to constraints on the microscopic parameters. Future multi-messenger searches at LIGO ($\delta c_g \lesssim 10^{-37}$) and eLISA ($\delta c_g \lesssim 10^{-24}$) have the potential of discovering BEC dark matter with repulsive self-interactions or rule it out conclusively.

We argued in favor of resolving the hierarchy problem by lowering the Planck scale and by introducing multiple new scales, and also argued in favor of considering axion-like particles as dark matter candidates. However, before we completely abandon supersymmetry, we have to appreciate that supersymmetry does not only have the potential to stabilize the electroweak scale and to provide a dark matter candidate, but supersymmetry is also theoretically well motivated. The Coleman-Mandula theorem proofs under the general assumptions of an interacting relativistic quantum field theory that the global symmetry group of the S-matrix has to factor into spacetime and particle symmetries. Supersymmetry is by far the most studied framework to circumvent the Coleman-Mandula theorem and to allow for a mixing of internal and external symmetries as we would expect to happen in a theory of everything. In chapter 5, we therefore took a closer look at the Coleman-Mandula theorem and pointed out different frameworks apart from supersymmetry which evade the no-go theorem. Finally, we introduced a radically new concept of effective spacetime and demonstrated the mixing of global spacetime and particle symmetries. We assumed that spacetime is given by a direct product of 4-dimensional Minkowski spacetime $\mathcal{M}_4$ and a d-dimensional hidden space Σ_d. We then proposed to identify fundamental particles as irreducible representations of the product spacetime where we additionally have to assume that a mechanism distinguishes the Minkowski spacetime $\mathcal{M}_4$ and the hidden space Σ_d locally. The structure of the product spacetime then permits a mixing of internal and external symmetries if the spacetime symmetry group of the hidden space Σ_d has a compact subgroup. We explicitly discussed a toy model which motivates the existence of three Standard Model generations and relates the measured fermion masses to field properties in the hidden space Σ_d. However, this can only be regarded as a first step. Future investigations including particle interactions and the emergence of the effective product spacetime have to reveal the full potential of our proposed spacetime concept.

We do not know where the thrilling pursuit of nature's fundamental concepts takes us next. However, we do hope that the ideas presented in this thesis help to understand our fascinating world a little bit better.

CHAPTER 7

APPENDIX

7.1 Gauge Boson Decays Minimal Left-Right Symmetric Theory

7.1.1 Charged Decays

The partial widths of W_R^+ are given by

$$\Gamma(W_R^+ \to \bar{f}f) = \frac{g_R^2}{6\pi} M_{W_R} ,$$

where $\bar{f}f \in \{\overline{q_d}q_u, \bar{e}\nu_L, \bar{e}\nu_R\}$ and we neglected the final state masses.

7.1.2 Neutral Decays

The partial decay widths of $Z^{'}$ in the limit where the final state fermion masses are neglected are given by

$$\begin{aligned}
\Gamma(Z^{'} \to \overline{q_u}q_u) &= \frac{\cos^2(\theta_R)}{48\pi}\left(\frac{g_R^2}{2} + \frac{g_{BL}^4}{9g_R^2} - \frac{g_{BL}^2}{3}\right) M_{Z'} ,\\
\Gamma(Z^{'} \to \overline{q_d}q_d) &= \frac{\cos^2(\theta_R)}{48\pi}\left(\frac{g_R^2}{2} + \frac{g_{BL}^4}{9g_R^2} + \frac{g_{BL}^2}{3}\right) M_{Z'} ,\\
\Gamma(Z^{'} \to \overline{\nu_L}\nu_L) &= \frac{\cos^2(\theta_R)}{48\pi}\left(\frac{g_R}{2} - \frac{g_{BL}^2}{g_R}\right)^2 M_{Z'} ,\\
\Gamma(Z^{'} \to \overline{\nu_R}\nu_R) &= \frac{\cos^2(\theta_R)}{48\pi}\left(\frac{g_R}{2} - \frac{g_{BL}^2}{g_R}\right)^2 M_{Z'} ,\\
\Gamma(Z^{'} \to \bar{e}e) &= \frac{\cos^2(\theta_R)}{48\pi}\left(\frac{g_R^2}{2} + \frac{g_{BL}^4}{g_R^2} - g_{BL}^2\right) M_{Z'} ,\\
\Gamma(Z^{'} \to \delta^+\delta^-) &= \frac{g_{BL}^2 \sin^2(\theta_R)}{48\pi M_{Z'}^2}\left(M_{Z'}^2 - 4M_\delta^2\right)^{\frac{3}{2}} .
\end{aligned}$$

7.2 Scalar Potential Minimal Left-Right Symmetric Theory

The full scalar potential of the minimal left-right symmetric theory with Majorana neutrinos is given by

$$\begin{aligned}V = &- \mu_H^2(H_L^\dagger H_L + H_R^\dagger H_R) + \lambda_H((H_L^\dagger H_L)^2 + (H_R^\dagger H_R)^2)\\ &+ \lambda_{LR}(H_L^\dagger H_L)(H_R^\dagger H_R) - (\mu_\Phi^2)_{ij}\mathrm{Tr}(\Phi_i^\dagger \Phi_j) + \lambda_{ijkl}^{(1)}\mathrm{Tr}(\Phi_i^\dagger\Phi_j)\mathrm{Tr}(\Phi_k^\dagger\Phi_l)\\ &+ \lambda_{ijkl}^{(2)}\mathrm{Tr}(\Phi_i^\dagger\Phi_j\Phi_k^\dagger\Phi_l) + a_{ij}(H_L^\dagger H_L + H_R^\dagger H_R)\mathrm{Tr}(\Phi_i^\dagger\Phi_j) + b_{ij}(H_L^\dagger\Phi_i\Phi_j^\dagger H_L\\ &+ H_R^\dagger\Phi_i^\dagger\Phi_j H_R) + c_i(H_L^\dagger\Phi_i H_R + H_R^\dagger\Phi_i^\dagger H_L) - \mu_\delta^2\delta^-\delta^+ + \lambda_\delta(\delta^-\delta^+)^2\\ &+ d(H_L^\dagger H_L + H_R^\dagger H_R)\delta^-\delta^+ + e_{ij}\mathrm{Tr}(\Phi_i^\dagger\Phi_j)\delta^-\delta^+ + \lambda_i(H_L^T i\sigma_2\Phi_i H_R\delta^-\\ &- H_L^* i\sigma_2^T\Phi_i^\dagger H_R^\dagger\delta^+)\,, \end{aligned}\tag{7.1}$$

where we defined $\Phi_1 \equiv \Phi$ and $\Phi_2 \equiv \tilde{\Phi}$. We require the scalar potential to respect the discrete left-right parity symmetry

$$H_L \leftrightarrow H_R \quad \text{and} \quad \Phi_i \leftrightarrow \Phi_i^\dagger\,, \tag{7.2}$$

such that we find for the scalar couplings

$$\begin{aligned}&(\mu_\Phi^2)_{ij} = (\mu_\Phi^2)_{ji}\,, \quad \lambda_{ijkk}^{(1)} = \lambda_{jikk}^{(1)}\,, \quad \lambda_{ijkl}^{(1)} = \lambda_{klij}^{(1)} = \lambda_{jilk}^{(1)}\,,\\ &\lambda_{ijkl}^{(2)} = \lambda_{jkli}^{(2)} = \lambda_{klij}^{(2)} = \lambda_{lijk}^{(2)}\,, \quad a_{ij} = a_{ji}\,, \quad b_{ij} = b_{ji}\,, \quad e_{ij} = e_{ji}\,.\end{aligned}\tag{7.3}$$

7.3 Scalar Bi-Doublet Vacuum Expectation Value Separation

In order to have a low scale seesaw mechanism in the minimal left-right symmetric theory with Majorana neutrinos, we have to require small Dirac neutrino masses. As discussed in section 2.1, we find small Dirac neutrino masses for $v_1 \gg v_2$ where $v_2 \to 0$. In this appendix, we demonstrate how such a separation of the vacuum expectation values in the scalar Higgs bi-doublet can be accommodated.

We have to investigate if tadpoles in the scalar potential can violate the condition $v_1 \gg v_2$ with $v_2 \to 0$. The scalar potential which we therefore consider is given by

$$\begin{aligned}V \supset &- (\mu_\Phi^2)_{ij}\mathrm{Tr}(\Phi_i^\dagger\Phi_j) + b_{ij}(H_L^\dagger\Phi_i\Phi_j^\dagger H_L + H_R^\dagger\Phi_i^\dagger\Phi_j H_R)\\ &+ c_i(H_L^\dagger\Phi_i H_R + H_R^\dagger\Phi_i^\dagger H_L)\,.\end{aligned}\tag{7.4}$$

We further assume for simplicity $(\mu_\Phi^2)_{11} = (\mu_\Phi^2)_{22} = (\mu_\Phi^2)_{12} =: \mu_\Phi^2$ and $b_{12} = 0$. We can then derive from the minimum conditions

$$\begin{aligned} v_1 &= -\frac{v_L v_R \left(2c_1\mu_\Phi^2 + c_2\left(-2\mu_\Phi^2 + b_{11}(v_L^2+v_R^2)\right)\right)}{(v_L^2+v_R^2)\left(-2b_{22}\mu_\Phi^2 + b_{11}(-2\mu_\Phi^2 + b_{22}(v_L^2+v_R^2))\right)}\,, \\ v_2 &= -\frac{v_L v_R \left(2c_2\mu_\Phi^2 + c_1\left(-2\mu_\Phi^2 + b_{22}(v_L^2+v_R^2)\right)\right)}{(v_L^2+v_R^2)\left(-2b_{22}\mu_\Phi^2 + b_{11}(-2\mu_\Phi^2 + b_{22}(v_L^2+v_R^2))\right)}\,. \end{aligned} \tag{7.5}$$

In the limit where $\mu_\Phi \to 0$, the vacuum expectation values are given by

$$\begin{aligned} v_1 &\simeq -\frac{c_2 v_L v_R}{b_{22}(v_L^2+v_R^2)}\,, \\ v_2 &\simeq -\frac{c_1 v_L v_R}{b_{11}(v_L^2+v_R^2)}\,. \end{aligned} \tag{7.6}$$

Hence if the scalar couplings satisfy

$$\left|\frac{c_2}{b_{22}}\right| \gg \left|\frac{c_1}{b_{11}}\right|\,, \tag{7.7}$$

we find $v_1 \gg v_2$. Moreover, for $c_1 \to 0$ also $v_2 \to 0$. This proof of principles therefore demonstrates that the scalar potential can account for a separation of scales in a scalar bi-doublet representation in left-right symmetric theories.

7.4 Feynman Rules Minimal Left-Right Symmetric Theory

The Feynman rules in the minimal left-right symmetric theory with Majorana neutrinos are given by

- $\bar{q}q\gamma : -ieQ^q\gamma^\mu$,
- $\bar{q}qZ : -i(V_Z^q - A_Z^q\gamma^5)\gamma^\mu$,
- $\bar{q}qZ' : -i(V_{Z'}^q - A_{Z'}^q\gamma^5)\gamma^\mu$,
- $\bar{e}eZ' : -i(V_{Z'}^e - A_{Z'}^e\gamma^5)\gamma^\mu$,
- $\bar{\nu}\nu Z' : iA_{Z'}^\nu\gamma^5\gamma^\mu$,
- $\overline{\nu^c}\nu^c Z' : iA_{Z'}^{\nu^c}\gamma^5\gamma^\mu$,
- $\delta^+\delta^-\gamma : -ie(p_3 - p_4)^\mu$,
- $\delta^+\delta^- Z : -ia_Z(p_3 - p_4)^\mu$,
- $\delta^+\delta^- Z' : -ia_{Z'}(p_3 - p_4)^\mu$.

The couplings are defined by

$$
\begin{aligned}
V_Z^q &= \frac{1}{2}\cos(\theta_W)\left(g_L T^3_{L/R} - \frac{g_{BL}^2}{g_L}\cos^2(\theta_R)\left(\frac{1}{3} + T^3_{L/R}\right)\right) \,, \\
A_Z^q &= -\frac{T^3_{L/R}}{2}\cos(\theta_W)\left(\frac{g_R^2}{g_L}\sin^2(\theta_R) + g_L\right) \,, \\
V_{Z'}^q &= \frac{1}{2}\cos(\theta_R)\left(g_R T^3_{L/R} - \frac{1}{3}\frac{g_{BL}^2}{g_R}\right) \,, \\
A_{Z'}^q &= \frac{g_R}{2} T^3_{L/R}\cos(\theta_R)\,, \\
V_{Z'}^e &= \frac{1}{2}\cos(\theta_R)\left(\frac{g_{BL}^2}{g_R} - \frac{g_R}{2}\right) \,, \\
A_{Z'}^e &= -\frac{g_R}{4}\cos(\theta_R)\,, \\
A_{Z'}^\nu &= A_{Z'}^{\nu^c} = \frac{1}{2}\cos(\theta_R)\left(\frac{g_R}{2} - \frac{g_{BL}^2}{g_R}\right) \,, \\
a_Z &= -g_{BL}\sin(\theta_W)\cos(\theta_R)\,, \\
a_{Z'} &= -g_{BL}\sin(\theta_R)\,,
\end{aligned}
$$

with the fundamental electron charge given by

$$
e = g_L \sin(\theta_W) = \frac{g_L g_R g_{BL}}{\sqrt{g_L^2 g_R^2 + g_{BL}^2(g_L^2 + g_R^2)}} \,,
$$

and $T^3_{L/R}$ the $SU(2)_{L/R}$ isospin of the quarks.

7.5 Leptophobic Gauge Boson Z_B Decays

The decays of the gauge boson Z_B are determined by the baryon number of the quarks and leptobaryons. The partial decay widths are

$$
\begin{aligned}
\Gamma(Z_\mathrm{B} \to \chi\chi) &= \frac{\alpha_\mathrm{B} B_\chi^2}{6} M_{Z_\mathrm{B}} \left(1 - 4\frac{m_\chi^2}{M_{Z_\mathrm{B}}^2}\right)^{\frac{3}{2}} \,, \\
\Gamma(Z_\mathrm{B} \to \bar{q}q) &= \frac{\alpha_\mathrm{B}}{9} M_{Z_\mathrm{B}} \left(1 + 2\frac{m_q^2}{M_{Z_\mathrm{B}}^2}\right)\sqrt{1 - 4\frac{m_q^2}{M_{Z_\mathrm{B}}^2}} \,.
\end{aligned} \tag{7.8}
$$

7.6 Baryonic Higgs $H_{\rm B}$ Decays

The possible tree-level partial decay widths of the baryonic Higgs $H_{\rm B}$ are given by

$$\begin{aligned}
\Gamma(H_{\rm B} \to \chi\chi) &= \frac{\alpha_{\rm B} B_{H_{\rm B}}^2 \cos^2(\theta)}{4} \frac{m_\chi^2}{M_{Z_{\rm B}}^2} M_{H_{\rm B}} \left(1 - 4\frac{m_\chi^2}{M_{H_{\rm B}}^2}\right)^{\frac{3}{2}} ,\\
\Gamma(H_{\rm B} \to Z_{\rm B} Z_{\rm B}) &= \frac{\alpha_{\rm B} B_{H_{\rm B}}^2 \cos^2(\theta)}{8} \frac{M_{H_{\rm B}}^3}{M_{Z_{\rm B}}^2} \left(1 - 4\frac{M_{Z_{\rm B}}^2}{M_{H_{\rm B}}^2} + 12\frac{M_{Z_{\rm B}}^4}{M_{H_{\rm B}}^4}\right) \sqrt{1 - 4\frac{M_{Z_{\rm B}}^2}{M_{H_{\rm B}}^2}} ,\\
\Gamma(H_{\rm B} \to WW) &= \frac{G_F \sin^2(\theta)}{8\sqrt{2}\pi} M_{H_{\rm B}}^3 \left(1 - 4\frac{M_W^2}{M_{H_{\rm B}}^2} + 12\frac{M_W^4}{M_{H_{\rm B}}^4}\right) \sqrt{1 - 4\frac{M_W^2}{M_{H_{\rm B}}^2}} ,\\
\Gamma(H_{\rm B} \to ZZ) &= \frac{G_F \sin^2(\theta)}{16\sqrt{2}\pi} M_{H_{\rm B}}^3 \left(1 - 4\frac{M_Z^2}{M_{H_{\rm B}}^2} + 12\frac{M_Z^4}{M_{H_{\rm B}}^4}\right) \sqrt{1 - 4\frac{M_Z^2}{M_{H_{\rm B}}^2}} ,\\
\Gamma(H_{\rm B} \to \bar{q}q) &= \frac{3 m_q^2 \sin^2(\theta) G_F}{4\pi\sqrt{2}} M_{H_{\rm B}} \left(1 - 4\frac{m_q^2}{M_{H_{\rm B}}^2}\right)^{\frac{3}{2}} ,\\
\Gamma(H_{\rm B} \to HH) &= \frac{c_{HHH_B}^2}{8\pi M_{H_{\rm B}}} \sqrt{1 - 4\frac{M_H^2}{M_{H_{\rm B}}^2}} ,
\end{aligned} \tag{7.9}$$

with

$$c_{HHH_B} = \frac{\sin(2\theta)(2M_H^2 + M_{H_{\rm B}}^2)}{4} \left(\frac{\cos(\theta)}{v_H} + \frac{\sin(\theta)}{v_{\rm B}}\right) . \tag{7.10}$$

For small mixing angles the loop mediated decays to electroweak gauge bosons become relevant. From the effective Lagrangian (2.101), we can derive the one-loop contributions of $H_{\rm B} \to WW, ZZ, Z\gamma, \gamma\gamma$ for $\theta \to 0$ when the above tree-level decays vanish

$$\begin{aligned}
\Gamma(H_{\rm B} \to WW) &= \frac{\alpha_{\rm B} M_{H_{\rm B}}^3}{32\pi^4 M_{Z_{\rm B}}^2} \frac{9 g_L^4}{4} ,\\
\Gamma(H_{\rm B} \to ZZ) &= \frac{\alpha_{\rm B} M_{H_{\rm B}}^3}{32\pi^4 M_{Z_{\rm B}}^2} \frac{g_L^4}{8\cos^4(\theta_w)} \left(3 - 6\sin^2(\theta_w) + 4\sin^4(\theta_w)\right)^2 ,\\
\Gamma(H_{\rm B} \to Z\gamma) &= \frac{\alpha_{\rm B} M_{H_{\rm B}}^3}{32\pi^4 M_{Z_{\rm B}}^2} \frac{e^2 g_L^2}{4} \left(3 - 4\sin(\theta_w)\right)^2 ,\\
\Gamma(H_{\rm B} \to \gamma\gamma) &= \frac{\alpha_{\rm B} M_{H_{\rm B}}^3}{32\pi^4 M_{Z_{\rm B}}^2} 2e^4 .
\end{aligned}$$

7.7 Fermion Masses 433 Theory

We continue to assume the vacuum expectation value hierarchy $v_{33} \gg v_R \gg v_{1,2}$. However, in contrast to section 3.1.2, we take mass corrections of order $\mathcal{O}(v_R/v_{33})$ into account. We assume that left-right symmetry is already broken and thus Φ_3 already acquired the vacuum expectation values v_{33} and v_R. The fermionic mass eigenstates involving Standard Model fermions are then given by

$$\begin{aligned}
D'^c &= c_\alpha D^c + s_\alpha d^c\,, \quad d'^c = c_\alpha d^c - s_\alpha D^c\,,\\
E'^- &= c_\alpha E^- - s_\alpha e^-\,, \quad e'^- = c_\alpha e^- + s_\alpha E^-\,,\\
N_1' &= c_\alpha N_1 - s_\alpha \nu\,, \quad \nu' = c_\alpha \nu + s_\alpha N_1\,,
\end{aligned}$$

where the mixing angle α is defined by

$$\tan\alpha = \frac{v_R}{v_{33}}\,. \tag{7.11}$$

We used the abbreviations $s_\alpha \equiv \sin(\alpha)$ and $c_\alpha \equiv \cos(\alpha)$. Thus, the Lagrangian containing Standard Model fermions and scalar fields which did not yet acquire a vacuum expectation value can be rewritten as

$$\begin{aligned}
-\mathcal{L} \supset\, & m_{D'} D D'^c + m_{L'}(N_1' N_2 - E^+ E'^-) + y_1 d(c_\alpha d'^c + s_\alpha D'^c)(\varphi_1^0)_1\\
& + y_2 u u^c (\varphi_2^0)_2 + h_1 N_2 N_3 (\varphi_1^0)_1 - h_1 e^+(c_\alpha e'^- - s_\alpha E'^-)(\varphi_1^0)_1\\
& + h_2(c_\alpha N_1' + s_\alpha \nu')N_3(\varphi_2^0)_2 - h_2(c_\alpha \nu' - s_\alpha N_1')\nu^c(\varphi_2^0)_2\,,
\end{aligned} \tag{7.12}$$

with

$$m_{D'} = y_3 v_{33}\sqrt{1 + \frac{v_R^2}{v_{33}^2}}\,, \quad m_{L'} = h_3 v_{33}\sqrt{1 + \frac{v_R^2}{v_{33}^2}}\,. \tag{7.13}$$

If now $(\phi_1^0)_1$ and $(\phi_2^0)_2$ acquire electroweak vacuum expectation values, we find for the Standard Model fermion masses

$$m_d = y_1 v_1 c_\alpha\,, \quad m_u = y_2 v_2\,, \quad m_e = h_1 v_1 c_\alpha\,, \quad m_\nu = h_2 v_2 c_\alpha\,. \tag{7.14}$$

The mass of the Standard Model singlet N_3 can be approximated at tree-level by

$$m_{N_3} \simeq \frac{(h_1 v_1)(h_2 v_2 c_\alpha)}{m_{L'}}\,, \tag{7.15}$$

and thus is despite the inclusion of fermion mass mixing still the lightest particle in the theory. However, due to loop-corrections the mass of N_3 increases and scales with v_{33}. The masses of the heavy fields D, D'^c, E^+, E'^-, N_1' and N_2 will get corrections of order $\mathcal{O}(v_{1,2}/v_{33})$ which we neglected. In the limit of $v_{33}, v_R \to \infty$, we arrive at the established Standard Model of particle physics.

7.7.1 Radiative Neutrino Masses including Mixing

We simplified the discussion of the radiative neutrino masses by considering the toy model

$$\mathcal{L} \supset -M_\Phi^2 \Phi\Phi^* - \lambda\Phi\Phi\Phi - \frac{h}{2} LL\Phi + \text{h.c.}\,. \tag{7.16}$$

Taking the above fermion mass mixing into account, the relevant interactions take the form

$$\begin{aligned}
-\mathcal{L} \supset h \Bigg[& \left[(c_\alpha \nu' - s_\alpha N_1')\left(c_\alpha E'^- + s_\alpha e'^-\right) - (c_\alpha N_1' + s_\alpha \nu')\left(c_\alpha e'^- - s_\alpha E'^-\right)\right] H^+ \\
& + \left[\left(c_\alpha e'^- - s_\alpha E'^-\right)\nu^c - \left(c_\alpha E'^- + s_\alpha e'^-\right) N_3\right]\varphi^+ - E^+ N_3 \varphi^- \\
& + \left[\nu^c E^+ - (c_\alpha N_1' + s_\alpha \nu')\, e^+\right] H^- \Bigg] \\
& + 3\lambda \Bigg[- H^- H^+ \varphi_1^0 + H^+ \varphi^- H_L^0 + H^- \varphi^+ H_R^0 - \varphi^+ \varphi^- \phi^0 \Bigg] + \text{h.c.}\,.
\end{aligned} \tag{7.17}$$

7.7.2 Fermion Mass Matrices 433 Theory

The full quark mass terms at tree-level are given by

$$-\mathcal{L} \supset (y_2 v_2) u^c u + \begin{pmatrix} d^c & D^c \end{pmatrix} \begin{pmatrix} y_1 v_1 & y_3 v_R \\ 0 & y_3 v_{33} \end{pmatrix} \begin{pmatrix} d \\ D \end{pmatrix}.$$

The full charged lepton mass term at tree-level is given by

$$-\mathcal{L} \supset \begin{pmatrix} e^+ & E^+ \end{pmatrix} \begin{pmatrix} -h_1 v_1 & 0 \\ h_3 v_R & -h_3 v_{33} \end{pmatrix} \begin{pmatrix} e^- \\ E^- \end{pmatrix}.$$

The full neutral lepton mass term at tree-level is given by

$$-\mathcal{L} \supset \begin{pmatrix} \nu\, \nu^c\, N_1\, N_2\, N_3 \end{pmatrix} \begin{pmatrix} 0 & -h_2 v_2 & 0 & -h_3 v_R & 0 \\ -h_2 v_2 & 0 & 0 & 0 & 0 \\ 0 & 0 & 0 & h_3 v_{33} & h_2 v_2 \\ -h_3 v_R & 0 & h_3 v_{33} & 0 & h_1 v_1 \\ 0 & 0 & h_2 v_2 & h_1 v_1 & 0 \end{pmatrix} \begin{pmatrix} \nu \\ \nu^c \\ N_1 \\ N_2 \\ N_3 \end{pmatrix}.$$

LIST OF ABBREVIATIONS

333 . . . . . . Trinification $SU(3)_C \otimes SU(3)_L \otimes SU(3)_R$

433 . . . . . . Gauge theory based on $SU(4)_C \otimes SU(3)_L \otimes SU(3)_R$

444 . . . . . . Gauge theory based on $SU(4)_C \otimes SU(4)_L \otimes SU(4)_R$

AGILE . . . . . Astro-rivelatore Gamma a Immagini LEggero

AMON . . . . Astrophysical Multimessenger Observatory Network

ATLAS . . . . A Toroidal LHC Apparatus

B . . . . Baryon Number

BBN . . . . . . Big Bang Nucleosynthesis

BEC . . . . . . Bose-Einstein Condensate

BH . . . . Black Hole

BR . . . . Branching Ratio

CERN . . . . . Conseil Européen pour la Recherche Nucléaire

CKM . . . . . Cabibbo-Kobayashi-Maskawa

CMB . . . . . . Cosmic Microwave Background

CMS . . . . . . Compact Muon Solenoid

CP . . . . Charge Parity

DFSZ . . . . . Dine-Fischler-Srednicki-Zhitnitsky

DM . . . . . . Dark Matter

DSph . . . . . Dwarf Spheroidal Galaxy

eLISA . . . . . Evolved Laser Interferometer Space Antenna

EM . . . . . . Electromagnetic

EW . . . . . . Electroweak

Fermi-GBM . . Fermi Gamma Burst Monitor

GUT . . . . . . Grand Unified Theory

GW	Gravitational Wave
H.E.S.S.	High Energy Stereoscopic System
INTEGRAL	International Gamma-Ray Astrophysics Laboratory
IPTA	International Pulsar Timing Array
KSVZ	Kim-Shifman-Vainshtein-Zakharov
L	Lepton Number
LHC	Large Hadron Collider
LIGO	Laser Interferometer Gravitational-Wave Observatory
LO	Leading Order
LR	Left-Right
MSTW	Martin-Stirling-Thorne-Watt
NS	Neutron Star
PMNS	Pontecorvo-Maki-Nakagawa-Sakata
PQ	Peccei-Quinn
QCD	Quantum Chromodynamics
SM	Standard Model of particle physics
UV	Ultraviolet (high energy)
VBF	Vector Boson Fusion
WIMP	Weakly Interacting Massive Particle
WISP	Weakly Interacting Slim Particle

Chapter 8

Bibliography

[1] P. Fileviez Perez, C. Murgui, and S. Ohmer, "*Simple Left-Right Theory: Lepton Number Violation at the LHC*," Phys. Rev. **D94** (2016) no. 5, 051701, arXiv:1607.00246.

[2] S. Ohmer and H. H. Patel, "*Leptobaryons as Majorana Dark Matter*," Phys. Rev. **D92** (2015) no. 5, 055020, arXiv:1506.00954.

[3] P. Fileviez Perez, S. Ohmer, and H. H. Patel, "*Minimal Theory for Lepto-Baryons*," Phys.Lett. **B735** (2014) 283, arXiv:1403.8029.

[4] P. Fileviez Perez and S. Ohmer, "*Unification and Local Baryon Number*," Phys. Lett. **B768** (2017) 86–91, arXiv:1612.07165.

[5] P. S. B. Dev, M. Lindner, and S. Ohmer, "*Gravitational waves as a new probe of Bose–Einstein condensate Dark Matter*," Phys. Lett. **B773** (2017) 219–224, arXiv:1609.03939.

[6] M. Lindner and S. Ohmer, "*Emerging Internal Symmetries from Effective Spacetimes*," Phys. Lett. **B773** (2017) 231–235, arXiv:1703.10188.

[7] D. Hanneke, S. F. Hoogerheide, and G. Gabrielse, "*Cavity Control of a Single-Electron Quantum Cyclotron: Measuring the Electron Magnetic Moment*," Phys. Rev. **A83** (2011) 052122, arXiv:1009.4831.

[8] **ATLAS**, G. Aad *et al.*, "*Observation of a new particle in the search for the Standard Model Higgs boson with the ATLAS detector at the LHC*," Phys.Lett. **B716** (2012) 1–29, arXiv:1207.7214.

[9] **CMS**, S. Chatrchyan *et al.*, "*Observation of a new boson at a mass of 125 GeV with the CMS experiment at the LHC*," Phys. Lett. **B716** (2012) 30–61, arXiv:1207.7235.

[10] S. L. Glashow, "*Partial-symmetries of weak interactions*," Nuclear Physics **22** (1961) no. 4, 579 – 588.

[11] S. Weinberg, "*A Model of Leptons*,"Phys. Rev. Lett. **19** (Nov, 1967) 1264–1266.

[12] A. Salam, "*Weak and Electromagnetic Interactions*," Conf.Proc.C680519 (1968) 367–377.

[13] P. W. Higgs, "*Broken Symmetries and the Masses of Gauge Bosons*," Phys. Rev. Lett. **13** (1964) 508–509.

[14] F. Englert and R. Brout, "*Broken Symmetry and the Mass of Gauge Vector Mesons*," Phys. Rev. Lett. **13** (1964) 321–323.

[15] G. S. Guralnik, C. R. Hagen, and T. W. B. Kibble, "*Global Conservation Laws and Massless Particles*," Phys. Rev. Lett. **13** (1964) 585–587.

[16] N. Cabibbo, "*Unitary Symmetry and Leptonic Decays*," Phys. Rev. Lett. **10** (1963) 531–533.

[17] M. Kobayashi and T. Maskawa, "*CP Violation in the Renormalizable Theory of Weak Interaction*," Prog.Theor.Phys. **49** (1973) 652–657.

[18] B. Pontecorvo, "*Mesonium and anti-mesonium*," Sov.Phys.JETP **6** (1957) 429.

[19] Z. Maki, M. Nakagawa, and S. Sakata, "*Remarks on the unified model of elementary particles*," Prog.Theor.Phys. **28** (1962) 870–880.

[20] **Planck**, P. A. R. Ade *et al.*, "*Planck 2015 results. XIII. Cosmological parameters*," Astron. Astrophys. **594** (2016) A13, `arXiv:1502.01589`.

[21] V. Rubin, N. Thonnard, and J. Ford, W.K., "*Rotational properties of 21 SC galaxies with a large range of luminosities and radii, from NGC 4605 /R = 4kpc/ to UGC 2885 /R = 122 kpc/*," Astrophys.J. **238** (1980) 471.

[22] K. G. Begeman, A. H. Broeils, and R. H. Sanders, "*Extended rotation curves of spiral galaxies: Dark haloes and modified dynamics*," Mon. Not. Roy. Astron. Soc. **249** (1991) 523.

[23] D. Clowe, M. Bradac, A. H. Gonzalez, M. Markevitch, S. W. Randall, *et al.*, "*A direct empirical proof of the existence of dark matter*," Astrophys.J. **648** (2006) L109–L113, `arXiv:astro-ph/0608407`.

[24] M. Bradac, S. W. Allen, T. Treu, H. Ebeling, R. Massey, R. G. Morris, A. von der Linden, and D. Applegate, "*Revealing the properties of dark matter in the merging cluster MACSJ0025.4-1222*," Astrophys. J. **687** (2008) 959, `arXiv:0806.2320`.

[25] **WMAP**, G. Hinshaw *et al.*, "*Nine-Year Wilkinson Microwave Anisotropy Probe (WMAP) Observations: Cosmological Parameter Results*," Astrophys.J.Suppl. **208** (2013) 19, `arXiv:1212.5226`.

[26] M. Milgrom, "*A Modification of the Newtonian dynamics as a possible alternative to the hidden mass hypothesis*," Astrophys.J. **270** (1983) 365–370.

[27] J. Moffat, "*Scalar-tensor-vector gravity theory*," JCAP **0603** (2006) 004, `arXiv:gr-qc/0506021`.

[28] F. Zwicky, "*Die Rotverschiebung von extragalaktischen Nebeln*," Helv.Phys.Acta **6** (1933) 110–127.

[29] D. Tytler, J. M. O'Meara, N. Suzuki, and D. Lubin, "*Review of Big Bang nucleosynthesis and primordial abundances*," Phys.Scripta **T85** (2000) 12, `arXiv:astro-ph/0001318`.

[30] V. Springel, C. S. Frenk, and S. D. White, "*The large-scale structure of the Universe*," Nature **440** (2006) 1137, `arXiv:astro-ph/0604561`.

[31] M. Bartelmann and P. Schneider, "*Weak gravitational lensing*," Phys.Rept. **340** (2001) 291–472, `arXiv:astro-ph/9912508`.

[32] J. R. Ellis, J. Hagelin, D. V. Nanopoulos, K. A. Olive, and M. Srednicki, "*Supersymmetric Relics from the Big Bang*," Nucl.Phys. **B238** (1984) 453–476.

[33] A. K. Gupta, J. Hughes, J. Preskill, and M. B. Wise, "*Magnetic Wormholes and Topological Symmetry*," Nucl.Phys. **B333** (1990) 195.

[34] L. Abbott and P. Sikivie, "*A Cosmological Bound on the Invisible Axion*," Phys.Lett. **B120** (1983) 133–136.

[35] J. M. Cline, K. Kainulainen, P. Scott, and C. Weniger, "*Update on scalar singlet dark matter*," Phys. Rev. **D88** (2013) 055025, `arXiv:1306.4710`. [Erratum: Phys. Rev.D92,no.3,039906(2015)].

[36] T. Hambye, F. S. Ling, L. Lopez Honorez, and J. Rocher, "*Scalar Multiplet Dark Matter*," JHEP **07** (2009) 090, `arXiv:0903.4010`. [Erratum: JHEP05,066(2010)].

[37] A. Kusenko, "*Sterile neutrinos: The Dark side of the light fermions*," Phys.Rept. **481** (2009) 1–28, `arXiv:0906.2968`.

[38] B. Carr, F. Kuhnel, and M. Sandstad, "*Primordial Black Holes as Dark Matter*," Phys. Rev. **D94** (2016) no. 8, 083504, `arXiv:1607.06077`.

[39] S. Bird, I. Cholis, J. B. Muñoz, Y. Ali-Haïmoud, M. Kamionkowski, E. D. Kovetz, A. Raccanelli, and A. G. Riess, "*Did LIGO detect dark matter?*," Phys. Rev. Lett. **116** (2016) no. 20, 201301, `arXiv:1603.00464`.

[40] A. Boyarsky, J. Lesgourgues, O. Ruchayskiy, and M. Viel, "*Lyman-alpha constraints on warm and on warm-plus-cold dark matter models*," JCAP **0905** (2009) 012, `arXiv:0812.0010`.

[41] M. Viel, G. D. Becker, J. S. Bolton, and M. G. Haehnelt, "*Warm dark matter as a solution to the small scale crisis: New constraints from high redshift Lyman-alpha forest data*," Phys. Rev. **D88** (2013) 043502, `arXiv:1306.2314`.

[42] **XENON1T**, E. Aprile, "*The XENON1T Dark Matter Search Experiment*," Springer Proc. Phys. **148** (2013) 93–96, `arXiv:1206.6288`.

[43] **XENON**, E. Aprile *et al.*, "*Physics reach of the XENON1T dark matter experiment*," JCAP **1604** (2016) no. 04, 027, `arXiv:1512.07501`.

[44] **H.E.S.S.**, A. Abramowski *et al.*, "*Search for a Dark Matter annihilation signal from the Galactic Center halo with H.E.S.S*," Phys. Rev. Lett. **106** (2011) 161301, `arXiv:1103.3266`.

[45] **H.E.S.S.**, A. Abramowski *et al.*, "*Search for Photon-Linelike Signatures from Dark Matter Annihilations with H.E.S.S.*," Phys. Rev. Lett. **110** (2013) 041301, `arXiv:1301.1173`.

[46] **H.E.S.S.**, A. Abramowski *et al.*, "*Search for dark matter annihilation signatures in H.E.S.S. observations of Dwarf Spheroidal Galaxies*," Phys. Rev. **D90** (2014) 112012, `arXiv:1410.2589`.

[47] **ATLAS, CMS**, J. Pazzini, "*Dark Matter search at LHC*," Nuovo Cim. **C40** (2017) no. 1, 3.

[48] **ADMX**, S. J. Asztalos *et al.*, "*A SQUID-based microwave cavity search for dark-matter axions*," Phys. Rev. Lett. **104** (2010) 041301, `arXiv:0910.5914`.

[49] **LIGO Scientific**, J. Aasi *et al.*, "*Advanced LIGO*," Class. Quant. Grav. **32** (2015) 074001, `arXiv:1411.4547`.

[50] L. J. Hall, D. Pinner, and J. T. Ruderman, "*A Natural SUSY Higgs Near 126 GeV*," JHEP **04** (2012) 131, `arXiv:1112.2703`.

[51] J. Cao, Z. Heng, J. M. Yang, and J. Zhu, "*Status of low energy SUSY models confronted with the LHC 125 GeV Higgs data*," JHEP **10** (2012) 079, `arXiv:1207.3698`.

[52] K. A. Meissner and H. Nicolai, "*Conformal Symmetry and the Standard Model*," Phys. Lett. **B648** (2007) 312–317, `arXiv:hep-th/0612165`.

[53] A. J. Helmboldt, P. Humbert, M. Lindner, and J. Smirnov, "*Minimal conformal extensions of the Higgs sector*," JHEP **07** (2017) 113, `arXiv:1603.03603`.

[54] N. Arkani-Hamed, S. Dimopoulos, and G. Dvali, "*The Hierarchy problem and new dimensions at a millimeter*," Phys.Lett. **B429** (1998) 263–272, `arXiv:hep-ph/9803315`.

[55] G. F. Giudice and M. McCullough, "*A Clockwork Theory*," JHEP **02** (2017) 036, `arXiv:1610.07962`.

[56] E. Noether, "*Invariant Variation Problems*," Gott.Nachr. **1918** (1918) 235–257, `arXiv:physics/0503066`.

[57] E. P. Wigner, "*On Unitary Representations of the Inhomogeneous Lorentz Group*," Annals Math. **40** (1939) 149–204. [Reprint: Nucl. Phys. Proc. Suppl.6,9(1989)].

[58] G. Lüders, "*Det. Kong. Danske Videnskabernes Selskab*," Mat.-fys. Medd. 28, No. 5 (1954) .

[59] W. Pauli, "*Niels Bohr and the Development of Physics*," McGraw-Hill, New York (1955) 30–51.

[60] O. W. Greenberg, "*Why is CPT fundamental?*," Found. Phys. **36** (2006) 1535–1553, `arXiv:hep-ph/0309309`.

[61] C. S. Wu, E. Ambler, R. W. Hayward, D. D. Hoppes, and R. P. Hudson, "*Experimental Test of Parity Conservation in Beta Decay*," Phys. Rev. **105** (1957) no. 4, 1413–1415.

[62] J. C. Pati and A. Salam, "*Lepton Number as the Fourth Color*," Phys. Rev. D **10** (1974) 275.

[63] R. N. Mohapatra and J. C. Pati, "*A Natural Left-Right Symmetry*," Phys. Rev. D **11** (1975) 2558.

[64] G. Senjanovic, "*Spontaneous Breakdown of Parity in a Class of Gauge Theories*," Nucl. Phys. B **153** (1979) 334.

[65] G. Senjanovic and R. N. Mohapatra, "*Exact Left-Right Symmetry and Spontaneous Violation of Parity*," Phys. Rev. D **12** (1975) 1502.

[66] S. Coleman and J. Mandula, "*All Possible Symmetries of the S Matrix*," Phys. Rev. **159** (1967) 1251–1256.

[67] A. Maiezza, M. Nemevsek, F. Nesti, and G. Senjanovic, "*Left-Right Symmetry at LHC*," Phys. Rev. **D82** (2010) 055022, `arXiv:1005.5160`.

[68] G. Senjanovic, "*Neutrino mass: From LHC to grand unification*," Riv. Nuovo Cim. **34** (2011) 1–68.

[69] G. C. Branco and G. Senjanovic, "*The Question of Neutrino Mass*," Phys. Rev. D **18** (1978) 1621.

[70] P. Minkowski, "*$\mu \to e\gamma$ at a Rate of One Out of 10^9 Muon Decays?*," Phys. Lett. **67B** (1977) 421–428.

[71] T. Yanagida, "*HORIZONTAL SYMMETRY AND MASSES OF NEUTRINOS*," Conf. Proc. **C7902131** (1979) 95–99.

[72] M. Gell-Mann, P. Ramond, and R. Slansky, "*Complex Spinors and Unified Theories*," Conf. Proc. **C790927** (1979) 315–321, `arXiv:1306.4669`.

[73] S. Glashow, "*Quarks and Leptons*," Cargèse lectures, eds. M. Lévy et al. Plenum (1980, New York) 707.

[74] R. N. Mohapatra and G. Senjanovic, "*Neutrino Mass and Spontaneous Parity Violation*," Phys. Rev. Lett. **44** (1980) 912.

[75] W. Konetschny and W. Kummer, "*Nonconservation of Total Lepton Number with Scalar Bosons*," Phys. Lett. **70B** (1977) 433–435.

[76] T. P. Cheng and L.-F. Li, "*Neutrino Masses, Mixings and Oscillations in SU(2) x U(1) Models of Electroweak Interactions*," Phys. Rev. **D22** (1980) 2860.

[77] J. Schechter and J. W. F. Valle, "*Neutrino Masses in SU(2) x U(1) Theories*," Phys. Rev. **D22** (1980) 2227.

[78] R. N. Mohapatra and G. Senjanovic, "*Neutrino Masses and Mixings in Gauge Models with Spontaneous Parity Violation*," Phys. Rev. **D23** (1981) 165.

[79] R. Foot, H. Lew, X. G. He, and G. C. Joshi, "*Seesaw Neutrino Masses Induced by a Triplet of Leptons*," Z. Phys. **C44** (1989) 441.

[80] P. Fileviez Perez, "*Type III Seesaw and Left-Right Symmetry*," JHEP **0903** (2009) 142, `arXiv:0809.1202`.

[81] A. Zee, "*A Theory of Lepton Number Violation, Neutrino Majorana Mass, and Oscillation*," Phys. Lett. B **93** (1980) 389.

[82] P. B. Pal, "*PseudoDirac neutrinos in the left-right model*," DOE-ER-40224-144, OITS-434 .

[83] L. Wolfenstein, "*Different Varieties of Massive Dirac Neutrinos*," Nucl. Phys. **B186** (1981) 147–152.

[84] M. Kobayashi and C. S. Lim, "*Pseudo Dirac scenario for neutrino oscillations*," Phys. Rev. **D64** (2001) 013003, `arXiv:hep-ph/0012266`.

[85] Y. B. Zeldovich, I. Y. Kobzarev, and L. B. Okun, "*Cosmological Consequences of the Spontaneous Breakdown of Discrete Symmetry*," Zh. Eksp. Teor. Fiz. **67** (1974) 3, [Sov. Phys. JETP **40** (1974) 1].

[86] F. del Aguila, J. de Blas, and M. Perez-Victoria, "*Electroweak Limits on General New Vector Bosons*," JHEP **09** (2010) 033, `arXiv:1005.3998`.

[87] Y. Zhang, H. An, X. Ji, and R. N. Mohapatra, "*General CP Violation in Minimal Left-Right Symmetric Model and Constraints on the Right-Handed Scale*," Nucl. Phys. B **802** (2008) 247, `arXiv:0712.4218`.

[88] M. Blanke, A. J. Buras, K. Gemmler, and T. Heidsieck, "*Delta* $F = 2$ *observables and* $B \to X_q\gamma$ *decays in the Left-Right Model: Higgs particles striking back*," JHEP **1203** (2012) 024, arXiv:1111.5014.

[89] S. Bertolini, A. Maiezza, and F. Nesti, "*Present and Future K and B Meson Mixing Constraints on TeV Scale Left-Right Symmetry*," Phys. Rev. D **89** (2014) no.9, 095028, arXiv:1403.7112.

[90] W.-Y. Keung and G. Senjanovic, "*Majorana Neutrinos and the Production of the Right-handed Charged Gauge Boson*," Phys. Rev. Lett. **50** (1983) 1427.

[91] M. Nemevsek, F. Nesti, G. Senjanovic, and Y. Zhang, "*First Limits on Left-Right Symmetry Scale from LHC Data*," Phys. Rev. **D83** (2011) 115014, arXiv:1103.1627.

[92] S. Alekhin *et al.*, "*A facility to Search for Hidden Particles at the CERN SPS: the SHiP physics case*," Rept. Prog. Phys. **79** (2016) no. 12, 124201, arXiv:1504.04855.

[93] J. Barry and W. Rodejohann, "*Lepton number and flavour violation in TeV-scale left-right symmetric theories with large left-right mixing*," JHEP **09** (2013) 153, arXiv:1303.6324.

[94] **ATLAS**, M. Aaboud *et al.*, "*Search for top squarks in final states with one isolated lepton, jets, and missing transverse momentum in* $\sqrt{s} = 13$ *TeV* pp *collisions with the ATLAS detector*," Phys. Rev. **D94** (2016) no. 5, 052009, arXiv:1606.03903.

[95] A. Martin, W. Stirling, R. Thorne, and G. Watt, "*Parton distributions for the LHC*," Eur.Phys.J. **C63** (2009) 189–285, arXiv:0901.0002.

[96] P. Fileviez Perez and C. Murgui, "*Lepton Flavour Violation in Left-Right Theory*," Phys. Rev. **D95** (2017) no. 7, 075010, arXiv:1701.06801.

[97] C. Murgui, "*Two Stories for Beyond the Standard Model*," Ruprecht-Karls-Universität Heidelberg (2016) .

[98] R. Kallosh, A. D. Linde, D. A. Linde, and L. Susskind, "*Gravity and global symmetries*," Phys.Rev. **D52** (1995) 912–935, arXiv:hep-th/9502069.

[99] T. Banks and N. Seiberg, "*Symmetries and Strings in Field Theory and Gravity*," Phys.Rev. **D83** (2011) 084019, arXiv:1011.5120.

[100] S. W. Hawking, "*Black hole explosions*," Nature **248** (1974) 30–31.

[101] S. W. Hawking, "*Particle Creation by Black Holes*," Commun. Math. Phys. **43** (1975) 199–220. [,167(1975)].

[102] J. D. Bekenstein, "*Black holes and entropy*," Phys. Rev. **D7** (1973) 2333–2346.

[103] J. D. Bekenstein, "*Generalized second law of thermodynamics in black hole physics*," Phys. Rev. **D9** (1974) 3292–3300.

[104] J. D. Bekenstein, "*A Universal Upper Bound on the Entropy to Energy Ratio for Bounded Systems*," Phys. Rev. **D23** (1981) 287.

[105] **Super-Kamiokande**, H. Nishino *et al.*, "*Search for Proton Decay via p -> e+ pi0 and p -> mu+ pi0 in a Large Water Cherenkov Detector*," Phys.Rev.Lett. **102** (2009) 141801, `arXiv:0903.0676`.

[106] H. Georgi and S. L. Glashow, "*Unity of All Elementary Particle Forces*," Phys. Rev. Lett. **32** (1974) 438.

[107] H. Georgi, H. R. Quinn, and S. Weinberg, "*Hierarchy of Interactions in Unified Gauge Theories*," Phys. Rev. Lett. **33** (1974) 451.

[108] H. Fritzsch and P. Minkowski, "*Unified Interactions of Leptons and Hadrons*," Annals Phys. **93** (1975) 193–266.

[109] P. Nath and P. Fileviez Perez, "*Proton stability in grand unified theories, in strings and in branes*," Phys. Rept. **441** (2007) 191, `hep-ph/0601023`.

[110] P. Fileviez Perez, "*New Paradigm for Baryon and Lepton Number Violation*," Phys. Rept. **597** (2015) 1, `arXiv:1501.01886`.

[111] P. Fileviez Perez and M. B. Wise, "*Baryon and lepton number as local gauge symmetries*," Phys. Rev. D **82** (2010) 011901, `arXiv:1002.1754`.

[112] P. Fileviez Perez and M. B. Wise, "*Breaking Local Baryon and Lepton Number at the TeV Scale*," JHEP **1108** (2011) 068, `arXiv:1106.0343`.

[113] T. R. Dulaney, P. Fileviez Perez, and M. B. Wise, "*Dark Matter, Baryon Asymmetry, and Spontaneous B and L Breaking*," Phys.Rev. **D83** (2011) 023520, `arXiv:1005.0617`.

[114] M. Duerr, P. Fileviez Perez, and M. B. Wise, "*Gauge Theory for Baryon and Lepton Numbers with Leptoquarks*," Phys. Rev. Lett. **110** (2013) 231801, `arXiv:1304.0576`.

[115] A. Joglekar, P. Schwaller, and C. E. Wagner, "*Dark Matter and Enhanced Higgs to Di-photon Rate from Vector-like Leptons*," JHEP **1212** (2012) 064, `arXiv:1207.4235`.

[116] P. Schwaller, T. M. P. Tait, and R. Vega-Morales, "*Dark matter and vectorlike leptons from gauged lepton number*," Phys.Rev. **D88** (2013) no. 3, 035001, `arXiv:1305.1108`.

[117] A. Sakharov, "*Violation of CP Invariance, c Asymmetry, and Baryon Asymmetry of the Universe*," Pisma Zh.Eksp.Teor.Fiz. **5** (1967) 32–35.

[118] W. Buchmuller, P. Di Bari, and M. Plumacher, "*Leptogenesis for pedestrians*," Annals Phys. **315** (2005) 305–351, `arXiv:hep-ph/0401240`.

[119] M.-C. Chen, "*TASI 2006 Lectures on Leptogenesis*," `arXiv:hep-ph/0703087`.

[120] J. A. Harvey and M. S. Turner, "*Cosmological baryon and lepton number in the presence of electroweak fermion number violation*," Phys.Rev. **D42** (1990) 3344–3349.

[121] M. E. Peskin and T. Takeuchi, "*New constraint on a strongly interacting Higgs sector*," Phys. Rev. Lett. **65** (1990) 964–967.

[122] H.-J. He, N. Polonsky, and S.-f. Su, "*Extra families, Higgs spectrum and oblique corrections*," Phys.Rev. **D64** (2001) 053004, `arXiv:hep-ph/0102144`.

[123] T. Appelquist and J. Carazzone, "*Infrared Singularities and Massive Fields*," Phys.Rev. **D11** (1975) 2856.

[124] X.-Y. Yang and J. Nie, "*Oblique parameters in gauged baryon and lepton numbers with a 125 GeV Higgs*," Chin.Phys. **C38** (2014) no. 5, 053101, `arXiv:1402.4916`.

[125] A. Hook, E. Izaguirre, and J. G. Wacker, "*Model Independent Bounds on Kinetic Mixing*," Adv. High Energy Phys. **2011** (2011) 859762, `arXiv:1006.0973`.

[126] **ATLAS, CMS**, G. Aad *et al.*, "*Measurements of the Higgs boson production and decay rates and constraints on its couplings from a combined ATLAS and CMS analysis of the LHC pp collision data at* $\sqrt{s} = 7$ *and 8 TeV*," JHEP **08** (2016) 045, `arXiv:1606.02266`.

[127] **Particle Data Group**, C. Patrignani *et al.*, "*Review of Particle Physics*," Chin. Phys. **C40** (2016) no. 10, 100001.

[128] M. Lindner, M. Sher, and H. W. Zaglauer, "*Probing Vacuum Stability Bounds at the Fermilab Collider*," Phys. Lett. **B228** (1989) 139–143.

[129] M. Cirelli, N. Fornengo, and A. Strumia, "*Minimal dark matter*," Nucl.Phys. **B753** (2006) 178–194, `arXiv:hep-ph/0512090`.

[130] B. W. Lee and S. Weinberg, "*Cosmological Lower Bound on Heavy Neutrino Masses*," Phys.Rev.Lett. **39** (1977) 165–168.

[131] P. Gondolo and G. Gelmini, "*Cosmic abundances of stable particles: Improved analysis*," Nucl.Phys. **B360** (1991) 145–179.

[132] C. M. Bender and S. Sarkar, "*Asymptotic Analysis of the Boltzmann Equation for Dark Matter Relics*," J. Math. Phys. **53** (2012) 103509, arXiv:1203.1822.

[133] J. Hisano, K. Ishiwata, and N. Nagata, "*Gluon contribution to the dark matter direct detection*," Phys.Rev. **D82** (2010) 115007, arXiv:1007.2601.

[134] **XENON**, E. Aprile *et al.*, "*First Dark Matter Search Results from the XENON1T Experiment*," arXiv:1705.06655.

[135] **ATLAS**, "*Search for light dijet resonances with the ATLAS detector using a Trigger-Level Analysis in LHC pp collisions at* $\sqrt{s} = 13$ *TeV*," ATLAS-CONF-2016-030 (2016) .

[136] **ATLAS**, M. Aaboud *et al.*, "*Search for new phenomena in dijet events using 37 fb*$^{-1}$ *of pp collision data collected at* $\sqrt{s}$ *=13 TeV with the ATLAS detector*," arXiv:1703.09127.

[137] **CMS**, V. Khachatryan *et al.*, "*Search for resonances and quantum black holes using dijet mass spectra in proton-proton collisions at* $\sqrt{s}$ *= 8 TeV*," Phys.Rev. **D91** (2015) no. 5, 052009, arXiv:1501.04198.

[138] **CMS**, V. Khachatryan *et al.*, "*Search for narrow resonances in dijet final states at* $\sqrt{(s)}$ *= 8 TeV with the novel CMS technique of data scouting*," Phys. Rev. Lett. **117** (2016) no. 3, 031802, arXiv:1604.08907.

[139] **CMS**, V. Khachatryan *et al.*, "*Search for narrow resonances decaying to dijets in proton-proton collisions at* $\sqrt{(s)}$ *= 13 TeV*," Phys. Rev. Lett. **116** (2016) no. 7, 071801, arXiv:1512.01224.

[140] **CMS**, "*Searches for dijet resonances in pp collisions at* $\sqrt{s} = 13$ TeV *using data collected in 2016.*," CMS-PAS-EXO-16-056 (2017) .

[141] T. Plehn, "*Lectures on LHC Physics*," Lect. Notes Phys. **844** (2012) 1–193, arXiv:0910.4182.

[142] A. Belyaev, N. D. Christensen, and A. Pukhov, "*CalcHEP 3.4 for collider physics within and beyond the Standard Model*," Comput. Phys. Commun. **184** (2013) 1729–1769, arXiv:1207.6082.

[143] H. H. Patel, "*Package-X: A Mathematica package for the analytic calculation of one-loop integrals*," Comput. Phys. Commun. **197** (2015) 276–290, arXiv:1503.01469.

[144] S. Weinberg, "*Baryon and Lepton Nonconserving Processes*," Phys. Rev. Lett. **43** (1979) 1566–1570.

[145] F. Wilczek and A. Zee, "*Operator Analysis of Nucleon Decay*," Phys. Rev. Lett. **43** (1979) 1571–1573.

[146] M. Duerr, P. Fileviez Perez, and M. Lindner, "*Left-Right Symmetric Theory with Light Sterile Neutrinos*," Phys. Rev. D **88** (2013) 051701, arXiv:1306.0568.

[147] G. M. Pelaggi, A. Strumia, and S. Vignali, "*Totally asymptotically free trinification*," JHEP **1508** (2015) 130, arXiv:1507.06848.

[148] G. M. Pelaggi, A. Strumia, and E. Vigiani, "*Trinification can explain the di-photon and di-boson LHC anomalies*," JHEP **1603** (2016) 025, arXiv:1512.07225.

[149] J. Hetzel, "*Phenomenology of a left-right-symmetric model inspired by the trinification model*," arXiv:1504.06739.

[150] J. Hetzel and B. Stech, "*Low-energy phenomenology of trinification: an effective left-right-symmetric model*," Phys. Rev. D **91** (2015) 055026, arXiv:1502.00919.

[151] J. Sayre, S. Wiesenfeldt, and S. Willenbrock, "*Minimal trinification*," Phys. Rev. D **73** (2006) 035013, hep-ph/0601040.

[152] K. S. Babu, X. G. He, and S. Pakvasa, "*Neutrino Masses and Proton Decay Modes in SU(3) X SU(3) X SU(3) Trinification*," Phys. Rev. D **33** (1986) 763.

[153] P. Fileviez Perez and M. B. Wise, "*Low Scale Quark-Lepton Unification*," Phys. Rev. D **88** (2013) 057703, arXiv:1307.6213.

[154] B. Fornal, A. Rajaraman, and T. M. P. Tait, "*Baryon Number as the Fourth Color*," Phys. Rev. D **92** (2015) no.5, 055022, arXiv:1506.06131.

[155] **CMS**, V. K. *et al.*, "*Search for vector-like charge 2/3 T quarks in proton-proton collisions at sqrt(s) = 8 TeV*," Phys. Rev. D **93** (2016) no.1, 012003, arXiv:1509.04177.

[156] **CMS**, V. K. *et al.*, "*Search for long-lived charged particles in proton-proton collisions at sqrt(s)= 13 TeV*," Phys. Rev. D **94** (2016) no.11, 112004, arXiv:1609.08382.

[157] P. F. de Salas, M. Lattanzi, G. Mangano, G. Miele, S. Pastor, and O. Pisanti, "*Bounds on very low reheating scenarios after Planck*," Phys. Rev. **D92** (2015) no. 12, 123534, arXiv:1511.00672.

[158] P. Fileviez Perez and S. Ohmer, "*Low Scale Unification of Gauge Interactions*," Phys. Rev. **D90** (2014) no. 3, 037701, arXiv:1405.1199.

[159] G. 't Hooft, "*Symmetry Breaking Through Bell-Jackiw Anomalies*," Phys. Rev. Lett. **37** (1976) 8–11.

[160] G. 't Hooft, "*Computation of the Quantum Effects Due to a Four-Dimensional Pseudoparticle*," Phys. Rev. **D14** (1976) 3432–3450. [Erratum: Phys. Rev.D18,2199(1978)].

[161] A. A. Belavin, A. M. Polyakov, A. S. Schwartz, and Yu. S. Tyupkin, "*Pseudoparticle Solutions of the Yang-Mills Equations*," Phys. Lett. **59B** (1975) 85–87.

[162] R. Jackiw and C. Rebbi, "*Vacuum Periodicity in a Yang-Mills Quantum Theory*," Phys. Rev. Lett. **37** (1976) 172–175.

[163] C. G. Callan, Jr., R. F. Dashen, and D. J. Gross, "*The Structure of the Gauge Theory Vacuum*," Phys. Lett. **63B** (1976) 334–340.

[164] P. Fileviez Perez and H. H. Patel, "*The Electroweak Vacuum Angle*," Phys. Lett. **B732** (2014) 241–243, `arXiv:1402.6340`.

[165] C. A. Baker *et al.*, "*An Improved experimental limit on the electric dipole moment of the neutron*," Phys. Rev. Lett. **97** (2006) 131801, `arXiv:hep-ex/0602020`.

[166] D. B. Kaplan and A. V. Manohar, "*Current Mass Ratios of the Light Quarks*," Phys. Rev. Lett. **56** (1986) 2004.

[167] T. Banks, Y. Nir, and N. Seiberg, "*Missing (up) mass, accidental anomalous symmetries, and the strong CP problem*," in *Yukawa couplings and the origins of mass. Proceedings, 2nd IFT Workshop, Gainesville, USA, February 11-13, 1994*, pp. 26–41. `arXiv:hep-ph/9403203`.

[168] S. Aoki *et al.*, "*Review of lattice results concerning low-energy particle physics*," Eur. Phys. J. **C77** (2017) no. 2, 112, `arXiv:1607.00299`.

[169] S. M. Barr, "*A Natural Class of Nonpeccei-quinn Models*," Phys. Rev. **D30** (1984) 1805.

[170] S. M. Barr, "*A Survey of a New Class of Models of CP Violation*," Phys. Rev. **D34** (1986) 1567.

[171] A. E. Nelson, "*Naturally Weak CP Violation*," Phys. Lett. **136B** (1984) 387–391.

[172] A. E. Nelson, "*Calculation of θ Barr*," Phys. Lett. **143B** (1984) 165–170.

[173] R. D. Peccei and H. R. Quinn, "*CP Conservation in the Presence of Instantons*," Phys. Rev. Lett. **38** (1977) 1440–1443.

[174] R. D. Peccei and H. R. Quinn, "*Constraints Imposed by CP Conservation in the Presence of Instantons*," Phys. Rev. **D16** (1977) 1791–1797.

[175] J. E. Kim, "*Weak Interaction Singlet and Strong CP Invariance*," Phys. Rev. Lett. **43** (1979) 103.

[176] M. A. Shifman, A. I. Vainshtein, and V. I. Zakharov, "*Can Confinement Ensure Natural CP Invariance of Strong Interactions?*," Nucl. Phys. **B166** (1980) 493–506.

[177] M. Dine, W. Fischler, and M. Srednicki, "*A Simple Solution to the Strong CP Problem with a Harmless Axion*," Phys. Lett. **104B** (1981) 199–202.

[178] A. R. Zhitnitsky, "*On Possible Suppression of the Axion Hadron Interactions. (In Russian)*," Sov. J. Nucl. Phys. **31** (1980) 260. [Yad. Fiz.31,497(1980)].

[179] S. Weinberg, "*A New Light Boson?*," Phys. Rev. Lett. **40** (1978) 223–226.

[180] F. Wilczek, "*Problem of Strong p and t Invariance in the Presence of Instantons*," Phys. Rev. Lett. **40** (1978) 279–282.

[181] W. A. Bardeen, R. D. Peccei, and T. Yanagida, "*CONSTRAINTS ON VARIANT AXION MODELS*," Nucl. Phys. **B279** (1987) 401–428.

[182] C. G. Callan, Jr., R. F. Dashen, and D. J. Gross, "*Toward a Theory of the Strong Interactions*," Phys. Rev. **D17** (1978) 2717.

[183] D. J. E. Marsh, "*Axion Cosmology*," Phys. Rept. **643** (2016) 1–79, `arXiv:1510.07633`.

[184] C. Vafa and E. Witten, "*Parity Conservation in QCD*," Phys. Rev. Lett. **53** (1984) 535.

[185] G. G. Raffelt, "*Stars as laboratories for fundamental physics*," University of Chicago Press (1996) 664 p (1996) .

[186] M. S. Turner, "*Windows on the Axion*," Phys. Rept. **197** (1990) 67–97.

[187] J. Preskill, M. B. Wise, and F. Wilczek, "*Cosmology of the Invisible Axion*," Phys. Lett. **120B** (1983) 127–132.

[188] M. Dine and W. Fischler, "*The Not So Harmless Axion*," Phys. Lett. **120B** (1983) 137–141.

[189] P. Arias, D. Cadamuro, M. Goodsell, J. Jaeckel, J. Redondo, and A. Ringwald, "*WISPy Cold Dark Matter*," JCAP **1206** (2012) 013, `arXiv:1201.5902`.

[190] E. Witten, "*Some Properties of O(32) Superstrings*," Phys. Lett. **149B** (1984) 351–356.

[191] M. Cicoli, M. Goodsell, and A. Ringwald, "*The type IIB string axiverse and its low-energy phenomenology*," JHEP **10** (2012) 146, `arXiv:1206.0819`.

[192] A. Suárez, V. H. Robles, and T. Matos, "*A Review on the Scalar Field/Bose-Einstein Condensate Dark Matter Model*," Astrophys. Space Sci. Proc. **38** (2014) 107–142, `arXiv:1302.0903`.

[193] M. Membrado, A. F. Pacheco, and J. Sañudo, "*Hartree solutions for the self-Yukawian boson sphere*," Phys. Rev. **A39** (1989) no. 8, 4207.

[194] B. Moore, "*Evidence against dissipationless dark matter from observations of galaxy haloes*," Nature **370** (1994) 629.

[195] R. A. Flores and J. R. Primack, "*Observational and theoretical constraints on singular dark matter halos*," Astrophys. J. **427** (1994) L1–4, `arXiv:astro-ph/9402004`.

[196] B. Moore, T. R. Quinn, F. Governato, J. Stadel, and G. Lake, "*Cold collapse and the core catastrophe*," Mon. Not. Roy. Astron. Soc. **310** (1999) 1147–1152, `arXiv:astro-ph/9903164`.

[197] W. J. G. de Blok, "*The Core-Cusp Problem*," Adv. Astron. **2010** (2010) 789293, `arXiv:0910.3538`.

[198] G. Kauffmann, S. D. M. White, and B. Guiderdoni, "*The Formation and Evolution of Galaxies Within Merging Dark Matter Haloes*," Mon. Not. Roy. Astron. Soc. **264** (1993) 201.

[199] A. A. Klypin, A. V. Kravtsov, O. Valenzuela, and F. Prada, "*Where are the missing Galactic satellites?*," Astrophys. J. **522** (1999) 82–92, `arXiv:astro-ph/9901240`.

[200] B. Moore, S. Ghigna, F. Governato, G. Lake, T. R. Quinn, J. Stadel, and P. Tozzi, "*Dark matter substructure within galactic halos*," Astrophys. J. **524** (1999) L19–L22, `arXiv:astro-ph/9907411`.

[201] J. S. Bullock, "*Notes on the Missing Satellites Problem*," `arXiv:1009.4505`.

[202] M. Boylan-Kolchin, J. S. Bullock, and M. Kaplinghat, "*Too big to fail? The puzzling darkness of massive Milky Way subhaloes*," Mon. Not. Roy. Astron. Soc. **415** (2011) L40, `arXiv:1103.0007`.

[203] M. Boylan-Kolchin, J. S. Bullock, and M. Kaplinghat, "*The Milky Way's bright satellites as an apparent failure of LCDM*," Mon. Not. Roy. Astron. Soc. **422** (2012) 1203–1218, `arXiv:1111.2048`.

[204] E. Papastergis, R. Giovanelli, M. P. Haynes, and F. Shankar, "*Is there a "too big to fail" problem in the field?*," Astron. Astrophys. **574** (2015) A113, `arXiv:1407.4665`.

[205] H.-Y. Schive, T. Chiueh, and T. Broadhurst, "*Cosmic Structure as the Quantum Interference of a Coherent Dark Wave*," Nature Phys. **10** (2014) 496–499, `arXiv:1406.6586`.

[206] S.-J. Sin, "*Late time cosmological phase transition and galactic halo as Bose liquid*," Phys. Rev. **D50** (1994) 3650–3654, `arXiv:hep-ph/9205208`.

[207] V. Sahni and L.-M. Wang, "*A New cosmological model of quintessence and dark matter*," Phys. Rev. **D62** (2000) 103517, `arXiv:astro-ph/9910097`.

[208] W. Hu, R. Barkana, and A. Gruzinov, "*Cold and fuzzy dark matter*," Phys. Rev. Lett. **85** (2000) 1158–1161, `arXiv:astro-ph/0003365`.

[209] T. Matos, A. Vazquez-Gonzalez, and J. Magana, "*ϕ^2 as Dark Matter*," Mon. Not. Roy. Astron. Soc. **393** (2009) 1359–1369, `arXiv:0806.0683`.

[210] J.-W. Lee and S. Lim, "*Minimum mass of galaxies from BEC or scalar field dark matter*," JCAP **1001** (2010) 007, `arXiv:0812.1342`.

[211] V. Lora, J. Magana, A. Bernal, F. J. Sanchez-Salcedo, and E. K. Grebel, "*On the mass of ultra-light bosonic dark matter from galactic dynamics*," JCAP **1202** (2012) 011, `arXiv:1110.2684`.

[212] L. Hui, J. P. Ostriker, S. Tremaine, and E. Witten, "*Ultralight scalars as cosmological dark matter*," Phys. Rev. **D95** (2017) no. 4, 043541, `arXiv:1610.08297`.

[213] P. J. E. Peebles, "*Fluid dark matter*," Astrophys. J. **534** (2000) L127, `arXiv:astro-ph/0002495`.

[214] J. Goodman, "*Repulsive dark matter*," New Astron. **5** (2000) 103, `arXiv:astro-ph/0003018`.

[215] A. Arbey, J. Lesgourgues, and P. Salati, "*Galactic halos of fluid dark matter*," Phys. Rev. **D68** (2003) 023511, `arXiv:astro-ph/0301533`.

[216] J. Eby, C. Kouvaris, N. G. Nielsen, and L. C. R. Wijewardhana, "*Boson Stars from Self-Interacting Dark Matter*," JHEP **02** (2016) 028, `arXiv:1511.04474`.

[217] J. Fan, "*Ultralight Repulsive Dark Matter and BEC*," Phys. Dark Univ. **14** (2016) 84–94, `arXiv:1603.06580`.

[218] M. Khlopov, B. A. Malomed, and I. B. Zeldovich, "*Gravitational instability of scalar fields and formation of primordial black holes*," Mon. Not. Roy. Astron. Soc. **215** (1985) 575–589.

[219] I. I. Tkachev, "*Coherent scalar field oscillations forming compact astrophysical objects*," Sov. Astron. Lett. **12** (1986) 305–308. [Pisma Astron. Zh.12,726(1986)].

[220] M. Colpi, S. L. Shapiro, and I. Wasserman, "*Boson Stars: Gravitational Equilibria of Selfinteracting Scalar Fields*," Phys. Rev. Lett. **57** (1986) 2485–2488.

[221] I. I. Tkachev, "*On the possibility of Bose star formation*," Phys. Lett. **B261** (1991) 289–293.

[222] E. W. Kolb and I. I. Tkachev, "*Axion miniclusters and Bose stars*," Phys. Rev. Lett. **71** (1993) 3051–3054, `arXiv:hep-ph/9303313`.

[223] J.-w. Lee and I.-g. Koh, "*Galactic halos as boson stars*," Phys. Rev. **D53** (1996) 2236–2239, `arXiv:hep-ph/9507385`.

[224] A. H. Guth, M. P. Hertzberg, and C. Prescod-Weinstein, "*Do Dark Matter Axions Form a Condensate with Long-Range Correlation?*," Phys. Rev. **D92** (2015) no. 10, 103513, `arXiv:1412.5930`.

[225] P. Sikivie and Q. Yang, "*Bose-Einstein Condensation of Dark Matter Axions*," Phys. Rev. Lett. **103** (2009) 111301, `arXiv:0901.1106`.

[226] N. Banik and P. Sikivie, "*Cosmic Axion Bose-Einstein Condensation*," in *Universal Themes of Bose-Einstein Condensation, edited by Nick P. Proukakis, David W. Snoke and Peter B. Littlewood, Cambridge University Press, June 2017, chapter 31, p. 608-619 (ISBN: 9781107085695)*. `arXiv:1501.05913`.

[227] T. Rindler-Daller and P. R. Shapiro, "*Angular Momentum and Vortex Formation in Bose-Einstein-Condensed Cold Dark Matter Haloes*," Mon. Not. Roy. Astron. Soc. **422** (2012) 135–161, `arXiv:1106.1256`.

[228] N. Banik and P. Sikivie, "*Axions and the Galactic Angular Momentum Distribution*," Phys. Rev. **D88** (2013) 123517, `arXiv:1307.3547`.

[229] F. Ferrer and J. A. Grifols, "*Bose-Einstein condensation, dark matter and acoustic peaks*," JCAP **0412** (2004) 012, `arXiv:astro-ph/0407532`.

[230] H. Velten and E. Wamba, "*Power spectrum for the Bose–Einstein condensate dark matter*," Phys. Lett. **B709** (2012) 1–5, `arXiv:1111.2032`.

[231] **Virgo, LIGO Scientific**, B. P. Abbott *et al.*, "*Observation of Gravitational Waves from a Binary Black Hole Merger*," Phys. Rev. Lett. **116** (2016) no. 6, 061102, `arXiv:1602.03837`.

[232] **Virgo, LIGO Scientific**, B. P. Abbott *et al.*, "*GW151226: Observation of Gravitational Waves from a 22-Solar-Mass Binary Black Hole Coalescence*," Phys. Rev. Lett. **116** (2016) no. 24, 241103, `arXiv:1606.04855`.

[233] **Virgo, LIGO Scientific**, B. P. Abbott *et al.*, "*GW170104: Observation of a 50-Solar-Mass Binary Black Hole Coalescence at Redshift 0.2*," Phys. Rev. Lett. **118** (2017) no. 22, 221101, `arXiv:1706.01812`.

[234] A. Ringwald, "*Exploring the Role of Axions and Other WISPs in the Dark Universe*," Phys. Dark Univ. **1** (2012) 116–135, `arXiv:1210.5081`.

[235] A. E. Nelson and J. Scholtz, "*Dark Light, Dark Matter and the Misalignment Mechanism*," Phys. Rev. **D84** (2011) 103501, `arXiv:1105.2812`.

[236] M. O. C. Pires and J. C. C. de Souza, "*Galactic cold dark matter as a Bose-Einstein condensate of WISPs*," JCAP **1211** (2012) 024, arXiv:1208.0301. [Erratum: JCAP1311,E01(2013)].

[237] A. Soni and Y. Zhang, "*Hidden SU(N) Glueball Dark Matter*," Phys. Rev. **D93** (2016) no. 11, 115025, arXiv:1602.00714.

[238] M. P. Hertzberg, "*Quantum and Classical Behavior in Interacting Bosonic Systems*," JCAP **1611** (2016) no. 11, 037, arXiv:1609.01342.

[239] C. Sabin, D. E. Bruschi, M. Ahmadi, and I. Fuentes, "*Phonon creation by gravitational waves*," New J. Phys. **16** (2014) 085003, arXiv:1402.7009.

[240] P. C. Peters, "*Index of refraction for scalar, electromagnetic, and gravitational waves in weak gravitational fields*," Phys. Rev. **D9** (1974) 2207–2218.

[241] T. Elghozi, N. E. Mavromatos, and M. Sakellariadou, "*Graviton propagation within the context of the D-material universe*," Eur. Phys. J. **C77** (2017) no. 7, 445, arXiv:1605.02680.

[242] R. G. Newton, "*Optical theorem and beyond*," American Journal of Physics **44** (1976) 639.

[243] C. W. Misner, K. S. Thorne, and J. A. Wheeler, *Gravitation*. W. H. Freeman, San Francisco, 1973.

[244] C. G. Boehmer and T. Harko, "*Can dark matter be a Bose-Einstein condensate?*," JCAP **0706** (2007) 025, arXiv:0705.4158.

[245] P. H. Chavanis, "*Mass-radius relation of Newtonian self-gravitating Bose-Einstein condensates with short-range interactions: I. Analytical results*," Phys. Rev. **D84** (2011) 043531, arXiv:1103.2050.

[246] P. H. Chavanis and L. Delfini, "*Mass-radius relation of Newtonian self-gravitating Bose-Einstein condensates with short-range interactions: II. Numerical results*," Phys. Rev. **D84** (2011) 043532, arXiv:1103.2054.

[247] G. D. Moore and A. E. Nelson, "*Lower bound on the propagation speed of gravity from gravitational Cherenkov radiation*," JHEP **09** (2001) 023, arXiv:hep-ph/0106220.

[248] V. Connaughton *et al.*, "*Fermi GBM Observations of LIGO Gravitational Wave event GW150914*," Astrophys. J. **826** (2016) no. 1, L6, arXiv:1602.03920.

[249] A. Nishizawa and T. Nakamura, "*Measuring Speed of Gravitational Waves by Observations of Photons and Neutrinos from Compact Binary Mergers and Supernovae*," Phys. Rev. **D90** (2014) no. 4, 044048, arXiv:1406.5544.

[250] X. Li, F.-W. Zhang, Q. Yuan, Z.-P. Jin, Y.-Z. Fan, S.-M. Liu, and D.-M. Wei, "*Implications of the Tentative Association Between Gw150914 and a Fermi-gbm Transient*," Astrophys. J. **827** (2016) no. 1, L16, `arXiv:1602.04460`.

[251] J. Ellis, N. E. Mavromatos, and D. V. Nanopoulos, "*Comments on Graviton Propagation in Light of GW150914*," Mod. Phys. Lett. **A31** (2016) no. 26, 1675001, `arXiv:1602.04764`.

[252] T. E. Collett and D. Bacon, "*Testing the speed of gravitational waves over cosmological distances with strong gravitational lensing*," Phys. Rev. Lett. **118** (2017) no. 9, 091101, `arXiv:1602.05882`.

[253] V. Branchina and M. De Domenico, "*Simultaneous observation of gravitational and electromagnetic waves*," `arXiv:1604.08530`.

[254] A. Loeb, "*Electromagnetic Counterparts to Black Hole Mergers Detected by LIGO*," Astrophys. J. **819** (2016) no. 2, L21, `arXiv:1602.04735`.

[255] M. Lyutikov, "*Fermi GBM signal contemporaneous with GW150914 - an unlikely association*," `arXiv:1602.07352`.

[256] S. E. Woosley, "*The Progenitor of Gw150914*," Astrophys. J. **824** (2016) no. 1, L10, `arXiv:1603.00511`.

[257] F. Fraschetti, "*Possible role of magnetic reconnection in the electromagnetic counterpart of binary black hole merger*," `arXiv:1603.01950`.

[258] S.-N. Zhang, Y. Liu, S. Yi, Z. Dai, and C. Huang, "*Do we expect to detect electromagnetic radiation from merging stellar mass black binaries like GW150914? No*," `arXiv:1604.02537`.

[259] A. Janiuk, M. Bejger, S. Charzyński, and P. Sukova, "*On the possible gamma-ray burst–gravitational wave association in GW150914*," New Astron. **51** (2017) 7–14, `arXiv:1604.07132`.

[260] J. Greiner, J. M. Burgess, V. Savchenko, and H. F. Yu, "*On the FERMI-GBM event seen 0.4 s after GW150914*," Astrophys. J. **827** (2016) no. 2, L38, `arXiv:1606.00314`.

[261] M. Tavani *et al.*, "*AGILE Observations of the Gravitational Wave Event GW150914*," Astrophys. J. **825** (2016) no. 1, L4, `arXiv:1604.00955`.

[262] V. Savchenko *et al.*, "*INTEGRAL upper limits on gamma-ray emission associated with the gravitational wave event GW150914*," Astrophys. J. **820** (2016) no. 2, L36, `arXiv:1602.04180`.

[263] **Swift**, P. A. Evans *et al.*, "*Swift follow-up of the Gravitational Wave source GW150914*," Mon. Not. Roy. Astron. Soc. **460** (2016) no. 1, L40–L44, `arXiv:1602.03868`.

[264] **Virgo, LIGO Scientific**, B. P. Abbott *et al.*, "*GW170814: A three-detector observation of gravitational waves from a binary black hole coalescence*," Submitted to: Phys. Rev. Lett. (2017) , arXiv:1709.09660.

[265] M. Rocha, A. H. G. Peter, J. S. Bullock, M. Kaplinghat, S. Garrison-Kimmel, J. Onorbe, and L. A. Moustakas, "*Cosmological Simulations with Self-Interacting Dark Matter I: Constant Density Cores and Substructure*," Mon. Not. Roy. Astron. Soc. **430** (2013) 81–104, arXiv:1208.3025.

[266] M. Markevitch, A. H. Gonzalez, D. Clowe, A. Vikhlinin, L. David, W. Forman, C. Jones, S. Murray, and W. Tucker, "*Direct constraints on the dark matter self-interaction cross-section from the merging galaxy cluster 1E0657-56*," Astrophys. J. **606** (2004) 819–824, arXiv:astro-ph/0309303.

[267] S. W. Randall, M. Markevitch, D. Clowe, A. H. Gonzalez, and M. Bradac, "*Constraints on the Self-Interaction Cross-Section of Dark Matter from Numerical Simulations of the Merging Galaxy Cluster 1E 0657-56*," Astrophys. J. **679** (2008) 1173–1180, arXiv:0704.0261.

[268] R. Massey, T. Kitching, and D. Nagai, "*Cluster Bulleticity*," Mon. Not. Roy. Astron. Soc. **413** (2011) 1709, arXiv:1007.1924.

[269] D. Harvey, R. Massey, T. Kitching, A. Taylor, and E. Tittley, "*The non-gravitational interactions of dark matter in colliding galaxy clusters*," Science **347** (2015) 1462–1465, arXiv:1503.07675.

[270] F. Kahlhoefer, K. Schmidt-Hoberg, J. Kummer, and S. Sarkar, "*On the interpretation of dark matter self-interactions in Abell 3827*," Mon. Not. Roy. Astron. Soc. **452** (2015) no. 1, L54–L58, arXiv:1504.06576.

[271] M. Vogelsberger, J. Zavala, and A. Loeb, "*Subhaloes in Self-Interacting Galactic Dark Matter Haloes*," Mon. Not. Roy. Astron. Soc. **423** (2012) 3740, arXiv:1201.5892.

[272] A. H. G. Peter, M. Rocha, J. S. Bullock, and M. Kaplinghat, "*Cosmological Simulations with Self-Interacting Dark Matter II: Halo Shapes vs. Observations*," Mon. Not. Roy. Astron. Soc. **430** (2013) 105, arXiv:1208.3026.

[273] J. Zavala, M. Vogelsberger, and M. G. Walker, "*Constraining Self-Interacting Dark Matter with the Milky Way's dwarf spheroidals*," Mon. Not. Roy. Astron. Soc. **431** (2013) L20–L24, arXiv:1211.6426.

[274] M. Kaplinghat, S. Tulin, and H.-B. Yu, "*Dark Matter Halos as Particle Colliders: Unified Solution to Small-Scale Structure Puzzles from Dwarfs to Clusters*," Phys. Rev. Lett. **116** (2016) no. 4, 041302, arXiv:1508.03339.

[275] T. Harko, "*Bose-Einstein condensation of dark matter solves the core/cusp problem*," JCAP **1105** (2011) 022, arXiv:1105.2996.

[276] V. H. Robles and T. Matos, "*Flat Central Density Profile and Constant DM Surface Density in Galaxies from Scalar Field Dark Matter*," Mon. Not. Roy. Astron. Soc. **422** (2012) 282–289, arXiv:1201.3032.

[277] A. Diez-Tejedor, A. X. Gonzalez-Morales, and S. Profumo, "*Dwarf spheroidal galaxies and Bose-Einstein condensate dark matter*," Phys. Rev. **D90** (2014) no. 4, 043517, arXiv:1404.1054.

[278] B. Li, T. Rindler-Daller, and P. R. Shapiro, "*Cosmological Constraints on Bose-Einstein-Condensed Scalar Field Dark Matter*," Phys. Rev. **D89** (2014) no. 8, 083536, arXiv:1310.6061.

[279] D. V. Semikoz and I. I. Tkachev, "*Kinetics of Bose condensation*," Phys. Rev. Lett. **74** (1995) 3093–3097, arXiv:hep-ph/9409202.

[280] A. Riotto and I. Tkachev, "*What if dark matter is bosonic and selfinteracting?*," Phys. Lett. **B484** (2000) 177–182, arXiv:astro-ph/0003388.

[281] L. Dolan and R. Jackiw, "*Symmetry Behavior at Finite Temperature*," Phys. Rev. **D9** (1974) 3320–3341.

[282] S. Weinberg, "*Gauge and Global Symmetries at High Temperature*," Phys. Rev. **D9** (1974) 3357–3378.

[283] J. I. Kapusta, "*Bose-Einstein Condensation, Spontaneous Symmetry Breaking, and Gauge Theories*," Phys. Rev. **D24** (1981) 426–439.

[284] **AMON core Team**, A. Keivani, H. Ayala, and J. DeLaunay, "*Astrophysical Multimessenger Observatory Network (AMON): Science, Infrastructure, and Status*," PoS **ICRC2017** (2017) 629, arXiv:1708.04724.

[285] **eLISA**, P. A. Seoane *et al.*, "*The Gravitational Universe*," arXiv:1305.5720.

[286] I. I. Shapiro, "*Fourth Test of General Relativity*," Phys. Rev. Lett. **13** (1964) 789–791.

[287] M. J. Longo, "*New Precision Tests of the Einstein Equivalence Principle From SN1987A*," Phys. Rev. Lett. **60** (1988) 173.

[288] L. M. Krauss and S. Tremaine, "*Test of the Weak Equivalence Principle for Neutrinos and Photons*," Phys. Rev. Lett. **60** (1988) 176.

[289] E. O. Kahya and S. Desai, "*Constraints on frequency-dependent violations of Shapiro delay from GW150914*," Phys. Lett. **B756** (2016) 265–267, arXiv:1602.04779.

[290] R. Takahashi, "*Arrival time differences between gravitational waves and electromagnetic signals due to gravitational lensing*," Astrophys. J. **835** (2017) no. 1, 103, arXiv:1606.00458.

[291] R. N. Manchester, "*The International Pulsar Timing Array*," Class. Quant. Grav. **30** (2013) 224010, arXiv:1309.7392.

[292] R. Haag, J. T. Lopuszanski, and M. Sohnius, "*All Possible Generators of Supersymmetries of the s Matrix*," Nucl. Phys. **B88** (1975) 257.

[293] E. Witten, "*The unity of fundamental interactions. Proceedings, International School of Subnuclear Physics, Erice 1981 , ed. A. Zichichi, Plenum Press, 1983, p.305*,".

[294] P. C. Argyres, "*An Introduction to Global Supersymmetry*,".

[295] O. Pelc and L. P. Horwitz, "*Generalization of the Coleman-Mandula theorem to higher dimension*," J. Math. Phys. **38** (1997) 139–172, arXiv:hep-th/9605147.

[296] S. Weinberg, "*The quantum theory of fields. Vol. 3: Supersymmetry*," Cambridge University Press (2000) .

[297] L. O'Raifeartaigh, "*Lorentz Invariance and Internal Symmetry*," Phys. Rev. **139** (1965) B1052–B1062.

[298] S. Abel, K. R. Dienes, and E. Mavroudi, "*Towards a nonsupersymmetric string phenomenology*," Phys. Rev. **D91** (2015) no. 12, 126014, arXiv:1502.03087.

[299] S. Hossenfelder, "*Minimal Length Scale Scenarios for Quantum Gravity*," Living Rev. Rel. **16** (2013) 2, arXiv:1203.6191.

[300] A. Kempf, G. Mangano, and R. B. Mann, "*Hilbert space representation of the minimal length uncertainty relation*," Phys. Rev. **D52** (1995) 1108–1118, arXiv:hep-th/9412167.

[301] J. Lukierski, A. Nowicki, and H. Ruegg, "*New quantum Poincare algebra and k deformed field theory*," Phys. Lett. **B293** (1992) 344–352.

[302] S. Majid and H. Ruegg, "*Bicrossproduct structure of kappa Poincare group and noncommutative geometry*," Phys. Lett. **B334** (1994) 348–354, arXiv:hep-th/9405107.

[303] R. Percacci, "*Mixing internal and spacetime transformations: Some examples and counterexamples*," J. Phys. **A41** (2008) 335403, arXiv:0803.0303.

[304] A. H. Chamseddine and V. Mukhanov, "*On Unification of Gravity and Gauge Interactions*," JHEP **03** (2016) 020, arXiv:1602.02295.

[305] F. Girelli, S. Liberati, and L. Sindoni, "*Planck-scale modified dispersion relations and Finsler geometry*," Phys. Rev. **D75** (2007) 064015, arXiv:gr-qc/0611024.

[306] A. N. Tawfik and A. M. Diab, "*Review on Generalized Uncertainty Principle*," Rept. Prog. Phys. **78** (2015) 126001, arXiv:1509.02436.

[307] P. Hořava, "*Quantum Gravity at a Lifshitz Point*," Phys. Rev. **D79** (2009) 084008, arXiv:0901.3775.

[308] M. Visser, "*Lorentz symmetry breaking as a quantum field theory regulator*," Phys. Rev. **D80** (2009) 025011, arXiv:0902.0590.

[309] J. Alexandre, "*Lifshitz-type Quantum Field Theories in Particle Physics*," Int. J. Mod. Phys. **A26** (2011) 4523–4541, arXiv:1109.5629.

[310] E. Wigner, "*On the Consequences of the Symmetry of the Nuclear Hamiltonian on the Spectroscopy of Nuclei*," Phys. Rev. **51** (193700) 106–119.

[311] M. Gell-Mann, "*Symmetries of baryons and mesons*," Phys. Rev. **125** (1962) 1067–1084.

[312] Y. Ne'eman, "*Derivation of strong interactions from a gauge invariance*," Nucl. Phys. **26** (1961) 222–229.

[313] F. Gürsey and L. A. Radicati, "*Spin and Unitary Spin Independence of Strong Interactions*," Phys. Rev. Lett. **13** (1964) 173–175.

[314] A. Pais, "*Implications of Spin-Unitary Spin Independence*," Phys. Rev. Lett. **13** (1964) 175–177.

[315] F. Gürsey, A. Pais, and L. A. Radicati, "*Spin and Unitary Spin Independence of Strong Interactions*," Phys. Rev. Lett. **13** (1964) no. 8, 299–301.

[316] R. P. Feynman, M. Gell-Mann, and G. Zweig, "*Group U(6) x U(6) generated by current components*," Phys. Rev. Lett. **13** (1964) 678–680.

[317] B. Sakita, "*Supermultiplets of elementary particles*," Phys. Rev. **136** (1964) B1756–B1760.

[318] A. Salam, R. Delbourgo, and J. A. Strathdee, "*The Covariant theory of strong interaction symmetries*," Proc. Roy. Soc. Lond. **A284** (1965) 146–158.

[319] M. A. B. Bég and A. Pais, "*Relativistic, Crossing-Symmetric, SU(6)-Invariant S-Matrix Theory*," Phys. Rev. Lett. **14** (1965) 267–270.

[320] B. Sakita and K. C. Wali, "*Relativistic Formulation of the SU(6) Symmetry Scheme*," Phys. Rev. **139** (1965) B1355–B1367.

[321] M. A. B. Bég and A. Pais, "*Covariance, SU(6), and Unitarity*," Phys. Rev. Lett. **14** (1965) 509–513.

[322] S. Coleman, "*Trouble with Relativistic SU(6)*," Phys. Rev. **138** (1965) B1262–B1267.

[323] S. Weinberg, "*Comments on Relativistic Supermultiplet Theories*," Phys. Rev. **139** (1965) B597–B601.

[324] W. D. McGlinn, "*Problem of Combining Interaction Symmetries and Relativistic Invariance*," Phys. Rev. Lett. **12** (1964) 467–469.

[325] O. W. Greenberg, "*Coupling of Internal and Space-Time Symmetries*," Phys. Rev. **135** (1964) 1447–1450.

[326] L. Michel, "*Relations between internal symmetry and relativistic invariance*," Phys. Rev. **137** (1965) B405–B408.

[327] L. Michel and B. Sakita, "*Group of invariance of a relativistic supermultiplet theory*," Annales Poincare Phys. Theor. **A11** (1965) 167–170.

[328] E. Recami, "*Tachyons, Monopoles, and Related Topics. Proceedings, First Session of the Interdisciplinary Seminars on Tachyons and Related Topics, Erice, 1-15 Sep 1976*," Amsterdam 1978, 285p .

[329] G. R. Dvali, G. Gabadadze, and G. Senjanovic, "*Constraints on extra time dimensions*," `arXiv:hep-ph/9910207`.

[330] T. Appelquist, H.-C. Cheng, and B. A. Dobrescu, "*Bounds on universal extra dimensions*," Phys. Rev. **D64** (2001) 035002, `arXiv:hep-ph/0012100`.

[331] H.-C. Cheng, K. T. Matchev, and M. Schmaltz, "*Radiative corrections to Kaluza-Klein masses*," Phys. Rev. **D66** (2002) 036005, `arXiv:hep-ph/0204342`.

[332] G. Servant and T. M. P. Tait, "*Is the lightest Kaluza-Klein particle a viable dark matter candidate?*," Nucl. Phys. **B650** (2003) 391–419, `arXiv:hep-ph/0206071`.

[333] G. Cacciapaglia, A. Deandrea, and J. Llodra-Perez, "*A Dark Matter candidate from Lorentz Invariance in 6D*," JHEP **03** (2010) 083, `arXiv:0907.4993`.

[334] B. A. Dobrescu and E. Ponton, "*Chiral compactification on a square*," JHEP **03** (2004) 071, `arXiv:hep-th/0401032`.

[335] T. Appelquist, B. A. Dobrescu, E. Ponton, and H.-U. Yee, "*Proton stability in six-dimensions*," Phys. Rev. Lett. **87** (2001) 181802, `arXiv:hep-ph/0107056`.

ACKNOWLEDGMENTS

Doing a PhD is never an easy quest. Without the encouragement, help, and love of my colleagues, friends, and family, writing this thesis would not have been possible. I would not have enjoyed the last three years half as much.

First and foremost, I would like to thank my PhD supervisor Manfred Lindner for accepting me as a PhD student, creating an inspiring working atmosphere and providing guidance when desperately needed. I would also like to take this opportunity to express my gratitude for the chance to attend international conferences, workshops and schools during my PhD. Next, I would like to thank Tilman Plehn for agreeing to referee this PhD thesis and Björn Malte Schäfer and Klaus Blaum for completing my examination committee.

My special gratitude goes to Pavel Fileviez Pérez for the delightful physics discussions, for sharing his deep physical insights, and for his patience during our joint projects. A particularly big thank you is directed to Bhupal Dev for his enthusiasm and persistence. The seminar invitation to Washington university in St. Louis was deeply appreciated. I would also like to thank Hiren H. Patel for his mentoring and being a role model. Hiren helped me to improve my standards. Clara Murgui deserves special thanks for her curiosity and eagerness in our discussions.

Keeping the division running smoothly is always challenging. I would therefore like to thank Anja Berneiser and Britta Schwarz for their dedication. My office mate Branimir Radovčić also deserves special mentioning. I always enjoyed our black board discussions in the office. The division thrives with the people. I would therefore like to thank my fellow PhD students Miguel Campos, Dominick Cichon, Christian Doering, Yannick Emonds, Alexander Helmboldt, Thomas Hugle, Pascal Humbert, Clarissa Martins Siqueira, Moritz Platscher, Ludwig Rauch, Thomas Rink, Natascha Rupp, and Johannes Welter, the master students Daniel Jimenez Tejero, Kevin Max, and Clara Miralles Vila, and the senior researchers Evgeny Akhmedov, Giorgio Arcadi, Michael Dürr, Florian Goertz, Kher Sham Lim, Rasmus Sloth Lundkvist, Farinaldo da Silva Queiroz, Werner Rodejohann, Kai Schmitz, Alexei Smirnov, Juri Smirnov, Stefan Vogl, Xunjie Xu, and Carlos Yaguna for pleasant lunch and coffee breaks.

I am in dept to Miguel Campos, Bhupal Dev, Pavel Fileviez Pérez, Florian Goertz, Franziska Müller, Branimir Radovčić and Jan Stockemer for proof-reading this thesis and supplying precious comments.

When studying physics, you are never a lone warrior but a team player. I would like to say thank you to Philippe d'Argent, David Gerick, Matthieu Kecke, and Dominik Mitzel for making studying physics a lot more fun.

This thesis would not have been possible without the love and support of my parents. The freedom and possibility to follow my interests and longings were always appreciated. I would not be were I am today without their ongoing assistance and inspiration. Last but not least, I would like to thank Franziska Müller for her unyielding support.